GDAŃSK UNIVERSITY OF TECHNOLOGY
FACULTY OF CHEMISTRY

The author of the PhD dissertation: M.Sc. Eng. Maksymilian Plata-Gryl

Scientific discipline: Chemical Sciences

DOCTORAL DISSERTATION

Title of PhD dissertation: Preparation and characterization of asphaltene based adsorbents for gas-solid adsorption systems

Title of PhD dissertation (in Polish): Badania nad adsorbentami na bazie frakcji asfaltenowej do procesów adsorpcji w układach gaz-ciało stałe

Supervisor *signature*
PhD. Sc. Eng., Grzegorz Boczkaj, Assoc. Prof. of GUT

Gdańsk, 2022

STATEMENT

The author of the PhD dissertation: M.Sc. Eng. Maksymilian Plata-Gryl

I, the undersigned, agree/~~do not agree*~~ that my PhD dissertation entitled:
Preparation and characterization of asphaltene based adsorbents for gas-solid adsorption systems may be used for scientific or didactic purposes.[1]

Gdańsk, 01.03.2022 .....

signature of the PhD student

Aware of criminal liability for violations of the Act of 4th February 1994 on Copyright and Related Rights (Journal of Laws 2006, No. 90, item 631) and disciplinary actions set out in the Law on Higher Education (Journal of Laws 2012, item 572 with later amendments),[2] as well as civil liability, I declare, that the submitted PhD dissertation is my own work.

I declare, that the submitted PhD dissertation is my own work performed under and in cooperation with the supervision of PhD. Sc. Eng., Grzegorz Boczkaj, Assoc. Prof. of GUT.

This submitted PhD dissertation has never before been the basis of an official procedure associated with the awarding of a PhD degree.

All the information contained in the above thesis which is derived from written and electronic sources is documented in a list of relevant literature in accordance with art. 34 of the Copyright and Related Rights Act.

I confirm that this PhD dissertation is identical to the attached electronic version.

Gdańsk, 01.03.2022 .....

signature of the PhD student

I, the undersigned, agree/~~do not agree*~~ to include an electronic version of the above PhD dissertation in the open, institutional, digital repository of Gdańsk University of Technology, Pomeranian Digital Library, and for it to be submitted to the processes of verification and protection against misappropriation of authorship.

Gdańsk, 01.03.2022 .....

signature of the PhD student

*) delete where appropriate.

[1] Decree of Rector of Gdansk University of Technology No. 34/2009 of 9th November 2009, TUG archive instruction addendum No. 8.

[2] Act of 27th July 2005, Law on Higher Education: Chapter 7, Criminal responsibility of PhD students, Article 226.

DESCRIPTION OF DOCTORAL DISSERTATION

The Author of the PhD dissertation: M.Sc. Eng. Maksymilian Plata-Gryl

Title of PhD dissertation: Preparation and characterization of asphaltene based adsorbents for gas-solid adsorption systems

Title of PhD dissertation in Polish: Badania nad adsorbentami na bazie frakcji asfaltenowej do procesów adsorpcji w układach gaz-ciało stałe

Language of PhD dissertation: English

Supervision: PhD. Sc. Eng., Grzegorz Boczkaj, Assoc. Prof. of GUT

Date of doctoral defense:

Keywords of PhD dissertation in Polish: asfalteny, materiały węglowe, lotne związki organiczne (LZO), adsorpcja, oczyszczanie gazów

Keywords of PhD dissertation in English: asphaltenes, carbon materials, volatile organic compounds (VOCs), adsorption, waste gas treatment, air purification

Summary of PhD dissertation in Polish: Tematyka badawcza pracy doktorskiej dotyczy przygotowania adsorbentów na bazie asfaltenów (porowaty nośnik pokryty warstwą asfaltenów). Szczególny nacisk położona na zbadanie właściwości adsorpcyjnych względem lotnych związków organicznych (LZO), w układzie gaz-ciało stałe. Badania wykazały, że asfalteny wyizolowane z asfaltów utlenionych silnie oddziałują z LZO. Właściwości sorpcyjne asfaltenów mogą zostać zmodyfikowane poprzez wprowadzenie dodatkowych grup funkcyjnych do ich struktury za pomocą reakcji chemicznych. Nitrowanie w sposób szczególny zwiększyło aktywność powierzchni asfaltenów w zakresie oddziaływań sorpcyjnych. Adsorpcja LZO na powierzchni zmodyfikowanego adsorbentu ma charakter fizyczny, z elementami chemisorpcji. Na podstawie entalpii adsorpcji wybranych LZO stwierdzono, że oddziaływania z powierzchnią asfaltenów nitrowanych są znacznie silniejsze niż w przypadku innych, standardowo używanych adsorbentów np. węgla aktywowanego. Krzywe przebicia złoża adsorbentu wykazały, że asfalteny nitrowane w znaczący sposób zwiększają pojemność sorpcyjną nośnika, oraz są odporne na działanie wysokiej temperatury, i mogą być wykorzystane w procesach cyklicznej adsorpcji zmienno-temperaturowej. Połączenie asfaltenów i łatwo dostępnego oraz taniego nośnika, może zostać wykorzystane do zagospodarowania i zwiększenia wartości materiałów odpadowych o niskiej wartości rynkowej.

Summary of PhD dissertation in English: The dissertation presents results of the experimental research on asphaltene-based adsorbents (support coated with asphaltene layer) for gas-solid adsorption systems, with special reference to volatile organic compounds (VOCs) removal from gas streams. Analysis of gas adsorption properties revealed that asphaltenes isolated from oxidized bitumen have strong affinity toward VOCs. Interactions with target gas molecules, and selectivity

were further enhanced by chemical modifications, of which nitration was the most beneficial for adsorption properties. Investigation of nitrated asphaltenes interaction with VOCs molecules revealed that the adsorption mechanism was driven by both physisorption and chemisorption. The strength of interactions with VOCs exceeds values reported for standard adsorbents. Fixed-bed adsorption studies revealed that facile coating of nitrated asphaltenes can significantly enhance adsorption capacity of a support material. Multiple adsorption-desorption cycles confirmed the durability of chemical modification and thermal resistance of asphaltene-based adsorbent. Utilization of asphaltenes and low cost supports, easily available in the target destination (e.g. diatomaceous earth or clays) can be an effective procedure for risk mitigation of hazardous VOCs, accompanied by effective waste management and low-value materials valorization.

ACKNOWLEDGEMENTS

To prof. Grzegorz Boczkaj,
for the patient guidance, knowledge sharing and encouragement he has provided throughout my time as his student. I have been privileged with having a supervisor who cared so much about my work, was always available when I had question and doubts, and was willing to proof read countless pages of my scribbles. His support and experience was invaluable for the successful completion of this work.

To my family,
for their continued support and encouragement during ups and downs of my research. I am indebted to them for their help.

To colleagues and members of the Department of Process Engineering and Chemical Technology,
for their friendship and support. Without them, completing this work would have been much more difficult.

To Gdańsk University of Technology and Faculty of Chemistry authorities,
for providing the funds to undertake this research, and giving the opportunity to meet so many interesting people.

The author gratefully acknowledge the financial support from the National Center for Research and Development, Warsaw, Poland – Project LIDER, no. LIDER/036/573/L-5/13/NCBR/2014.

This work was financially supported by the project “INTERPHD2” no. POWR.03.02.00-IP.08-00-DOC/16.

Contents

Abstract

Adsorption-based gas separation and purification have found widespread application in various industries, laboratories and environmental protection systems. Effectiveness of this techniques relies on the adsorbents – solid materials that selectively interact with molecules in a gas phase.

This dissertation presents results of the experimental research on asphaltene-based adsorbents for gas-solid adsorption systems, with special reference to volatile organic compounds (VOCs) removal from waste gas streams. Adsorbents were prepared by coating of a porous support material (surface area provider) with asphaltenes (adsorption active layer).

Thorough analysis of gas adsorption properties revealed that asphaltenes isolated from oxidized bitumen have strong affinity toward VOCs. Interactions with target gas molecules, and selectivity were further enhanced by chemical modifications. Out of numerous chemical modifications examined, nitration was the most beneficial for adsorption properties (*e.g.* adsorption capacity). Detailed analysis of nitrated asphaltenes interaction with VOCs molecules revealed that the adsorption mechanism was driven by both physisorption and chemisorption. The strength of interactions with VOCs exceeds values reported for standard adsorbents, *e.g.* activated carbons.

Fixed-bed adsorption studies revealed that facile coating of nitrated asphaltenes can significantly enhance adsorption capacity of a support material. Multiple adsorption-desorption cycles confirmed the durability of chemical modification and thermal resistance of asphaltene-based adsorbent. Utilization of asphaltenes (considered a waste material in petroleum industry) and low-cost supports, easily available in the target destination (*e.g.* diatomaceous earth or clays) can be an effective procedure for risk mitigation of hazardous VOCs, accompanied by effective waste management and low-value materials valorisation.

I. Introduction

The industrial development and economic growth critically depends on processes that deliver pure chemicals. Thus, gas separation and purification is indispensable, both in industrial and laboratory practice, and it contributes to a significant part of capital and operating costs of a given process and/or product [1,2].

Production of chemical compounds is the second largest sector of manufacturing, and estimates predict that it will triple by the end of 2050, as compared to 2010 [3]. Currently there are *ca.* 350 000 chemicals on the market, with novel one being constantly produced - almost 70 000 was registered in the last decade [4].

Mass production of targeted chemicals and their further processing has however a flipside. It produces unintended by-products, impurities and wastes that are emitted as liquid or gases [5]. Recent analyses suggest that chemical pollution has passed safe limit for natural environment [6]. The anthropogenic pollution can be found from the summit of Himalayans [7] to the deepest oceans [8]. Production and releases of hazardous chemicals are a threat to biological processes fundamental for all life. For examples, common gaseous pollutants like volatile organic compounds (VOCs), ozone or NO_x can reduce by 80% the ability of insects to pollinate flowers and crops [9,10].

Growing public awareness of environmental pollution forced an introduction of stronger regulation to timid and control emission of hazardous gases, as well as made the environment preservation an imperative for authorities [11]. On the other hand, it was realized by companies that pro-environmental approach can increase their profits [12–14].

Unfortunately, current regulation system is good for tackling well-defined threats like chlorofluorocarbons destroying ozone layer or CO_2 contributing to greenhouse effect. The galloping increase in production of common and novel chemicals exceed the ability of authorities and science to investigate and control their impact on natural environment and human health [15,16].

VOCs constitute a major group of hazardous chemicals and air pollutants emitted from industrial, agricultural and municipal sources [17]. Compounds of this group are defined as organic compounds having vapour pressure at least 0.01 kPa at standard conditions [18]. They can be present in the environment as gaseous airborne or adsorbed on solid (indoor surfaces, airborne particular matter) chemicals [19,20]. Noxious character of some VOCs is well-know and confirmed *e.g.* toxic effects, or participation in atmospheric photochemical reactions [21,22]. Extended exposure to VOCs is associated with increased risk of mutagenicity and carcinogenicity [23]. Apart from the adverse health effects, VOCs are also responsible for excessive odour emission and odour nuisance for residents, that affects directly the quality and comfort of life, even at very low concentrations - some VOCs (*e.g.* dimethyl sulphide or methyl mercaptan) have extremely low odour threshold value (below

ppb levels) [24,25]. The problem of VOCs emission is made even greater by the fact that many of them are emerging pollutants with vague hazardousness and without proper long-term risk assessment [15]. Additionally, even if toxic effect of individual VOC can be low, the aggregate effect may be significant. Due to lack of scientific certainty in this regards, a fair amount of precaution is required.

Measures undertaken to control emission of VOCs fall into two categories: process integrated and end-of-pipe solution. Process integrated actions are connected with process improvement, modernization and recycling aimed at preventing the production of hazardous wastes in the first place. However, this approach is significantly limited by technology and cost - replacement of traditional technologies is very difficult due to large-scale production. End-of-pipe solutions are usually separate stages in relation to the industrial processes, and are focused on removal of hazardous chemicals from waste streams [26–28].

End-of-pipe technologies used for reduction of VOCs emission can be based on their destruction or recovery. First group typically include different oxidation techniques, which at the cost of high energy consumption, decompose VOCs to CO_2 and H_2O. With destructive methods, problem of air pollution is however only partially solved because CO_2 is produced, as well some other secondary pollutants *e.g.* NO_x, O_3 or organic aerosols [29,30]. Second group, consist of methods used for selective separation and recovery of VOCs *e.g.* absorption, condensation, membrane separation or adsorption. These methods are generally viewed as more environmentally friendly, and more economical [19,31]. Figure 1 compiles various techniques for control of VOCs emission.

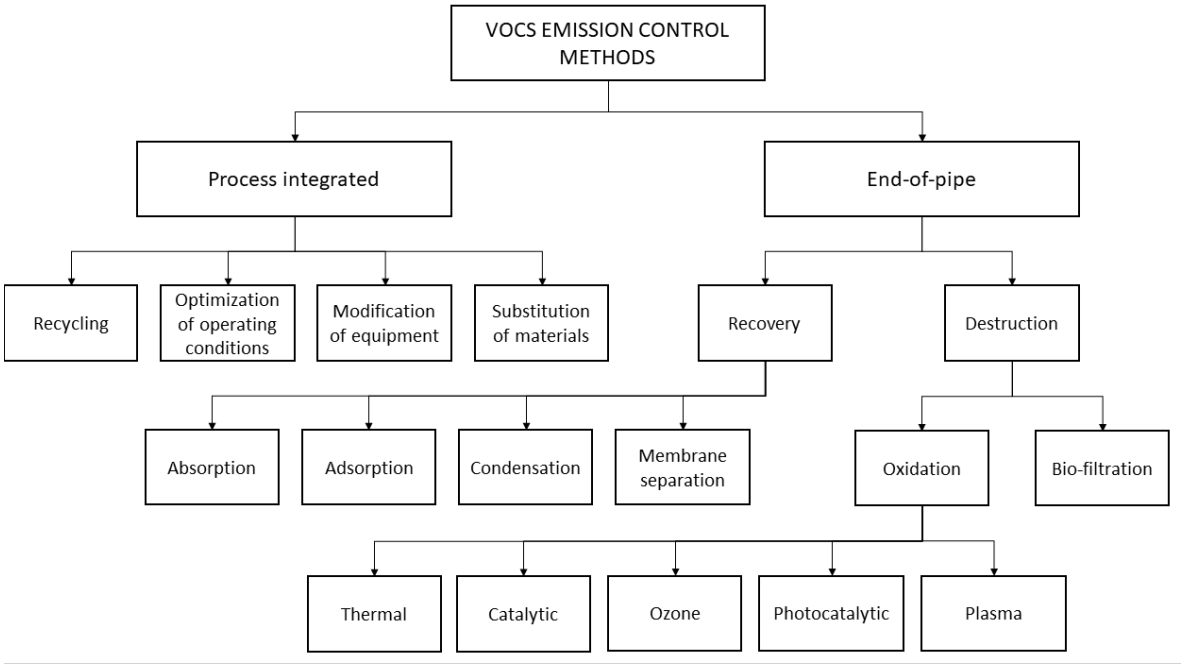

Figure 1. Methods for emission control of VOCs.

Among techniques presented in the Figure 1, adsorption has proved to be an effective method for VOCs abatement [32]. Adsorption in based on solid materials known as adsorbents to selectively interact with VOCs and separate them from gas streams. In typical gas purification applications, targeted molecules are concentrated on the surface of adsorbent until its capacity will be exceeded, or it will be recovered by thermal or vacuum methods. The possibility to reuse, both the adsorbent and separated VOCs, make adsorption economically viable strategy for VOCs emission control [32–34].

The key factor in adsorption technology are adsorbents. Adsorbent characteristic will determine the separation efficiency, investment and operating cost, as well as safety. Thus, finding or designing the material with optimal adsorption properties is crucial for successful commercial application [33,35,36]. Recently, a growing interest in adsorbents derived from wastes or solid industrial by-products is observed [37–39]. Such approach has a potential to tackle the problem of solid and gaseous wastes at once, addressing the challenges of climate change, biodiversity loss, waste production and pollution – it can be viewed as a combination of process integrated and end-of-pipe strategies.

II. Aims and objectives

The aim of this dissertation was to develop asphaltene-based adsorbent for adsorption separation processes, with special focus on waste gas treatment and removal of VOCs. Strictly speaking, two aspects were investigated: interactions between VOCs molecules and asphaltenes in the gas-solid systems, and adsorption equilibrium data (adsorption isotherms and breakthrough curves) analysis for representative VOCs.

The objectives of this work are to:

- Isolate high-purity asphaltenes from bitumen penetration grade 20/30.
- Modify isolated asphaltenes with different organic functionalities, investigate their effect on adsorbate-adsorbent interactions, and select the most promising material for comprehensive evaluation of adsorption potential.
- Characterize selected, modified asphaltenes surface properties and adsorption potential.
- Determine the VOCs uptake capabilities of modified asphaltene-based adsorbent.

III. Literature review

1. Adsorption

Adsorption is a phenomenon that occurs when molecules (adsorbate) present in a fluid are concentrated on a surface of a solid (adsorbent). Opposite phenomenon is called desorption, *i.e.* the adsorbate is released back to bulk phase. When the system is in equilibrium, adsorption and desorption rates are equal. Adsorption takes place spontaneously and to some extent on virtually any solid material - however, preferably on materials having molecular interactions with adsorbate and porous structure that provides high surface area. If the adsorption is accompanied by a dissolution in an adsorbent (absorption) the general term sorption is used [34]. The extent of adsorption is dependent on the nature of adsorbent, adsorbate and bulk phase. Figure 2 presents factors affecting adsorption in gas-solid systems.

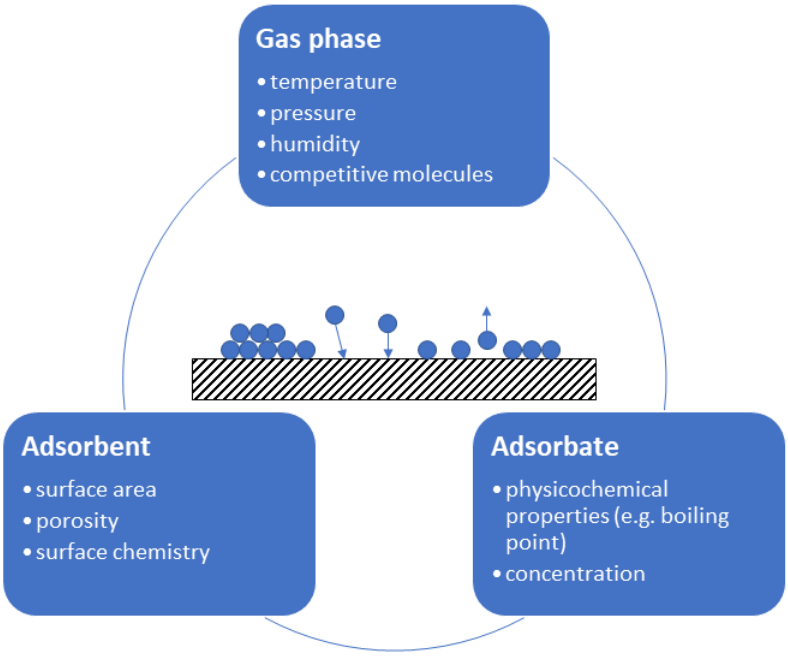

Figure 2. Factors affecting the adsorption process.

1.1. Classification of adsorption

Adsorption process can be divided into a sequence of steps including: (1) diffusion of an adsorbate from a bulk of a fluid to a vicinity of an interface with a solid surface, (2) diffusion of an adsorbate through a stationary fluid film (boundary layer) surrounding an adsorbent's surface, (3)

diffusion through pores (intraparticle diffusion) to adsorption sites and (4) adsorption of an adsorbate molecules on adsorption sites [40].

Two distinctive types of adsorption (fourth step) can be identified: physisorption and chemisorption. Physisorption is based on relatively weak van der Waals forces. Its specificity is low, but molecules can adsorb in multilayers. Enthalpy of adsorption accompanying physisorption is in the range of 10-40 kJ mol^{-1} – close to enthalpy of condensation. The advantage of weak adsorbat-adsorbent interactions is full reversibility of the adsorption, and lower energy consumption required for regeneration of adsorbent. The process is exothermic in nature, thus its magnitude is significant at relatively low temperature – the increase of temperature negatively affects adsorption [40–42].

Chemisorption involves transfer of electrons between molecules of adsorbate and adsorbent. Thus the strength of interaction close to the chemical bonding range, and enthalpy of adsorption oscillates in the range of 20-400 kJ mol^{-1}. Distinctive feature of chemisorption is that adsorbate molecules can bind only to specific active centres on the surface of the adsorbent. High specificity entails formation of maximum monolayer of adsorbate. The process can be both endothermic or exothermic. Because substantial amount of energy is required to activate chemisorption, temperature affects it positively (to some extent). Very strong adsorbate-adsorbent interactions makes it an irreversible process – in the sense that desorbed molecules differ from the adsorbed ones [34,43,44]. Table 1 compares both types of adsorption.

Table 1. Differences between physisorption and chemisorption.

Feature	**Physisorption**	**Chemisorption**
bonding forces	van der Waals	chemical bonding (transfer of electrons)
heat effect	exothermic	endothermic or exothermic
effect of temperature	• negative • significant at relatively low temperatures	• positive (to some extent – activated adsorption) • possible over a wide range of temperatures
change of enthalpy / kJ mol^{-1}	10 – 40	20 - 400
reversibility	reversible	irreversible (desorbed compound different from adsorbed one)
surface coverage	complete (up to multilayer)	incomplete (up to monolayer)
specificity	low	high
activation energy	small / none	large

Chemisorption is favoured in catalytic processes, while physisorption everywhere where is demand for high adsorption capacity, recovery of adsorbate and easy regeneration of adsorbent (*e.g.*

gas purification and/or storage, waste gas treatment, or analytical separations). Although the distinction between both types of adsorption is quite clear it is possible for both to occur simultaneously (to the benefit of overall process) [45].

Surface of macropores behaves similarly to flat surface and physisorption occurs with formation of mono and multilayers. In mesopores adsorption proceed via multilayer formation, up to the point where enhanced van der Waals interactions, between molecules in the confined space of mesopore induce condensation, and filling of the mesopore volume. In micropores, with width close to molecular dimension of adsorptive, the adsorption potential of pore walls overlap, which result in instant micropore filling, without differentiation on mono and multilayer formation. Out of whole porous network, filling of micropores occurs in the first place, at relatively low partial pressures. Capacity of micropores depends on the experimental conditions *i.e.* molecular size of adsorptive molecule and its accessibility to the pore (it can be negligible as in molecular sieves). More detailed description of physisorption mechanism can be found in books [46–48], and citations therein.

Adsorption data are presented in form of adsorption isotherms, as the amount adsorbed per gram of outgassed adsorbent (preferably in mol g^{-1}), in relation to the equilibrium relative pressure (p/p^0), *i.e.* concentration of this substance in the gas phase, where p^0 is the saturation pressure at the temperature of measurement.

1.2. Adsorbents

Adsorption is a general process and takes place whenever adsorptive molecule is in contact with a surface – thus, virtually any solid is an adsorbent. However, to apply adsorption as a separation unit operation in industry, adsorbent must have certain attributes.

Effective adsorbent is usually thought of as the one with high adsorption capacity, high selectivity, good kinetics, stable physicochemical structure, that is easy to regenerate and reuse, cheap and will generate minimal waste when disposed [40,47]. Moreover, every different application will have its own prerequisites and constrains placed on the adsorbent.

High adsorption capacity (amount of adsorbate adsorbed per unit mass of adsorbent) is the most important property of an adsorbent. It sets limits to the amount of adsorbent required, which in turn dictates the volume of vessels – both are crucial for capital cost of an adsorption unit. Surface area, pore size, and volume intuitively correlates with adsorption capacity, but the exact dependence may be more subtle, *e.g.* not all pores may be accessible for adsorptive molecules. Nevertheless, solids with extended porous network and developed surface area are sought after [49,50].

Selectivity of an adsorbent can be driven by chemical structure (specific interactions with adsorbate) or porous structure. To a great extent, pore size distribution of an adsorbent controls the diffusion of particles and mass transfer kinetics. Dimension of pores set steric restriction on diffusion of adsorptive molecules, limiting their access to them [51,52]. Importance of kinetics is most clearly seen in separation of nitrogen from air using carbon molecular sieves – the effectiveness of this separations is in the difference between diffusion rates of oxygen and nitrogen molecules [53]. Figure 3 presents pore width of some common adsorbents along with molecular size of selected molecules.

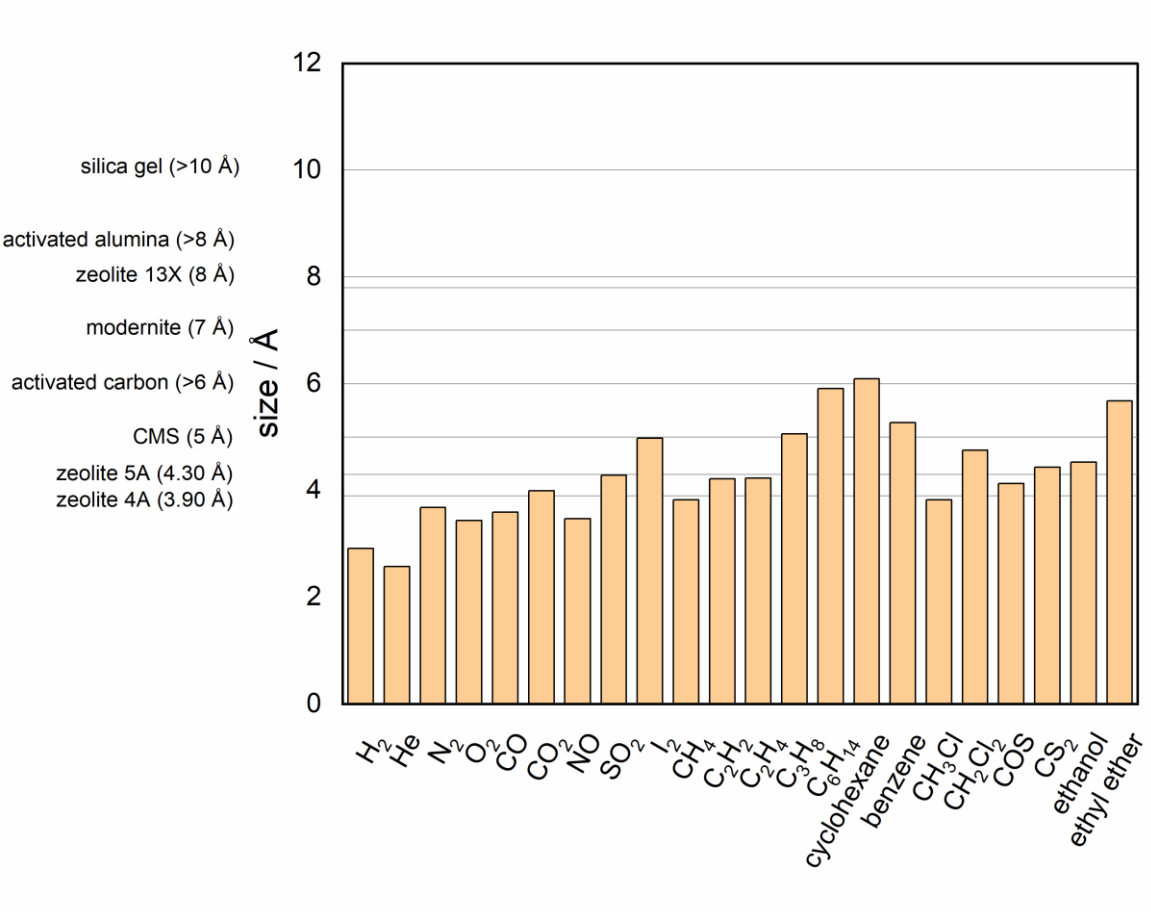

Figure 3. Pore size of typical adsorbents and effective sizes of common molecules.

Favourable kinetics is not only desirable for selectivity, but also for general efficiency of the process. Good kinetics yields a sharp breakthrough curves in fixed bed adsorption system and leads to efficient utilization of adsorbent, and short adsorption cycle time. Slow kinetic may be overcome by extending contact time inside adsorption unit, but it reduces the throughput [54–56].

Economic feasibility of adsorption process rely greatly on regenerability, and possibility of adsorbent operation in sequential cycles. Adsorbents can be regenerated by different methods *e.g.*

temperature or pressure swing [57]. Regardless of method, regeneration decrease the available adsorption capacity [57,58]. Moreover, adsorbent is subjected to other, chemical and physical, factors that can reduce its life-time, *e.g.* moisture [59]. To operate adsorbent over hundreds of cycles, with reproducible performance, it has to have robust and stable physicochemical structure [60]. Nevertheless, sooner or later, the adsorbent will be depleted and it will have to be disposed. Thus, ease and cost of waste adsorbent management and disposal have to be considered.

There is no single adsorbent that fulfils all requirements mentioned above, and very few that will be optimal. Moreover, industrial development is expanding the number of possible adsorption applications, each with its own priorities regarding adsorbent properties. To meet demands, researchers are constantly investigating new materials with improved adsorption performance. A brief description of available types of adsorbents is presented in the following part of the text.

Zeolites

Zeolites are microporous aluminosilicates with crystalline structure, found in natural deposits or synthesized in laboratories. Reader interested in zeolite synthesis will find different publications reviewing available methods, *e.g.* [61–67],but book [68] is especially recommended.

The zeolite framework is composed of SiO_4^{4-} and AlO_4^{5-} tetrahedra, arranged in a regular three-dimensional crystalline framework [63,68]. Atomic ratio of Si/Al is always above 1, and can be varied which affects the hydrophobicity/hydrophilicity of the material. Low silica zeolites very strongly interacts with polar molecules, while high-silica zeolites are nonpolar adsorbents [69].

The zeolite framework has a regular structure of cages, interconnected by windows of definite size – typically in the range of 3 – 12 Å. Presence of aluminium atoms produces a negative framework charge, that is balanced by alkali and/or earth-alkali cations [70]. Due to their distinctive characteristic, zeolites have found widespread application in industrial separation and catalysis [71] for treatment of natural gas [72], gas production and purification (especially dehydration) [73,74], for production of speciality and fine chemicals [75], as well as for gasoline production (catalytic cracking of gas oil) [76]. Zeolites are also utilized in the field of environmental protection. The subject of zeolites applications have been covered in numerous reviews and books [77].

Behind the excellent separation selectivity and adsorption capacity of zeolites are their high surface area, large pore volume, and precisely defined pore size. Unimodal distribution of pores size gives zeolites a molecular sieving properties, thus they are also called molecular sieves. Cages of zeolites can host a large number of molecules, which are selected based on their shape and size with respect to the size of window aperture [70,78]. It is worth mentioning, that molecular sieving

mechanism is temperature dependent, *i.e.* for some molecules it occurs only at specific temperatures [33,79].

Aperture size is controlled by the number, type and distribution of cations [68,70]. Because they are loosely connected to the framework, they can be easily exchanged to other cations, yielding molecular sieves with tuned selectivity. For example type 4A zeolite is synthesized in the sodium form with effective aperture of 3.8 Å, but after ion-exchange with K^+ a type 3A (aperture size 3.0 Å) is obtained. Type 3A zeolite is used for selective dehydration of gases and alcohols. It admits almost exclusively water molecules, and excludes all hydrocarbons, and essentially all permanent gases (except ammonia). Type 5A zeolite is produced by Na^+ exchange (in type 4A) to Ca^{2+} or Mg^{2+}. As a result aperture size is increased to 4.3 Å, because two Na^+ cations are exchanged to one divalent ion. This type of zeolite is commercially used for separation of paraffins, iso-paraffins and cyclic hydrocarbons – the cages of type 5A zeolite are accessible only to linear paraffins [33]. Apart from molecular sieving, zeolites can separate molecules by kinetic mechanism (differences in diffusivities) [80,81].

Recent example of tuning zeolites selectivity by cation exchange are so-called trapdoor zeolites. The exchanged cation is large enough to block the access to cavities to any molecule, below a specific critical temperature – above it the cation deviates from its original position in the aperture of window, and the access to the cavity is not restricted by it [82,83]. Such zeolites have a remarkably low BET surface area measured at cryogenic conditions. The optimal type of cations and composition range of zeolite for trapdoor effect was discussed in [83].

Trapdoor zeolites can ensure exclusive admission of a specific molecules to the cavity of zeolite based on a subtle difference in interaction with cation residing at window aperture. At a specific temperature, a guest molecule can induce temporary and reversible cation deviation from aperture, opening the access to the cavity. This new separation mechanism is independent of the molecule size. For example on chabazite zeolite exchanged with Cs^+ a preferable admission of larger CO molecule over smaller N_2 was observed [84]. Trapdoor zeolite was reported as efficient adsorbent for other difficult separation, *e.g.* for separation of hydrogen isotopologues at mild temperature conditions [85].

Activated carbons

Activated carbon (AC) is collect term for an amorphous, non-graphitized carbonaceous material, with high porosity and surface area. BET surface areas of ACs can reach up to few thousand square meters per gram [33]. Its excellent adsorption properties have been recognized since long time ago, and ACs are widely used for adsorption, in both gas-solid and liquid-solid systems [86].

Rapid development of modern society, and fast growing production caused increased pollution. Stricter regulations about water and air control, or recovery of valued chemicals demanded a proper separation and purification technologies. Adsorption with activated carbon turned out to be a robust and efficient solution. To this day ACs are a gold standard adsorbent [87]. The summary of current applications employing AC adsorbents can be found in [37,88,89].

AC is produced in two step process. Firstly, the precursor is carbonized to remove volatile matter, and increase carbon content [90]. As precursor, carbonaceous materials are used *e.g.* wood, peat, husks, fruit shells, bones, industrial biomass, petroleum coke [88]. Possibility of AC production from agricultural and industrial wastes have significantly increased the scientific interest [91,92].

Carbonization alone, is not enough to develop satisfactory porosity. Additionally, pores are filled with pyrolysis residues. Thus, as prepared char requires additional step *i.e.* activation – physical or chemical. Physical activation involves gasification of the carbonized precursor with mild oxidizing gases *e.g.* CO_2 or steam, at high temperatures (*ca.* 800-1000 °C). Chemical activation does not require separate carbonization step - the precursor is mixed with activators and thermally treated at temperatures ranging from 400 to 1000 °C. Comprehensive reviews about ACs production are available elsewhere [88,93–96].

Porosity and pore size distribution are ultimate factors shaping the excellent adsorption capacity of ACs. The structure is hierarchical with macro, meso and micropores present – smaller pores are branching off from bigger ones. Most of the total pore volume is located within micro and mesopores, which are responsible for outstanding capacity of ACs [33]. Nevertheless, macropores are necessary for fast mass transfer of adsorptive, from bulk phase to the surface of AC [97]. The fraction of given type of pores can be controlled by precursor, carbonization and activation parameters, and tailored for specific applications [98,99].

Surface chemistry of activated carbons have been a subject of multiple studies [100–107]. Heteroatoms within AC network are typically oxygen and hydrogen, and are arranged in functional groups with character similar to functional groups typical for aromatic compounds [108]. For as synthesized AC their amount relatively small and set nonpolar (or slightly polar) character to the surface. It has important practical implications. AC is one of the few adsorbents that does not require moisture removal from feed stream. Although nonpolar molecules bind stronger and preferably to the surface of AC, it cannot be viewed as hydrophobic adsorbent [109]. Additionally, nonpolar surface is capable of only weak van der Waals interactions with adsorbate, which can be relatively easily broken. This ensures facile regeneration and reuse of AC in cyclic processes [33,110].

Surface functional groups affects significantly only adsorption of polar molecules with strong, and permanent dipole moments. To enhance specific interactions ACs are subjected to chemical modifications. Oxidation is an example of chemical treatment used to tailor ACs adsorption

properties. Incorporation of oxygen containing functional groups change the character of the surface to hydrophilic, and enhance interactions with polar molecules – opposite effect can be achieved by thermal desorption of oxygen containing groups. Another example are nitrogen-enriched ACs, manufactured for the purpose of CO_2 adsorption. The modification of surface chemistry of ACs has been a subject of long-standing scientific interest, and numerous reviews are available, *e.g.* [111–114].

Carbon molecular sieves

Carbon molecular sieves (CMSs) are a subgroup of activated carbon, with purely microporous structure [33,115]. Narrow pore size distribution enables a separation mechanism based primarily on kinetics, rather than thermodynamic [116,117]. Similarly to zeolites, CMSs exhibit molecular sieving effect, and can selectively separate molecules based on differences in shape, size or diffusion rate [118]. The advantage over zeolites is that CMSs are less hydrophilic and can be used with wet-gas streams. On the other hand, engineering desired pore size in CMS is more challenging and the structure is less defined.

Due to its favourable selectivity of O_2/N_2, N_2/CH_4 or CO_2/CH_4, CMSs are used for production of nitrogen [115], and are attracting attention for *e.g.* methane upgrading [117,119], or propylene/propane separation [120,121]. The selectivity can be further enhanced by chemical modifications *e.g.* impregnation [117,122].

CMSs are manufactured by a similar method as ACs. The precursor used in the process can be biomass or coal [123]. Because carbonized precursor has a complex pore network and wide pore size distribution, it lacks appropriate selectivity [116]. Pore size (and selectivity) can be tuned in two ways: 1) controlled carbonization [124–126], and 2) chemical vapour deposition (CVD) [118].
In industrial practice, pore size of CMSs is controlled by CVD of hydrocarbons on the surface of carbonized precursor, in order to modify the available porosity. The deposition of hydrocarbons occurs at the entrance to pores, limiting their width to match the size of desired adsorbate. The pyrolytic carbon is obtained by thermal cracking of deposited hydrocarbons under an inert atmosphere [116,118,121]. A literature review on preparation of CMSs is presented in [123].

Metal-organic frameworks

Metal-organic frameworks (MOFs) are an emerging class of crystalline porous materials, with ultrahigh porosity and very low density. Constructed with the use of coordination chemistry, framework of MOF is composed of metal ion (or cluster of ions) and organic ligands (linkers). Final

structures inherits properties of both, inorganic and organic, building blocks, yielding materials with multifunctional characteristic. In combination with modular nature of MOFs, it produces a versatile and tunable material (with over 1000 experimentally known types) that is considered in the context of various applications. The interest in MOFs is further boosted by high crystallinity, which greatly simplify structural characterization, and predicting (or explaining) their properties, as well as by diverse functional groups on their frameworks that can be easily modified [127,128].

The most unique property of MOFs is exceptionally high porosity (up to 90 %) and surface area, that can be finely tuned by appropriate selection of building blocks - generally MOFs pore size distribution is within micropore range (from several angstroms to several nanometres) [129,130]. MOFs are among materials with the most developed surface area known. Samples with BET surface area as high as 7000 $m^2 g^{-1}$ were successfully synthesized, and theoretically achievable values are close to 15 000 $m^2 g^{-1}$ [131]. This naturally predestine MOFs for catalysis, gas storage and separation [132]. Also, adsorptive removal of hazardous materials from the environment have received a great deal of attention recently [133].

On the other hand, the biggest uniqueness of MOFs may be problematic in some applications - very narrow pores limits mass transfer and diffusion of molecules. To ensure better accessibility to pores, synthesis of mesoporous MOFs is under investigation [134]. Another practical limitation is their fragileness. Functional groups on the organic ligands are susceptible to elevated temperature or microwave radiation (often employed in synthesis), on the other hand MOFs synthesised at mild conditions are rarely chemically and thermally stable [135,136]. Last but not least, satisfactory water stability of MOFs is a major challenge - most of them are water-labile to some extent. It is probably the most problematic characteristic of MOFs, in regard to their future applications [137–139].

MOFs are viewed as materials capable of revolutionizing almost any area of life, thus they are extensively investigated. Comprehensive description is out of scope of this thesis, but more information can be easily found in many review articles that have been published, *e.g.* [128,132–139].

Alumina

Activated alumina is an adsorbent obtained by thermal dehydration of aluminium trihydrate or gibbsite. The final structure is composed of Al^{3+} and O^{2-} ions bonded in tetrahedral or octahedral coordination. Its physicochemical properties depends on the temperature, heating rate and atmosphere during production. The most popular form of alumina, used for adsorption and catalysis, is γ-alumina. It is the best known for its ultimate water adsorption capacity, being higher than in

zeolites, thus it is commonly applied as desiccant. Apart from that, it is used for removal of acidic gases from hydrocarbons, or for adsorption of polar compounds [33,140].

As mentioned above, textural properties depend on synthesis parameters [47]. The surface area is in the range *ca.* 200 – 500 m^2 g^{-1}. Random grouping of alumina oxides and hydroxides within alumina lattice creates a variety of micro and mesopores, with the pore size distribution in the range *ca.* 2 – 6 nm [33,141].

Surface of activated alumina contains both, basic and acidic sites. Besides, it can interact *via* multiple types of interactions *e.g* hydrogen bonding, van der Waals or dipole-dipole. Moreover, chemisorption was also observed. Acidity of alumina surface is its most distinctive property. Electron acceptor properties are provided by aluminium atoms [141,142]. In case of hydrated surface, Brøoensted acid sites are present, due to -OH groups. Acidity of the activated alumina surface can be controlled by treatment with acids [143].

Silica gel and Mobile Composition Matter (MCM)

Silica gels are amorphous, mesoporous adsorbents with pores larger than 2 nm. Generally, they are fabricated by polymerization of silicic acid, aggregation of colloidal silica, or sol-gel processing of silicon alkoxides. Adsorbent with different properties can be prepared, depending on synthesis parameters [33]. Silica gels are recognized as excellent desiccants [144]. They have the highest capacity for water among industrially relevant adsorbents, and are easy to regenerate (at *ca.* 150 °C, compared to 350 °C for zeolites), as they form relatively weak bonds with water [145,146].

Surface chemistry of silica gel is dominated by abundant hydroxyl groups, which participate in adsorption of molecules – hydrogen bonding is the most important type of interaction [147,148]. Presence of hydroxyl groups make them especially susceptible to chemical modifications, *e.g.* by reacting with organic ligands [149–152]. This feature is widely used for separation in liquid chromatography [153,154].

A more recent and promising type of silica adsorbents are MCM-type materials. It is a type of ordered mesoporous silicate prepared by hydrothermal process in presence of surfactant templates. MCM adsorbents gained attention because of its simple structure, ease of synthesis and feasible tailoring of its porosity and surface properties. The distinctive feature is its large uniform pore structure and very large pore volume. The pore size can be controlled in the range of 2 – 10 nm. In gas phase applications, MCM adsorbents are tested for adsorption of CO_2, CH_4, H_2S, SO_2, H_2, or VOCs. Recent progress in the adsorption of gas compounds was summarized in [155,156]. Different aspects of MCM-type materials have been reviewed and discussed extensively in [33,157–159].

Low-cost natural and waste-derived adsorbents

Increased production and consumption have emphasized issues of pollution and waste management. The broadness of the chemical pollution problem, has made it difficult to tackle theses global challenges with traditional or specialized (*e.g.* MOFs, CMSs) adsorbents, due to their specificity, selectivity, availability and/or price.

As it was mentioned before, adsorption occurs on virtually any surface, thus almost anything can be an adsorbent. Additionally, adsorption is versatile and robust technology, and there are "almost no limitations" to what can be put inside the adsorption column. This is provoking scientist to seek for low-cost alternatives of traditional adsorbents. As a low-cost alternative, a material that is readily available, requires little processing, and/or is by-product or waste material from another industry or agricultural activity, can be viewed. Apart from tackling problem of chemical pollution, such approach fits to the concept of circular economy, through effective waste management and valorisation. Natural materials that are cheap and abundant in nature can also be considered low-cost adsorbents.

Two strategies are observed in the scientific literature: 1) synthesis of traditional adsorbents *e.g.* ACs, zeolites, mesoporous silicas, from waste materials [160–167], 2) direct application of waste or natural materials for adsorption [168–172].

A considerable research interest is directed toward synthesis of ACs from alternative feedstocks, because it has become a standard adsorbent for remediation of municipal and industrial waste streams. Currently, ACs are obtained mostly by carbonization and activation of wood, anthracite and bituminous coal, lignite, peat, coconut shell, olive stones and almond shells – the last three can be considered a waste or by-product. Given the fact, that many industrial and agricultural wastes have a high carbon content, they can undergo controlled carbonization and activation, yielding AC as well. It may be especially interesting in the context of wastes that pose disposal problems due to their bulk volume, toxicity, or physical nature (e.g. petroleum wastes, old tires, rice hulls). Other alternative feedstocks include, *e.g.*: bark, sawdust, lignin, petroleum wastes, fly ash, chitosan, bagasse, seaweed, dead biomass, and many more. Produced ACs usually matches their traditional counterparts, in terms of adsorption properties. The literature on this subject has been discussed extensively in review papers, *e.g.* [93,95,173–176]

"Low-cost" of ACs from alternative feedstocks is significantly inflated by processing. The feedstock requires careful pre-treatment prior to carbonization and activation, that consumes significant amounts of energy. Additionally, any alterations in physicochemical properties of the feedstock, will require appropriate process parameters adjustment, to produce adsorbent with

reproducible characteristic. Thus, this strategy may be viewed more as a viable waste management, rather than a low-cost production of ACs.

In recent developments, researchers have succeeded in synthesizing other types of adsorbents from different types of waste materials, *e.g.* zeolites from fly ash [166,167], aluminium solid wastes [164], municipal glass [163], or mesoporous silica from rice husk ash [162], banana peel ash [161], fly ash [160]. Recent findings about zeolite synthesis from industrial and hazardous wastes were summarized in [165,177]

Second mentioned strategy, provide that natural or waste materials are directly applied as adsorbents – without significant transformation. For example fly ash was utilized as low-cost adsorbent for adsorption of SO_x, NO_x, VOCs, or mercury removal from flue gases [172]. The problem of greenhouse gas CO_2 emission, was tackled by adsorption with CaO recovered from eggshell [178], carbide slag [171], or paper mill wastes [170].

Similar effort are made toward application of low-cost materials that are abundant in nature. Clay minerals are probably the most explored materials, due to their layered structure, high ratio of surface to volume, and both, chemical and mechanical stability [179,180]. A comprehensive review of clay minerals application in adsorption from gaseous phase was presented in [169]. Diatomite is an example of naturally occurring mesoporous silica, used for adsorption of various hazardous compounds from gas phase, either in natural form, after modification [168,181,182] or as a part of composite adsorbent [183,184].

Low-cost adsorbents (natural or waste-derived) usually have lower adsorption capacity compared to their "lab-engineered" equivalents (ACs, zeolite, *etc.*) [87,185]. However, even if inferior in terms of adsorption capacity, they can potentially be feasible for adsorption, due to their abundance and cost effectiveness. Moreover, a viable procedures of chemical and/or physical modifications are available to help overcome this drawback (at least to some extent).

1.3. Modification of adsorbents

Application of a given adsorbent may be limited because of its lack of selectivity, low adsorption capacity, and susceptibility to temperature, humidity or chemical factors [186–188]. Modification of the surface properties is viewed as a valuable approach for overcoming shortcomings of the adsorbent, and extending its applicability [189,190].

Surface modification is the process of tailoring physical and/or chemical characteristic of adsorbent, in order to meet specific adsorption system requirements, and can be carried out by different methods. As a result of modification, textural properties and/or surface chemistry of

adsorbent is altered in order to enhance selective affinity to targeted molecules and/or increase adsorbent adsorption capacity [111,191–193].

Modifications of adsorbents can be classified into physical and chemical. Physical modification usually introduces alteration to textural characteristic of the adsorbent. The most typical example is the activation of a char using oxidizing gases such as CO_2 [194], steam [195] or air [196], in combination with high temperature. Such process creates new micropores and expands the existing ones, by reaction of gas molecules with carbon atoms of the char. Enlarged surface area has a direct reflection in increased adsorption capacity. Moreover, physical modification with oxidizing gases may introduce new oxygen containing surface groups, that will increase polarity of the surface and favour adsorption of *e.g.* polar VOCs [192].

By substituting oxidizing gas to inert, heat treatment can be used for selective removal of surface acidic functionalities - majority of oxygen containing functional groups decompose at temperatures up to 1000 °C. For carbonaceous adsorbents such process increase basicity and hydrophobicity of the surface [197]. For zeolites, post-synthetic thermal modification may be used to tailor the transport properties within pores [198].

Second type of modifications, *i.e.* chemical, change the type and quantity of surface functional groups, enhancing the interaction between target molecules and adsorbents surface. Functional groups of chemical agents can be attached to surface of adsorbent in two ways: 1) by grafting or impregnation. Grafting involves formation of new bonds between chemical agent and adsorbent surface, while impregnation deposits chemical agents on the surface *via* physical interactions [111]. Advantage of grafting is that it is more thermally stable, but the amount of chemical agent grafted on the surface is limited, compared do impregnation [199]. However, impregnation is the simplest method for adding new functionalities to the adsorbent surface (chemical agent dissolved in a volatile solvent is contacted with adsorbent, followed by solvent evaporation) [199]. It should be noted, that addition of functional groups can reduce the accessible pore volume of an adsorbent [200].

Regardless of the method, chemical modification aims at introducing specific functional groups, usually containing heteroatoms, that will interact selectively with targeted molecules. Typically, these are oxygen and nitrogen, containing functional groups, metal/metal oxides, and hydrocarbon-type functional groups (e.g. alkyl, alkene, arene).

Oxygen atoms are commonly introduced as phenol, carboxylic, quinone, lactone, carbonyl, ether, ester and hydroxyl groups. Their presence on the surface of an adsorbent is determinant for its acid nature and polarity. Moreover, they increase hydrophilicity of the adsorbent. Especially, presence of surface hydroxyl and carboxylic groups enhance dispersibility in water [201]. Although, enhanced affinity toward water is unfavourable for adsorption performance and limits applicability of an

adsorbent in humid conditions, oxygen functional groups can improve sorption properties toward polar VOCs [200], CO_2 [202], or heteroaromatic nitrogen compounds [203]. Ester groups were reported to play an important role in mercury adsorption from flue gases [204,205].

Oxygen containing groups can be a source of various types of interactions with adsorptive molecule. Carboxylic groups can enhance physisorption of molecules by an oxygen lone pair donation, and by hydrogen bond interactions – carbonyl part can act as Lewis base, and hydroxy group as a Lewis acid [206]. Similarly, unpaired electrons of oxygen in carbonyl and ether moieties can enhance adsorption of polar and polarisable molecules, through electron acceptor-donor interactions [207,208]. Polar hydroxyl group has a capability to interact *via* H-bonding, both as a H-donor and H-acceptor [187]. Moreover hydroxyl groups can be responsible for dipole-induced dipole interactions with VOCs molecules [209].

Doping adsorbents with nitrogen is a common practice for increasing their basicity. Nitrogen atoms can donate a lone pair of electron, which can interact with adsorptive by Lewis acid-base interactions [210]. Increased basicity is also related to enhanced dipole-dipole and hydrogen-bonding interactions [211]. Similarly to O-containing functional groups, presence of nitrogen group increase hydrophilicity of the adsorbent surface, and compromise performance under humid conditions [212]. Nitrogen on the surface of adsorbents is typically detected in the form of amine, nitro, imine, amide, nitrile pyrrole, pyridine, and pyridone.

The most popular are amine functionalised adsorbents, because this type of modification is known to promote selective adsorption of CO_2 *via* strong chemisorptive interactions [213]. The flipside of enhanced interactions is the requirement of higher temperature for regeneration of such adsorbent [214]. Amine functional groups are also effective in enhancing adsorption of VOCs [215] and SO_2 [194].

Basic amide groups potentially introduce two adsorption sites to the surface of an adsorbent: one acting as electron donor (-C=O), the second one as acceptor ($-NH_x$). Additionally, amide groups is able to establish hydrogen bonds and interacting with π electrons [216]. Contrary to amide group, polar nitro groups have acidic character - two electron rich atoms of oxygen can interact with electron deficient parts of adsorptive through electron donor-acceptor interactions [217]. Nitrile and pyrrole are weak basic functional groups. With the latter, adsorptive can interact with hydrogen or nitrogen atom, *via* Lewis acid/base interactions and hydrogen bonding [218]. Pyrrole groups exhibit high thermal stability. For porous carbon, no significant decrease of their content was observed below 700 ^{o}C [219].

Metals and metal oxides can be used to change the surface chemistry, as well as polarity of adsorbent, and to increase selectivity of adsorbent [220]. The adsorption mechanism is very often changed from physisorption to chemisorption [221]. Beneficial effect of metal/metal oxide doping for

adsorption of VOCs was observed for different types of adsorbents *e.g.* mesoporous silica [222], MOFs [223], and ACs [224]. Modification of ACs with metallic oxides have successfully increased adsorption capacity for SO_2 removal from flue gas [225].

The most obvious example of hydrocarbon-type functional group modification is introduction of alkyl chains in order to deactivate the surface of adsorbent and make it more hydrophobic. Hydrophobic adsorbent are superior for adsorption of VOCs from humid environment [226]. Beside, alkene groups were reported to positively contribute to adsorption of polarizable molecules, through π-π interactions [227,228].

Modification of adsorbents properties to increase their adsorption performance has been a subject of long-standing scientific interest. Methodology of surface functional groups introduction depends on multiple factors: nature of the material being functionalized, reagents and targeted adsorptive/application. Information presented above skims only the surface of available knowledge. Reviewing all possible modification methods of different adsorbents goes beyond the scope of this work. Comprehensive reviews dedicated to specific adsorbents and specific applications are available in the literature – for example surface modification of activated carbons for adsorption of VOCs [189], SO_2 and NO_x [111] or modification methods of adsorbents for adsorption of elemental mercury from flue gases [191].

1.4. Adsorbent characterization techniques

In practical context, information about equilibrium, kinetic and thermodynamic of adsorption system are the most illustrative and useful for optimization of adsorption process. However, to a great extent, these are derivatives of adsorbents physicochemical properties *e.g.* surface chemistry, surface area, or porosity (the adsorbate and bulk phase properties are also relevant, but typically are independent variables).

Advancement in the field of adsorption technique is centred around development of adsorbents. Since adsorption occurs on virtually any solid surface, a multitude of materials are of interest to researchers, not to mention numerous modified variants. Figure 4 shows the number of papers, published over the span of last 20 years, including phrases “novel adsorbent” or “new adsorbent” in the title.

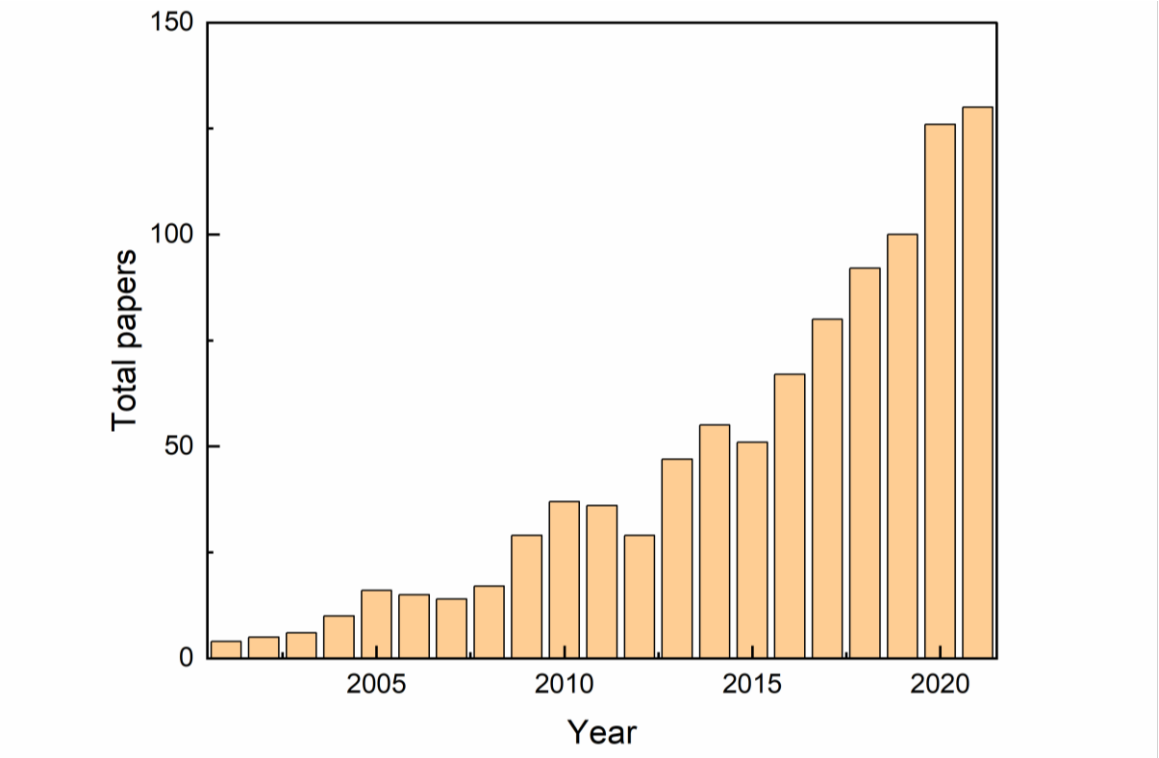

Figure 4. The number of papers about adsorbents, having "new" or "novel" in the title, published over the span of last 20 (Source: PubMed, 2022).

Rational design of an adsorbent requires knowledge about its structure. Unfortunately, one comprehensive tool for adsorbent properties characterization does not exist. Proper description usually depend upon combination of several techniques. Additionally, selection of a suitable method is dictated by the nature of the material under investigation, *e.g.* analysis of amorphous sample with X-ray diffraction (XRD) will provide little insight, if not at all. It would be ideal to use a full range of available characterization techniques, but very often available resources are limited, especially if the material is not completely new, and ground-breaking.

Analysis of 144 papers from journals listed in Journal Citation Reports (JCR) gave an overview of the most frequently used characterization techniques. The results are presented in the Figure 5. Reviewed publications were published between 2008 – 2021 (75% after 2017), and were related to adsorbents used for gas phase separations *i.e.* MOFs (19 % of publications), zeolites (20 %), carbonaceous adsorbents (33 %), composites (17 %), and others (11%).

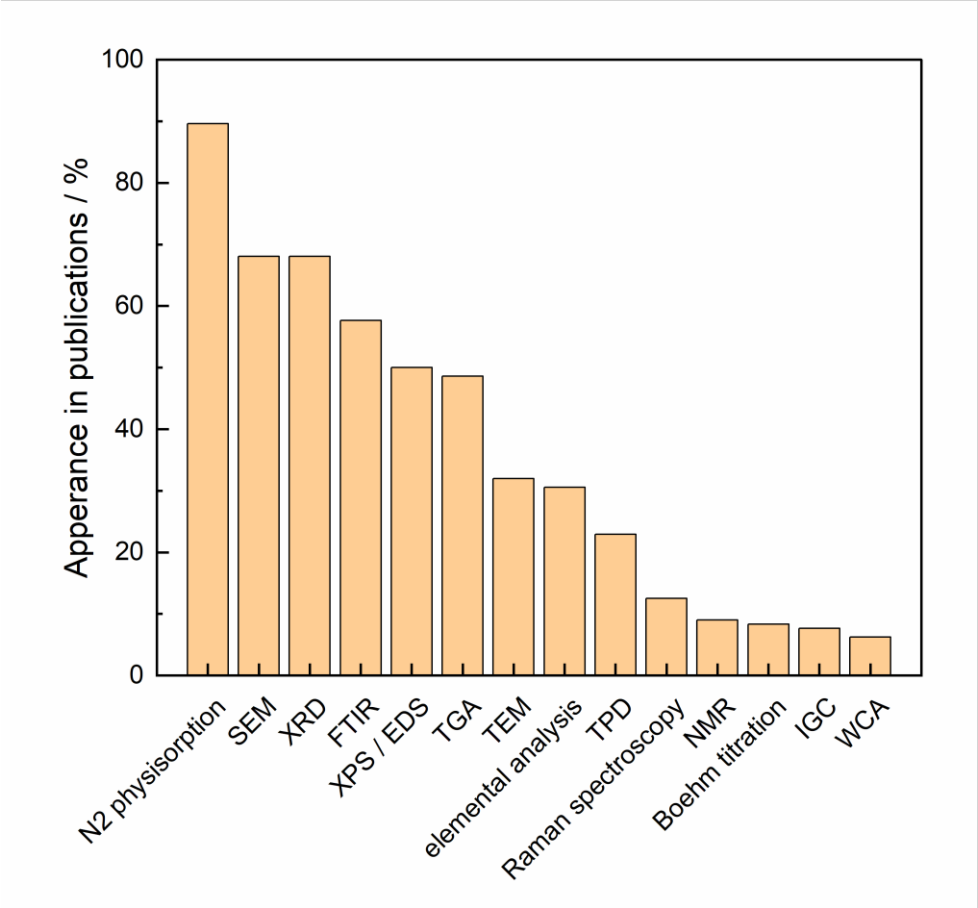

Figure 5. Frequency of application of a given technique to adsorbents characterization.

It is impossible to select the perfect set of experimental techniques suitable for all adsorbents, nor to use all known to science. Nevertheless there are few methods that are universal, easily available, and can add up to a toolkit, which will provide maximum information, with as little effort as possible, *i.e.* N_2 adsorption at cryogenic temperature (77 K), Fourier-transform infrared spectroscopy (FTIR), elemental analysis, and inverse gas chromatography (IGC). Such selection should give comprehensive outlook on adsorbent properties, with reasonable demand for technical resources and workload - especially at the early stage of research, when multiple samples are preliminary screened. This set of techniques was used in the research presented in this dissertation.

Nitrogen adsorption at cryogenic temperature is a must-have for adsorbent characterization. It provides information about textural properties, *i.e.* surface area and porosity, which are closely linked to adsorbate uptake.

Types of atoms within adsorbent structure are crucial for adsorbent physicochemical properties. Unfortunately, there is no all-in-one tool for elemental analysis. The choice of technique will be dictated by the elements to be analysed, and their location *i.e.* in the bulk or on the surface. For

carbonaceous adsorbents it is typical to measure the content of carbon, hydrogen, nitrogen, sulphur and oxygen with CHNS elemental analysers (so-called ultimate analysis).

FTIR technique allows to detect arrangement of atoms on the surface of the adsorbent. Functional groups are responsible for specific interactions with adsorbate molecules, and act as adsorption active centres. It is the most popular technique for analysis of surface chemistry.

Even though so far IGC is not routinely employed for adsorbent characterization, it direct measures interactions between gas molecules and solid surface. Thus, it can be invaluable tool for adsorbent characterization. It is a variant of gas chromatography – adsorbent under investigation is placed inside chromatographic column and retention of a pure probe compounds, with known properties, is monitored. Depending on experimental conditions, different properties of adsorbent surface can derived from retention times of probes, *e.g.* dispersive and specific component of the surface free energy, acid-base properties, surface roughness, enthalpy of adsoprtion, adsorption isotherms, adsorption potential distribution, or specific surface area. The undisputable advantage of this technique is that access to standard gas chromatograph is enough to conduct experiments – although dedicated instruments are available.

Description of these methods can be found in the following chapters. Other techniques were excluded due to reasons listed below:

Scanning electron microscopy (SEM) / transmission electron microscopy (TEM) – sophisticated equipment; tedious sample preparation; information about single particles – results may be susceptible to inhomogeneity of material,

X-ray diffraction (XRD) – sophisticated equipment; generally not useful for amorphous materials,

X-ray photoelectron spectroscopy (XPS) – sophisticated equipment; information similar to the one provided by FTIR and elemental analysis; small area of a surface probed,

Temperature programmed desorption (TPD) – information only about thermally labile surface functional groups (mainly oxygen containing),

Boehm titration – determination of only four types of oxygen containing surface functional groups; limited to carbonaceous adsorbent,

Raman spectroscopy – sophisticated equipment; similar to FTIR,

Nuclear magnetic resonance (NMR) – sophisticated equipment.

1.4.1. Low temperature N_2 physisorption

Textural characterization of material is mandatory to evaluate its applicability as adsorbent. Surface area, pore size distribution, and porosity translate directly into adsorption capacity

[229,230]. Moreover, porous structure controls transport phenomena and diffusion of molecules, and therefore also selectivity of separations [116,120].

The most popular, and generally accepted, method of texture characterization is physical adsorption of gases. It determines the amount of gas adsorbed by an adsorbent at specific temperature and pressure, and with the aid of appropriate computational methods provides information about pore volume, pore size distribution, and specific surface area [41,231].

As a standard test method, gas physisorption has been extensively used by scientist over the years. Implementation of this technique was recently boosted by development of nanoporous materials with tailored porous structures [232]. Countless analysis of different materials revealed strengths, weaknesses and existing challenges that needs to be solved. Numerous reviews have been dedicated to physisorption characterization of porous materials (adsorbents in particular), where detailed discussion about experimental and theoretical aspects of physisorption characterization can be found [41,42,232–234]. For a reader interested in this subject, a IUPAC technical report "*Physisorption of gases, with special reference to the evaluation of surface area and pore size distribution"* is recommended as a first read [41]. Thus, the information presented below is by no means meant to be comprehensive description of physisorption characterization of textural properties of adsorbents.

Adsorbents surface area and features of the porous network are extracted from the shape of adsorption isotherm of gas, measured in the pressure range from vacuum ($P/P_0 = 0$) to saturation ($P/P_0 = 1$). Standard adsorptive for textural characterization is nitrogen, and its adsorption is measured at a liquid nitrogen temperature (77 K). Because, nitrogen as adsorptive has some certain limitations, *e.g.* nitrogen is not suitable for analysis of pores with size less than 0.7 nm, due to very slow diffusion and equilibration, and quadrupolar moment of N_2 can result in enhanced interaction with heterogenous surface. Thus other adsorptives, like argon (at 87 K) or carbon dioxide (at 273 K), can be used. The choice of adsorptive for textural characterization was exhaustively discussed in review papers [42,232,234]. Despite limitations, nitrogen is the first choice for economic reasons.

Physisorption isotherm can be generally divided into six types, which are closely related to specific pore structures [41]. Classification proposed by the IUPAC is presented in the Figure 6. Type I isotherm is characteristic for microporous solids, with mainly narrow micropores (< 2 nm), and small external surfaces. The uptake is limited by micropore volume, and steep rise at low partial pressure is due to micropore filling. Type II isotherm is observed for adsorption of gases on non-porous or macroporous materials. First knee of the isotherm corresponds to formation of monolayer coverage. In Type III isotherm monolayer formation cannot be distinguished, and adsorbent-adsorbate interactions are relatively weak. Type IV is given by mesoporous adsorbent. Similarly to type II, first knee is related to monolayer coverage and beginning of multilayer formation. It is then followed by

pore condensation (second knee), with final saturation plateau. Type V is similar to type III, but pore filling is additionally observed. Type VI isotherm represent layer-by-layer adsorption on uniform nonporous surfaces.

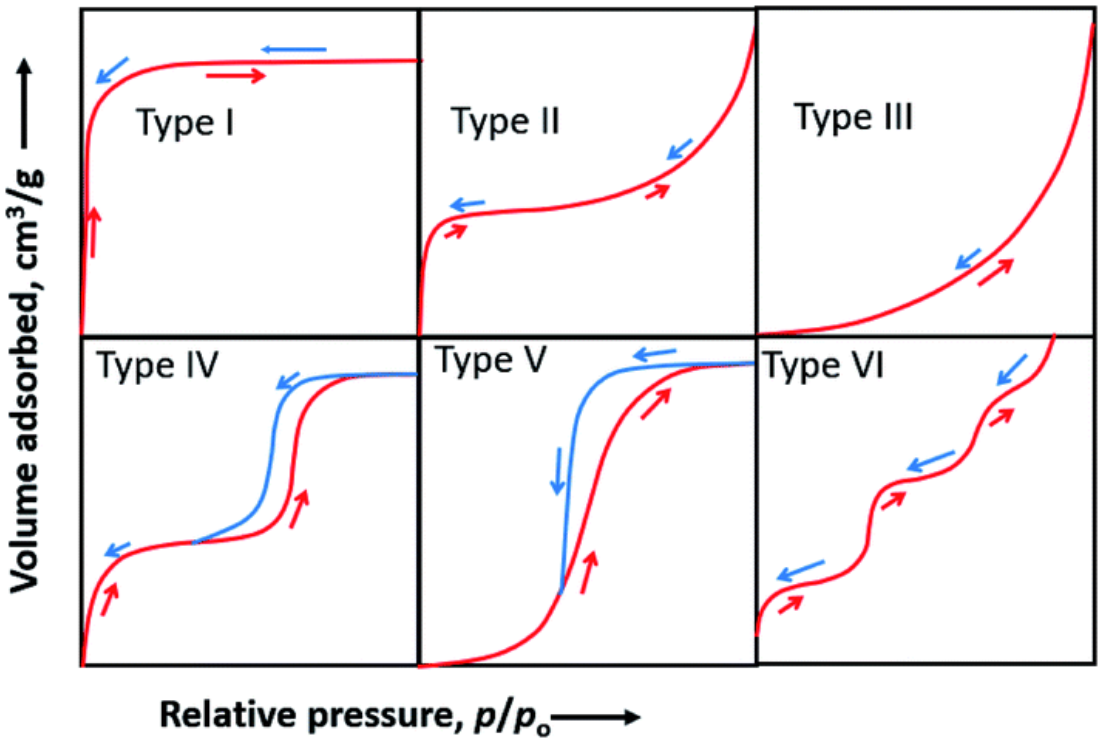

Figure 6. Classification of adsorption isotherms according to IUPAC recommendations [41]. Red and blue lines represent adsorption and desorption branch, respectively. Reprinted from [235].

For some systems (Type IV and Type V isotherms) capillary condensation may be accompanied by hysteresis (adsorption isotherm does not coincide with desorption isotherm), in the multilayer range of isotherm. Similarly to adsorption isotherm, hysteresis loops can be classified into 5 general types, which are closely correlated to a specific pore structure. Empirical classification of hysteresis loops, along with explanation of particular pore features represented by them, was presented in IUPAC technical report [41].

Specific surface area is the most basic parameter derived from adsorption isotherm. It is calculated from the monolayer capacity, using the BET (Brunauer, Emmett, and Teller) method, despite well-known shortcomings of this method. BET theory is based on simplified model of physisorption on homogenous surfaces. Applicability of this approach is always limited to a part of isotherm, usually below p/p^0 of about 0.30, where monolayer is created and multilayer starts to form. BET area of and adsorbent can be regarded as the area available for the adsorption only for non-porous, macroporous, or mesoporous materials (with type II or a type IV isotherm). For microporous, the process of monolayer-multilayer formation and micropore filling cannot be

distinguished, and the range of relative pressures where BET method should be applied is very low, and hard to localize. Thus, the BET area derived for microporous adsorbents should be regarded as apparent surface area, rather than probe accessible. Nevertheless, BET-area is a valuable tool for characterization of materials, and can be regarded as "fingerprint" of the adsorbent. Critical evaluation of the BET method can be found in [41,232]

Determination of pore volume and pore size is much more straightforward, regardless of the pore size of adsorbent. The pore volume is derived from the amount of adsorptive adsorbed at relative pressure close to unity - assuming that adsorbate in the pores is in liquid state. The pore size distribution, and pore volume in relation to pore size can be determined by different methods *e.g.* Kelvin equation based approaches, Dubinin-Radushkevitch method, standard and comparison isotherm concepts, or density functional theory (DFT). DFT is currently considered superior to other methods, providing more reliable results of pore size analysis [41,42,233].

1.4.2. Ultimate analysis

Textural properties of an adsorbent are deemed as dominant for adsorption performance, especially in gas-solid systems. However the role of chemical structure is undeniable, although somewhat covert due to complex interaction mechanism between adsorbate and surface atoms.

Chemical composition of an adsorbent is determined by elemental analysis. It is useful for detecting changes in the composition of adsorbent samples, in regard to synthesis and modification stages. For example, for optimization of synthesis procedure [236], or to determine optimum loading of a dopant [237]. Unfortunately, there is no one-in-all tool that allow to study full range of elements within sample.

For carbonaceous adsorbents it is typical to quantify carbon, hydrogen, nitrogen and sulphur (determined from the gaseous products of its complete combustion) – oxygen content is calculated by difference. It is so-called ultimate analysis [236,238,239]. If other atoms (*e.g.* metals) are of concern, different techniques have to be used, *e.g.* emission spectroscopy combined with inductively coupled plasma [240–242].

Atoms constituting adsorbent decides about: physicochemical properties [243], selectivity [188,238,244], thermal stability [245,246], adsorption capacity [240,241], or hydrophobicity [236,239]. For example it is a common practice to increase affinity toward CO_2 by doping with nitrogen [237,247–249], or to manipulate hydrophobicity of the surface by introduction or removal of oxygen atoms. Ratio of the O/C atoms provides information about polarity of an adsorbent [239], and can be useful for predicting selectivity. It was observed that O-containing moieties favours adsorption of polar VOCs, over hydrophobic ones [236]. Kim and co-workers have used the elemental

analysis to calculate sulphur accumulation on the surface of an adsorbent, and determine its resistance to SO_2 present in gas streams [188].

The disadvantage of elemental (ultimate) analysis by combustion, is that it analyses bulk of the samples. For some samples, especially chemically modified, the dopant loading may be non-homogenous, with a higher degree of doping on the surface, as compared to inner pores [241,250].

Ultimate analysis is very frequently followed by other structural analysis techniques to determine the arrangement of atoms on the surface, *i.e.* to detect specific functional groups that are responsible for specific properties of adsorbent and interactions with molecules in gas phase.

1.4.3. Fourier transform infrared spectroscopy

Fourier transform infrared spectroscopy (FTIR) is an analytical technique used to study structural properties of materials. Absorption of a given wavelength of the infrared radiation by a sample is closely related to the type of chemical bond, and can be assigned to specific functional groups. Hence, the position of absorption bands in spectrum can reveal the chemical structure of the adsorbent surface [251]. This information can be further used to explain adsorbents performance, if the adsorption process is controlled by specific interactions with surface functional groups [209,229]

Adsorbents are usually sampled as pellets prepared by mixing with IR non-absorbing salt e.g. KBr [252]. Alternative sampling method, getting more attention recently, is ATR (attenuated total reflectance) [228,253]. It allows for quick analysis without special sample preparation. The sample is placed on a crystal of the ATR, and the only requirement is a firm contact between the sample and the crystal. Solid adsorbents can be analysed as a powders or thin films. If adsorbent is soluble in a volatile solvent, it can be dissolved, deposited in the surface of the crystal, and evaporated, leaving an uniform film of the adsorbent [254,255].

The absorption bands position, and intensity are main diagnostic tools. Functional groups and chemical bonds are identified based on experience, and previously published data for similar materials [209,215,252]. If a material has a well-defined structure like *e.g.* MOFs, the spectrum can be used to confirm the identity by comparing it to literature data [253], or even to propose the structure of MOF-forming unit [256]. For composites it is possible to identify individual components based on the characteristic vibration bands [257].

The shifts, appearance/disappearance of adsorption bands, and changes in their intensities are useful in assessing effect of synthesis or modification procedure on the surface structure – the evolution of surface functionalities can be followed [258,259]. Appearance of new absorption bands can be considered as a proof of a successful modification by e.g. grafting [187], cross-linking [260],

impregnation [215], or covalent anchoring [248]. On the other hand, lack of changes in the spectrum can be also a useful information about adsorbent's framework stability after incorporation of e.g. metals [261].

While qualitative interpretation of spectra is quite straightforward, the quantitative analysis is very difficult. Samples can be compared semi-quantitatively with specific indices - a ratio between a peak area (or band intensity) of a given surface species and a peak of invariant peak, *i.e.* peak for a structural feature that is not affected during modification or synthesis. For example, nitrile and C-O indices were used to study functionalization of polyacrylonitrile nanofibers with β-cyclodextrin for adsorption of formaldehyde [260]. Similar approach was applied to characterization of asphaltenes, and gave information about carbonyl abundance index, aromaticity, average number of carbons per alkyl side chain, alkyl side chain length, or degree of substitution on the peripheral carbon of aromatic ring [262].

Beside structural characterization, FTIR technique can be used to investigate the adsorption process itself. The involvement of a specific functional group in the adsorption process can be assessed by shifts in wavenumber values and peaks intensity changes after adsorption [263,264]. Use of a specific probe molecule can help in identification of acidic and basic adsorption centres [265,266]. For example, pyridine is used to provide information about Lewis and Brøensted acid sites, and information about strength of acid sites can be obtained by stepwise desorption at different temperatures [267].

FTIR is an adequate technique to observe formation of hydrogen bonds between adsorbate and adsorbent, because OH or NH_2 groups are clearly visible on the spectrum above 3000 cm^{-1} wavenumber [228,268] – however it may be difficult to distinguish them if both groups are present [228]. Shift of their position after adsorption may indicate hydrogen bond formation [269,270]. Additionally, from absorption bands of OH or NH_2 group, the hydrophobicity of adsorbents can compared, as their hydrophilic character is responsible for high water affinity (hydrophobicity can be also evaluated based on signal from CH_2 and CH_3 groups) [271,272].

The issue, with analysis in this part of spectrum, is related to the adsorbents tendency to bound water molecules from gas phase (especially hydrophilic ones). The broad bands above 3000 cm^{-1} which are usually ascribed to OH group vibrations can in fact be a signal from weakly bonded water on the surface or within the pores of [230,261,273].

1.4.4. Inverse gas chromatography

Adsorbent design requires a deep understanding of surface phenomena. Detailed picture about solid surface properties can be obtained by "observation" of its interactions with gas molecules. An inverse gas chromatography (IGC) technique turns out to be useful tool for this purpose.

Compared to analytical gas chromatography (GC), the role of the phases in the IGC is inverted. The stationary phase is under investigation, while compounds in the mobile phase probes the surface of the adsorbent. A great advantage of IGC is that experimental setup is similar to standard gas chromatograph, and no special sample preparation is required. It allows to conduct fast and accurate measurements over a wide range of temperatures, both at low and high pressures of test probes vapours [274,275]. Moreover, solid adsorbent may be fibrous, crystalline or amorphous powders, or even semi-solid [276].

Adsorbent is analysed by injection of a pure test probe, with well-known physicochemical properties. Probes with different polarities, acidities, molecular areas, and electron donor/acceptor properties are used to determine the respective properties of the adsorbent surface, based on the analysis of the retention time, and peak elution profiles. Important properties of adsorbents such as thermodynamic interaction parameters [275], specific surface area [277], surface energy heterogeneity [278], acid-base properties [279], adsorption isotherms [280], surface free energy [281] or polar functionalities [282] on the surface can be determined.

IGC experiments can be conducted in two different modes *i.e.* at infinite dilution (ID) or at finite concentration (FC) [274]. In IGC-ID a very small quantity of test probe is introduced into the system. Under such conditions the surface coverage is close to zero, the Henry's law is obeyed and only adsorbate-adsorbent interactions are observed. Because, the amount of probe is limited, it is assumed that probe molecules interact mainly with high-energy adsorption sites on the surface [283]. In some cases it may be a disadvantage, because the distribution of the active sites may be more relevant than the nature of the high-energy ones. IGC-ID mode is typically used for determination of thermodynamic parameters,, Henry's constants, dispersive components of the surface free energy, or acid-base properties of surface [276,284].

IGC-FC is a useful mode for measuring adsorption isotherms, surface energy heterogeneity, surface area, porosity. The amount of injected probe is increased, so the less active adsorption sites are involved in interactions with probe molecules [275,285]. A good overview of IGC approaches to determination of surface heterogeneity can be found in [278]. In combination with thermal desorption, IGC-FC can discriminate the contribution of micro and mesopores to the adsorption [286].

During the years, IGC has become an accurate, reliable and fast method for physicochemical characterization of solid. It is extensively applied for characterization of various solid materials: zeolites [277], silica [287], composite materials, polymers [288], cellulose [289], pharmaceutical solids [290], alumina [286], clays [291], carbonaceous materials (coal, activated carbon, carbon nanotubes, graphene, carbon black, graphite etc.) [284,292]. A search made on the Web of Science in 2022 provided over 2000 articles where IGC was applied for characterization of materials properties.

Physicochemical characterization of solid materials by IGC has been a subject of long-standing scientific interest, and many reviews [275,276,278,283,284,293] and books [274] of the subject are available where the theoretical, methodological and practical issues are discussed in details. Below basic concepts of IGC are described briefly.

Rohrschneider-McReynolds constants

Rohrschneider-McReynolds constants are a systematic approach used in gas chromatography to compare retention characteristic of stationary phases (sorbents) [294–296]. The retention of a molecule on a given sorbent is a result of various intermolecular interactions, which were divided by Rohrschneider into five types, represented by five test compounds:

$$RI = xX + yY + zZ + uU + sS \quad (1)$$

where RI is the retention index for a given compound. X, Y, Z, U, S, are the Rohrschneider-McReynolds constants for a stationary phase, and x, y, z, u, s are test probe's empirical coefficients. For test compounds selected by Rohrschneider and McReynolds, probe's empirical coefficients are equal to 1. Meaning of the Rohrschneider-McReynolds constants is presented in the Table 2.

Table 2. Meaning of the Rohrschneider-McReynolds constants.

Constant	**Test probe**	**Molecular interactions**
X	benzene	weak dispersion forces, polarizability of the adsorbent
Y	1-butanol	hydrogen bonding ability of the adsorbent
Z	2-pentanone	polarizability, part of the dipolar character of the adsorbent
U	1-nitropropane	electron donor, electron acceptor, and dipolar character of the adsorbent
S	pyridine	acidic (electron acceptor) character of the adsorbent

Constants represent contribution from various types of molecular interactions to the adsorption, and are calculated as a difference in retention indices, of test compounds, for adsorbent of interest and nonpolar reference adsorbent. For nonpolar adsorbent, by definition, the constants are equal to 0. As a standard nonpolar stationary phase squalane is typically used, however other nonpolar adsorbents can be also used e.g. Carbopack B [297], DB1 (100% polydimethylsiloxane) [298], or graphitized thermally carbon black [243,299]. The choice of reference column can lead to a negative values of constant [298,300,301], which points to a lower activity of the adsorbent, with regard to a given type of interaction.

Retention indices can be calculated by measuring retention time of a test probe in isothermal conditions (Kovats retention index) or in programmed temperature (Linear Retention Index, LRI), in reference to n-alkanes retention. Both n-alkanes, and test probes have to be analysed in the same conditions. The method of calculation is graphically presented in the Figure 7. Although it is possible to calculate them from linear regression equation, it is more accurate to calculate the retention index with the following equation:

$$RI = 100\left(\frac{t'_{r,x} - t'_{r,n}}{t'_{r,n+1} - t'_{r,n}}\right) + 100n \qquad (2)$$

where $t'_{r,x}$ is the retention time of a compound of interest, $t'_{r,n}$ and $t'_{r,n+1}$ are the retention time of n-alkanes eluting before and after the compound of interest, respectively, and z is the carbon atom number in the n-alkane molecule eluting before compound of interest.

Constants measure the extent of polar attractive interactions of a given type between adsorbate and adsorbent, and are used to estimate selectivity of an adsorbent. Although the whole sets of constants should be considered to get a complete idea about adsorption characteristic, usually it is represented by a single parameter called polarity - a sum or average value of 5 constants. Polarity is a measure of the strength of interactions between test probe and stationary phase (sorbent) [298,301–303]. The more polar is the adsorbent, the greater is the test probe retention.

The Rohrschneider-McReynolds constant are common in gas chromatography, where they became a standard method used to describe selectivity of stationary phases [298,300,302]. Nevertheless, the can be easily applied to analysis of adsorbents' adsorption performance toward VOCs, using packed columns [297,301,304,305]. The Rohrschneider-McReynolds concept led to development of Abraham's model [306,307].

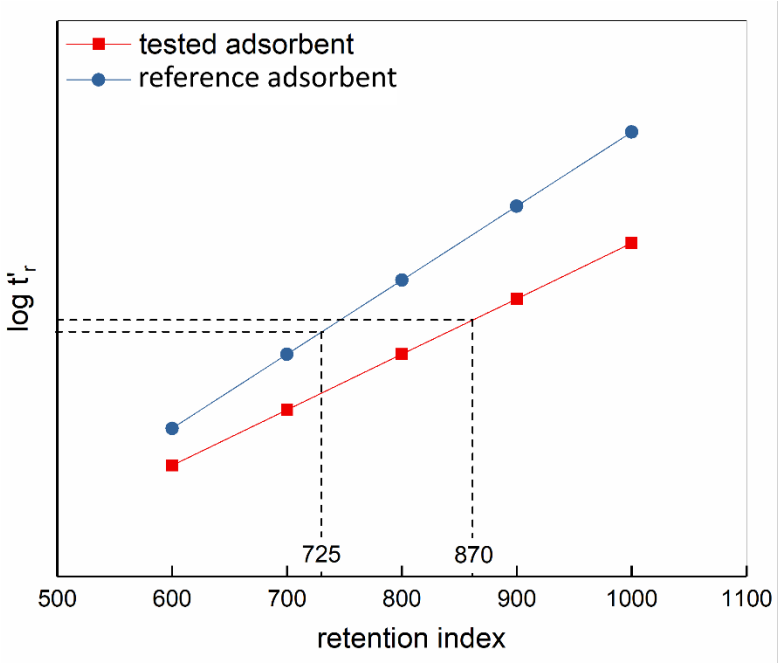

Figure 7. Graphical representation of retention indices determination. Lines represents n-alkane reference line for adsorbents.

Free surface energy

Surface activity is an important feature of the adsorbent surface. It can be described in terms of surface energy, which is directly correlated with intermolecular interactions. Surface free energy (γ_S) is a combination of dispersive and specific (or polar) interactions [281]:

$$\gamma_S = \gamma_S^D + \gamma_S^{SP} \tag{3}$$

where γ_S^D and γ_S^{SP} are dispersive and specific components of the surface free energy. The value of the dispersive component is frequently used to compare different adsorbents activity, and to evaluate effects of modifications [284].

Calculations of the γ_S^D are based on the retention of n-alkanes probe at ID conditions, because they are capable to interact only *via* dispersive interactions. The net retention volume (V_N) of the probe is calculated by following equation:

$$V_N = j \cdot F \cdot (t_R - t_0) \tag{4}$$

where j is the James-Martin mobile phase compressibility correction factor, F is the flow rate of carrier gas, t_R is the retention time of a probe compounds, and t_0 is the retention time of

noninteracting probe (dead-time). To eliminate effects of temperature and solid, specific retention volume (V_g) can be calculated:

$$V_g = \frac{V_N}{m} \cdot \frac{273.15}{T} \tag{5}$$

where T is the measurement absolute temperature, and m is the mass of the solid in the column.

Surface free energy components are calculated with thermodynamic equations, *i.e.* with the standard Gibbs free energy change of adsorption (ΔG_{ad}):

$$\Delta G_{ad} = R \cdot T \cdot \ln V_N + C \tag{6}$$

where R is the gas constant and C is related to the reference state. Similarly to γ_S, ΔG_{ad} is the sum of the dispersive (ΔG_{ad}^D) and specific components (ΔG_{ad}^{SP}):

$$\Delta G_{ad} = \Delta G_{ad}^D + \Delta G_{ad}^{SP} \tag{7}$$

If n-alkanes are used, no specific interactions are observed and $\Delta G_{ad} = \Delta G_{ad}^D$. Generally, two methods are used to calculate γ_S^D, *i.e.* Schultz method and Dorris-Gray method. According to Schultz method, it can be derived from the following relationship [308]:

$$\Delta G_{ad} = 2 \cdot N_A \cdot a \cdot \sqrt{\gamma_S^D \cdot \gamma_L^D} + C \tag{8}$$

where N_A is the Avogadro's number, a is the cross-sectional area of the probe molecule, and γ_L^D is the dispersive component of the surface free energy of the liquid probe molecule. Plotting the ΔG_{ad} as a function of $a\sqrt{\gamma_L^D}$ produces a straight line, called the "alkane line", with the slope being equal to γ_S^D of the solid under investigation.

In Dorris-Gray method, γ_S^D is related to the number of methylene groups in n-alkane molecule, and can be calculated by the following equation [309]:

$$\gamma_S^D = \frac{(-\Delta G_{CH2})^2}{4 \cdot N^2 \cdot (a_{CH2})^2 \cdot \gamma_{CH2}} \tag{9}$$

where a_{CH2} is the methylene group surface area and ΔG_{CH2} is the free energy of adsorption per methylene group. Value of the ΔG_{CH2} is derived from the slope of the ΔG_{ad} versus the number of carbon atoms in the n-alkane molecule. γ_{CH2} is the surface energy of the polyethylene-type polymer with finite molecular weight, which is approximately 35.6 mJ m^{-2}. More accurately it can be calculated by following relationship [275]:

$$\gamma_{CH2} = 35.6 + 0.058 \cdot (293 - T) \quad (10)$$

The graphical illustration of the Schultz and Dorris-Gray method is depicted in the Figure 8. Comparison of both methods revealed that Dorris-Gray method produces greater values of γ_S^D, and is more accurate, compared to values obtained through Schultz method. More in depth comparison of both methods can be found in [308].

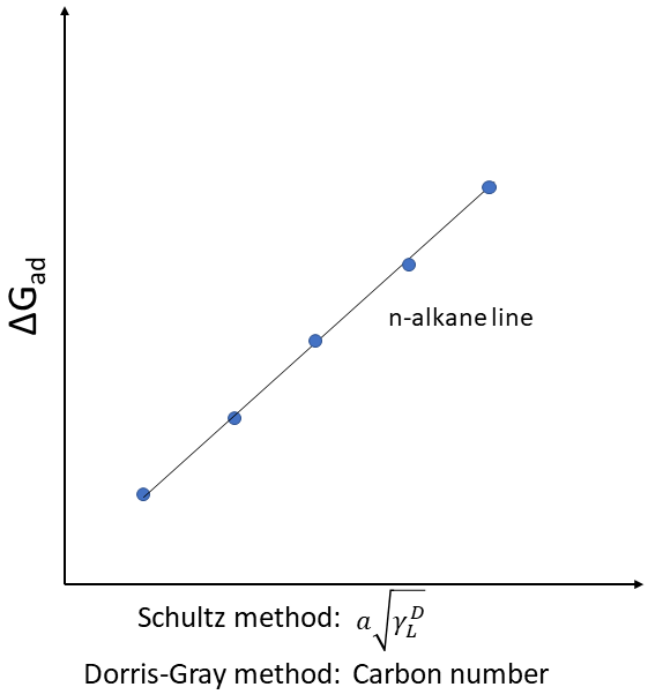

Figure 8. The typical diagram for determining dispersive components of the surface free energy by Schultz and Dorris-Gray methods.

A comprehensive insight in to specific surface interactions can provide better understanding of adsorbents adsorption properties, and their ability to change after chemical modification. Specific interactions of solid are probed with polar probes, with precisely known characteristic. Polar probe

interactions with solid surfaces originate from both dispersive and specific interactions. To separate and evaluate ΔG_{ad}^{SP}, ΔG_{ad} of a polar compounds is subtracted from ΔG_{ad} of hypothetical n-alkane having the same reference property, *e.g.* saturated vapour pressure, $a\sqrt{\gamma_L^D}$, or topological index [280–282,284,310].

Specific interactions encompass different categories of interactions, but special attention was devoted to acid-base properties *i.e.* electron donor/acceptor properties. Based on the Good-Van Oss theory, γ_S^{SP} can be divided into electron acceptor γ_S^+ and electron donor γ_S^- components, that can be calculated according to the following equation [311]:

$$\Delta G_A^{SP} = 2 \cdot N \cdot a \cdot \left((\gamma_L^+ \cdot \gamma_S^-)^{1/2} + (\gamma_L^- \cdot \gamma_S^+)^{1/2} \right) \quad (11)$$

where γ_L^+ and γ_L^- are the electron donor and acceptor parameters of the probe molecules. If monopolar acid (*e.g.* methylene chloride) and monopolar base (*e.g.* ethyl acetate) are used, the Equation 1 reduces to the following two equations [312]:

$$\gamma_S^- = \frac{\left(\Delta G_A^{SP}\right)^2}{4 \cdot N^2 \cdot a^2 \cdot \gamma_l^+} \quad (12)$$

$$\gamma_S^+ = \frac{\left(\Delta G_A^{SP}\right)^2}{4 \cdot N^2 \cdot a^2 \cdot \gamma_l^-} \quad (13)$$

knowing this, the γ_S^{SP} is calculated as:

$$\gamma_S^{SP} = 2\sqrt{\gamma_S^+ \gamma_S^-} \quad (14)$$

As it was mentioned before, IGC-ID probes only adsorption sites with the highest energy. To overcome this problem, surface energy and its components can be calculated as a function of surface coverage, if larger amount of probes are injected [279,292,313–316].

Adsorption isotherms

The method of IGC-FC was developed to readily obtain adsorption isotherms, in the range that can be hard to analyse by classical volumetric or gravimetric methods. The general approach to evaluate adsorbents performance, is to compare their maximum possible adsorption capacity. For

this a high adsorbate pressures (> 1000 Pa) are required, but it may be misleading for a prediction of performance in practical applications. In real-world scenarios, the pollutants levels can be well below 1 Pa [317]. IGC is well suited for measuring adsorption isotherms at low partial pressures of adsorbates. For calculations two methods can be used, *i.e.* peak maximum (PM) and elution characteristic point (ECP) [274].

In the PM method, the retention volumes and partial pressures are obtained from the maxima of chromatographic peaks recorder for different amounts of injected probes, whereas in ECP method they are derived from the tailing of peak for high concentration of probe compound. The advantage of the ECP method is that full isotherm can be determined from one peak. However, the linearity of the detector must be established. It is ensured when tails of peaks from several injections, of different concentrations, superimpose. Detailed descriptions of both measurement procedures are given in [274].

IGC-FC was demonstrated to be a fast and accurate technique for determination of isotherms, adsorption capacity or BET surface areas [276,280,318]. Thus, IGC can be used as an extremely fast tool for BET surface measurements, especially in screening studies at the early stage of adsorbent development.

Adsorption potential distribution

Adsorbents are porous materials with chemically and structurally heterogenous surfaces. Chemical heterogeneity is generated by functional groups or impurities present on the surface. Various functional groups, and their arrangement results in energetic heterogeneity of adsorption centres. For practical reasons, adsorption energy distribution may be more important than the existence, and type of high energy sites – as measured by IGC-FC [235,278,284].

The information about surface heterogeneity can be presented as adsorption energy distribution or adsorption potential distribution, and is encoded in the pressure dependence of adsorption Hence, it can be extracted from the adsorption isotherm. Both approaches assumes that adsorption energy is continuously distributed, the surface is a collection of homogenous patches (isoenergetic domains), and that the measured sorption isotherm is a sum of local sorption isotherms [283,319].

Determination of adsorption energy distribution is not a trivial task and requires quite complicated mathematical calculations, as well as assumptions about local isotherm model [319,320]. Detailed description of the method of adsorption energy distribution calculation from the chromatographic signal can be found in [321].

Adsorption potential distribution is a less complicated method for surface heterogeneity determination, and it generally gives the same information as the adsorption energy distribution

[283,322]. Adsorption potential (A) is defined as the change in the Gibbs free energy, and is related to the equilibrium pressure [322]:

$$A = RT \ln\left(\frac{P_0}{P}\right) \tag{15}$$

The distribution of adsorption potential (Φ) is calculated from the following equation:

$$\Phi = -\frac{dn}{dA} \tag{16}$$

where n is the adsorbed amount of the probe.

Both adsorption potential and adsorption energy distribution depend on test probe used in experiment. Thus, using different probes can reveal different interactions and evolution of surface chemical and/or physical structure [323]. Surface energy site maps have reported for different materials: carbon blacks [323], silicas [319], graphite [292], porous glass, alumina, activated carbons [279], silica gels [313], natural fibres [314],

1.5. Modelling of adsorption

The best adsorbent for a given process is selected based on results of several experiments. Adsorption isotherms and breakthrough curves are typically used to design adsorption process. Experimental data is modelled with theoretical, semi-empirical or empirical models in order to predict adsorption parameters and scale-up the adsorption system [324,325].

1.5.1. Isotherms

A fundamental tool for adsorbent selection is the equilibrium adsorption isotherm, measured for constituents of the gas mixture, under conditions similar to operational. Analysis of adsorption equilibrium involves experimental measurement and data representation by isotherm models (equations), which are used to correlate adsorption data for adsorbent characterization, and to design industrial gas adsorption process. By considering the equilibrium data, and both adsorbent and adsorbate properties, the isotherm model can help to explain the adsorption mechanism [34,40]. Additionally, the adsorption isotherm can be useful in determination of the adsorbent regeneration method [326].

Generally, single component adsorption isotherms are used as first approximation. Mixed gas adsorption models are used when more accurate estimates for equilibrium adsorption are required [327]. Numerous theoretical and semi-empirical models have been proposed to described sorption equilibrium. Their extensive descriptions can be found in books and review papers [33,34,40,328,329]. Here, two most common (and the most frequently used) models are briefly presented *i.e.* Langmuir and Freundlich.

As to the methodology of gas adsorption measurement, various methods are available: volumetric/manometric, gravimetric, their combinations, as well as gas flow methods. Their detailed presentation is beyond the scope of the present dissertation, but comprehensive review of available methodologies can be found in [47,329], and citations therein.

Langmuir model is based on assumptions that the surface of an adsorbent is energetically homogenous, *i.e.* all adsorption centres have the same adsorption potential and can accommodate exactly one adsorbate molecule per each. Thus, adsorption is restricted to monolayer formation. Additionally, lateral interactions between adsorbed molecules are neglected [330]. The nonlinear mathematical form of this model is as follows:

$$q = \frac{q_0 K_L \frac{P}{P_0}}{1 + K_L \frac{P}{P_0}} \tag{17}$$

where q is the equilibrium adsorption capacity, P is the vapour pressure of adsorptive at equilibrium, P_0 is the saturated vapour pressure adsorptive, q_0 is the maximum (monolayer) adsorption capacity, and K_L is the Langmuir constant.

To evaluate the favourability of adsorption process, separation factor R_L can be calculated using Langmuir constant K_L:

$$R_L = \frac{1}{1 + K_L \frac{P}{P_0}} \tag{18}$$

Adsorption is unfavourable when $R_L > 1$, linear if $R_L = 1$, favourable when $0 < R_L < 1$, and irreversible at $R_L = 0$ [331]. Langmuir isotherm model is typically used for quantifying and comparing adsorption capacity of different adsorbents [332].

At low pressures Langmuir isotherm obeys the Henry's law, and reduces to Henry's isotherm:

$$q = K_H P \tag{19}$$

Value of the Henry's constant K_H is important for selectivity of separation, because it is exponentially proportional to the heat of adsorption Q, which in turn is equal to the bond energy between the adsorbate and adsorbent. Adsorption equilibrium selectivity α_{12} of compound 1 and 2 can be calculated as a ratio of Henry's constants [333]:

$$\alpha_{12} = \frac{K_{H,1}}{K_{H,2}} \tag{20}$$

It should be noted however, that its predictive value is valid only at low gas pressure, and low adsorption loading [334].

Freundlich isotherm is an empirical model describing adsorption on solids with heterogenous surfaces (*e.g.* activated carbons [335]). However it can be theoretically derived. Freundlich model assumes that the adsorption centres are patchwise distributed, *i.e.* adsorption centres with the same adsorption energy are grouped together, and there is no interactions between these groups. Similarly to Langmuir model, each adsorption centre can accommodate only one molecule [40]. The equation takes the following form:

$$q = K_F \left(\frac{P}{P_0}\right)^{\frac{1}{n}} \tag{21}$$

where K_F and n are temperature dependent Freundlich constants. K_F is correlated with adsorption capacity, while n with intensity of adsorption. The Freundlich isotherm applicability is limited at low and high pressures. At low, it does not have a proper Henry law behaviour, and at high it does not have a finite limit of adsorption capacity [336].

1.5.2. Breakthrough curves

Most of the industrial and environmental adsorption processes are operated under dynamic conditions – with constant flow of feed gas through a column with a fixed bed of an adsorbent. Thus dynamic sorption analysis is fundamental from practical point of view. It allows to investigate sorption kinetic and equilibria, co-adsorption, selectivity, and transfer of lab-scale process to industrial scale. Moreover, dynamic sorption analysis is required because in technical flow process,

for a certain type of purification or separation, adsorption capacity derived from adsorption isotherm is not completely accessible [337,338].

Breakthrough curves are a record of an adsorptive concentration in the gas phase at the outlet of an adsorption column as a function of time. They are used as a predictive simulation of industrial scale gas adsorption and can be viewed as the final characterization of an adsorbent [339]. Figure 9 presents a typical shape of the breakthrough curve for a single adsorptive in the feed.

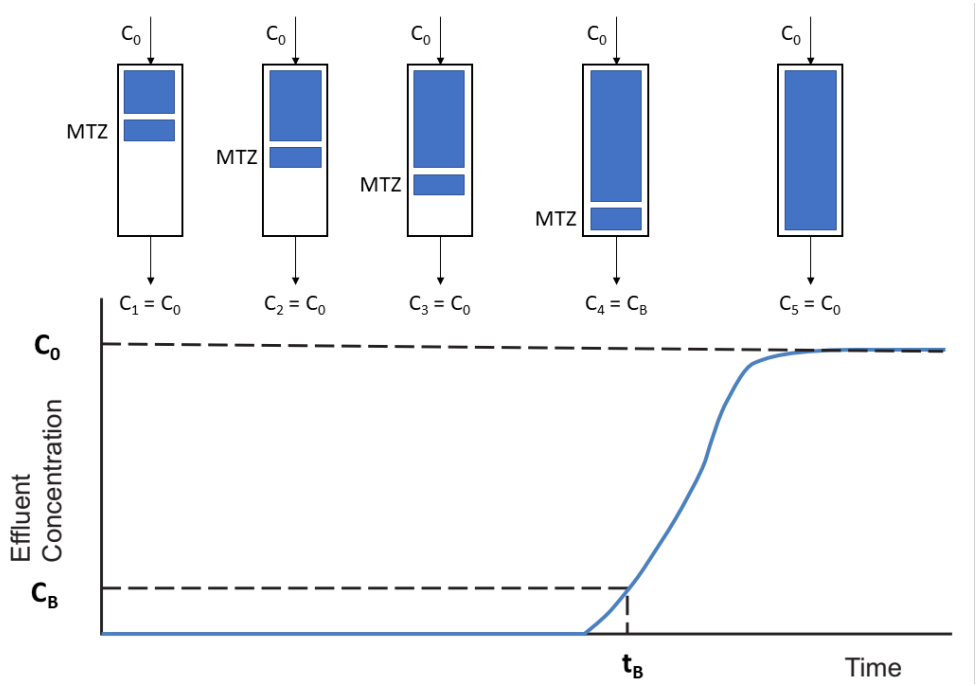

Figure 9. Breaktrough curve for a single adsorptive in gas feed. C_0 – inlet adsorptive concentration, C_B – outlet adsorptive concentration at breaktrough time (t_B). MTZ – mass transfer zone.

At the beginning the gas with well-defined concentration of adsorptive is fed to a column with fresh bed of the adsorbent and is completely withheld by adsorption on its surface. As the measurement proceed, and the volume of treated gas increase, the part of the bed is eventually in equilibrium and no more molecules can be adsorbed. The length of the adsorbent bed over which the adsorbate concentration changes is called mass transfer zone. It progress along the column, exhausting the adsorbent bed. Eventually, a traces of adsorptive are detected at the column outlet followed by steep increase of the adsorptive concentration in the gas stream. Finally, the adsorbent is exhausted and adsorptive molecules are simply passing through the column, without being adsorbed (“*gas breaks through*”). In practice, the adsorption process is conducted until the adsorptive concentration in outlet gas reaches specified, breakthrough concentration (C_B). After this time (breakthrough time, t_B) the adsorbent bed have to be regenerated [340,341].

The shape of the breakthrough curves determines the extent to which the adsorption capacity can be utilized. The more steep the curve, the smaller is the mass transfer zone, and consequently the bigger part of the adsorbent bed is exhausted at the breakthrough time [258,272] – it is crucial for determining the length of adsorption column required in final applications, and total costs of adsorption unit.

Maximum adsorption capacity q_{max} of the adsorbent, under dynamic conditions, can be obtained from the following equation:

$$q_{max} = F \int_{t=0}^{t_e} (C_0 - C_t) dt \tag{22}$$

where F is the gas flowrate, C_0 is the adsorptive concentration in the feed, C_t is the adsorptive concentration, at the outlet of the column, at given time, and t_e is the adsorbent bed exhaustion time. The adsorption capacity until the breakthrough can be obtained by changing the integral bound t_e to t_B – it gives technically usable sorption capacity.

The length of the mass transfer zone can be evaluated according to the following equation:

$$MTZ = L\left(\frac{t_e - t_B}{t_e}\right) \tag{23}$$

where L is the length of the adsorbent bed. The value of MTZ will determine the performance of the column and the length of unused bed (at breakthrough time).

The design of adsorption process requires establishment of mathematical model that adequately describes adsorption in the fixed bed column and allow to predict the breakthrough [342]. Frequently used models are: Bohart-Adams, Thomas, Yoon-Nelson, Clark, and Dose-response models [343,344].

2. Asphaltenes

Crude oil is constituted by countless types of hydrocarbon molecules - a single heavy-oil sample can contain more than 20 000 different chemical compounds [345]. Due to is complexity determination of its composition on a molecular level is doomed to failure (at least for now). For practical reasons a group type composition is determined. The most typical is so-called SARA analysis, based on solubility of molecules in organic solvents, which separates crude oil into four fractions of

increasing polarity, namely: saturates, aromatics, resins, and asphaltenes [346–348]. Figure 10 presents the general scheme of the SARA group type composition analysis of petroleum products.

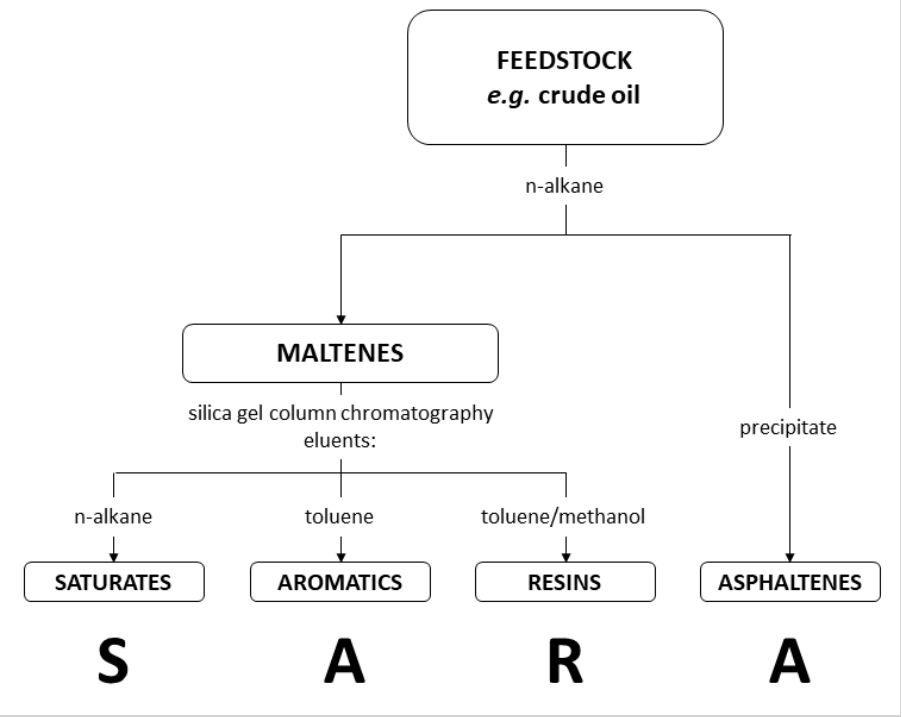

Figure 10. General scheme of the SARA group type composition of petroleum products.

Precipitated asphaltenes are a dark brown amorphous solid [349], without definite melting point - they degrade at temperatures above 350 °C [350,351]. Similarly to its original source, it is a heterogenous fraction of polyfunctional compounds, polydisperse in molecular weight, structure and functionalities [46,352–354]. According to the division presented in the Figure 10, asphaltenes are defined as fraction of crude oil insoluble in light n-alkanes (*e.g.* n-heptane), and soluble in light aromatic hydrocarbons (*e.g.* benzene or toluene). In crude oil and products of it processing they are present in concentration up to tens of percents. As the most aromatic, polar, and heaviest fraction, asphaltenes quantitatively remain in a residue from vacuum distillation [355–357]. Their content can be increased by oxidation – air blowing process used for upgrading properties of vacuum residue in bitumen production process [358].

Although asphaltenes are a class of compounds with complex structure, they are certain common points in their structure. Asphaltenes are hosts for majority of heteroatoms present in crude oil. Apart from C and H, their molecular structure contains N, O, S, and metals (mainy V, Fe, and Ni). The H:C ratio is stable and close to 1 - nearly 90 % of hydrogen atoms are bonded to sp^3 carbon. Higher variability is observed for N, O, S, and depends on the source of asphaltenes. Sulphur atoms exist mainly as thiophene and sulphide, oxygen as carboxyl and hydroxyl groups, and most of

the nitrogen is bonded in aromatic structures (pyrrolic and pyridinic). Metals are present at mg/g level as metalloporphyrins [12,13,16–18].

Structurally, asphaltenes are polycyclic aromatic hydrocarbons (PAHs) with a single core assembled from 4-10 aromatic rings [46,359], with peripheral aliphatic or naphthenic substituents – so-called island or continental structure [362]. Aliphatic chains are formed mostly by short alkyl groups (length of 1-4 carbons) [46]. Direct molecular imaging and analysis of UV-Vis spectra of asphaltenes suggest that the diameter of average molecule is in the range of 10 – 30 Å [359,363]. Molecular mass of compounds within this fraction varies between approx. 500 and 1000 g mol^{-1}, with mean value at 750 g mol^{-1} [353,359]. Figure 11 presents chemical structures of asphaltenes. They were proposed based on atomic force microscopy (AFM) measurements and scanning tunnelling microscopy (STM) orbital images [364]. More detailed information regarding asphaltenes separations methods and structure can be found in review papers [348,365] and books [346,347].

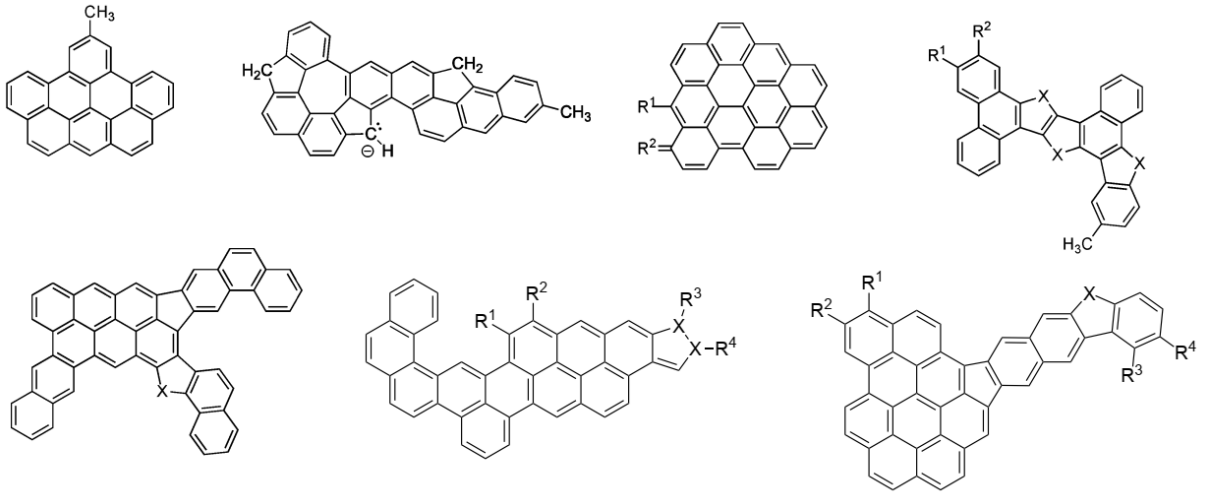

Figure 11. Chemical structures of asphaltenes proposed based on AFM and STM measurements. X represents unknown part within carbon framework (*e.g.* CH, CH_2, N, NH, O, or S). R indicates unknown side group [364].

Complex structure and numerous functionalities within asphaltenes structure are a source of numerous interactions *e.g.* vand der Waals, Coulombic, hydrogen bonding or π-π stacking [366]. Acid-base surface characteristic is related to presence of heteroatoms. Acidic centres contains oxygen and sulphur. Basic sites are due to N, O, or S in aromatic ring or on alkyl chain [360,367]. Asphaltenes are considered surface active molecules, as they tend to adsorb on both liquid/liquid and liquid/solid interfaces. Analysis of adsorption on solid surfaces, revealed a physisorption mechanism and multilayer formation [352].

Asphaltenes, mostly considered as problematic, are named “the cholesterol of petroleum” [368]. This fraction is responsible for serious problems, both in downstream and upstream processes, that can derail exploration and production. The precipitation and deposition can occur in the well-tubing, and in the refinery equipment, which must be in consequence taken out of service for their removal [369]. Moreover, asphaltenes can act as oil-water stabilizers, hindering separation of emulsified water and oil. Present in heavy oil and residuum, asphaltenes affect hydroprocessing by acting as coke precursor, deactivating catalyst, and in consequence limiting efficiency of conversion and refining [369].

So far, asphaltenes are used only in asphalts and insulation as composite materials. The demand for “pure” asphaltenes does not exist. Considering the large oil production worldwide, asphaltenes can be an easily available by-product; currently without any real market value. Hence, there is a potential economic and environmental benefit in finding innovative applications for this “valuable” waste product of petroleum industry. Several new applications are currently under investigation, and were reviewed by Kamkar *et al*. [370] – including the one presented in this dissertation.

IV. Results and discussion

1. Scalable isolation method of high purity asphaltene from bitumen (Paper 1)

Preliminary studies have demonstrated the applicability of asphaltenes in the field of separation processes. Especially in gas-solid adsorption systems, asphaltenes as adsorbents revealed unique selectivity and retention toward VOCs [304].

Development and commercialization of asphaltene-based adsorbents (or other functional materials) requires considerable amounts of this fraction. Unfortunately, standard test methods of asphaltene isolation were designed to work with small samples for technical analysis purposes. While suitable for process control in petrochemical industry or small scale research, they are inadequate for isolation of material to be used in separation processes. Research and development of asphaltene-based adsorbents demand a reliable, reproducible and uncomplicated method of asphaltenes precipitation, with high yield and purity.

Paper 1 presents results of work on improvement of asphaltenes isolation from bitumens. Parameters of the precipitation were selected based on comprehensive review of literature. Proposed procedure incorporates n-heptane as a solvent in 1:40 feedstock to solvent ratio (g mL^{-1}). The mixture is heated for 1 h at boiling point of n-heptane and set aside for 1h before separation of asphaltenes. As a reference procedure, a standard test method ASTM D4124 was used.

The most significant change in comparison to standard method is in separation and purification steps. Precipitated asphaltenes are filtered through cellulosic thimble that is subsequently placed in Soxhlet type extractor, where asphaltenes undergo extensive washing with boiling n-heptane.

Efficiency of separation and purity of isolated fraction was controlled by thin-layer chromatography with flame ionization detection (TLC-FID) technique. The normal phase separation mechanism was used, resulting in so-called SARA (Saturates, Aromatics, Resins, Asphaltenes) analysis. Results revealed that washing (purification) step is crucial for purity of asphaltenes fraction. A presence of noticeable amounts of resins and aromatic compounds was observed in samples isolated by standard test method. It leads to a false positive error, i.e. higher content of asphaltenes in bitumen samples, and may be relevant for technical analysis or researchers investigating asphaltenes physicochemical properties. In respect to adsorption applications, presence of resins may cause problems with thermal degradation of adsorbent and adsorptive properties reproducibility.

The issue of impurities in asphaltene fraction was corrected by extensive purification in Soxhlet extractor. Results of analysis of the asphaltene fraction content in bitumen and purity are presented in the Table 3. The improved procedure is characterized by increased purity (above 97 %), increased reproducibility and precision, as well as reduced labour and solvent consumption. The simplicity of the proposed procedure enable easier scale-up necessary for obtaining high quantities of pure asphaltenes.

Table 3. Comparison of yield and purity of asphaltene fractions isolated with improved procedure and standard test method.

	ASTM D4124			**Improved procedure**		
	Mean	**STD**	**CV**	**Mean**	**STD**	**CV**
Yield of asphaltenes [wt.%]	10.14	0.46	4.49	8.79	0.35	3.99
Purity [%]	95.80	0.30	0.31	97.39	0.76	0.78

Procedures used in the above-mentioned research, results and their discussion are presented in detail in the paper published in the *Journal of Petroleum Science and Engineering* "An Improved scalable method of isolating asphaltenes" **(Paper 1)**. The paper presents also a thorough analysis of scale-up potential of improved isolation method.

2. Chemical modification of asphaltenes, their characteristic and adsorption properties (Papers 2 & 3)

Chemical structure of asphaltenes makes them a suitable platform for incorporation of different chemical groups. Added functionalities, introduced during chemical modification, can create synergy between their properties, and that of pristine asphaltenes, resulting in enhanced adsorptive properties *i.e.* adsorption capacity and selectivity.

In the initial stage of asphaltene-based adsorbent development, a series of chemically modified asphaltene fractions was produced. Successful introduction of new functional groups was proved by FTIR, elemental and IGC analysis. Effects of modifications on asphaltenes adsorption performance was evaluated by Rohrschneider-McReynolds constants. Their values revealed that adsorption characteristic was influenced the most by nitration and cyanation. Thus, this samples were selected for further research. Values of Rohrschneider-McReynolds constants for pristine, nitrated, and cyanated asphaltenes are presented in the Table 4.

For both samples a substantial increase of retention was observed, regardless the nature of test probe. It indicates that chemical modifications enhance a wide range of interactions. Such outcome is desired if the adsorbent is meant to target different types of molecules in waste gas. For nitrated asphaltenes overall strength of interactions is more or less evenly distributed between all measured types, while for cyanated asphaltenes electrondonor properties (S') increased much more, compared to other types of interactions. Cyanated asphaltenes should favourably adsorb basic compounds *e.g.* nitrogen volatile organic compounds (NVOCs). The sum of Rohrschneider-McReynolds constants indicate that both adsorbents fall into category of polar adsorbents. Apart from changing interactions with chemical compounds, presence of functional groups on the surface of modified asphaltenes affects also hydrophobicity. Contrary to pristine, modified asphaltenes are easily wetted with water. It should be not without significance for adsorption of polar VOCs.

Table 4. Rohrschneider-McReynolds constants for asphaltene-based adsorbents.

Asphaltenes type	X'	Y'	Z'	U'	S'	Sum
Asphaltenes	88	97	172	182	171	710
Cyanated asphaltenes	102	293	276	325	785	1781
Nitrated asphaltenes	203	356	404	389	482	1834

X' – benzene / weak dispersion forces and polarizability of adsorbent; Y' – 1-butanol / hydrogen bonding ability of the adsorbent; Z' – 2-pentanone / polarizability, part of the dipolar character of the adsorbent; U' – 1-nitropropane / electrondonor, electronacceptor and dipolar character of the adsorbent; S' – pyridine / acidic (electronacceptor) character of the adsorbent.

To present a more detailed description of asphaltene-based adsorbents surface properties, samples were subjected to analysis with IGC technique. Results revealed that facile chemical modifications significantly enhanced adsorbate-adsorbent interactions. Higher surface activity of chemically modified asphaltenes originates from increased dispersive (γ_S^D) and specific (γ_S^{SP}) components of free surface energy. The most noticeable increase was reported for nitrated asphaltenes *i.e.* 380 mJ m^{-2} at 30 ^{o}C (extrapolated), compared to 118 and 106 mJ m^{-2} for cyanated and pristine asphaltenes, respectively. The value of γ_S^D of nitrated asphaltene is similar to values observed for activated carbons, zeolites or alumina. Retention of polar test compounds demonstrated that modification introduced a substantial amount of acidic and basic adsorption centres on the adsorbents surface.

In case of nitrated asphaltenes, acidic centres originate from presence of oxygen containing functional groups, while basic come from doped nitrogen (-NO_2 groups). Elemental analysis revealed

that nitrogen and oxygen content increased after modification from 1.28 and 1.79 wt% to 6.25 and 18.81 wt%, respectively. It indicates that approx. 3.6 mmol of $-NO_2$ were introduced per gram of nitrated asphaltenes, along with other oxygen-containing groups. It follows from the oxidative properties of nitric acid used for modification.

Measured enthalpies of adsorption revealed that chemical modifications altered the adsorption mechanism. On pristine asphaltenes adsorption is driven predominantly by physisorption, whereas that of modified asphaltenes is driven by both physisorption and chemisorption. Presence of the latter is caused by chemical reaction between surface functional groups and adsorbed gas molecules, and indicates catalytic properties of asphaltenes.

Moreover, conducted analyses demonstrated that asphaltene-based adsorbents can withstand multiple adsorption-desorption cycles without adsorption performance deterioration. Thus, it is possible to use them in continuous processes where adsorbent is regenerated by temperature and/or pressure swinging.

Comprehensive description of experimental procedures and abovementioned findings, about surface and adsorption properties of chemically modified asphaltenes, was presented in **Paper 2** and **Paper 3**, as well as in corresponding Supporting Informations. **Paper 2**, published in the journal *Separation and Purification Technology*, was dedicated to nitrated asphaltenes, whereas research about cyanated asphaltenes was presented on the *46th International Conference of the Slovak Society of Chemical Engineering* and published in the journal *Chemical Papers* (**Paper 2**).

3. Removal of VOCs from gas phase in fixed bed columns with nitrated asphaltenes (Paper 4)

During the process of adsorbent development the natural order of things is to test its applicability under dynamic conditions – in fixed-bed system, as it is preferred technique in industrial applications.

For tests, the adsorbent was prepared by coating a porous support with 10 wt.-% of nitrated asphaltenes. As asphaltenes itself have low surface area, there was a demand to use a proper porous support material. On the other hand, it gives the opportunity to utilize natural or waste materials that are easily available on site, *e.g.* natural clays or diatomaceous earth. This part of the studies revealed that nitrated asphaltenes are solely responsible for interactions with adsorbate, while the support provides only the surface area and porosity required for efficient adsorption. As such, the adsorption capacity will depend to some extent on the type of support used. This approach can be

used for effective removal of hazardous chemical compounds from gas streams, accompanied by waste management and valorisation of low value or waste materials.

As a support, the diatomaceous earth was used, because of its low-cost, abundance, highly developed porosity in the range of macro and mesopores, high mechanical and chemical resistance, and rigid structure. Effective deposition of nitrated asphaltenes was confirmed by FTIR analysis.

Adsorbents performance in fixed-bed system was evaluated by measuring breakthrough curves for pyridine, benzene, and 1-nitropropane. Measurements were done at 30 °C and two relative humidity levels (5 and 80 %). For comparison, adsorption column with uncoated diatomaceous earth was prepared and tested as well.

Results revealed a noticeable increase of maximum adsorption capacity for all test compound, in favour of nitrated asphaltene-based adsorbent. For pyridine, benzene, and 1-nitropropane it changed more than 11, 7, 3 times, respectively. Higher adsorption capacity is advantageous as it increase service life of a column bed, and decrease the required adsorbent mass.

The shape of breakthrough curves indicated that deposition of nitrated asphaltenes improved adsorption efficiency and effective bed usage. The length of mass transfer zone was reduced by more than 1.5, 2, and 3 times for benzene, 1-nitropropane, and pyridine, respectively. The performance gains are highlighted better by the change of the effective adsorption capacity *i.e.* the part of adsorption capacity consumed at the breakthrough. It changed from 33.4 to 84.0 % for 1-nitropropane, from 29.4 to 68.7 % for benzene, and from 58.8 to 92.3 for pyridine.

The breakthrough capacity was compared with values reported in the literature [87] for different adsorbents. Because the adsorbent was designed in a way that nitrated asphaltenes can be used as active component coated on the surface of a porous support, the breakthrough capacity was normalized against the specific surface area of adsorbents – adsorption capacity at breakthrough per square meter of surface. For nitrated asphaltene-based adsorbent this value is much higher than for other adsorbents in the comparison, *e.g.* it is over two times higher than for Carbotrap or Tenax TA.

Breakthrough data were modelled by three models: Bohart-Adams, Thomas, and Yoon-Nelson. It revealed that coating of diatomaceous earth with asphaltenes did not change significantly the kinetics of the adsorption process, except adsorption of benzene. However the drop in the adsorption rate was compensated by increased adsorption capacity.

In real-case scenarios, process streams frequently are humid, and molecules of target gas compete with water molecules to access adsorption centres. As a result, a decrease of adsorption capacity is observed – it is common phenomenon for majority of adsorbents used in practice, also observed in the case of nitrated-asphaltene based adsorbent. During measurements under humid conditions, the adsorbent bed was depleted by benzene and 1-nitropropane about 6, and 2 times

faster, respectively, compared to dry conditions. Nevertheless, it partially retains its favourable adsorption properties. Similar drop of adsorption capacity was observed for activated carbon [371].

Reusability of the adsorbent was evaluated by 10 cycles benzene adsorption-desorption measurements - the desorption was performed by temperature swing up to 250 °C. No significant changes in adsorption capacity were observed for subsequent adsorption cycles, indicating satisfactory reusability. Moreover, it confirms durability of chemical modification with $–NO_2$ groups, and good thermal stability of the adsorbent.

Since the nitrated asphaltene-based adsorbent and uncoated support have similar porosity and surface area, the differences in the adsorption performance, observed during breakthrough experiments, have to be a result of increased strength of adsorbate-adsorbent interactions, originating from the chemical structure of the surface and presence of the specific sorption sites. These properties, underlying the exceptional adsorption characteristic, were revealed by IGC analysis.

High adsorption capacity of nitrated asphaltene-based adsorbent is explained by increased dispersive and specific components of the surface free energy. The role of dispersive forces is highlighted by good correlation of adsorption capacity and polarizability of test probes. In the area of specific interactions, the electrondonor character of the surface was especially noticeable. The strength of interactions with test compounds was comparable to the ones observed for graphene or metal organic frameworks, while leaving behind activated carbons, as demonstrated by enthalpies of adsorption. Their values revealed the contribution of chemisorption to adsorption mechanism, and confirmed the potential catalytic properties of asphaltene reported in the previous work.

The mechanism of adsorbate interactions with adsorbents surface was investigated with FTIR measurements before and after adsorption. In the spectrum, a characteristic shifts of absorption bands were observed, indicating specific interactions between adsorbate molecules and functional groups of the adsorbent.

The research about use of asphaltenes for removal of VOCs in fixed-bed adsorption systems is presented completely in the paper published in the *Chemical Engineering Journal* "Characterization of diatomaceous earth coated with nitrated asphaltenes as superior adsorbent for removal of VOCs from gas phase in fixed bed column" (**Paper 4**).

V. Dissertation summary

The aim of the research, presented in this dissertation, was to evaluate adsorption potential of asphaltenes and develop asphaltene-based adsorbent for gas-solid separations. The steps in the research work included isolation of asphaltene fraction from bitumen, chemical modification of asphaltenes, evaluation of their surface adsorption characteristic, and analysis of asphaltene-based adsorbent potential for VOCs removal from gas phase in fixed bed columns. The main conclusions of this dissertation are as follows:

1) Asphaltenes isolated by standard test methods, used in petroleum industry for technical analysis, contain significant amounts of resins that can deteriorate asphaltene adsorbents quality *e.g.* thermal stability or reproducibility of adsorption characteristic.
2) Purification of precipitated asphaltenes is the indispensable step to obtain high purity asphaltene fraction. Extended washing with boiling n-heptane in Soxhlet type extractor is sufficient to yield fraction with over 97 % content of asphaltenes. Moreover, cellulosic thimble used for Soxhlet extractor is an efficient filtrating material for precipitation step.
3) In the light of the above, an improved procedure of asphaltenes isolation was proposed. It is characterized by increased reproducibility and precision, as well as reduced labour and materials consumption. The simplicity of the proposed procedure enable easier scale-up necessary for obtaining high quantities of pure asphaltenes, necessary for research and development of asphaltene-based adsorbents.
4) As isolated asphaltenes, applied as adsorbent in gas-solid systems, have interesting selectivity and retention toward VOCs. However, their competitiveness and scope of application can be broaden by chemical modifications of the surface. Studies demonstrated that facile chemical modification of asphaltenes surface improve interaction with target gas molecules, resulting in higher adsorption capacity and efficiency. Out of numerous chemical modifications examined, nitrated asphaltenes present the most valuable change of adsorption characteristic.
5) Chemical modifications of asphaltenes alters the adsorption mechanism. Values of enthalpies of adsorption revealed that on pristine asphaltenes adsorption is driven predominantly by physisorption, whereas that of modified asphaltenes is driven by both physisorption and chemisorption. The strength of interactions with VOCs exceeds values reported for standard adsorbents, *e.g.* activated carbons, reported in the literature.
6) Presence of chemisorption indicates potential for catalytic activity of modified asphaltenes and creates new opportunities to apply asphaltenes in heterogenous catalysis.

7) Asphaltenes (nonporous in nature) can be easily coated on a surface of a porous material (support), acting as a adsorption active layer responsible for interactions with target gas molecules, while the support acts as surface are provider. Utilization of asphaltenes (considered a waste material in petroleum industry) and low-cost supports easily available in the target destination (*e.g.* diatomaceous earth or clays) can be an effective procedure for risk mitigation of hazardous VOCs, accompanied by effective waste management and low-value materials valorisation.
8) Facile coating of nitrated asphaltenes can significantly enhance adsorption capacity of a support material, as demonstrated by dynamic, fixed-bed adsorption studies with nitrated-asphaltenes based adsorbent (diatomaceous earth coated with 10 wt.-% of nitrated asphaltenes). The breakthrough capacity for benzene, normalized against the specific surface area of adsorbents (adsorption capacity at breakthrough per meter square of surface), for nitrated asphaltene-based adsorbent was superior compared to values reported for standard adsorbents.
9) Multiple adsorption tests demonstrated durability of chemical modification and thermal resistance of asphaltene-based adsorbent. It can withstand multiple adsorption-desorption cycles without performance deterioration. Hence, it is possible to use it in continuous processes, where adsorbent is regenerated by temperature and/or pressure swinging.

Presented results demonstrate the applicability of asphaltene-based adsorbents in adsorption processes, especially in waste gas purification. Asphaltenes as such present advantageous adsorption properties, but adding new functionalities to their structure *via* facile chemical modifications, give new and unique quality to asphaltene-based adsorbents. When applied as a layer deposited on a surface of a porous support, goals of hazardous VOCs removal from gas streams, and low-value materials valorisation can be achieved at the same time.

VI. References

[1] F.G. Kerry, Industrial Gas Handbook, 1st ed., CRC Press, Boca Raton, 2007.

[2] P. Pullumbi, F. Brandani, S. Brandani, Gas separation by adsorption: technological drivers and opportunities for improvement, Curr. Opin. Chem. Eng. 24 (2019) 131–142. doi.org/10.1016/j.coche.2019.04.008.

[3] Chemicals for a sustainable future. Report of the EEA Scientific Committee Seminar., Copenhagen, 2017.

[4] Z. Wang, G.W. Walker, D.C.G. Muir, K. Nagatani-Yoshida, Toward a Global Understanding of Chemical Pollution: A First Comprehensive Analysis of National and Regional Chemical Inventories, Environ. Sci. Technol. 54 (2020) 2575–2584. doi.org/10.1021/acs.est.9b06379.

[5] L. Shao, Grand Challenges in Emerging Separation Technologies, Front. Environ. Chem. 1 (2020) 1–5. doi.org/10.3389/fenvc.2020.00003.

[6] L. Persson, B.M. Carney Almroth, C.D. Collins, S. Cornell, C.A. de Wit, M.L. Diamond, P. Fantke, M. Hassellöv, M. MacLeod, M.W. Ryberg, P. Søgaard Jørgensen, P. Villarrubia-Gómez, Z. Wang, M.Z. Hauschild, Outside the Safe Operating Space of the Planetary Boundary for Novel Entities, Environ. Sci. Technol. 56 (2022) 1510–1521. doi.org/10.1021/acs.est.1c04158.

[7] K.R. Miner, H. Clifford, T. Taruscio, M. Potocki, G. Solomon, M. Ritari, I.E. Napper, A.P. Gajurel, P.A. Mayewski, Deposition of PFAS 'forever chemicals' on Mt. Everest, Sci. Total Environ. 759 (2021) 144421. doi.org/10.1016/j.scitotenv.2020.144421.

[8] S. Dasgupta, X. Peng, S. Chen, J. Li, M. Du, Y.H. Zhou, G. Zhong, H. Xu, K. Ta, Toxic anthropogenic pollutants reach the deepest ocean on Earth, Geochemical Perspect. Lett. 7 (2018) 22–26. doi.org/10.7185/geochemlet.1814.

[9] J.M.W. Ryalls, B. Langford, N.J. Mullinger, L.M. Bromfield, E. Nemitz, C. Pfrang, R.D. Girling, Anthropogenic air pollutants reduce insect-mediated pollination services, Environ. Pollut. 297 (2022) 118847. doi.org/10.1016/j.envpol.2022.118847.

[10] C.M. Reitmayer, R.D. Girling, C.W. Jackson, T.A. Newman, Repeated short-term exposure to diesel exhaust reduces honey bee colony fitness, Environ. Pollut. 300 (2022) 118934. doi.org/10.1016/j.envpol.2022.118934.

[11] A. Sikora, European Green Deal – legal and financial challenges of the climate change, ERA Forum. 21 (2020) 681–697. doi.org/10.1007/s12027-020-00637-3.

[12] A. Carfora, G. Scandurra, A. Thomas, Determinants of environmental innovations supporting small- and medium-sized enterprises sustainable development, Bus. Strateg. Environ. 30 (2021) 2621–2636. doi.org/10.1002/bse.2767.

[13] D.I. Leyva-de la Hiz, V. Ferron-Vilchez, J.A. Aragon-Correa, Do Firms' Slack Resources Influence the Relationship Between Focused Environmental Innovations and Financial Performance? More is Not Always Better, J. Bus. Ethics. 159 (2019) 1215–1227. doi.org/10.1007/s10551-017-3772-3.

[14] A. Triguero, L. Moreno-Mondéjar, M.A. Davia, Eco-innovation by small and medium-sized firms in Europe: From end-of-pipe to cleaner technologies, Innov. Manag. Policy Pract. 17 (2015) 24–40. doi.org/10.1080/14479338.2015.1011059.

[15] C.E. Enyoh, A.W. Verla, W. Qingyue, F.O. Ohiagu, A.H. Chowdhury, E.C. Enyoh, T. Chowdhury, E.N. Verla, U.P. Chinwendu, An overview of emerging pollutants in air: Method of analysis and potential public health concern from human environmental exposure, Trends Environ. Anal. Chem. 28 (2020) e00107. doi.org/10.1016/j.teac.2020.e00107.

[16] V. Dulio, B. van Bavel, E. Brorström-Lundén, J. Harmsen, J. Hollender, M. Schlabach, J. Slobodnik, K. Thomas, J. Koschorreck, Emerging pollutants in the EU: 10 years of NORMAN in support of environmental policies and regulations, Environ. Sci. Eur. 30 (2018) 1-13. doi.org/10.1186/s12302-018-0135-3.

[17] R. Koppmann, ed., Volatile Organic Compounds in the Atmosphere, Blackwell Publishing, 2007.

[18] J.H. Duffus, M. Nordberg, D.M. Templeton, Glossary of terms used in toxicology, 2nd edition (IUPAC Recommendations 2007), Pure Appl. Chem. 79 (2007) 1153-1344. doi.org/10.1351/pac200779071153.

[19] F.I. Khan, A. Kr. Ghoshal, A.K. Ghoshal, Removal of volatile organic compounds from polluted air, J. Loss Prev. Process Ind. 13 (2000) 527–545. doi.org/10.1016/S0950-4230(00)00007-3.

[20] I. Kourtchev, C. Giorio, A. Manninen, E. Wilson, B. Mahon, J. Aalto, M. Kajos, D. Venables, T. Ruuskanen, J. Levula, M. Loponen, S. Connors, N. Harris, D. Zhao, A. Kiendler-Scharr, T. Mentel, Y. Rudich, M. Hallquist, J.F. Doussin, W. Maenhaut, J. Bäck, T. Petäjä, J. Wenger, M. Kulmala, M. Kalberer, Enhanced volatile organic compounds emissions and organic aerosol mass increase the oligomer content of atmospheric aerosols, Sci. Rep. 6 (2016) 35038. doi.org/10.1038/srep35038.

[21] A. Hartikainen, P. Yli-Pirilä, P. Tiitta, A. Leskinen, M. Kortelainen, J. Orasche, J. Schnelle-Kreis, K.E.J. Lehtinen, R. Zimmermann, J. Jokiniemi, O. Sippula, Volatile Organic Compounds from Logwood Combustion: Emissions and Transformation under Dark and Photochemical Aging Conditions in a Smog Chamber, Environ. Sci. Technol. 52 (2018) 4979–4988. doi.org/10.1021/acs.est.7b06269.

[22] S. Bakand, C. Winder, C. Khalil, A. Hayes, A novel in vitro exposure technique for toxicity testing of selected volatile organic compounds, J. Environ. Monit. 8 (2006) 100–105.

doi.org/10.1039/b509812b.

[23] A.J. Li, V.K. Pal, K. Kannan, A review of environmental occurrence, toxicity, biotransformation and biomonitoring of volatile organic compounds, Environ. Chem. Ecotoxicol. 3 (2021) 91–116. doi.org/10.1016/j.enceco.2021.01.001.

[24] E. Kabir, K.H. Kim, An on-line analysis of 7 odorous volatile organic compounds in the ambient air surrounding a large industrial complex, Atmos. Environ. 44 (2010) 3492–3502. doi.org/10.1016/j.atmosenv.2010.06.021.

[25] M. Pawnuk, A. Grzelka, U. Miller, I. Sówka, Prevention and reduction of odour nuisance in waste management in the context of the current legal and technological solutions, J. Ecol. Eng. 21 (2020) 34–41. doi.org/10.12911/22998993/125455.

[26] A. Mantovani, O. Tarola, C. Vergari, End-of-pipe or cleaner production? How to go green in presence of income inequality and pro-environmental behavior, J. Clean. Prod. 160 (2017) 71–82. doi.org/10.1016/j.jclepro.2017.01.110.

[27] K.A. Zotter, “End-of-pipe” versus “process-integrated” water conservation solutions: A comparison of planning, implementation and operating phases, J. Clean. Prod. 12 (2004) 685–695. doi.org/10.1016/S0959-6526(03)00115-X.

[28] W. Yizhong, H. Ye, W. Qunwei, Z. Dequn, S. Bin, Cleaner production vs end-of-pipe treatment: Evidence from industrial SO2 emissions abatement in China, J. Environ. Manage. 277 (2021) 111429. doi.org/10.1016/j.jenvman.2020.111429.

[29] M. Ehn, J.A. Thornton, E. Kleist, M. Sipilä, H. Junninen, I. Pullinen, M. Springer, F. Rubach, R. Tillmann, B. Lee, F. Lopez-Hilfiker, S. Andres, I.H. Acir, M. Rissanen, T. Jokinen, S. Schobesberger, J. Kangasluoma, J. Kontkanen, T. Nieminen, T. Kurtén, L.B. Nielsen, S. Jørgensen, H.G. Kjaergaard, M. Canagaratna, M.D. Maso, T. Berndt, T. Petäjä, A. Wahner, V.M. Kerminen, M. Kulmala, D.R. Worsnop, J. Wildt, T.F. Mentel, A large source of low-volatility secondary organic aerosol, Nature. 506 (2014) 476–479. doi.org/10.1038/nature13032.

[30] J. Niu, X. Du, J. Ran, R. Wang, Dry (CO 2) reforming of methane over Pt catalysts studied by DFT and kinetic modeling, Appl. Surf. Sci. 376 (2016) 79–90. doi.org/10.1016/j.apsusc.2016.01.212.

[31] Y.S. Son, Decomposition of VOCs and odorous compounds by radiolysis: A critical review, Chem. Eng. J. 316 (2017) 609–622. doi.org/10.1016/j.cej.2017.01.063.

[32] T. Brinkmann, G. Giner Santonja, H. Yukseler, S. Roudier, L. Delgado Sancho, Best Available Techniques (BAT) Reference Document for Common Waste Water and Waste Gas Treatment/Management Systems in the Chemical Sector. Industrial Emissions Directive 2010/75/EU (Integrated Pollution Prevention and Control), Luxembourg, 2016.

[33] R.T. Yang, Adsorbents: fundamentals and applications, John Wiley & Sons, INC., New Jersey,

2003.

[34] D.M. Ruthven, Principles of Adsorption and Adsorption Processes, 1st ed., Wiley-Interscience, 1984.

[35] X. Li, L. Zhang, Z. Yang, P. Wang, Y. Yan, J. Ran, Adsorption materials for volatile organic compounds (VOCs) and the key factors for VOCs adsorption process: A review, Sep. Purif. Technol. 235 (2020) 116213. doi.org/10.1016/j.seppur.2019.116213.

[36] F. Rezaei, P. Webley, Structured adsorbents in gas separation processes, Sep. Purif. Technol. 70 (2010) 243–256. doi.org/10.1016/j.seppur.2009.10.004.

[37] S. Wong, N. Ngadi, I.M. Inuwa, O. Hassan, Recent advances in applications of activated carbon from biowaste for wastewater treatment: A short review, J. Clean. Prod. 175 (2018) 361–375. doi.org/10.1016/j.jclepro.2017.12.059.

[38] Y. Dai, Q. Sun, W. Wang, L. Lu, M. Liu, J. Li, S. Yang, Y. Sun, K. Zhang, J. Xu, W. Zheng, Z. Hu, Y. Yang, Y. Gao, Y. Chen, X. Zhang, F. Gao, Y. Zhang, Utilizations of agricultural waste as adsorbent for the removal of contaminants: A review, Chemosphere. 211 (2018) 235–253. doi.org/10.1016/j.chemosphere.2018.06.179.

[39] W.H. Chan, M.N. Mazlee, Z.A. Ahmad, M.A.M. Ishak, J.B. Shamsul, The development of low cost adsorbents from clay and waste materials: a review, J. Mater. Cycles Waste Manag. 19 (2017) 1–14. doi.org/10.1007/s10163-015-0396-5.

[40] D.D. Do, Adsorption Analysis: Equilibria and Kinetics (Series on Chemical Engineering), Imperial College Press, London, 1998.

[41] M. Thommes, K. Kaneko, A. V. Neimark, J.P. Olivier, F. Rodriguez-Reinoso, J. Rouquerol, K.S.W. Sing, Physisorption of gases, with special reference to the evaluation of surface area and pore size distribution (IUPAC Technical Report), Pure Appl. Chem. 87 (2015) 1051–1069. doi.org/10.1515/pac-2014-1117.

[42] K.A. Cychosz, M. Thommes, Progress in the Physisorption Characterization of Nanoporous Gas Storage Materials, Engineering. 4 (2018) 559–566. doi.org/10.1016/j.eng.2018.06.001.

[43] M. Králik, Adsorption, chemisorption, and catalysis, Chem. Pap. 68 (2014) 1625–1638. doi.org/10.2478/s11696-014-0624-9.

[44] F. Ding, B.I. Yakobson, Challenges in hydrogen adsorptions: From physisorption to chemisorption, Front. Phys. 6 (2011) 142–150. doi.org/10.1007/s11467-011-0171-6.

[45] L.J. Ma, T. Han, J. Jia, H.S. Wu, Cooperative physisorption and chemisorption of hydrogen on vanadium-decorated benzene, RSC Adv. 10 (2020) 37770–37778. doi.org/10.1039/d0ra06057g.

[46] V. Calemma, R. Rausa, P. D'Antona, L. Montanari, Characterization of asphaltenes molecular structure, Energy Fuels. 12 (1998) 422–428. doi.org/10.1021/ef9701854.

[47] F. Rouquerol, J. Rouquerol, K.S.W. Sing, P.L. Llewellyn, G. Maurin, Adsorption by Powders and Porous Solids, Academic Press, London, 2013.

[48] S.J. Gregg, K.S.W. Sing, Adsorption, Surface Area and Porosity, Academic Press, London, 1982.

[49] A.K. Rajagopalan, A.M. Avila, A. Rajendran, Do adsorbent screening metrics predict process performance? A process optimisation based study for post-combustion capture of CO2, Int. J. Greenh. Gas Control. 46 (2016) 76–85. doi.org/10.1016/j.ijggc.2015.12.033.

[50] R. Kumar, Pressure Swing Adsorption Process: Performance Optimum and Adsorbent Selection, Ind. Eng. Chem. Res. 33 (1994) 1600–1605. doi.org/10.1021/ie00030a021.

[51] X. Hu, S. Brandani, A.I. Benin, R.R. Willis, Development of a semiautomated zero length column technique for carbon capture applications: Study of diffusion behavior of CO2 in MOFs, Ind. Eng. Chem. Res. 54 (2015) 5777–5783. doi.org/10.1021/acs.iecr.5b00515.

[52] C.R. Reid, K.M. Thomas, Adsorption kinetics and size exclusion properties of probe molecules for the selective porosity in a carbon molecular sieve used for air separation, J. Phys. Chem. B. 105 (2001) 10619–10629. doi.org/10.1021/jp0108263.

[53] D.M. Ruthven, S. Farooq, Air separation by pressure swing adsorption, Gas Sep. Purif. 4 (1990) 141–148. doi.org/10.1016/0950-4214(90)80016-E.

[54] N. Álvarez-Gutiérrez, M. V. Gil, F. Rubiera, C. Pevida, Kinetics of CO2 adsorption on cherry stone-based carbons in CO2/CH4 separations, Chem. Eng. J. 307 (2017) 249–257. doi.org/10.1016/j.cej.2016.08.077.

[55] J.C. Knox, A.D. Ebner, M.D. Levan, R.F. Coker, J.A. Ritter, Limitations of Breakthrough Curve Analysis in Fixed-Bed Adsorption, Ind. Eng. Chem. Res. 55 (2016) 4734–4748. doi.org/10.1021/acs.iecr.6b00516.

[56] Y. Yang, C. Sun, B. Lin, Q. Huang, Surface modified and activated waste bone char for rapid and efficient VOCs adsorption, Chemosphere. 256 (2020) 127054. doi.org/10.1016/j.chemosphere.2020.127054.

[57] J. Elfving, C. Bajamundi, J. Kauppinen, T. Sainio, Modelling of equilibrium working capacity of PSA, TSA and TVSA processes for CO2 adsorption under direct air capture conditions, J. CO2 Util. 22 (2017) 270–277. doi.org/10.1016/j.jcou.2017.10.010.

[58] P. Zhang, X. Bu, Y. Yang, L. Wang, Technical-economic evaluation of an energy-integrated temperature swing adsorption process for compressed air drying, Comput. Chem. Eng. 157 (2022) 107621. doi.org/10.1016/j.compchemeng.2021.107621.

[59] Y. Liu, K. Mallouk, H. Emamipour, M.J. Rood, X. Liu, Z. Yan, Isobutane adsorption with carrier gas recirculation at different relative humidities using activated carbon fiber cloth and electrothermal regeneration, Chem. Eng. J. 360 (2019) 1011–1019. doi.org/10.1016/j.cej.2018.02.095.

[60] M. Jahandar Lashaki, S. Khiavi, A. Sayari, Stability of amine-functionalized CO2 adsorbents: A multifaceted puzzle, Chem. Soc. Rev. 48 (2019) 3320–3405. doi.org/10.1039/c8cs00877a.

[61] F. Mumtaz, M.F. Irfan, M.R. Usman, Synthesis methods and recent advances in hierarchical zeolites: a brief review, J. Iran. Chem. Soc. 18 (2021) 2215–2229. doi.org/10.1007/s13738-021-02183-2.

[62] C.S. Cundy, P.A. Cox, The hydrothermal synthesis of zeolites: History and development from the earliest days to the present time, Chem. Rev. 103 (2003) 663–701. doi.org/10.1021/cr020060i.

[63] J. Yu, Synthesis of zeolites, in: J. Cejka, H. van Bekkum, A. Corma, F. Schueth (Eds.), Introd. to Zeolite Sci. Pract., 3rd ed., Elsevier, Amsterdam, 2007.

[64] X. Meng, X. Feng-Shou, Green routes for synthesis of zeolites, Chem. Rev. 114 (2014) 1521–1543. doi.org/10.7536/PC150112.

[65] Z. Liu, J. Zhu, T. Wakihara, T. Okubo, Ultrafast synthesis of zeolites: Breakthrough, progress and perspective, Inorg. Chem. Front. 6 (2019) 14–31. doi.org/10.1039/c8qi00939b.

[66] R. Chaves Lima, L. Bieseki, P. Vinaches Melguizo, S.B. Castella Pergher, Environmentaly Friendly Zeolites, Synthesis and Source Materials, 1st ed., Springer International Publishing, 2019.

[67] J. Čejka, R. Millini, M. Opanasenko, D.P. Serrano, W.J. Roth, Advances and challenges in zeolite synthesis and catalysis, Catal. Today. 345 (2020) 2–13. doi.org/10.1016/j.cattod.2019.10.021.

[68] S. Mintova, N. Barrier, eds., Verified Syntheses of Zeolitic Materials, 3rd ed., Synthesis Commission of the International Zeolite Association, 2016.

[69] C. Wang, H. Guo, S. Leng, J. Yu, K. Feng, L. Cao, J. Huang, Regulation of hydrophilicity/hydrophobicity of aluminosilicate zeolites: a review, Crit. Rev. Solid State Mater. Sci. 46 (2021) 330–348. doi.org/10.1080/10408436.2020.1819198.

[70] B. Sels, L. Kustov, Zeolites and Zeolite-Like Materials, 1st ed., Elsevier, Amsterdam, 2016.

[71] B.M. Weckhuysen, J. Yu, Recent advances in zeolite chemistry and catalysis, Chem. Soc. Rev. 44 (2015) 7022–7024. doi.org/10.1039/c5cs90100f.

[72] S.U. Nandanwar, D.R. Corbin, M.B. Shiflett, A Review of Porous Adsorbents for the Separation of Nitrogen from Natural Gas, Ind. Eng. Chem. Res. 59 (2020) 13355–13369. doi.org/10.1021/acs.iecr.0c02730.

[73] M.G.R.S. Santos, L.M.S. Correia, J.L. de Medeiros, O. de Q.F. Araújo, Natural gas dehydration by molecular sieve in offshore plants: Impact of increasing carbon dioxide content, Energy Convers. Manag. 149 (2017) 760–773. doi.org/10.1016/j.enconman.2017.03.005.

[74] E.J. Shokroo, D.J. Farsani, H.K. Meymandi, N. Yadollahi, Comparative study of zeolite 5A and zeolite 13X in air separation by pressure swing adsorption, Korean J. Chem. Eng. 33 (2016)

1391–1401. doi.org/10.1007/s11814-015-0232-6.

[75] X. Feng, Z. Zong, S.K. Elsaidi, J.B. Jasinski, R. Krishna, P.K. Thallapally, M.A. Carreon, Kr/Xe Separation over a Chabazite Zeolite Membrane, J. Am. Chem. Soc. 138 (2016) 9791–9794. doi.org/10.1021/jacs.6b06515.

[76] E. Kianfar, S. Hajimirzaee, S. mousavian, A.S. Mehr, Zeolite-based catalysts for methanol to gasoline process: A review, Microchem. J. 156 (2020) 104822. doi.org/10.1016/j.microc.2020.104822.

[77] S. Kulprathipanja, Zeolites in Industrial Separation and Catalysis, 1st ed., Wiley, 2010.

[78] M. Thommes, Textural Characterization of Zeolites and Ordered Mesoporous Materials by Physical Adsorption, in: J. Cejka, H. van Bekkum, A. Corma, F. Schuth (Eds.), Introd. to Zeolite Sci. Pract., 3rd ed., Amsterdam, 2007.

[79] K. Kotoh, S. Takashima, Y. Nakamura, Molecular-sieving effect of zeolite 3A on adsorption of H2, HD and D2, Fusion Eng. Des. 84 (2009) 1108–1112. doi.org/10.1016/j.fusengdes.2009.01.052.

[80] J.A. Thompson, Acid gas adsorption on zeolite SSZ-13: Equilibrium and dynamic behavior for natural gas applications, AIChE J. 66 (2020) e16549. doi.org/10.1002/aic.16549.

[81] R. Krishna, Thermodynamically Consistent Methodology for Estimation of Diffusivities of Mixtures of Guest Molecules in Microporous Materials, ACS Omega. 4 (2019) 13520–13529. doi.org/10.1021/acsomega.9b01873.

[82] T. De Baerdemaeker, D. De Vos, Gas separation: Trapdoors in zeolites, Nat. Chem. 5 (2013) 89–90. doi.org/10.1038/nchem.1560.

[83] J. Shang, G. Li, R. Singh, P. Xiao, J.Z. Liu, P.A. Webley, Determination of composition range for “molecular trapdoor” effect in chabazite zeolite, J. Phys. Chem. C. 117 (2013) 12841–12847. doi.org/10.1021/jp4015146.

[84] J. Shang, G. Li, R. Singh, Q. Gu, K.M. Nairn, T.J. Bastow, N. Medhekar, C.M. Doherty, A.J. Hill, J.Z. Liu, P.A. Webley, Discriminative separation of gases by a “molecular trapdoor” mechanism in chabazite zeolites, J. Am. Chem. Soc. 134 (2012) 19246–19253. doi.org/10.1021/ja309274y.

[85] A.J.W. Physick, D.J. Wales, S.H.R. Owens, J. Shang, P.A. Webley, T.J. Mays, V.P. Ting, Novel low energy hydrogen-deuterium isotope breakthrough separation using a trapdoor zeolite, Chem. Eng. J. 288 (2016) 161–168. doi.org/10.1016/j.cej.2015.11.040.

[86] T.J. Bandosz, Activated Carbon Surfaces in Environmental Remediation, 1st ed., Academic Press, 2006.

[87] J.E. Szulejko, K.H. Kim, J. Parise, Seeking the most powerful and practical real-world sorbents for gaseous benzene as a representative volatile organic compound based on performance metrics, Sep. Purif. Technol. 212 (2019) 980–985. doi.org/10.1016/j.seppur.2018.11.001.

[88] P. González-García, Activated carbon from lignocellulosics precursors: A review of the synthesis methods, characterization techniques and applications, Renew. Sustain. Energy Rev. 82 (2018) 1393–1414. doi.org/10.1016/j.rser.2017.04.117.

[89] Y. Chen, Y. Zhu, Z. Wang, Y. Li, L. Wang, L. Ding, X. Gao, Y. Ma, Y. Guo, Application studies of activated carbon derived from rice husks produced by chemical-thermal process - A review, Adv. Colloid Interface Sci. 163 (2011) 39–52. doi.org/10.1016/j.cis.2011.01.006.

[90] C. Rodríguez Correa, M. Stollovsky, T. Hehr, Y. Rauscher, B. Rolli, A. Kruse, Influence of the Carbonization Process on Activated Carbon Properties from Lignin and Lignin-Rich Biomasses, ACS Sustain. Chem. Eng. 5 (2017) 8222–8233. doi.org/10.1021/acssuschemeng.7b01895.

[91] A. Zubrik, M. Matik, S. Hredzák, M. Lovás, Z. Danková, M. Kováčová, J. Briančin, Preparation of chemically activated carbon from waste biomass by single-stage and two-stage pyrolysis, J. Clean. Prod. 143 (2017) 643–653. doi.org/10.1016/j.jclepro.2016.12.061.

[92] E. Köseoɬlu, C. Akmil-Başar, Preparation, structural evaluation and adsorptive properties of activated carbon from agricultural waste biomass, Adv. Powder Technol. 26 (2015) 811–818. doi.org/10.1016/j.apt.2015.02.006.

[93] Z. Heidarinejad, M.H. Dehghani, M. Heidari, G. Javedan, I. Ali, M. Sillanpää, Methods for preparation and activation of activated carbon: a review, Environ. Chem. Lett. 18 (2020) 393–415. doi.org/10.1007/s10311-019-00955-0.

[94] W. Ao, J. Fu, X. Mao, Q. Kang, C. Ran, Y. Liu, H. Zhang, Z. Gao, J. Li, G. Liu, J. Dai, Microwave assisted preparation of activated carbon from biomass: A review, Renew. Sustain. Energy Rev. 92 (2018) 958–979. doi.org/10.1016/j.rser.2018.04.051.

[95] A. Jain, R. Balasubramanian, M.P. Srinivasan, Hydrothermal conversion of biomass waste to activated carbon with high porosity: A review, Chem. Eng. J. 283 (2016) 789–805. doi.org/10.1016/j.cej.2015.08.014.

[96] Y. Gao, Q. Yue, B. Gao, A. Li, Insight into activated carbon from different kinds of chemical activating agents: A review, Sci. Total Environ. 746 (2020) 141094. doi.org/10.1016/j.scitotenv.2020.141094.

[97] W. Rudzinski, T. Panczyk, Kinetics of gas adsorption in activated carbons, studied by applying the statistical rate theory of interfacial transport, J. Phys. Chem. B. 105 (2001) 6858–6866. doi.org/10.1021/jp004166y.

[98] M.K.B. Gratuito, T. Panyathanmaporn, R.A. Chumnanklang, N. Sirinuntawittaya, A. Dutta, Production of activated carbon from coconut shell: Optimization using response surface methodology, Bioresour. Technol. 99 (2008) 4887–4895. doi.org/10.1016/j.biortech.2007.09.042.

[99] S. Khalili, B. Khoshandam, M. Jahanshahi, Optimization of production conditions for synthesis

of chemically activated carbon produced from pine cone using response surface methodology for CO2 adsorption, RSC Adv. 5 (2015) 94115–94129. doi.org/10.1039/c5ra18986a.

[100] H.P. Boehm, Chemical Identification of Surface Groups, Adv. Catal. 16 (1966) 179–274. doi.org/10.1016/S0360-0564(08)60354-5.

[101] H.P. Boehm, Investigations of Surface Oxides of Carbon, 2 (1963) 221. doi.org/10.1002/anie.196302212.

[102] H.P. Boehm, Some aspects of the surface chemistry of carbon blacks and other carbons, Carbon N. Y. 32 (1994) 759–769. doi.org/10.1016/0008-6223(94)90031-0.

[103] H.P. Boehm, Surface oxides on carbon and their analysis: a critical assessment, Carbon N. Y. 40 (2002) 145–149. doi.org/10.1016/S0008-6223(01)00165-8.

[104] M. V. Lopez-Ramon, F. Stoeckli, C. Moreno-Castilla, F. Carrasco-Marin, On the characterization of acidic and basic surface sites on carbons by various techniques, Carbon N. Y. 37 (1999) 1215–1221. doi.org/10.1016/S0008-6223(98)00317-0.

[105] T.J. Bandosz, J. Jagiello, J.A. Schwarz, Comparison of Methods to Assess Surface Acidic Groups on Activated Carbons, Anal. Chem. 64 (1992) 891–895. doi.org/10.1021/ac00032a012.

[106] T.J. Bandosz, J. Jagiełło, J.A. Schwarz, A. Krzyzanowski, Effect of surface chemistry on sorption of water and methanol on activated carbons, Langmuir. 12 (1996) 6480–6486. doi.org/10.1021/la960340r

[107] P. Burg, M.H. Abraham, D. Cagniant, Methods of determining polar and non-polar sites on carbonaceous adsorbents. The contribution of the linear solvation energy relationship approach, Carbon 41 (2003) 867–879. doi.org/10.1016/S0008-6223(03)00018-6.

[108] I.I. Salame, T.J. Bandosz, Surface Chemistry of Activated Carbons: Combining the Results of Temperature-Programmed Desorption, Boehm, and Potentiometric Titrations., J. Colloid Interface Sci. 240 (2001) 252–258. doi.org/10.1006/jcis.2001.7596.

[109] D.D. Do, H.D. Do, Model for water adsorption in activated carbon, Carbon 38 (2000) 767–773. doi.org/10.1016/S0008-6223(99)00159-1.

[110] R.C. Bansal, G. Meenakshi, Activated Carbon Adsorption, 1st ed., CRC Press, Boca Raton, 2005.

[111] A.A. Abdulrasheed, A.A. Jalil, S. Triwahyono, M.A.A. Zaini, Y. Gambo, M. Ibrahim, Surface modification of activated carbon for adsorption of SO2 and NOX: A review of existing and emerging technologies, Renew. Sustain. Energy Rev. 94 (2018) 1067–1085. doi.org/10.1016/j.rser.2018.07.011.

[112] M.S. Shafeeyan, W.M.A.W. Daud, A. Houshmand, A. Shamiri, A review on surface modification of activated carbon for carbon dioxide adsorption, J. Anal. Appl. Pyrolysis. 89 (2010) 143–151. doi.org/10.1016/j.jaap.2010.07.006.

[113] Z. Chen, S. Deng, H. Wei, B. Wang, J. Huang, G. Yu, Activated carbons and amine-modified

materials for carbon dioxide capture -- A review, Front. Environ. Sci. Eng. 7 (2013) 326–340. doi.org/10.1007/s11783-013-0510-7.

[114] A. Srivastava, B. Gupta, A. Majumder, A.K. Gupta, S.K. Nimbhorkar, A comprehensive review on the synthesis, performance, modifications, and regeneration of activated carbon for the adsorptive removal of various water pollutants, J. Environ. Chem. Eng. 9 (2021) 106177. doi.org/10.1016/j.jece.2021.106177.

[115] A. Dąbrowski, Adsorption - From theory to practice, Adv. Colloid Interface Sci. 93 (2001) 135–224. doi.org/10.1016/S0001-8686(00)00082-8.

[116] J. Liu, Y. Liu, D. Kayrak Talay, E. Calverley, M. Brayden, M. Martinez, A new carbon molecular sieve for propylene/propane separations, Carbon 85 (2015) 201–211. doi.org/10.1016/j.carbon.2014.12.089.

[117] Z. Yang, D. Wang, Z. Meng, Y. Li, Adsorption separation of CH4/N2 on modified coal-based carbon molecular sieve, Sep. Purif. Technol. 218 (2019) 130–137. doi.org/10.1016/j.seppur.2019.02.048.

[118] H. Demiral, İ. Demiral, Preparation and characterization of carbon molecular sieves from chestnut shell by chemical vapor deposition, Adv. Powder Technol. 29 (2018) 3033–3039. doi.org/10.1016/j.apt.2018.07.015.

[119] Y. Park, D.K. Moon, D. Park, M. Mofarahi, C.H. Lee, Adsorption equilibria and kinetics of CO2, CO, and N2 on carbon molecular sieve, Sep. Purif. Technol. 212 (2019) 952–964. doi.org/10.1016/j.seppur.2018.11.069.

[120] M. Andrade, F. Relvas, A. Mendes, Highly propylene equilibrium selective carbon molecular sieve adsorbent, Sep. Purif. Technol. 245 (2020) 116853. doi.org/10.1016/j.seppur.2020.116853.

[121] J. Liu, C. Han, M. McAdon, J. Goss, K. Andrews, High throughput development of one carbon molecular sieve for many gas separations, Microporous Mesoporous Mater. 206 (2015) 207–216. doi.org/10.1016/j.micromeso.2014.11.030.

[122] Y. Feng, W. Yang, N. Wang, W. Chu, D. Liu, Effect of nitrogen-containing groups on methane adsorption behaviors of carbon spheres, J. Anal. Appl. Pyrolysis. 107 (2014) 204–210. doi.org/10.1016/j.jaap.2014.02.021.

[123] A.R. Mohamed, M. Mohammadi, G.N. Darzi, Preparation of carbon molecular sieve from lignocellulosic biomass: A review, Renew. Sustain. Energy Rev. 14 (2010) 1591–1599. doi.org/10.1016/j.rser.2010.01.024.

[124] M. Rungta, L. Xu, W.J. Koros, Carbon molecular sieve dense film membranes derived from Matrimid® for ethylene/ethane separation, Carbon N. Y. 50 (2012) 1488–1502. doi.org/10.1016/j.carbon.2011.11.019.

[125] X. Ning, W.J. Koros, Carbon molecular sieve membranes derived from Matrimid® polyimide for nitrogen/methane separation, Carbon 66 (2014) 511–522. doi.org/10.1016/j.carbon.2013.09.028.

[126] J. Liu, J. Goss, T. Calverley, Y. Liu, C. Broomall, J. Kang, R. Golombeski, D. Anaya, B. Moe, K. Mabe, G. Watson, A. Wetzel, Carbon molecular sieve fiber with 3.4–4.9 Angstrom effective micropores for propylene/propane and other gas separations, Microporous Mesoporous Mater. 305 (2020) 110341. doi.org/10.1016/j.micromeso.2020.110341.

[127] H. Li, M. Eddaoudi, M. O'Keeffe, O.M. Yaghi, Design and synthesis of an exceptionally stable and highly porous metal-organic framework, Nature. 402 (1999) 276–279. doi.org/10.1038/46248

[128] K.K. Gangu, S. Maddila, S.B. Mukkamala, S.B. Jonnalagadda, A review on contemporary Metal-Organic Framework materials, Inorganica Chim. Acta. 446 (2016) 61–74. doi.org/10.1016/j.ica.2016.02.062.

[129] O.K. Farha, A.Ö. Yazaydin, I. Eryazici, C.D. Malliakas, B.G. Hauser, M.G. Kanatzidis, S.T. Nguyen, R.Q. Snurr, J.T. Hupp, De novo synthesis of a metal-organic framework material featuring ultrahigh surface area and gas storage capacities, Nat. Chem. 2 (2010) 944–948. doi.org/10.1038/nchem.834.

[130] H. Furukawa, N. Ko, Y.B. Go, N. Aratani, S.B. Choi, E. Choi, A.Ö. Yazaydin, R.Q. Snurr, M. O'Keeffe, J. Kim, O.M. Yaghi, Ultrahigh porosity in metal-organic frameworks, Science 329 (2010) 424–428. doi.org/10.1126/science.1192160.

[131] O.K. Farha, I. Eryazici, N.C. Jeong, B.G. Hauser, C.E. Wilmer, A.A. Sarjeant, R.Q. Snurr, S.T. Nguyen, A.Ö. Yazaydin, J.T. Hupp, Metal-organic framework materials with ultrahigh surface areas: Is the sky the limit?, J. Am. Chem. Soc. 134 (2012) 15016–15021. doi.org/10.1021/ja3055639.

[132] B. Li, H.M. Wen, Y. Cui, W. Zhou, G. Qian, B. Chen, Emerging Multifunctional Metal–Organic Framework Materials, Adv. Mater. 28 (2016) 8819–8860. doi.org/10.1002/adma.201601133.

[133] N.A. Khan, Z. Hasan, S.H. Jhung, Adsorptive removal of hazardous materials using metal-organic frameworks (MOFs): A review, J. Hazard. Mater. 244–245 (2013) 444–456. doi.org/10.1016/j.jhazmat.2012.11.011.

[134] W. Xuan, C. Zhu, Y. Liu, Y. Cui, Mesoporous metal–organic framework materials, Chem. Soc. Rev. 41 (2012) 1677–1695. doi.org/10.1039/c1cs15196g.

[135] N. Stock, S. Biswas, Synthesis of metal-organic frameworks (MOFs): Routes to various MOF topologies, morphologies, and composites, Chem. Rev. 112 (2012) 933–969. doi.org/10.1021/cr200304e.

[136] Z. Wang, S.M. Cohen, Postsynthetic modification of metal–organic frameworks, Chem. Soc.

Rev. 38 (2009) 1315–1329. doi.org/10.1039/b802258p.

[137] S. Yuan, L. Feng, K. Wang, J. Pang, M. Bosch, C. Lollar, Y. Sun, J. Qin, X. Yang, P. Zhang, Q. Wang, L. Zou, Y. Zhang, L. Zhang, Y. Fang, J. Li, H.C. Zhou, Stable Metal–Organic Frameworks: Design, Synthesis, and Applications, Adv. Mater. 30 (2018) 1704303. doi.org/10.1002/adma.201704303.

[138] M. Ding, X. Cai, H.L. Jiang, Improving MOF stability: Approaches and applications, Chem. Sci. 10 (2019) 10209–10230. doi.org/10.1039/c9sc03916c.

[139] N.C. Burtch, H. Jasuja, K.S. Walton, Water stability and adsorption in metal-organic frameworks, Chem. Rev. 114 (2014) 10575–10612. doi.org/10.1021/cr5002589.

[140] L.D. Hart, E. Lense, eds., Alumina Chemicals: Science and Technology Handbook, Wiley, 1990.

[141] S. Sircar, M.B. Rao, T.C. Golden, Drying of gases and liquids by activated alumina, in: A. Dąbrowski, V.A. Tertykh (Eds.), Adsorption on New and Modified Inorganic Sorbents, Elsevier, 1996.

[142] B.C. Gates, J.R. Katzer, G.C.A. Schuit, Chemistry of Catalytic Processes, McGraw-Hill, New York, 1979.

[143] J.B. Peri, A model for the surface of a silica-alumina catalyst, J. Catal. 41 (1976) 227–239. doi.org/10.1016/0021-9517(76)90338-9.

[144] K.G. Wynnyk, B. Hojjati, R.A. Marriott, Sour Gas and Water Adsorption on Common High-Pressure Desiccant Materials: Zeolite 3A, Zeolite 4A, and Silica Gel, J. Chem. Eng. Data. 64 (2019) 3156–3163. doi.org/10.1021/acs.jced.9b00233.

[145] K.L. Yan, Q. Wang, Adsorption characteristics of the silica gels as adsorbent for gasoline vapors removal, IOP Conf. Ser. Earth Environ. Sci. 153 (2018). doi.org/10.1088/1755-1315/153/2/022010.

[146] C.A. Grande, D.G.B. Morence, A.M. Bouzga, K.A. Andreassen, Silica Gel as a Selective Adsorbent for Biogas Drying and Upgrading, Ind. Eng. Chem. Res. 59 (2020) 10142–10149. doi.org/10.1021/acs.iecr.0c00949.

[147] J.B. Peri, A.L. Hensley, The surface structure of silica gel, J. Phys. Chem. 72 (1968) 2926–2933. doi.org/10.1021/j100854a041.

[148] R.M. Almeida, C.G. Pantano, Structural investigation of silica gel films by infrared spectroscopy, J. Appl. Phys. 68 (1990) 4225–4232. doi.org/10.1063/1.346213.

[149] Y. Zhang, K. Chen, C. Lv, T. Wu, Y. Wen, H. He, S. Yu, L. Wang, Adsorption Separation of CO2/CH4 from Landfill Gas by Ethanolamine-Modified Silica Gel, Water. Air. Soil Pollut. 232 (2021). doi.org/10.1007/s11270-021-05001-w.

[150] K. Wang, H. Shang, L. Li, X. Yan, Z. Yan, C. Liu, Q. Zha, Efficient CO 2 capture on low-cost silica gel modified by polyethyleneimine, J. Nat. Gas Chem. 21 (2012) 319–323.

doi.org/10.1016/S1003-9953(11)60371-X.

[151] K. Hu, W. Zhang, H. Yang, Y. Cui, J. Zhang, W. Zhao, A. Yu, S. Zhang, Calixarene ionic liquid modified silica gel: A novel stationary phase for mixed-mode chromatography, Talanta. 152 (2016) 392–400. doi.org/10.1016/j.talanta.2016.02.038.

[152] A. Banaei, S. Ebrahimi, H. Vojoudi, S. Karimi, A. Badiei, E. Pourbasheer, Adsorption equilibrium and thermodynamics of anionic reactive dyes from aqueous solutions by using a new modified silica gel with 2,2"-(pentane-1,5-diylbis(oxy))dibenzaldehyde, Chem. Eng. Res. Des. 123 (2017) 50–62. doi.org/10.1016/j.cherd.2017.04.032.

[153] W. Zhao, J. Chu, F. Xie, Q. Duan, L. He, S. Zhang, Preparation and evaluation of pillararene bonded silica gel stationary phases for high performance liquid chromatography, J. Chromatogr. A. 1485 (2017) 44–51. doi.org/10.1016/j.chroma.2016.12.019.

[154] S. Ji, Y. Zheng, F. Zhang, X. Liang, B. Yang, A polyvinyl alcohol-coated silica gel stationary phase for hydrophilic interaction chromatography, Analyst. 140 (2015) 6250–6253. doi.org/10.1039/c5an01159k.

[155] J.A.S. Costa, R.A. de Jesus, D.O. Santos, J.F. Mano, L.P.C. Romão, C.M. Paranhos, Recent progresses in the adsorption of organic, inorganic, and gas compounds by MCM-41-based mesoporous materials, Microporous Mesoporous Mater. 291 (2020) 109698. doi.org/10.1016/j.micromeso.2019.109698.

[156] E. Dündar-Tekkaya, Y. Yürüm, Mesoporous MCM-41 material for hydrogen storage: A short review, Int. J. Hydrogen Energy. 41 (2016) 9789–9795. doi.org/10.1016/j.ijhydene.2016.03.050.

[157] V.A. Ostroumova, A.L. Maksimov, MWW-Type Zeolites: MCM-22, MCM-36, MCM-49, and MCM-56 (A Review), Pet. Chem. 59 (2019) 788–801. doi.org/10.1134/S0965544119080140.

[158] S. Bhattacharyya, G. Lelong, M.L. Saboungi, Recent progress in the synthesis and selected applications of MCM-41: A short review, J. Exp. Nanosci. 1 (2006) 375–395. doi.org/10.1080/17458080600812757.

[159] P. Selvam, S.K. Bhatia, C.G. Sonwane, Recent advances in processing and characterization of periodic mesoporous MCM-41 silicate molecular sieves, Ind. Eng. Chem. Res. 40 (2001) 3237–3261. doi.org/10.1021/ie0010666.

[160] M.G. Miricioiu, V.C. Niculescu, Fly ash, from recycling to potential raw material for mesoporous silica synthesis, Nanomaterials. 10 (2020) 1–14. doi.org/10.3390/nano10030474.

[161] D.F. Mohamad, N.S. Osman, M.K.H.M. Nazri, A.A. Mazlan, M.F. Hanafi, Y.A.M. Esa, M.I.I.M. Rafi, M.N. Zailani, N.N. Rahman, A.H.A. Rahman, N. Sapawe, Synthesis of Mesoporous Silica Nanoparticle from Banana Peel Ash for Removal of Phenol and Methyl Orange in Aqueous Solution, Mater. Today Proc. 19 (2019) 1119–1125. doi.org/10.1016/j.matpr.2019.11.004.

[162] Y. Liu, Y. Guo, W. Gao, Z. Wang, Y. Ma, Z. Wang, Simultaneous preparation of silica and activated carbon from rice husk ash, J. Clean. Prod. 32 (2012) 204–209. doi.org/10.1016/j.jclepro.2012.03.021.

[163] R. Terzano, C. D'Alessandro, M. Spagnuolo, M. Romagnoli, L. Medici, Facile Zeolite Synthesis from Municipal Glass and Aluminum Solid Wastes, Clean - Soil, Air, Water. 43 (2015) 133–140. doi.org/10.1002/clen.201400091.

[164] M. Yoldi, E.G. Fuentes-Ordoñez, S.A. Korili, A. Gil, Zeolite synthesis from aluminum saline slag waste, Powder Technol. 366 (2020) 175–184. doi.org/10.1016/j.powtec.2020.02.069.

[165] M. Yoldi, E.G. Fuentes-Ordoñez, S.A. Korili, A. Gil, Zeolite synthesis from industrial wastes, Microporous Mesoporous Mater. 287 (2019) 183–191. doi.org/10.1016/j.micromeso.2019.06.009.

[166] K.M. Lee, Y.M. Jo, Synthesis of zeolite from waste fly ash for adsorption of CO2, J. Mater. Cycles Waste Manag. 12 (2010) 212–219. doi.org/10.1007/s10163-010-0290-0.

[167] L. Liu, R. Singh, P. Xiao, P.A. Webley, Y. Zhai, Zeolite synthesis from waste fly ash and its application in CO2 capture from flue gas streams, Adsorption. 17 (2011) 795–800. doi.org/10.1007/s10450-011-9332-8.

[168] Y. Mu, M. Cui, S. Zhang, J. Zhao, C. Meng, Q. Sun, Comparison study between a series of new type functional diatomite on methane adsorption performance, Microporous Mesoporous Mater. 267 (2018) 203–211. doi.org/10.1016/j.micromeso.2018.03.037.

[169] K. Wal, P. Rutkowski, W. Stawiński, Application of clay minerals and their derivatives in adsorption from gaseous phase, Appl. Clay Sci. 215 (2021) 54–66. doi.org/10.1016/j.clay.2021.106323.

[170] Y. Li, R. Sun, Studies on adsorption of carbon dioxide on alkaline paper mill waste using cyclic process, Energy Convers. Manag. 82 (2014) 46–53. doi.org/10.1016/j.enconman.2014.03.004.

[171] S. Wu, Y. Li, J. Zhao, C. Lu, Z. Wang, Simultaneous CO2/SO2 adsorption performance of carbide slag in adsorption/desorption cycles, Can. J. Chem. Eng. 94 (2016) 33–40. doi.org/10.1002/cjce.22369.

[172] S. Wang, H. Wu, Environmental-benign utilisation of fly ash as low-cost adsorbents, J. Hazard. Mater. 136 (2006) 482–501. doi.org/10.1016/j.jhazmat.2006.01.067.

[173] O. Ioannidou, A. Zabaniotou, Agricultural residues as precursors for activated carbon production-A review, Renew. Sustain. Energy Rev. 11 (2007) 1966–2005. doi.org/10.1016/j.rser.2006.03.013.

[174] M.A. Yahya, Z. Al-Qodah, C.W.Z. Ngah, Agricultural bio-waste materials as potential sustainable precursors used for activated carbon production: A review, Renew. Sustain. Energy Rev. 46 (2015) 218–235. doi.org/10.1016/j.rser.2015.02.051.

[175] Suhas, P.J.M. Carrott, M.M.L. Ribeiro Carrott, Lignin - from natural adsorbent to activated carbon: A review, Bioresour. Technol. 98 (2007) 2301–2312. doi.org/10.1016/j.biortech.2006.08.008.

[176] M. Danish, T. Ahmad, A review on utilization of wood biomass as a sustainable precursor for activated carbon production and application, Renew. Sustain. Energy Rev. 87 (2018) 1–21. doi.org/10.1016/j.rser.2018.02.003.

[177] V.P. Mallapur, J.U.K. Oubagaranadin, A Brief Review on the Synthesis of Zeolites from Hazardous Wastes, Trans. Indian Ceram. Soc. 76 (2017) 1–13. doi.org/10.1080/0371750X.2016.1231086.

[178] S.L. Hsieh, F.Y. Li, P.Y. Lin, D.E. Beck, R. Kirankumar, G.J. Wang, S. Hsieh, CaO recovered from eggshell waste as a potential adsorbent for greenhouse gas CO2, J. Environ. Manage. 297 (2021) 113430. doi.org/10.1016/j.jenvman.2021.113430.

[179] S. Harti, G. Cifredo, J.M. Gatica, H. Vidal, T. Chafik, Physicochemical characterization and adsorptive properties of some Moroccan clay minerals extruded as lab-scale monoliths, Appl. Clay Sci. 36 (2007) 287–296. doi.org/10.1016/j.clay.2006.10.004.

[180] M.L. Pinto, J. Pires, J. Rocha, Porous materials prepared from clays for the upgrade of landfill gas, J. Phys. Chem. C. 112 (2008) 14394–14402. doi.org/10.1021/jp803015d.

[181] W. Yu, L. Deng, P. Yuan, D. Liu, W. Yuan, P. Liu, H. He, Z. Li, F. Chen, Surface silylation of natural mesoporous/macroporous diatomite for adsorption of benzene, J. Colloid Interface Sci. 448 (2015) 545–552. doi.org/10.1016/j.jcis.2015.02.067.

[182] D.P. Bernabe, R.A.S. Herrera, B.T. Doma, M.L. Fu, Y. Dong, Y.F. Wang, Adsorption of low concentration formaldehyde in air using ethylene-diamine- modified diatomaceous earth, Aerosol Air Qual. Res. 15 (2015) 1652–1661. doi.org/10.4209/aaqr.2015.05.0292.

[183] G. Zhang, Y. Liu, Z. Hashisho, Z. Sun, S. Zheng, L. Zhong, Adsorption and photocatalytic degradation performances of TiO2/diatomite composite for volatile organic compounds: Effects of key parameters, Appl. Surf. Sci. 525 (2020). doi.org/10.1016/j.apsusc.2020.146633.

[184] W. Yuan, P. Yuan, D. Liu, L. Deng, J. Zhou, W. Yu, F. Chen, A hierarchically porous diatomite/silicalite-1 composite for benzene adsorption/desorption fabricated via a facile pre-modification in situ synthesis route, Chem. Eng. J. 294 (2016) 333–342. doi.org/10.1016/j.cej.2016.02.099.

[185] K.H. Kim, J.E. Szulejko, N. Raza, V. Kumar, K. Vikrant, D.C.W. Tsang, N.S. Bolan, Y.S. Ok, A. Khan, Identifying the best materials for the removal of airborne toluene based on performance metrics - A critical review, J. Clean. Prod. 241 (2019) 118408. doi.org/10.1016/j.jclepro.2019.118408.

[186] T.C. Drage, A. Arenillas, K.M. Smith, C.E. Snape, Thermal stability of polyethylenimine based

carbon dioxide adsorbents and its influence on selection of regeneration strategies, Microporous Mesoporous Mater. 116 (2008) 504–512. doi.org/10.1016/j.micromeso.2008.05.009.

[187] S. Liu, Y. Peng, J. Chen, W. Shi, T. Yan, B. Li, Y. Zhang, J. Li, Engineering surface functional groups on mesoporous silica: towards a humidity-resistant hydrophobic adsorbent, J. Mater. Chem. A. 6 (2018) 13769–13777. doi.org/10.1039/c8ta04082f.

[188] C. Kim, W. Choi, M. Choi, SO 2 -Resistant Amine-Containing CO 2 Adsorbent with a Surface Protection Layer, ACS Appl. Mater. Interfaces. 11 (2019) 16586–16593. doi.org/10.1021/acsami.9b02831.

[189] X. Wang, H. Cheng, G. Ye, J. Fan, F. Yao, Y. Wang, Y. Jiao, W. Zhu, H. Huang, D. Ye, Key factors and primary modification methods of activated carbon and their application in adsorption of carbon-based gases: A review, Chemosphere. 287 (2022) 131995. doi.org/10.1016/j.chemosphere.2021.131995.

[190] S.M. Abegunde, K.S. Idowu, O.M. Adejuwon, T. Adeyemi-Adejolu, A review on the influence of chemical modification on the performance of adsorbents, Resour. Environ. Sustain. 1 (2020) 100001. doi.org/10.1016/j.resenv.2020.100001.

[191] W. Xu, A. Hussain, Y. Liu, A review on modification methods of adsorbents for elemental mercury from flue gas, Chem. Eng. J. 346 (2018) 692–711. doi.org/10.1016/j.cej.2018.03.049.

[192] L. Zhu, D. Shen, K.H. Luo, A critical review on VOCs adsorption by different porous materials: Species, mechanisms and modification methods, J. Hazard. Mater. 389 (2020) 122102. doi.org/10.1016/j.jhazmat.2020.122102.

[193] B. Petrovic, M. Gorbounov, S. Masoudi Soltani, Influence of surface modification on selective CO2 adsorption: A technical review on mechanisms and methods, Microporous Mesoporous Mater. 312 (2021) 110751. doi.org/10.1016/j.micromeso.2020.110751.

[194] J. Shao, J. Zhang, X. Zhang, Y. Feng, H. Zhang, S. Zhang, H. Chen, Enhance SO2 adsorption performance of biochar modified by CO2 activation and amine impregnation, Fuel. 224 (2018) 138–146. doi.org/10.1016/j.fuel.2018.03.064.

[195] O. Hwang, S.R. Lee, S. Cho, K.S. Ro, M. Spiehs, B. Woodbury, P.J. Silva, D.W. Han, H. Choi, K.Y. Kim, M.W. Jung, Efficacy of Different Biochars in Removing Odorous Volatile Organic Compounds (VOCs) Emitted from Swine Manure, ACS Sustain. Chem. Eng. 6 (2018) 14239–14247. doi.org/10.1021/acssuschemeng.8b02881.

[196] S.M. Hong, H.J. Yoon, Y. Choi, Y.Z. Cho, S. Mun, V.G. Pol, K.B. Lee, Solving two environmental problems simultaneously: Scalable production of carbon microsheets from structured packing peanuts with tailored microporosity for efficient CO2 capture, Chem. Eng. J. 379 (2020) 122219. doi.org/10.1016/j.cej.2019.122219.

[197] N. Wibowo, L. Setyadhi, D. Wibowo, J. Setiawan, S. Ismadji, Adsorption of benzene and toluene from aqueous solutions onto activated carbon and its acid and heat treated forms: Influence of surface chemistry on adsorption, J. Hazard. Mater. 146 (2007) 237–242. doi.org/10.1016/j.jhazmat.2006.12.011.

[198] C. Zhang, W.J. Koros, Tailoring the Transport Properties of Zeolitic Imidazolate Frameworks by Post-Synthetic Thermal Modification, ACS Appl. Mater. Interfaces. 7 (2015) 23407–23411. doi.org/10.1021/acsami.5b07769.

[199] S. Builes, L.F. Vega, Effect of immobilized amines on the sorption properties of solid materials: Impregnation versus grafting, Langmuir. 29 (2013) 199–206. doi.org/10.1021/la3038507.

[200] Y. An, Q. Fu, D. Zhang, Y. Wang, Z. Tang, Performance evaluation of activated carbon with different pore sizes and functional groups for VOC adsorption by molecular simulation, Chemosphere. 227 (2019) 9–16. doi.org/10.1016/j.chemosphere.2019.04.011.

[201] Z. Wu, P.A. Webley, D. Zhao, Comprehensive study of pore evolution, mesostructural stability, and simultaneous surface functionalization of ordered mesoporous carbon (FDU-15) by wet oxidation as a promising adsorbent, Langmuir. 26 (2010) 10277–10286. doi.org/10.1021/la100455w.

[202] M.G. Plaza, K.J. Thurecht, C. Pevida, F. Rubiera, J.J. Pis, C.E. Snape, T.C. Drage, Influence of oxidation upon the CO2 capture performance of a phenolic-resin-derived carbon, Fuel Process. Technol. 110 (2013) 53–60. doi.org/10.1016/j.fuproc.2013.01.011.

[203] X. Han, H. Lin, Y. Zheng, The role of oxygen functional groups in the adsorption of heteroaromatic nitrogen compounds, J. Hazard. Mater. 297 (2015) 217–223. doi.org/10.1016/j.jhazmat.2015.04.056.

[204] J. Zhang, Y. Duan, Q. Zhou, C. Zhu, M. She, W. Ding, Adsorptive removal of gas-phase mercury by oxygen non-thermal plasma modified activated carbon, Chem. Eng. J. 294 (2016) 281–289. doi.org/10.1016/j.cej.2016.02.002.

[205] P. Sun, B. Zhang, X. Zeng, G. Luo, X. Li, H. Yao, C. Zheng, Deep study on effects of activated carbon's oxygen functional groups for elemental mercury adsorption using temperature programmed desorption method, Fuel. 200 (2017) 100–106. doi.org/10.1016/j.fuel.2017.03.031.

[206] R. Dawson, D.J. Adams, A.I. Cooper, Chemical tuning of CO2 sorption in robust nanoporous organic polymers, Chem. Sci. 2 (2011) 1173–1177. doi.org/10.1039/c1sc00100k.

[207] B. Sajjadi, W.Y. Chen, N.O. Egiebor, A comprehensive review on physical activation of biochar for energy and environmental applications, Rev. Chem. Eng. 35 (2019) 735–776. doi.org/10.1515/revce-2017-0113.

[208] Y. You, J. Deng, X. Tan, N. Gorjizadeh, M. Yoshimura, S.C. Smith, V. Sahajwalla, R.K. Joshi, On

the mechanism of gas adsorption for pristine, defective and functionalized graphene, Phys. Chem. Chem. Phys. 19 (2017) 6051–6056. doi.org/10.1039/c6cp07654h.

[209] H. Liu, Y. Yu, Q. Shao, C. Long, Porous polymeric resin for adsorbing low concentration of VOCs: Unveiling adsorption mechanism and effect of VOCs' molecular properties, Sep. Purif. Technol. 228 (2019) 115755. doi.org/10.1016/j.seppur.2019.115755.

[210] K.V. Kumar, K. Preuss, L. Lu, Z.X. Guo, M.M. Titirici, Effect of Nitrogen Doping on the CO2 Adsorption Behavior in Nanoporous Carbon Structures: A Molecular Simulation Study, J. Phys. Chem. C. 119 (2015) 22310–22321. doi.org/10.1021/acs.jpcc.5b06017.

[211] Y. Zhao, X. Liu, K.X. Yao, L. Zhao, Y. Han, Superior capture of CO2 achieved by introducing extra-framework cations into N-doped microporous carbon, Chem. Mater. 24 (2012) 4725–4734. doi.org/10.1021/cm303072n.

[212] T. Horikawa, N. Sakao, T. Sekida, J. Hayashi, D.D. Do, M. Katoh, Preparation of nitrogen-doped porous carbon by ammonia gas treatment and the effects of N-doping on water adsorption, Carbon 50 (2012) 1833–1842. doi.org/10.1016/j.carbon.2011.12.033.

[213] A.A. Azmi, A.H. Ruhaimi, M.A.A. Aziz, Efficient 3-aminopropyltrimethoxysilane functionalised mesoporous ceria nanoparticles for CO2 capture, Mater. Today Chem. 16 (2020) 100273. doi.org/10.1016/j.mtchem.2020.100273.

[214] P.J. Milner, R.L. Siegelman, A.C. Forse, M.I. Gonzalez, T. Runčevski, J.D. Martell, J.A. Reimer, J.R. Long, A Diaminopropane-Appended Metal-Organic Framework Enabling Efficient CO2 Capture from Coal Flue Gas via a Mixed Adsorption Mechanism, J. Am. Chem. Soc. 139 (2017) 13541–13553. doi.org/10.1021/jacs.7b07612.

[215] M.I. Swasy, M.L. Campbell, B.R. Brummel, F.D. Guerra, M.F. Attia, G.D. Smith, F. Alexis, D.C. Whitehead, Poly(amine) modified kaolinite clay for VOC capture, Chemosphere. 213 (2018) 19–24. doi.org/10.1016/j.chemosphere.2018.08.156.

[216] V. Safarifard, S. Rodríguez-Hermida, V. Guillerm, I. Imaz, M. Bigdeli, A.A. Tehrani, J. Juanhuix, A. Morsali, M.E. Casco, J. Silvestre-Albero, E. V. Ramos-Fernandez, D. Maspoch, Influence of the Amide Groups in the CO2/N2 Selectivity of a Series of Isoreticular, Interpenetrated Metal-Organic Frameworks, Cryst. Growth Des. 16 (2016) 6016–6023. doi.org/10.1021/acs.cgd.6b01054.

[217] A. Torrisi, C. Mellot-Draznieks, R.G. Bell, Impact of ligands on CO2 adsorption in metal-organic frameworks: First principles study of the interaction of CO2 with functionalized benzenes. II. Effect of polar and acidic substituents, J. Chem. Phys. 132 (2010). doi.org/10.1063/1.3276105.

[218] X. Ma, L. Li, R. Chen, C. Wang, H. Li, S. Wang, Heteroatom-doped nanoporous carbon derived from MOF-5 for CO 2 capture, Appl. Surf. Sci. 435 (2018) 494–502. doi.org/10.1016/j.apsusc.2017.11.069.

[219] G.P. Hao, W.C. Li, D. Qian, A.H. Lu, Rapid synthesis of nitrogen-doped porous carbon monolith for CO2 capture, Adv. Mater. 22 (2010) 853–857. doi.org/10.1002/adma.200903765.

[220] K. Zhou, W. Ma, Z. Zeng, X. Ma, X. Xu, Y. Guo, H. Li, L. Li, Experimental and DFT study on the adsorption of VOCs on activated carbon/metal oxides composites, Chem. Eng. J. 372 (2019) 1122–1133. doi.org/10.1016/j.cej.2019.04.218.

[221] I.A. Aguayo-Villarreal, M.A. Montes-Morán, V. Hernández-Montoya, A. Bonilla-Petriciolet, A. Concheso, C.K. Rojas-Mayorga, J. González, Importance of iron oxides on the carbons surface vs the specific surface for VOC's adsorption, Ecol. Eng. 106 (2017) 400–408. doi.org/10.1016/j.ecoleng.2017.05.043.

[222] S. Peng, W. Li, Y. Deng, W. Li, X. Ma, Y. Chen, Removal of low concentration CH3SH with regenerable Cu-doped mesoporous silica, J. Colloid Interface Sci. 513 (2018) 903–910. doi.org/10.1016/j.jcis.2017.12.005.

[223] D. Wang, G. Wu, Y. Zhao, L. Cui, C.H. Shin, M.H. Ryu, J. Cai, Study on the copper(II)-doped MIL-101(Cr) and its performance in VOCs adsorption, Environ. Sci. Pollut. Res. 25 (2018) 28109–28119. doi.org/10.1007/s11356-018-2849-6.

[224] W.D.P. Rengga, A. Chafidz, M. Sudibandriyo, M. Nasikin, A.E. Abasaeed, Silver nano-particles deposited on bamboo-based activated carbon for removal of formaldehyde, J. Environ. Chem. Eng. 5 (2017) 1657–1665. doi.org/10.1016/j.jece.2017.02.033.

[225] J.A. Arcibar-Orozco, J.R. Rangel-Mendez, T.J. Bandosz, Reactive adsorption of SO2 on activated carbons with deposited iron nanoparticles, J. Hazard. Mater. 246–247 (2013) 300–309. doi.org/10.1016/j.jhazmat.2012.12.001.

[226] Y. Lv, J. Sun, G. Yu, W. Wang, Z. Song, X. Zhao, Y. Mao, Hydrophobic design of adsorbent for VOC removal in humid environment and quick regeneration by microwave, Microporous Mesoporous Mater. 294 (2020) 109869. doi.org/10.1016/j.micromeso.2019.109869.

[227] N. Saad, M. Chaaban, D. Patra, A. Ghanem, H. El-Rassy, Molecularly imprinted phenyl - functionalized silica aerogels: Selective adsorbents for methylxanthines and PAHs, Microporous Mesoporous Mater. 292 (2020) 109759. doi.org/10.1016/j.micromeso.2019.109759.

[228] H. Molavi, A. Eskandari, A. Shojaei, S.A. Mousavi, Enhancing CO2/N2 adsorption selectivity via post-synthetic modification of NH2-UiO-66(Zr), Microporous Mesoporous Mater. 257 (2018) 193–201. doi.org/10.1016/j.micromeso.2017.08.043.

[229] M.C. Almazán-Almazán, M. Pérez-Mendoza, M. Domingo-García, I. Fernández-Morales, F. del Rey-Bueno, A. García-Rodríguez, F.J. López-Garzón, The role of the porosity and oxygen groups on the adsorption of n-alkanes, benzene, trichloroethylene and 1,2-dichloroethane on active carbons at zero surface coverage, Carbon 45 (2007) 1777–1785.

doi.org/10.1016/j.carbon.2007.05.003.

[230] S. Ullah, M.A. Bustam, M.A. Assiri, A.G. Al-Sehemi, G. Gonfa, A. Mukhtar, F.A. Abdul Kareem, M. Ayoub, S. Saqib, N.B. Mellon, Synthesis and characterization of mesoporous MOF UMCM-1 for CO2/CH4 adsorption; an experimental, isotherm modeling and thermodynamic study, Microporous Mesoporous Mater. 294 (2020) 109844. doi.org/10.1016/j.micromeso.2019.109844.

[231] International Organization for Standarization, ISO 9277 : Determination of the specific surface area of solids by gas adsorption — BET method, 2010.

[232] K.A. Cychosz, R. Guillet-Nicolas, J. García-Martínez, M. Thommes, Recent advances in the textural characterization of hierarchically structured nanoporous materials, Chem. Soc. Rev. 46 (2017) 389–414. doi.org/10.1039/c6cs00391e.

[233] K. Sing, The use of nitrogen adsorption for the characterisation of porous materials, Colloids Surfaces A Physicochem. Eng. Asp. 187–188 (2001) 3–9. doi.org/10.1016/S0927-7757(01)00612-4.

[234] M. Thommes, K.A. Cychosz, Physical adsorption characterization of nanoporous materials: Progress and challenges, Adsorption. 20 (2014) 233–250. doi.org/10.1007/s10450-014-9606-z.

[235] K.V. Kumar, S. Gadipelli, B. Wood, K.A. Ramisetty, A.A. Stewart, C.A. Howard, D.J.L. Brett, F. Rodriguez-Reinoso, Characterization of the adsorption site energies and heterogeneous surfaces of porous materials, J. Mater. Chem. A. 7 (2019) 10104–10137. doi.org/10.1039/c9ta00287a.

[236] R. Chen, N. Han, L. Li, S. Wang, X. Ma, C. Wang, H. Li, H. Li, L. Zeng, Fundamental understanding of oxygen content in activated carbon on acetone adsorption desorption, Appl. Surf. Sci. 508 (2020) 145211. doi.org/10.1016/j.apsusc.2019.145211.

[237] J.M. Park, D.K. Yoo, S.H. Jhung, Selective CO2 adsorption over functionalized Zr-based metal organic framework under atmospheric or lower pressure: Contribution of functional groups to adsorption, Chem. Eng. J. 402 (2020) 126254. doi.org/10.1016/j.cej.2020.126254.

[238] N.H.M. Hossein Tehrani, M.S. Alivand, A. Rashidi, K. Rahbar Shamskar, M. Samipoorgiri, M.D. Esrafili, D. Mohammady Maklavany, M. Shafiei-Alavijeh, Preparation and characterization of a new waste-derived mesoporous carbon structure for ultrahigh adsorption of benzene and toluene at ambient conditions, J. Hazard. Mater. 384 (2020). doi.org/10.1016/j.jhazmat.2019.121317.

[239] X. Zhang, X. Miao, W. Xiang, J. Zhang, C. Cao, Ball milling biochar with ammonia hydroxide or hydrogen peroxide enhances its adsorption of phenyl volatile organic compounds (VOCs), J. Hazard. Mater. 403 (2021) 123540. doi.org/10.1016/j.jhazmat.2020.123540.

[240] M.F. de Aguiar, G.L. V Coelho, Adsorption of sulfur compounds from natural gas by different

adsorbents and desorption using supercritical CO 2, J. Environ. Chem. Eng. 5 (2017) 4353–4364. doi.org/10.1016/j.jece.2017.07.079.

[241] A.A. Dabbawala, I. Ismail, B. V. Vaithilingam, K. Polychronopoulou, G. Singaravel, S. Morin, M. Berthod, Y. Al Wahedi, Synthesis of hierarchical porous Zeolite-Y for enhanced CO2 capture, Microporous Mesoporous Mater. 303 (2020) 110261. doi.org/10.1016/j.micromeso.2020.110261.

[242] Y. Wu, D. Yuan, D. He, J. Xing, S. Zeng, S. Xu, Y. Xu, Z. Liu, Decorated Traditional Zeolites with Subunits of Metal–Organic Frameworks for CH4/N2 Separation, Angew. Chemie - Int. Ed. 58 (2019) 10241–10244. doi.org/10.1002/anie.201905014.

[243] M. Maciejewska, M. Rogulska, Synthesis and characterization of VP–DMN polymeric sorbents, Adsorption. 25 (2019) 419–427. doi.org/10.1007/s10450-019-00031-7.

[244] Y. Li, R. Xu, B. Wang, J. Wei, L. Wang, M. Shen, J. Yang, Enhanced n-doped porous carbon derived from koh-activated waste wool: A promising material for selective adsorption of CO2/CH4 and CH4/N2, Nanomaterials. 9 (2019). doi.org/10.3390/nano9020266.

[245] J. Zhu, L. Wu, Z. Bu, S. Jie, B.G. Li, Polyethylenimine-Grafted HKUST-Type MOF/PolyHIPE Porous Composites (PEI@PGD-H) as Highly Efficient CO2 Adsorbents, Ind. Eng. Chem. Res. 58 (2019) 4257–4266. doi.org/10.1021/acs.iecr.9b00213.

[246] D. Nakrani, M. Belani, H.C. Bajaj, R.S. Somani, P.S. Singh, Concentrated colloidal solution system for preparation of uniform Zeolite-Y nanocrystals and their gas adsorption properties, Microporous Mesoporous Mater. 241 (2017) 274–284. doi.org/10.1016/j.micromeso.2016.12.039.

[247] A. Gholidoust, J.D. Atkinson, Z. Hashisho, Enhancing CO2 Adsorption via Amine-Impregnated Activated Carbon from Oil Sands Coke, Energy and Fuels. 31 (2017) 1756–1763. doi.org/10.1021/acs.energyfuels.6b02800.

[248] D.K. Yoo, T.U. Yoon, Y.S. Bae, S.H. Jhung, Metal-organic framework MIL-101 loaded with polymethacrylamide with or without further reduction: Effective and selective CO2 adsorption with amino or amide functionality, Chem. Eng. J. 380 (2020) 122496. doi.org/10.1016/j.cej.2019.122496.

[249] M. He, T. Xu, Z. Jiang, L. Yang, Y. Zou, F. Xia, X. Wang, X. Wang, Y. He, Incorporation of bifunctional aminopyridine into an NbO-type MOF for the markedly enhanced adsorption of CO2 and C2H2 over CH4, Inorg. Chem. Front. 6 (2019) 1177–1183. doi.org/10.1039/c9qi00195f.

[250] X. Su, L. Bromberg, V. Martis, F. Simeon, A. Huq, T.A. Hatton, Postsynthetic Functionalization of Mg-MOF-74 with Tetraethylenepentamine: Structural Characterization and Enhanced CO2 Adsorption, ACS Appl. Mater. Interfaces. 9 (2017) 11299–11306.

doi.org/10.1021/acsami.7b02471.

[251] B.C. Smith, Fundamentals of Fourier Transform Infrared Spectroscopy, 2nd ed., CRC Press, 2011.

[252] A. Pophali, K.M. Lee, L. Zhang, Y.C. Chuang, L. Ehm, M.A. Cuiffo, G.P. Halada, M. Rafailovich, N. Verma, T. Kim, First synthesis of poly(furfuryl) alcohol precursor-based porous carbon beads as an efficient adsorbent for volatile organic compounds, Chem. Eng. J. 373 (2019) 365–374. doi.org/10.1016/j.cej.2019.05.029.

[253] L. Asgharnejad, A. Abbasi, A. Shakeri, Ni-based metal-organic framework/GO nanocomposites as selective adsorbent for CO2 over N2, Microporous Mesoporous Mater. 262 (2018) 227–234. doi.org/10.1016/j.micromeso.2017.11.038.

[254] M. Plata-Gryl, M. Momotko, S. Makowiec, G. Boczkaj, Highly effective asphaltene-derived adsorbents for gas phase removal of volatile organic compounds, Sep. Purif. Technol. 224 (2019) 315–321. doi.org/10.1016/j.seppur.2019.05.041.

[255] M. Plata-Gryl, M. Momotko, S. Makowiec, G. Boczkaj, Application of cyanated asphaltenes in gas-phase adsorption processes for removal of volatile organic compounds, Chem. Pap. 74 (2020) 995–1008. doi.org/10.1007/s11696-019-00938-z.

[256] G. Sargazi, D. Afzali, A. Mostafavi, A novel microwave assisted reverse micelle fabrication route for Th (IV)-MOFs as highly efficient adsorbent nanostructures with controllable structural properties to CO and CH 4 adsorption: Design, and a systematic study, Appl. Organomet. Chem. 33 (2019) 1–12. doi.org/10.1002/aoc.4816.

[257] S. Kayal, A. Chakraborty, Activated carbon (type Maxsorb-III) and MIL-101(Cr) metal organic framework based composite adsorbent for higher CH4 storage and CO2 capture, Chem. Eng. J. 334 (2018) 780–788. doi.org/10.1016/j.cej.2017.10.080.

[258] M. Zhu, K. Zhou, X. Sun, Z. Zhao, Z. Tong, Z. Zhao, Hydrophobic N-doped porous biocarbon from dopamine for high selective adsorption of p-Xylene under humid conditions, Chem. Eng. J. 317 (2017) 660–672. doi.org/10.1016/j.cej.2017.02.114.

[259] X. Wang, C. Ma, J. Xiao, Q. Xia, J. Wu, Z. Li, Benzene/toluene/water vapor adsorption and selectivity of novel C-PDA adsorbents with high uptakes of benzene and toluene, Chem. Eng. J. 335 (2018) 970–978. doi.org/10.1016/j.cej.2017.10.102.

[260] D. Noreña-Caro, M. Álvarez-Láinez, Functionalization of polyacrylonitrile nanofibers with β-cyclodextrin for the capture of formaldehyde, Mater. Des. 95 (2016) 632–640. doi.org/10.1016/j.matdes.2016.01.106.

[261] L. Zhu, X. Lv, S. Tong, T. Zhang, Y. Song, Y. Wang, Z. Hao, C. Huang, D. Xia, Modification of zeolite by metal and adsorption desulfurization of organic sulfide in natural gas, J. Nat. Gas Sci. Eng. 69 (2019) 102941. doi.org/10.1016/j.jngse.2019.102941.

[262] L.M. Petrova, N.A. Abbakumova, T.R. Foss, G. V. Romanov, Structural features of asphaltene and petroleum resin fractions, Pet. Chem. 51 (2011) 252–256. doi.org/10.1134/S0965544111040062.

[263] Y. Li, Y. Guo, T. Zhu, S. Ding, Adsorption and desorption of SO2, NO and chlorobenzene on activated carbon, J. Environ. Sci. (China). 43 (2016) 128–135. doi.org/10.1016/j.jes.2015.08.022.

[264] F. Meng, M. Song, Y. Wei, Y. Wang, The contribution of oxygen-containing functional groups to the gas-phase adsorption of volatile organic compounds with different polarities onto lignin-derived activated carbon fibers, Environ. Sci. Pollut. Res. 26 (2019) 7195–7204. doi.org/10.1007/s11356-019-04190-6.

[265] S.W. Bian, J. Baltrusaitis, P. Galhotra, V.H. Grassian, A template-free, thermal decomposition method to synthesize mesoporous MgO with a nanocrystalline framework and its application in carbon dioxide adsorption, J. Mater. Chem. 20 (2010) 8705–8710. doi.org/10.1039/c0jm01261k.

[266] H. Valdés, A.L. Riquelme, V.A. Solar, F. Azzolina-Jury, F. Thibault-Starzyk, Removal of chlorinated volatile organic compounds onto natural and Cu-modified zeolite: The role of chemical surface characteristics in the adsorption mechanism, Sep. Purif. Technol. 258 (2021) 118080. doi.org/10.1016/j.seppur.2020.118080.

[267] D.T. Yazici, C. Bilgiç, Determining the surface acidic properties of solid catalysts by amine titration using Hammett indicators and FTIR-pyridine adsorption methods, Surf. Interface Anal. 42 (2010) 959–962. doi.org/10.1002/sia.3474.

[268] R. Chen, Z. Yao, N. Han, X. Ma, L. Li, S. Liu, H. Sun, S. Wang, L. Li, S. Wang, Insights into the Adsorption of VOCs on a Cobalt-Adeninate Metal-Organic Framework (Bio-MOF-11), ACS Omega. 5 (2020) 15402–15408. doi.org/10.1021/acsomega.0c01504.

[269] Z. Yang, H. Miao, Z. Rui, H. Ji, Enhanced formaldehyde removal from air using fully biodegradable chitosan grafted β-Cyclodextrin adsorbent withweak chemical interaction, Polymers (Basel). 11 (2019). doi.org/10.3390/polym11020276.

[270] A.H. Mamaghani, F. Haghighat, C.S. Lee, Gas phase adsorption of volatile organic compounds onto titanium dioxide photocatalysts, Chem. Eng. J. 337 (2018) 60–73. doi.org/10.1016/j.cej.2017.12.082.

[271] Z. Cheng, K. Feng, Y. Su, J. Ye, D. Chen, S. Zhang, X. Zhang, D.D. Dionysiou, Novel biosorbents synthesized from fungal and bacterial biomass and their applications in the adsorption of volatile organic compounds, Bioresour. Technol. 300 (2020) 122705. doi.org/10.1016/j.biortech.2019.122705.

[272] H. Wang, T. Wang, L. Han, M. Tang, J. Zhong, W. Huang, R. Chen, VOC adsorption and

desorption behavior of hydrophobic, functionalized SBA-15, J. Mater. Res. 31 (2016) 516–525. doi.org/10.1557/jmr.2016.40.

[273] G. Autie-Castro, M.A. Autie, E. Rodríguez-Castellón, C. Aguirre, E. Reguera, Cu-BTC and Fe-BTC metal-organic frameworks: Role of the materials structural features on their performance for volatile hydrocarbons separation, Colloids Surfaces A Physicochem. Eng. Asp. 481 (2015) 351–357. doi.org/10.1016/j.colsurfa.2015.05.044.

[274] J.R. Conder, C.L. Young, Physicochemical Measurements by Gas Chromatography, Wiley, 1979.

[275] A. Voelkel, B. Strzemiecka, K. Adamska, K. Milczewska, Inverse gas chromatography as a source of physiochemical data, J. Chromatogr. A. 1216 (2009) 1551–1566. doi.org/10.1016/J.CHROMA.2008.10.096.

[276] S. Mohammadi-Jam, K.E. Waters, Inverse gas chromatography applications: A review, Adv. Colloid Interface Sci. 212 (2014) 21–44. doi.org/10.1016/j.cis.2014.07.002.

[277] F. Thielmann, D.A. Butler, D.R. Williams, E. Baumgarten, Characterisation of microporous materials by dynamic sorption methods, Stud. Surf. Sci. Catal. 129 (2000) 633–638. doi.org/10.1016/s0167-2991(00)80266-9.

[278] B. Charmas, R. Leboda, Effect of surface heterogeneity on adsorption on solid surfaces, J. Chromatogr. A. 886 (2000) 133–152. doi.org/10.1016/s0021-9673(00)00432-5.

[279] A. Pal, A. Kondor, S. Mitra, K. Thu, S. Harish, B.B. Saha, On surface energy and acid–base properties of highly porous parent and surface treated activated carbons using inverse gas chromatography, J. Ind. Eng. Chem. 69 (2019) 432–443. doi.org/10.1016/j.jiec.2018.09.046.

[280] V.Y. Gus'kov, A.G. Ganieva, F.K. Kudasheva, Monolayer capacity estimation by inverse gas chromatography at finite concentrations, Colloids Surfaces A Physicochem. Eng. Asp. 513 (2017) 95–101. doi.org/10.1016/j.colsurfa.2016.11.039.

[281] S.C. Das, I. Larson, D.A.V. Morton, P.J. Stewart, Determination of the polar and total surface energy distributions of particulates by inverse gas chromatography, Langmuir. 27 (2011) 521–523. doi.org/10.1021/la104135z.

[282] S. Dong, M. Brendlé, J.B. Donnet, Study of solid surface polarity by inverse gas chromatography at infinite dilution, Chromatographia. 28 (1989) 469–472. doi.org/10.1007/BF02261062.

[283] F. Thielmann, Introduction into the characterisation of porous materials by inverse gas chromatography, J. Chromatogr. A. 1037 (2004) 115–123. doi.org/10.1016/J.CHROMA.2004.03.060.

[284] F. Gholami, M. Tomas, Z. Gholami, S. Mirzaei, M. Vakili, Surface Characterization of Carbonaceous Materials Using Inverse Gas Chromatography: A Review, Electrochem. 1 (2020) 367–387. doi.org/10.3390/electrochem1040024.

[285] F. Thielmann, D.A. Butler, D.R. Williams, Characterization of porous materials by finite concentration inverse gas chromatography, Colloids Surfaces A Physicochem. Eng. Asp. 187–188 (2001) 267–272. doi.org/10.1016/S0927-7757(01)00640-9.

[286] F. Thielmann, E. Baumgarten, Characterization of Microporous Aluminas by Inverse Gas Chromatography, J. Colloid Interface Sci. 229 (2000) 418–422. doi.org/10.1006/jcis.2000.6958.

[287] M. Rückriem, A. Inayat, D. Enke, R. Gläser, W.D. Einicke, R. Rockmann, Inverse gas chromatography for determining the dispersive surface energy of porous silica, Colloids Surfaces A Physicochem. Eng. Asp. 357 (2010) 21–26. doi.org/10.1016/j.colsurfa.2009.12.001.

[288] Y. Yampolskii, N. Belov, Investigation of Polymers by Inverse Gas Chromatography, Macromolecules. 48 (2015) 6751–6767. doi.org/10.1021/acs.macromol.5b00895.

[289] J.A.F. Gamelas, The surface properties of cellulose and lignocellulosic materials assessed by inverse gas chromatography: A review, Cellulose. 20 (2013) 2675–2693. doi.org/10.1007/s10570-013-0066-5.

[290] L. Lapčík, M. Otyepka, E. Otyepková, B. Lapčíková, R. Gabriel, A. Gavenda, B. Prudilová, Surface heterogeneity: Information from inverse gas chromatography and application to model pharmaceutical substances, Curr. Opin. Colloid Interface Sci. 24 (2016) 64–71. doi.org/10.1016/j.cocis.2016.06.010.

[291] E.H. Denis, C.G. Fraga, N.L. Huggett, W.C. Weaver, L.A. Rush, B.P. Dockendorff, A.S. Breton-Vega, A.J. Carman, Physicochemical Gas-Solid Sorption Properties of Geologic Materials Using Inverse Gas Chromatography, Langmuir. 37 (2021) 6887–6897. doi.org/10.1021/acs.langmuir.0c03676.

[292] F. Thielmann, D. Pearse, Determination of surface heterogeneity profiles on graphite by finite concentration inverse gas chromatography, J. Chromatogr. A. 969 (2002) 323–327. doi.org/10.1016/S0021-9673(02)00896-8.

[293] A. Voelkel, Inverse gas chromatography in characterization of surface, Chemom. Intell. Lab. Syst. 72 (2004) 205–207. doi.org/10.1016/j.chemolab.2004.01.016.

[294] W.O. McReynolds, Characterization of some liquid phases, J. Chromatogr. Sci. 8 (1970) 685–691. doi.org/10.1093/chromsci/8.12.685.

[295] L. Rohrschneider, A method of characterization of the liquids used for separation in gas chromatography, J. Chromatogr. A. 22 (1966) 6–22.

[296] R. Rajkó, T. Körtvélyesi, K. Sebok-Nagy, M. Görgényi, Theoretical characterization of McReynolds' constants, Anal. Chim. Acta. 554 (2005) 163–171. doi.org/10.1016/j.aca.2005.08.024.

[297] A.I. Makarycheva, Y.G. Slizhov, V.P. Kirin, Adsorption properties of new Silochrome-based chelate-containing gas chromatographic materials, Russ. J. Appl. Chem. 90 (2017) 533–540.

doi.org/10.1134/S1070427217040073.

[298] Q. Qu, Y. Shen, C. Gu, Z. Gu, Q. Gu, C. Wang, X. Hu, Capillary column coated with graphene oxide as stationary phase for gas chromatography, Anal. Chim. Acta. 757 (2012) 83–87. doi.org/10.1016/j.aca.2012.10.032.

[299] M. Maciejewska, J. Osypiuk-Tomasik, Sorption on porous copolymers of 1-vinyl-2-pyrrolidonedivinylbenzene, J. Therm. Anal. Calorim. 114 (2013) 749–755. doi.org/10.1007/s10973-013-3107-2.

[300] Y. V. Patrushev, E.Y. Yakovleva, I.K. Shundrina, D.P. Ivanov, T.S. Glazneva, The properties of capillary columns with sorbents based on poly-(1-trimethylsilyl-1-propyne) modified with nitrous oxide, J. Chromatogr. A. 1406 (2015) 291–298. doi.org/10.1016/j.chroma.2015.06.013.

[301] Z.Y. Gu, D.Q. Jiang, H.F. Wang, X.Y. Cui, X.P. Yan, Adsorption and separation of xylene isomers and ethylbenzene on two Zn-terephthalate metal-organic frameworks, J. Phys. Chem. C. 114 (2010) 311–316. doi.org/10.1021/jp9063017.

[302] X. Yang, C. Li, M. Qi, L. Qu, Graphene-ZIF8 composite material as stationary phase for high-resolution gas chromatographic separations of aliphatic and aromatic isomers, J. Chromatogr. A. 1460 (2016) 173–180. doi.org/10.1016/j.chroma.2016.07.029.

[303] J. Zheng, C. Lu, J. Huang, L. Chen, C. Ni, X. Xie, F. Zhu, D. Wu, G. Ouyang, Fabrication of powdery polymer aerogel as the stationary phase for high-resolution gas chromatographic separation, Talanta. 186 (2018) 445–451. doi.org/10.1016/j.talanta.2018.04.096.

[304] G. Boczkaj, M. Momotko, D. Chruszczyk, A. Przyjazny, M. Kamiński, Novel stationary phases based on asphaltenes for gas chromatography, J. Sep. Sci. 39 (2016) 2527–2536. doi.org/10.1002/jssc.201600183.

[305] M. Plata-Gryl, M. Momotko, S. Makowiec, G. Boczkaj, Application of cyanated asphaltenes in gas-phase adsorption processes for removal of volatile organic compounds, Chem. Pap. 74 (2020) 995–1008. doi.org/10.1007/s11696-019-00938-z.

[306] M.H. Abraham, C.F. Poole, S.K. Poole, Classification of stationary phases and other materials by gas chromatography, J. Chromatogr. A. 842 (1999) 79–114. doi.org/10.1016/S0021-9673(98)00930-3.

[307] M.H. Abraham, A. Ibrahim, A.M. Zissimos, Determination of sets of solute descriptors from chromatographic measurements, J. Chromatogr. A. 1037 (2004) 29–47. doi.org/10.1016/j.chroma.2003.12.004.

[308] B. Shi, Y. Wang, L. Jia, Comparison of Dorris-Gray and Schultz methods for the calculation of surface dispersive free energy by inverse gas chromatography, J. Chromatogr. A. 1218 (2011) 860–862. doi.org/10.1016/j.chroma.2010.12.050.

[309] G.M. Dorris, D.G. Gray, Adsorption of n-alkanes at zero surface coverage on cellulose paper

and wood fibers, J. Colloid Interface Sci. 77 (1980) 353–362. doi.org/10.1016/0021-9797(80)90304-5.

[310] E. Brendlé, E. Papirer, A new topological index for molecular probes used in inverse gas chromatography 2. Application for the evaluation of the solid surface specific interaction potential, J. Colloid Interface Sci. 194 (1997) 217–224. doi.org/10.1006/jcis.1997.5105.

[311] C.J. van Oss, R.J. Good, M.K. Chaudhury, Additive and nonadditive surface tension components and the interpretation of contact angles, Langmuir. 4 (1988) 884–891. doi.org/10.1021/la00082a018.

[312] C.J. van Oss, Acid-base interfacial interactions in aqueous media, Colloids Surfaces A Physicochem. Eng. Asp. 78 (1993) 1–49. doi.org/10.1016/0927-7757(93)80308-2.

[313] M.L. Palash, A. Pal, T.H. Rupam, B.D. Park, B.B. Saha, Surface energy characterization of different particulate silica gels at infinite dilution, Colloids Surfaces A Physicochem. Eng. Asp. 603 (2020). doi.org/10.1016/j.colsurfa.2020.125209.

[314] A. Legras, A. Kondor, M. Alcock, M.T. Heitzmann, R.W. Truss, Inverse gas chromatography for natural fibre characterisation: dispersive and acid-base distribution profiles of the surface energy, Cellulose. 24 (2017) 4691–4700. doi.org/10.1007/s10570-017-1443-2.

[315] R. Ho, J.Y.Y. Heng, A review of inverse gas chromatography and its development as a tool to characterize anisotropic surface properties of pharmaceutical solids, KONA Powder Part. J. 30 (2012) 164–180. doi.org/10.14356/kona.2013016.

[316] R.R. Smith, D.R. Williams, D.J. Burnett, J.Y.Y. Heng, A new method to determine dispersive surface energy site distributions by inverse gas chromatography, Langmuir. 30 (2014) 8029–8035. doi.org/10.1021/la500688d.

[317] J.E. Szulejko, K.H. Kim, Is the maximum adsorption capacity obtained at high VOC pressures (>1000 Pa) really meaningful in real-world applications for the sorptive removal of VOCs under ambient conditions (<1 Pa)?, Sep. Purif. Technol. 228 (2019) 115729. doi.org/10.1016/j.seppur.2019.115729.

[318] S. Lazarević, Ž. Radovanović, D. Veljović, A. Onjia, D. Janaćković, R. Petrović, Characterization of sepiolite by inverse gas chromatography at infinite and finite surface coverage, Appl. Clay Sci. 43 (2009) 41–48. doi.org/10.1016/J.CLAY.2008.07.013.

[319] J. Jagiełło, G. Ligner, E. Papirer, Characterization of silicas by inverse gas chromatography at finite concentration: Determination of the adsorption energy distribution function, J. Colloid Interface Sci. 137 (1990) 128–136. doi.org/10.1016/0021-9797(90)90049-T.

[320] H. Balard, D. Maafa, A. Santini, J.B. Donnet, Study by inverse gas chromatography of the surface properties of milled graphites, J. Chromatogr. A. 1198–1199 (2008) 173–180. doi.org/10.1016/j.chroma.2008.05.012.

[321] H. Balard, Estimation of the surface energetic heterogeneity of a solid by inverse gas chromatography, Langmuir. 13 (1997) 1260–1269. doi.org/10.1002/masy.19961080107.

[322] M. Jaroniec, K.P. Gadkaree, J. Choma, Relation between adsorption potential distribution and pore volume distribution for microporous carbons, Colloids Surfaces A Physicochem. Eng. Asp. 118 (1996) 203–210. doi.org/10.1016/S0927-7757(96)03685-0.

[323] J.. Donnet, E. Custodéro, T.. Wang, G. Hennebert, Energy site distribution of carbon black surfaces by inverse gas chromatography at finite concentration conditions, Carbon N. Y. 40 (2002) 163–167. doi.org/10.1016/S0008-6223(01)00168-3.

[324] H. Sui, P. Jiang, X. Li, J. Liu, X. Li, L. He, Binary Adsorption Equilibrium and Breakthrough of n-Butyl Acetate and p-Xylene on Granular Activated Carbon, Ind. Eng. Chem. Res. 58 (2019) 8279–8289. doi.org/10.1021/acs.iecr.9b00022.

[325] P. Bollini, N.A. Brunelli, S.A. Didas, C.W. Jones, Dynamics of CO2 adsorption on amine adsorbents. 2. insights into adsorbent design, Ind. Eng. Chem. Res. 51 (2012) 15153–15162. doi.org/10.1021/ie3017913.

[326] S.G. Ramalingam, P. Pré, S. Giraudet, L. Le Coq, P. Le Cloirec, O. Baudouin, S. Déchelotte, Different families of volatile organic compounds pollution control by microporous carbons in temperature swing adsorption processes, J. Hazard. Mater. 221–222 (2012) 242–247. doi.org/10.1016/j.jhazmat.2012.04.037.

[327] D.A. Kennedy, M. Mujcin, E. Trudeau, F.H. Tezel, Pure and Binary Adsorption Equilibria of Methane and Nitrogen on Activated Carbons, Desiccants, and Zeolites at Different Pressures, J. Chem. Eng. Data. 61 (2016) 3163–3176. doi.org/10.1021/acs.jced.6b00245.

[328] M.A. Al-Ghouti, D.A. Da'ana, Guidelines for the use and interpretation of adsorption isotherm models: A review, J. Hazard. Mater. 393 (2020) 122383. doi.org/10.1016/j.jhazmat.2020.122383.

[329] J. Keller, R. Staudt, Gas Adsorption Equilibria: Experimental Methods and Adsorptive Isotherms, Springer, Boston, 2005.

[330] I. Langmuir, The adsorption of gases on plane surfaces of glass, mica and platinum, J. Am. Chem. Soc. 40 (1918) 1361–1403. doi.org/10.1021/ja02242a004

[331] N. Dammak, N. Fakhfakh, S. Fourmentin, M. Benzina, Treatment of gas containing hydrophobic VOCs by adsorption process on raw and intercalated clays, Res. Chem. Intermed. 41 (2015) 5475–5493. doi.org/10.1007/s11164-014-1675-9.

[332] H. Bekhti, H. Bouchafaa, R. Melouki, A. Travert, Y. Boucheffa, Adsorption of CO2 over MgO−Impregnated NaYzeolites and modeling study, Microporous Mesoporous Mater. 294 (2020) 109866. doi.org/10.1016/j.micromeso.2019.109866.

[333] H. Wang, B. Wang, J. Li, T. Zhu, Adsorption equilibrium and thermodynamics of

acetaldehyde/acetone on activated carbon, Sep. Purif. Technol. 209 (2019) 535–541. doi.org/10.1016/j.seppur.2018.07.076.

[334] D. Saha, Z. Bao, F. Jia, Deng, Adsorption of CO2, CH4, N2O, and N2 on MOF-5, MOF-177, and zeolite 5A, Environ. Sci. Technol. 44 (2010) 1820–1826. pubs.acs.org/doi/abs/10.1021/es9032309.

[335] M.E. Ramos, P.R. Bonelli, A.L. Cukierman, M.M.L. Ribeiro Carrott, P.J.M. Carrott, Adsorption of volatile organic compounds onto activated carbon cloths derived from a novel regenerated cellulosic precursor, J. Hazard. Mater. 177 (2010) 175–182. doi.org/10.1016/j.jhazmat.2009.12.014.

[336] F.D. Yu, L.A. Luo, G. Grevillot, Adsorbption isotherms of VOCs onto an activated carbon monolith: Experimental measurement and correlation with different models, J. Chem. Eng. Data. 47 (2002) 467–473. doi.org/10.1021/je010183k.

[337] A. Möller, R. Eschrich, C. Reichenbach, J. Guderian, M. Lange, J. Möllmer, Dynamic and equilibrium-based investigations of CO2-removal from CH4-rich gas mixtures on microporous adsorbents, Adsorption. 23 (2017) 197–209. doi.org/10.1007/s10450-016-9821-x.

[338] P.G. Aguilera, F.J. Gutiérrez Ortiz, Prediction of fixed-bed breakthrough curves for H2S adsorption from biogas: Importance of axial dispersion for design, Chem. Eng. J. 289 (2016) 93–98. doi.org/10.1016/j.cej.2015.12.075.

[339] R. Valenciano, E. Aylón, M.T. Izquierdo, A critical short review of equilibrium and kinetic adsorption models for vocs breakthrough curves modelling, Adsorpt. Sci. Technol. 33 (2015) 851–870. doi.org/10.1260/0263-6174.33.10.851.

[340] J. Nastaj, B. Ambrozek, Analysis of gas dehydration in TSA system with multi-layered bed of solid adsorbents, Chem. Eng. Process. Process Intensif. 96 (2015) 44–53. doi.org/10.1016/j.cep.2015.08.001.

[341] N. Jiang, Y. Shen, B. Liu, D. Zhang, Z. Tang, G. Li, B. Fu, CO2 capture from dry flue gas by means of VPSA, TSA and TVSA, J. CO2 Util. 35 (2020) 153–168. doi.org/10.1016/j.jcou.2019.09.012.

[342] M.S. Shafeeyan, W.M.A. Wan Daud, A. Shamiri, A review of mathematical modeling of fixed-bed columns for carbon dioxide adsorption, Chem. Eng. Res. Des. 92 (2014) 961–988. doi.org/10.1016/j.cherd.2013.08.018.

[343] K.H. Chu, Breakthrough curve analysis by simplistic models of fixed bed adsorption: In defense of the century-old Bohart-Adams model, Chem. Eng. J. 380 (2020) 122513. doi.org/10.1016/j.cej.2019.122513.

[344] N. Fakhfakh, N. Dammak, M. Benzina, Breakthrough modeling and experimental design for o-xylene dynamic adsorption onto clay material, Environ. Sci. Pollut. Res. 25 (2018) 18263–18277. doi.org/10.1007/s11356-017-9386-6.

[345] K. Akbarzadeh, A. Hammami, A. Kharrat, D. Zhang, S. Allenson, J. Creek, S. Kabir, A. Jamaluddin, A.G. Marshall, R.P. Rodgers, O.C. Mullins, T. Solbakken, Asphaltenes—problematic but rich in potential, Oilf. Rev. 19 (2007) 22–43.

[346] T.F. Yen, G. V Chilingarian, eds., Asphaltenes and Asphalts, 1, 1st ed., Elsevier, 1994.

[347] O.C. Mullins, E.Y. Sheu, A. Hammami, A.G. Marshall, Asphaltenes, Heavy Oils, and Petroleomics, 1st ed., Springer, New York, 2007.

[348] O.C. Mullins, The asphaltenes, Annu. Rev. Anal. Chem. 4 (2011) 393–418. doi.org/10.1146/annurev-anchem-061010-113849.

[349] E.B. Sirota, Physical structure of asphaltenes, Energy Fuels. 19 (2005) 1290–1296. doi.org/10.1021/ef049795b.

[350] S.E. Moschopedis, S. Parkash, J.G. Speight, Thermal decomposition of asphaltenes, Fuel 57 (1978) 431–434. doi.org/10.1007/BF00911837.

[351] V. Calemma, R. Rausa, Thermal decomposition behaviour and structural characteristics of asphaltenes, J. Anal. Appl. Pyrolysis. 40–41 (1997) 569–584. doi.org/10.1016/S0165-2370(97)00016-8.

[352] J. Sjöblom, S. Simon, Z. Xu, Model molecules mimicking asphaltenes, Adv. Colloid Interface Sci. 218 (2015) 1–16. doi.org/10.1016/j.cis.2015.01.002.

[353] H. Groenzin, O.C. Mullins, Molecular size and structure of asphaltenes, Pet. Sci. Technol. 19 (2001) 219–230. doi.org/10.1081/LFT-100001236.

[354] E. Buenrostro-Gonzalez, H. Groenzin, C. Lira-Galeana, O.C. Mullins, The Overriding Chemical Principles that Define Asphaltenes, Energy Fuels. 15 (2001) 972–978. doi.org/10.1021/ef0100449

[355] J.G. Speight, Petroleum asphaltenes - Part 1: Asphaltenes, resins and the structure of petroleum, Oil Gas Sci. Technol. 59 (2004) 467–477. doi.org/10.2516/ogst:2004032.

[356] J.G. Speight, Petroleum Chemistry and Refining, Taylor & Francis, Washington, 1998.

[357] H. Alboudwarej, J. Beck, W.Y. Svrcek, H.W. Yarranton, K. Akbarzadeh, Sensitivity of asphaltene properties to separation techniques, Energy Fuels. 16 (2002) 462–469. doi.org/10.1021/ef010213p.

[358] S.E. Moschopedis, J.G. Speight, Oxidation of a bitumen, Fuel. 54 (1975) 210–212. doi.org/10.1016/0016-2361(75)90014-9

[359] H. Groenzin, O.C. Mullins, Molecular size and structure of asphaltenes from various sources, Energy Fuels. 14 (2000) 677–684. doi.org/10.1021/EF990225Z.

[360] S.M. Hashmi, K.X. Zhong, A. Firoozabadi, Acid-base chemistry enables reversible colloid-to-solution transition of asphaltenes in non-polar systems, Soft Matter. 8 (2012) 8778–8785. doi.org/10.1039/c2sm26003d.

[361] O.C.M. and E.Y. Sheu, Structures and Dynamics of Asphaltenes, Springer, New York, 2013.

[362] H. Sabbah, A.L. Morrow, A.E. Pomerantz, R.N. Zare, Evidence for island structures as the dominant architecture of asphaltenes, Energy Fuels. 25 (2011) 1597–1604. doi.org/10.1021/ef101522w.

[363] T.F. Yen, J. Gordon Erdman, S.S. Pollack, Investigation of the structure of petroleum asphaltenes by X-ray diffraction, Anal. Chem. 33 (1961) 1587-1594. doi.org/10.1021/ac60179a039

[364] B. Schuler, G. Meyer, D. Peña, O.C. Mullins, L. Gross, Unraveling the molecular atructures of asphaltenes by atomic force microscopy, J. Am. Chem. Soc. 137 (2015) 9870–9876. doi.org/10.1021/jacs.5b04056.

[365] P. Zuo, S. Qu, W. Shen, Asphaltenes: Separations, structural analysis and applications, J. Energy Chem. 34 (2019) 186–207. doi.org/10.1016/j.jechem.2018.10.004.

[366] J. Murgich, Intermolecular forces in aggregates of asphaltenes and resins, Pet. Sci. Technol. 20 (2002) 983–997. doi.org/10.1081/LFT-120003692.

[367] M.A. Desando, J.A. Ripmeester, Chemical derivatization of Athabasca oil sand asphaltene for analysis of hydroxyl and carboxyl groups via nuclear magnetic resonance spectroscopy, Fuel. 81 (2002) 1305–1319. doi.org/10.1016/S0016-2361(02)00040-6.

[368] S.L. Kokal, S.G. Sayegh, Asphaltenes: the cholesterol of petroleum, in: SPE Middle East Oil Show, 1995: p. paper SPE 29787. doi.org/http://dx.doi.org/10.2118/29787-MS.

[369] I. Gawel, D. Bociarska, P. Biskupski, Effect of asphaltenes on hydroprocessing of heavy oils and residua, Appl. Catal. A Gen. 295 (2005) 89–94. doi.org/10.1016/j.apcata.2005.08.001.

[370] M. Kamkar, G. Natale, A review on novel applications of asphaltenes: A valuable waste, Fuel. 285 (2021) 119272. doi.org/10.1016/j.fuel.2020.119272.

[371] A. Veksha, E. Sasaoka, M.A. Uddin, The influence of porosity and surface oxygen groups of peat-based activated carbons on benzene adsorption from dry and humid air, Carbon 47 (2009) 2371–2378. doi.org/10.1016/j.carbon.2009.04.028.

VII. Scientific achievements

Publications in peer-reviewed journals:

Fundamental for dissertation:

1. **M. Plata-Gryl**, M. Momotko, S. Makowiec, G. Boczkaj, Characterization of diatomaceous earth coated with nitrated asphaltenes as superior adsorbent for removal of VOCs from gas phase in fixed bed column, *Chem. Eng. J.* 427 (2022) 130653.

   (IF: 13.273, Q1 – Engineering, Chemical)

2. **M. Plata-Gryl**, M. Momotko, S. Makowiec, G. Boczkaj, Highly effective asphaltene-derived adsorbents for gas phase removal of volatile organic compounds, *Sep. Purif. Technol.* 224 (2019) 315.

   (IF: 5.774, Q1 - Engineering, Chemical)

3. **M. Plata-Gryl**, M. Motoko, S. Makowiec, G. Boczkaj, Application of cyanated asphaltenes in gas-phase adsorption process for removal of volatile organic compounds, *Chem. Pap.* 74 (2020) 995.

   (IF: 2.097, Q3 - Chemistry, Multidisciplinary)

4. **M. Plata-Gryl**, C. Jungnickel, G. Boczkaj, An improved scalable method of isolating asphaltenes, *J. Pet. Sci. Eng.* 167 (2018) 608.

   (IF: 2.886, Q1 - Engineering, Petroleum)

Additional:

1. K. Fedorov, **M. Plata-Gryl**, J.A. Khan, G. Boczkaj, Ultrasound-assisted heterogeneous activation of persulfate and peroxymonosulfate by asphaltenes for the degradation of BTEX in water, *J. Hazard. Mater.* 397 (2020) 1228040.

   (IF: 10.588, Q1 – Engineering, Environmental)

2. **M. Plata-Gryl**, M. Momotko, G. Boczkaj, Adsorption properties characterization of asphaltenes by inverse gas chromatography, *Cam. Sep.* 10 (2018) 29.

   (IF: - , Q: -)

3. **M. Plata-Gryl**, G. Boczkaj, Sorption properties of asphaltene stationary phases for gas chromatography separations, *Cam. Sep.* 9 (2017) 23.

   (IF: - , Q: -)

4. A. Miciak, M. Momotko, **M. Plata-Gryl**, G. Boczkaj, The research on properties of asphaltene stationary phase to separate mixtures of optically active compounds with the use of gas chromatography technique, *Cam. Sep.* 9 (2017) 5.

   (IF: - , Q: -)

(Impact Factors and Quartile of journal, in the moment of publication, are given according to Web of Science database.)

Internship:

15.11.2020-15.05.2021, Prof. Dr. Roger Gläser group at Universität Leipzig, Faculty of Chemistry and Mineralogy, Institute of Chemical Technology, Topic: characterization of microporous zeolites for the separation of dihydrogen isotopologues.

Patent:

1. G. Boczkaj, S. Makowiec, M. Momotko, **M. Plata-Gryl**, Sposób otrzymywania sorbentu, zwłaszcza do chromatografii gazowej, Pat. 236734, 2018.

Patent application:

1. G. Boczkaj, M. Momotko, **M. Plata-Gryl**, S. Makowiec, Sposób otrzymywania sorbentu zwłaszcza do oczyszczania gazów, P.428252, 2018.

Scientific projects:

1. Preparation and investigation of carbon-based 3D porous structures (aerogels) structural properties and intermolecular interactions at solid/gas interface, funded by National Science Centre, 2020-2023, Principal investigator: **M. Plata-Gryl**.

Conference presentations:

1. **M. Plata-Gryl**, M. Momotko, S. Makowiec, G. Boczkaj, Application of cyanated asphaltenes in gas phase adsorption processes for removal of volatile organic compounds, 46th International Conference of the Slovak Society of Chemical Engineering, Tatrianske Matliare, Slovakia, 2019.

2. **M. Plata-Gryl**, G. Boczkaj, New method of isolation of asphatlenes having reproducible purity and sorptive properties as sorbents for separation techniques, Central European Conference ECOpole'17, Polanica Zdrój, Poland, 2017.

3. M. Momotko, **M. Plata-Gryl**, S. Makowiec, G. Boczkaj, Selectivity tunning of asphaltene based sorbents by means of chemical modifications, 10th International Conference on Instrumental Methods of Analysis: Modern Trends and Applications, Greece, 2017.

4. G. Boczkaj, **M. Plata-Gryl**, M. Momotko, Studies on reproducibility of isolation of pure asphaltene fraction and its properties for separation techniques, 10th International Conference on Instrumental Methods of Analysis: Modern Trends and Applications, Greece, 2017.

5. G. Boczkaj, M. Momotko, **M. Plata-Gryl**, New developments in stationary phases for gas chromatography, 22nd International Symposium on Separation Sciences, Toruń, 2016.

6. M. Momotko, **M. Plata-Gryl**, G. Boczkaj, Studies on separation of asphaltene stationary phases for gas chromatography, 22nd International Symposium on Separation Sciences, Toruń, 2016.

VIII. List of attachments/publications

Attachment / Paper 1

M. Plata-Gryl, C. Jungnickel, G. Boczkaj, An improved scalable method of isolating asphaltenes, *J. Pet. Sci. Eng.* 167 (2018) 608.

Attachment / Paper 2

M. Plata-Gryl, M. Momotko, S. Makowiec, G. Boczkaj, Highly effective asphaltene-derived adsorbents for gas phase removal of volatile organic compounds, *Sep. Purif. Technol.* 224 (2019) 315.

Attachment / Paper 3

M. Plata-Gryl, M. Motoko, S. Makowiec, G. Boczkaj, Application of cyanated asphaltenes in gas-phase adsorption process for removal of volatile organic compounds, *Chem. Pap.* 74 (2020) 995.

Attachment / Paper 4

M. Plata-Gryl, M. Momotko, S. Makowiec, G. Boczkaj, Characterization of diatomaceous earth coated with nitrated asphaltenes as superior adsorbent for removal of VOCs from gas phase in fixed bed column, *Chem. Eng. J.* 427 (2022) 130653.

(All publications are attached with authors' contribution statements.)

Journal of Petroleum Science and Engineering 167 (2018) 608–614

Contents lists available at ScienceDirect

Journal of Petroleum Science and Engineering

journal homepage: www.elsevier.com/locate/petrol

An improved scalable method of isolating asphaltenes

Maksymilian Plata-Gryl[a], Christian Jungnickel[b], Grzegorz Boczkaj[a,*]

[a] Gdansk University of Technology, Faculty of Chemistry, Department of Chemical and Process Engineering, Poland
[b] Gdansk University of Technology, Faculty of Chemistry, Department of Colloid and Lipid Science, Poland

ARTICLE INFO

Keywords:
Asphaltenes
Bitumen
Soxhlet
Precipitation
Sorbents
Extraction

ABSTRACT

A new, improved and scalable procedure of asphaltene fraction isolation is presented and compared to standard test methods. The new procedure uses 1:40 feedstock to solvent (n-heptane) ratio (g/mL), filtration through a cellulosic thimble and extensive washing in a Soxhlet type extractor. The group type composition and purity of the asphaltene fractions have been examined using thin-layer chromatography with flame-ionization detection. This study revealed that the new procedure provides a higher purity of asphaltene fraction resulting in a more accurate determination of its content in bitumens when comparing to the standard test method. Moreover, an attempt of evaluation of the scale-up possibility of the proposed and standard test methods was made, revealing that new procedure is more scalable than standard test methods. It is possible to obtain large quantities of a high purity asphaltene fraction even on a process scale. This feature is crucial for technical analytics, for researchers studying asphaltenes characteristic as well as for other novel applications of asphaltenes such as its use as sorbents in separation techniques.

1. Introduction

Asphaltenes are the most aromatic group of chemical compounds present in the crude oil and the heaviest products of its processing; they quantitatively remain in a residue from vacuum distillation. Due to their complex composition, asphaltenes are a class of compounds defined on the basis of solubility (Linton, 1894; Marcusson, 1911; Parr et al., 1909) rather than molecular structure. They are insoluble in n-alkanes *e.g.* n-heptane, and soluble in toluene or benzene (Ferris et al., 1967; Hubbard and Stanfield, 1948; Kleinschmidt, 1955; Mitchell and Speight, 1973; O'Donnell et al., 1951; Strieter, 1941). In terms of molecular structure, asphaltenes are polycyclic aromatic compounds (PACs) comprised of 4–10 fused aromatic rings, peripherally attached alkyl chains and polar functional groups *e.g.* carboxylic acids, phenol, and pyridines (Groenzin and Mullins, 2000; Mullins, 2011, 2010). They consist mostly of hydrogen and carbon, with H:C ratio of about 1–1.2, and additionally heteroatoms such as oxygen, sulfur, nitrogen and trace amounts of vanadium and nickel can be found in their backbone (Leyva et al., 2013; Trejo et al., 2004). Typical asphaltene molecules have an average molecular weight of 750 g/mole (Badre et al., 2006; Groenzin and Mullins, 2000; Pomerantz et al., 2015) and are arranged into planar type structures with a tendency to form nanoaggregates (about six asphaltene molecules) and clusters (about eight nanoaggregates) (Mullins, 2010; Pomerantz et al., 2015; Schuler et al., 2015).

Asphaltenes exhibit wide range of interactions *e.g.* van der Waals, Coulombic, hydrogen bonding, and π-π stacking (Murgich, 2002). Because of their physicochemical similarity to resins, asphaltenes exhibit strong sorption interactions with them. In solution, asphaltene-resin interactions can be favoured over asphaltene-asphaltene interactions (Speight, 2004). Resins can adsorb in the form of multilayers on the surface of the asphaltenes and penetrate their microporous structure (León et al., 2002; Liao et al., 2005). This is beneficial when considering stability of refinery process streams, as resins stabilize asphaltenes in colloidal form (Aguiar and Mansur, 2015; Andersen and Speight, 2001; Koots and Speight, 1975), but can be a drawback if the purpose is to isolate pure asphaltenes.

Asphaltenes are of crucial importance in the petroleum industry, mainly due to the several technological issues created by them in crude oil processing *i.e.* formation of emulsions, fouling, well-bore and pipelines clogging, coke formation, and catalyst deactivation in conversion processes (Akbarzadeh et al., 2007; Almehaideb, 2004; Idris and Okoro, 2013; Kokal and Sayegh, 1995; Ramirez-Jaramillo et al., 2006). Currently, asphaltenes are utilized only in the production of bitumens, bitumen mixtures and mineral rubber (Rostler and Sternberg, 1949). Their content in bitumen is increased by oxidation (air blowing process) (Moschopedis and Speight, 1975) for upgrading of primary properties of vacuum residue, measured by penetration, softening point and breaking point parameters. They describe the stiffness and behavior of bitumen in high and low temperatures of its usage.

Recently, Boczkaj et al. (2016) showed that asphaltenes present the

* Corresponding author. Gdansk University of Technology, Faculty of Chemistry, Department of Chemical and Process Engineering, 80 – 233 Gdansk, G. Narutowicza St. 11/12, Poland.
E-mail address: grzegorz.boczkaj@pg.edu.pl (G. Boczkaj).

https://doi.org/10.1016/j.petrol.2018.04.039
Received 19 October 2017; Received in revised form 21 March 2018; Accepted 15 April 2018
Available online 17 April 2018
0920-4105/

possibility of being applied as a sorbent in separation techniques. Their unique selectivity, high thermal stability and low production cost makes it an interesting material for stationary phases for gas chromatography, as well as for preparative and process separations (Boczkaj et al., 2016, 2015). However, current methods of isolation are not sufficient for providing large scale quantities of this material. Therefore a new method is required.

Traditionally, asphaltenes are isolated by means of precipitation with saturated hydrocarbons, such as *n*-pentane and *n*-heptane (ASTM D2007; 2003; ASTM D3279; 2001; ASTM D4124; 2001; ASTM D6560; 2000). Precipitation conditions *i.e.* type of solvent type, solvent to feedstock ratio, standing time and temperature have a significant impact on the yield of obtained asphaltenes and co-precipitated resins (Andersen and Birdi, 1990; H. Alboudwarej et al., 2002; Mitchell and Speight, 1973; Speight et al., 1984). Thus, asphaltene fractions isolated under different conditions are not identical and consequently have different properties. Although some groups indicate that the mechanism of precipitation is independent of the isolation method, but rather that the quantity of isolated asphaltenes is of the same magnitude, their characteristic should also be the same (Andersen and Birdi, 1990).

The type of solvent and its amount have the most evident effect on the precipitate. The yield of asphaltenes increases with increasing number of carbons in an n-alkane and reaches a plateau using n-heptane. The usage of n-heptane as a solvent is favoured when asphaltenes are the subject of research, because their properties are virtually stable for n-alkanes above n-hexane (Andersen and Birdi, 1990;Alboudwarej et al., 2002; Mitchell and Speight, 1973; Speight et al., 1984). Studies revealed that to provide efficient separation of asphaltenes, at least 30 mL of solvent to each gram of feedstock is necessary (Alboudwarej et al., 2002; Speight et al., 1984). Although settling time can have a significant impact on the obtained asphaltene fraction purity, it varies considerably in standard test methods; from 30 min (ASTM D2007; 2003) up to 16 h (ASTM D4124; 2001). Studies revealed that to ensure stable yields of asphaltenes, standing time of about 8–10h is needed. Extending this time above 16h may lead to the adsorption of resins from the liquid on the asphaltenes surface (Speight et al., 1984).

A number of studies investigated the effect of temperature on asphaltenes precipitation. However in this case, conflicting information emerges, with some report a decrease in asphaltenes yield with increasing temperature (Ali and Al-Ghannam, 1981; Mitchell and Speight, 1973) and the possibility of enhanced co-precipitation of resins (Speight et al., 1984), while others indicate increased yield in higher temperatures (Andersen, 1994; Andersen and Birdi, 1990; Hu and Guo, 2001). Andersen and Birdi (1990) observed an increased yield of precipitate followed by decrease after reaching maximum at 25 °C. He ascribed it to enhanced adsorption of smaller molecules and further rupture of those interactions (desorption of molecules) as the temperature increases further. However, the most recent studies seem to confirm a decrease in yield of asphaltenes with increasing temperature (Andersen, 1995, 1994; Andersen et al., 1998, 1997; Andersen and Stenby, 1996; Hu and Guo, 2001; Maqbool et al., 2011) and a lower content of resins when precipitation is carried out at higher temperatures (Pineda et al., 2007). UV fluorescence studies revealed that when temperature decreases more compounds with smaller fused rings precipitate. Conversely, when the precipitation temperature increases, the isolated fraction is dominated by larger aromatic structures (Andersen and Birdi, 1990). This result is supported by molecular weight studies, as molecular mass increase when asphaltenes are precipitated at elevated temperatures. Another consequence of increased precipitation temperature is higher aromaticity (*i.e.* lower H/C ratio) and polarity of isolated fraction (Andersen, 1995, 1994; Andersen et al., 1997; Pineda et al., 2007). In the scope of the definition and up-to-date structural information about asphaltenes, as well as being insoluble in n-alkanes and consisting of aromatic core of 4–10 fused rings, the variation of temperature affects the precipitate yield due to the co-precipitation of smaller molecules (*e.g.* resins). Although, one need to remember that there is no distinct border between asphaltenes and resins.

The last step of almost all precipitation procedures include washing of the isolated asphaltenes to remove adsorbed resins as well as other components of the primary material (ASTM D2007; 2003; ASTM D3279; 2001; ASTM D4124; 2001; ASTM D6560; 2000). If asphaltenes-resins interactions are adsorptive, then it should be possible to remove resins with re-precipitations and/or intensive washing with the correct solvent. The second phenomenon that can hinder the isolation of pure asphaltenes is to block access of the solvent by occlusion, thus retaining resins (or generally other than asphaltene fractions) by asphaltenes (Derakhshesh et al., 2013; Liao et al., 2006, 2005; Strausz et al., 2006). Although, the importance of the washing step is recognised intuitively, it is the most imprecise and ambiguous step. Usually it is performed on a filter with the solvent used for the precipitation. A common criterion is to continue washing until the effluent is colourless (ASTM D4124; 2001). This implies arbitrariness and leads to different extents of washing. Another popular method of washing is to use a reflux extractor (ASTM D6560; 2000). Results presented in (Alboudwarej et al., 2002) revealed that using Soxhlet's extractor led to removal of 22% w/w of maltenes from filter-washed asphaltenes.

As we have shown, a number of methods and refinements exist to isolate asphaltenes, but none allow for large scale production of a consistently pure product. Therefore, the aim of this paper was to propose simplified, reproducible, easy to scale – up procedure of asphaltenes isolation, which will give at least similar results as the standard test method. It would be of great importance, not only for studies in our research group (Boczkaj et al., 2016), but for researchers studying asphaltenes characteristic and technical analysis of petroleum products as well. Usually asphaltenes are characterized by their average properties *e.g.* elemental composition and molar mass. In this paper, thin-layer chromatography with flame ionization detection (TLC-FID) was used to compare group type composition of asphaltene fractions obtained by studied methods. Moreover operation effectiveness, scale-up possibility as well as economic aspects of this methods were evaluated.

2. Experimental

2.1. Materials

Bitumen 20/30 SDA (Lotos Group, Gdansk, Poland) and n-heptane EMPLURA® (Merck, Germany) were used to isolate the asphaltene fraction. Depending on the isolation method used, mixture was filtered through a 0.45 μm PTFE membrane filter (Achrom, Belgium) or a standard single thickness 33 × 100 mm cellulose thimble (VWR, United States). During hydrocarbon group type analysis of the isolated fractions, the following analytical grade chemicals were used: dichloromethane (POCH, Poland), methanol (POCH, Poland), toluene (POCH, Poland) and hexane (Merck, Germany). To filter samples prior to analysis, 0.45 μm PTFE syringe filters (Achrom, Belgium) were used.

2.2. Apparatus

To perform filtration a vacuum glass set (Glassco, India) was used. Isolated samples were washed in a Soxhlet type extractor. Weight measurements were performed with a WLC 6/A2 (readability 0.1 g) and WPA 180/C (readability 0.1 mg) balances (RADWAG, Poland).

To analyze the group type composition of the isolated fractions by means of TLC-FID technique an Iatroscan Mk. V (Iatron Lab., Japan), silica gel Chromarods S5 (Iatron Lab., Japan), 3200/IS-01 semiautomatic sampler (SES, Germany), 7102 KH 2 μL syringe (Hamilton, USA), TLC TK-8 Chromarods dryer (Iatron Lab., Japan), chromatographic chambers, AD converter, and corresponding software (Chomik, Poland) were used.

2.3. Procedures

2.3.1. Asphaltene fractions isolation

2.3.1.1. Procedure ASTM D4124. The reference samples of asphaltene fraction were isolated using the conditions described in ASTM D4124 (ASTM D4124; 2001). As a reference standard method of isolation ASTM D4124 was selected, because it exploits high solvent to feedstock ratio (100 mL: 1 g), long contact time (ca.16 h) and extensive washing of isolated asphaltenes (till effluent is colorless). This should ensure high purity (low content of resins) of the asphaltene fraction. Bitumen was heated in an oven at 70 °C for 1 h and 6 g (weighed to the nearest 0.1 g) were placed in 1 L flask, which was gently heated to disperse bitumen on the bottom and lower sides of the flask. Next, the n-heptane was added in the ratio of 100 mL per 1 g of bitumen. The mixture was heated to boiling and refluxed for 1 h with occasionally stirring. After the mixture was allowed to cool for 16 h, it was filtered through 0.45 μm PTFE membrane filter under the vacuum. The precipitate was washed with hot n-heptane until a colorless filtrate was obtained. The filtrate was consequently washed with 80 mL of fresh n-heptane, and heated for 30 min with occasional stirring and filtered again through a fresh tared PTFE membrane filter. The asphaltene cake was washed with hot n-heptane till the filtrate was colorless, dried (1 h at 100 °C) and weighed.

2.3.1.2. Procedure B1 and B16. The novel procedure of isolation proposed and tested in this paper is as follows: bitumen is heated in an oven at 70 °C for 1 h and 15 g of it is placed in 1 L round-bottom flask. The flask is gently heated to disperse bitumen on the bottom and lower sides of the flask. Next, the n-heptane is added in the ratio of 40 mL per 1g of the bitumen. The mixture is brought to a boil and refluxed for 1h with occasional stirring. Then it is set aside for 1 h (procedure B1) and 16h (procedure B16) to cool and the content of the flask is filtered through a tared cellulose thimble. In procedure B1 the filtration started at temperature of the mixture being 55 °C, and in B16 procedure at 20 °C. The thimble is placed in a Soxhlet extractor and washed with n-heptane for 24 h. Next, it is dried at 100 °C for 1h and weighed.

Figs. 1 and 2 present steps of standard and proposed procedures for isolation of asphaltene fraction and experimental glassware setup, respectively.

2.3.2. Hydrocarbon group type analysis of isolated fractions

The group type composition of bitumen and the isolated fractions was investigated by TLC-FID technique which allows a relatively fast analysis. A normal phase separation mechanism is used, resulting in a so-called SARA (Saturates, Aromatics, Resins, Asphaltenes) analysis. In this conditions asphaltenes are defined as a group of compounds having the highest retention.

Samples were prepared by dissolving the samples in dichloromethane to yield concentration of 2 mg/mL. This prevents overloading of the stationary phase and leads to a better separation of asphaltenes and resins. To remove any undissolved particles, the samples were filtered through 0.45 μm PTFE syringe filters. Before spotting the samples, the Chromarods were activated in the flame of FID detector: once in time of 35 s and twice in 50 s. Then, they were placed in desiccator for 10 min to cool down.

1 μL of the samples were spotted in a small aliquots on the three Chromarods each, to obtain quantitative results. Next, the Chromarods with the spotted samples were placed in the dryer (set to 70 °C) for 3 min. A three-step elution sequence was used, with eluents in the following order:

1. Dichloromethane:methanol (95:5 v/v) elution up to 45% of a stationary phase height
2. Toluene elution up to 80% of a stationary phase height
3. n-hexane (95% water saturated) elution up to 100% of a stationary phase height

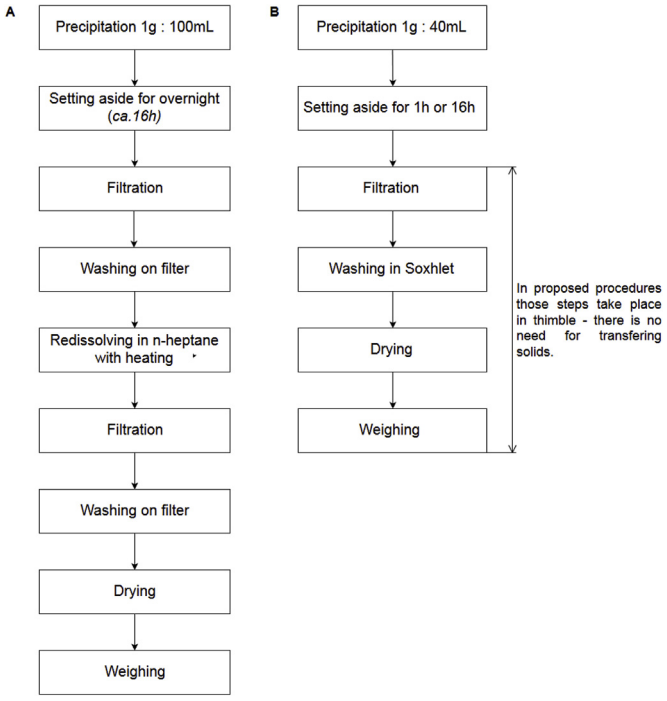

Fig. 1. Scheme of studied procedures for isolation of asphaltene fraction. A) standard test method ASTM D4124. B) Proposed procedures. For two tested variants B1 and B16 the scheme is the same, only time of setting aside changes (1 h vs 16 h).

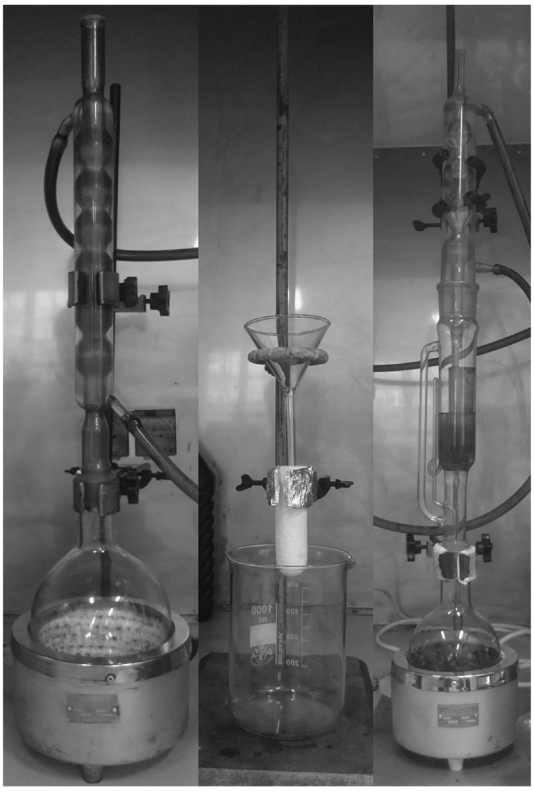

Fig. 2. Experimental glassware setup. From left: precipitation set, filtration set, washing (Soxhlet) set.

The set of solvents used in this work is a typical set used for hydrocarbons group type analysis of petroleum heavy fractions using TLC-

FID technique (Sharma et al., 1998). However, atypical is the sequence of the elution, which is contrary to what can be typically found in literature (Jiang et al., 2008; Sharma et al., 1998). In our work we developed the Chromarods beginning with the solvent ensuring the elution of asphaltene fraction. It follows from the high amount of asphaltene in the sample which are not solubilized and eluted by n-hexane (which is used as the first solvent in typical procedures). In our opinion fractions other than asphaltenes (i.e. saturates and aromatics) can be trapped under asphaltenes and shielded/covered by them, hence not eluted by the n-hexane. First solvent (dichloromethane:methanol) eluted all components of the spotted sample and increased accessibility of two other solvents to the whole amount of the sample. This approach was validated in our lab during a series of quality control analysis of bitumen, performed for a local refinery in Gdansk.

Each TLC chamber was lined with chromatographic paper, filled with eluent and left for saturation for 15 min. The Chromarods were placed in the chamber and eluted accordingly. Before elution with toluene and n-hexane the frame with rods was held in headspace of eluent for 5 min to saturate the stationary phase with vapors of the eluent. After each elution step the rods were dried for 3 min (or longer if a scent of a solvent was noticeable) and left in desiccator for 10 min to cool down.

Detection was carried out in a TLC-FID analyzer. Rod scanning time was set to 35 s, hydrogen and air flow were 150 mL/min and 1800 mL/min respectively. Chromatograms were integrated with a normalization method. Obtained results were used comparatively for evaluation of purity of asphaltene fraction obtained by means of studied in this paper methods of isolation.

2.4. Quality assurance of data

The average results for isolation of asphaltene fraction, by each procedure, are the mean values of three separate isolations. The average yield is a mass ratio of asphaltene fraction and feedstock (bitumen). For TLC-FID analysis, each sample was spotted on three rods to provide quantitative data. The average of asphaltenes content was calculated as a mean of the means for individual samples isolated with given procedure. The relative standard deviation (RSD%), which expresses the precision and repeatability was calculated as a ratio of standard deviation to the mean value of asphaltenes content, multiplied by one hundred.

To compare the accuracy of investigated procedures, mean results (which were obtained by the same analyst) were evaluated by means of F-Snedecor test, to confirm the homogeneity of variances and next with t-Student test. t-Student test is used for determining whether the observed difference between obtained means is statistically significant or not. F-Snedecor test is performed to check whether the variances of the two samples are equal and if t-Student test without correction can be used.

3. Results and discussion

Fig. 3 shows exemplary TLC-FID chromatograms (SARA analysis) of analyzed sample isolated by B1 (B) procedure and feedstock bitumen (A). A baseline separation between resins and asphaltenes is obtained, allowing to control the precipitation.

Table 1 presents results of TLC-FID analysis of obtained asphaltene fractions. Table 2 presents differences between values of parameters given in Table 1 for the tested procedures.

Isolated asphaltene fractions were dark brown, black mat solids. Quantitative analysis revealed some differences which are consistent with obtained yields of asphaltene fractions. It is clear from data in Table 1 that ASTM standard test method has a false positive error i.e. it reports higher content of asphaltenes in bitumen due to the presence of impurities of resins fraction co-precipitating or adsorbing on asphaltenes. The studied alternative procedures exhibit an improved purity of obtained asphaltene fraction. It is possible, that in the case of bitumens having lower content of asphaltenes and higher of resins, this error for ASTM methods would be higher.

The average result of asphaltene fraction yield was 10.14% w/w from the ASTM D4124 procedure and 8.79% w/w from the new B1 procedure. This difference is mainly the result of lower resins content when proposed B1 procedure is used. These conclusions are supported by the TLC-FID data, which revealed that the asphaltenes content in isolated fraction is higher by 1.59% for B1 procedure.

The lowest yield of asphaltene fraction was obtained for our procedure with B1 contact time. At the same time this procedure gave the highest purity of asphaltenes. This indicates that B1 procedure, involving the washing in the Soxhlet, washed out more maltenes than the ASTM D4124, in which washing of the filter cake is performed manually. Additionally, the developed procedures have improved reproducibility, as the RSD% value is lower, comparing with ASTM method.

The second variant of the procedure, in which contact time was the same as in ASTM D4124 method, gave the results between standard and B1 procedures. The yield of asphaltene fraction was higher and purity of asphaltenes lower than in B1 procedure. Probably, it is due to a lower temperature of a mixture at the beginning of filtration and resulting higher adsorption of resins in B16 procedure. Still, this method provided higher purity of asphaltenes than ASTM method. This result clearly indicates the problem of the presence of resins fractions in precipitated asphaltenes fraction, which is almost completely solved in the developed method for optimized conditions of settling the solution, filtration and Soxhlet extraction stages.

The precision and repeatability of each procedure was sufficient and comparable, as the RSD% value was below 5% (Table 1). Table 3 presents values of calculated and critical parameters for the t-Student and F-Snedecor test. The t-Student test revealed statistical difference between mean results for ASTM D4124 and proposed B1 procedure. No statistical difference was observed for B16 and ASTM D4124 method. Between B16 and B1 procedures difference in purity of asphaltene fraction was insignificant, while difference in yield of asphaltene fraction was slightly significant. Comparison of standard deviations revealed that both proposed methods were slightly more precise than the standard test method.

As abovementioned, the goal of this research was to develop simple, cost-effective and easy to scale-up procedure of asphaltenes isolation which will give at least similar results, in terms of asphaltene purity, as standard test method. This has been achieved by lowering the feedstock to solvent ratio from 1g per 100 mL to 1g per 40 mL (this ratio is reported in some of ASTM methods as allowable) along with modification of purification step. As shown in Table 4 solvent consumption in B1 procedure was calculated as three times lower than in ASTM D4124. For ASTM D4124 calculation has been made on the basis of the amount of the solvent used in abovementioned experiment, while for the other two standard test methods quantities of solvent and feedstock specified in standard test method were used.

The studies revealed, that washing step is crucial for final asphaltenes purity. Lower solvent consumption allowed the use of bigger quantities of feedstock without fall-off in asphaltene fraction purity (in fact, a higher purity was obtained). This may be not only important for process scale isolation, but also in terms of asphaltenes research. Due to the high complexity of petroleum and its subfractions, asphaltenes are still relatively unknown and poorly studied group of chemical compounds. One of the difficulties associated with the correct characterization of asphaltenes is the lack of one universal and standardized method of isolation. Different research teams isolate asphaltenes by means of different ASTM or other standard methods described in the literature or perform isolation by means of their own developed procedures. This affects strongly the purity of asphaltenes and reproducibility of results, thus making comparisons limited. Proposed simple, reproducible procedure giving high quantities of asphaltene fraction with very low resins content is an important contribution to this issue.

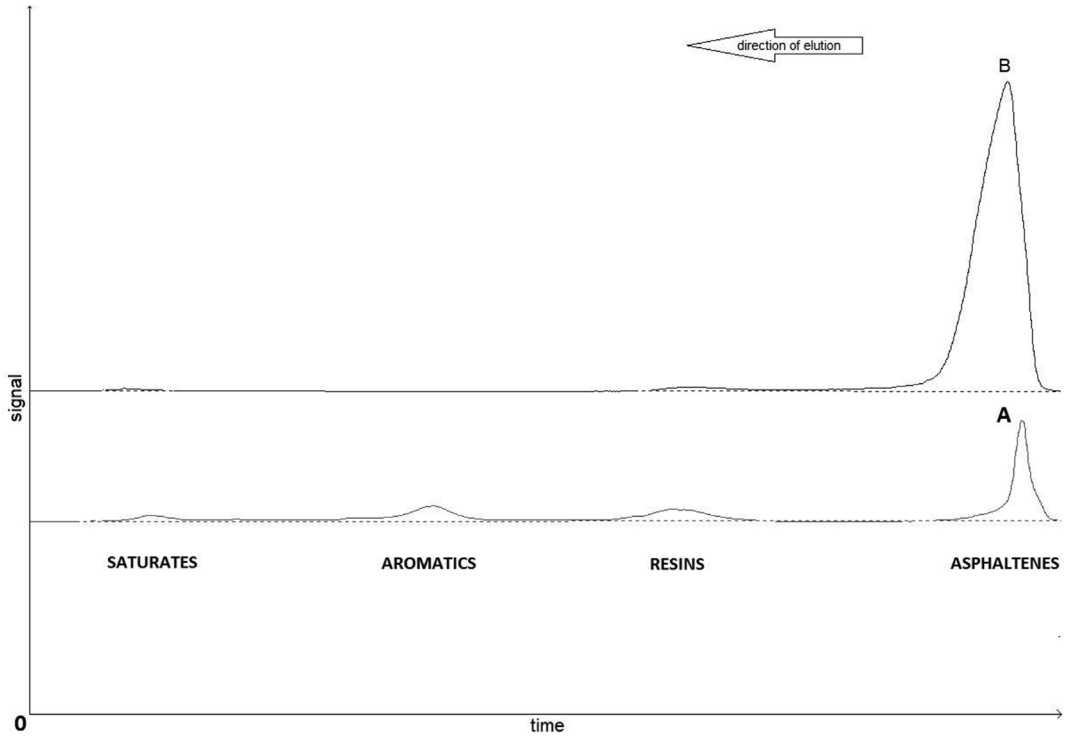

Fig. 3. Exemplary TLC-FID chromatograms of SARA fractionation. A) feedstock – bitumen 20/30 SDA and B) the asphaltene fraction isolated with tested B1 procedure.

Table 4 compares selected parameters of investigated procedures and two additional standard test methods.

3.1. Time consumption

B1 procedure is the most time consuming but it is caused by the most extensive washing among compared procedures. This extended purification is a must to obtain pure asphaltenes fraction and accurate results of determination.

In the case of standard test methods the isolation procedure time can be extended by problems with filtration rate. When isolating asphaltene fraction according to ASTM D4124-01, 0.45 μm PTFE filters were used and especially in the case of higher amounts of asphaltene fraction, the filters have tendency to clog, thus decreasing the rate of filtration and significantly increasing the time of the filtration stage. The same issue may be observed in ASTM D3297 and D6560 procedures which utilize glass filter pads and cellulose quantitative filters, respectively. In B1 procedure filtration under vacuum with sub micrometer filter was replaced with simple filtration through cellulose thimble, in which the washing step is carried out later. No issues with filtration were observed when filtering through thimble and filtrations were completed in time under 15 min. To check if no asphaltenes are going through thimble during filtration, effluent was filtered through 0.45 μm PTFE membrane filter and no solid particles were retained.

Table 2
Differences between results for tested procedures.

	ASTM D4124 – B16	ASTM D4124 – B1	B16 – B1
Yield of asphaltene fraction [% m/m]	0.55 ± 0.14	1.35 ± 0.11	0.80 ± 0.03
Asphaltenes content [%]	0.69 ± 0.17	1.59 ± 0.46	0.90 ± 0.29

3.2. Solvent consumption, washing and purity of asphaltene fraction

The B1 procedure has the lowest solvent consumption yet the most extensive washing of the isolated fraction, giving the highest purity of asphaltene fraction. ASTM D3279 procedure consumes almost three times more solvent than B1 procedure and washing step is very limited. Although there is no data available about purity of asphaltene fraction isolated with ASTM D3279, because it is similar to ASTM D4124, the purity probably will not exceed the one obtained with ASTM D4124.

ASTM D6560 uses similar amount of n-heptane but incorporates dissolution/re-precipitation with toluene. It also involves washing in reflux extractor. However, contrary to Soxhlet extractor used in B1 procedure, it is constructed in a way that the solvent is constantly drained from sample. In Soxhlet extractor a chamber is flooded with hot solvent and periodically emptied by siphon. This ensures longer contact time and in case of bigger sample the whole asphaltene fraction should be evenly washed. ASTM D6560 procedure is somewhat alike to B1 in

Table 1
Comparison of asphaltenes isolation results obtained with tested procedures.

Method	ASTM D4124			B16			B1		
	Mean	STD	RSD%	Mean	STD	RSD%	Mean	STD	RSD%
Yield of asphaltene fraction [% m/m]	10.14	0.46	4.49	9.59	0.32	3.34	8.79	0.35	3.99
Asphaltene fraction purity [%]	95.80	0.30	0.31	96.49	0.47	0.49	97.39	0.76	0.78

Table 3
Comparison of variances and means for two sets of results.

	ASTM D4124 – B16	ASTM D4124 – B1	B16 – B1
	F-Snedecor		
	F_{cr} ($\alpha = 0.05$, $f_1 = f_2 = 2$) = 19.00		
	F		
Yield of asphaltene fraction [% m/m]	2.07	1.73	1.20
Asphaltenes content [%]	2.45	6.42	2.61
	t-Student		
	t_{cr} ($\alpha = 0.05$, $f = n_1 + n_2 - 2 = 4$) = 2.776		
	t		
Yield of asphaltene fraction [% m/m]	1.70	4.04	2.92
Asphaltenes content [%]	2.14	3.37	1.74

terms of solvent consumption and washing and can yield asphaltene fractions of similar purity.

3.3. Arbitrariness and laboriousness

Filtration in thimble and further Soxhlet washing allowed to omit a part of ASTM D4124 test method in which filter cake is transferred to beaker for extra washing and avoid manual washing of filter cake, which lowered the labor consumption and reduced arbitrariness.

Washing of asphaltene fraction in Soxhlet for a fixed amount of time eliminates the necessity of setting arbitrary end time of washing. Arbitrariness was evaluated on the basis of the precision of end points. In case of B1 and ASTM D3279 procedures end points are quantitative whereas in ASTM D4124 it is qualitative (color of effluent). In ASTM D6560 the washing step end point is measured in hours, however it is not fixed and only minimal time of washing is given.

3.4. Scaling up/automation

Table 5 presents the results of scaling up possibility evaluation. To estimate scaling up difficulty, the isolation process was divided into three parts: precipitation, filtration and washing. To every stage two numbers were ascribed: one representing its significance (wage) and second one describing difficulty of scaling up this stage. Difficulty was multiplied by significance of considered step and sum of those multiplications was treated as scaling up possibility parameter. Table 6 presents scale which was used to determine overall scale up possibility of the procedure.

Precipitation step was considered as having the lowest significance for the differentiation of the procedures because in every procedure it is conducted in the same way and only volume of a solvent differs. This difference was used to determine difficulty of scaling up. The bigger the feedstock to solvent ratio the bigger the vessel needed for precipitation step.

When evaluating filtration step, time and power consumption were taken under consideration. In case of ASTM D4124 significant problems with filtration resulting in extended filtration time were discussed above. Additionally in ASTM D4124 and D3279 procedures vacuum is used for filtration which increases power consumption. Those remarks are also true for washing step.

Due to the availability of wide range of Soxhlet dimensions, proposed procedure can be easily scaled up, from laboratory scale to automated. Continuous washing with hot solvent is also easier to implement on a process scale, than filtration through sub micrometer filters. Moreover, in B1 procedure after filtration asphaltenes remain in thimble in which they are washed and it should be easy to make it “one-pot” process. Additionally in B1 procedure asphaltenes are not dissolved in toluene after washing with n-heptane as in ASTM D6560 and there is no need for evaporation to reprecipitate asphaltenes.

3.5. Safety

Conducting purification step in Soxhlet extractor reduces risk to safety and health. In ASTM D4124 procedure washing with hot solvent is done manually and redissolving of asphaltene fraction in hot n-heptane takes place in an open beaker. The lack of proper attention can lead to overheating of the mixture, which may result in bumping, thus representing a hazard.

4. Conclusion

The procedures of asphaltene fraction isolation developed and tested in this paper provided higher purity of isolated fractions (containing less resins) and are characterized by improved reproducibility and precision comparing to standard test method, which is corroborated by the RSD% values.

Implementation of filtration through cellulose thimble and washing off isolated fraction in Soxhlet extractor is less laborious, less arbitrariness and easy to scale-up. This simplicity makes the scale-up easier which in connection with smaller solvent consumption per 1g of feedstock can lead to obtaining higher quantities of asphaltene fraction, which may be especially interesting for researchers working on characterization of asphaltenes *e.g.* structural analysis and further if kilograms of asphaltenes are needed for different studies. In this field particularly important are studies on bitumen properties related to asphaltene content and their physico-chemical character.

As abovementioned, asphaltenes are currently under investigation in terms of their sorption properties and employing them in separation techniques (Boczkaj et al., 2016, 2015). Such sorbents can be used in process scale separations or as a stationary phase for gas chromatography. In this case further scaling-up will be needed and previously mentioned advantages of proposed procedures can be crucial for isolating large quantities of this material. Furthermore, in process scale

Table 4
Comparison of procedures for isolation of asphaltene fraction.

	B1	ASTM D4124-01	ASTM D3279-07	ASTM D6560-00 (IP 143/01)
Time consumption	*ca.* 28h	*ca.* 20h	*ca.* 3h	*ca.* 10h
Solvent consumption	50 mL/g	*ca.* 150 mL/g	*ca.* 130 mL/g	*heptane: ca.* 50 mL/g toluene: *ca.* 10 mL/g
Washing	24h Soxhlet	on filter washing, until filtrate is colorless	on filter, 3 × 10 mL	min. 1h reflux extractor
Laboriousness	+	–	+	- -
Purity of asphaltene fraction	97.39 ± 0.76	95.80 ± 0.30	NA	NA
Scaling up/automation	easy	difficult	moderate	moderate
Safety	safe	hazardous steps	safe	safe
Arbitrariness	+ +	–	+ +	+

Table 5
Collation of grades ascribed to isolation process stages describing its importance and difficulty of scaling up.

Stage	Wage	B1		ASTM D4124-01		ASTM D3279-07		ASTM D6560-00	
		Difficulty	Mult.	Difficulty	Mult.	Difficulty	Mult.	Difficulty	Mult.
Precipitation	1	2	2	4	4	4	4	2	2
Filtration	2	2	4	5	10	3	6	3	6
Washing	3	2	6	4	12	3	9	4	12
Scaling up parameter			12		26		19		20

Table 6
Scale used to determine the possibility of process scale up.

Scaling up parameter	Scaling-up difficulty
≤15	easy
15–20	moderate
> 20	difficult

isolation, washing step can be based on the same principle as in Soxhlet extractor (recirculation of the hot solvent) and in turn will result in cost reduction of this step.

Acknowledgement

The authors gratefully acknowledge the financial support from the National Center for Research and Development, Warsaw, Poland – Project LIDER, no. LIDER/036/573/L-5/13/NCBR/2014.

References

Aguiar, J.I.S., Mansur, C.R.E., 2015. Study of the interaction between asphaltenes and resins by microcalorimetry and ultraviolet-visible spectroscopy. Fuel 140, 462–469.
Akbarzadeh, K., Hammami, A., Kharrat, A., Zhang, D., Allenson, S., Creek, J., Kabir, S., Jamaluddin, A., Marshall, A.G., Rodgers, R.P., Mullins, O.C., Solbakken, T., 2007. Asphaltenes—problematic but rich in potential. Oilf. Rev. 22–43.
Alboudwarej, H., Beck, J., Svrcek, A, W.Y., Yarranton, H.W., Akbarzadeh, K., 2002. Sensitivity of asphaltene properties to separation techniques. Energy Fuels. 16, 462–469.
Ali, L.H., Al-Ghannam, K.A., 1981. Investigations into asphaltenes in heavy crude oils. I. Eff. Temp. Precip. by alkane solvents. Fuel 60, 1043–1046.
Almehaideb, R.A., 2004. Asphaltene precipitation and deposition in the near wellbore region: a modeling approach. J. Pet. Sci. Eng. 42, 157–170.
Andersen, S.I., 1994. Effect of precipitaiton temperature on the composition of n-heptane asphaltenes. Fuel Sci. Technol. Int. 12, 51–74.
Andersen, S.I., 1995. Effect of precipitation temperature on the composition of n-heptane asphaltenes Part 2. Fuel Sci. Technol. Int. 13, 579–604.
Andersen, S.I., Birdi, K.S., 1990. Influence of temperature and solvent on the precipitation of asphaltenes. Fuel Sci. Technol. Int. 8, 593–615.
Andersen, S.I., Speight, J.G., 2001. Petroleum resins: separation, character, and role in petroleum. Pet. Sci. Technol. 19, 1–34.
Andersen, S.I., Stenby, E.H., 1996. Thermodynamics o asphaltene precipitation and dissolution investigation of temperature and solvent effects. Fuel Sci. Technol. Int. 14, 261–287.
Andersen, S.I., Keul, A., Stenby, E., 1997. Variation in composition of subfractions of petroleum asphaltenes. Pet. Sci. Technol. 15, 611–645.
Andersen, S.I., Lindeloff, N., Stenby, E.H., 1998. Investigation of asphaltene precipitation at elevated temperature. Pet. Sci. Technol. 16, 323–334.
ASTM D2007, 2003. Standard test Method for Characteristic Groups in Rubber Extender and Processing Oils and other Petroleum – Derived Oils by the Clay – Gel Absorption Chromatographic Method.
ASTM D3279, 2001. Standard Test Method for n-Heptane Insolubles.
ASTM D4124, 2001. Standard Test Method for Separation of Asphalt into Four Fractions.
ASTM D6560, 2000. Standard test Method for Determination of Asphaltenes (Heptane Insolubles) In crude Petroleum and Petroleum Products.
Badre, S., Carla Goncalves, C., Norinaga, K., Gustavson, G., Mullins, O.C., 2006. Molecular size and weight of asphaltene and asphaltene solubility fractions from coals, crude oils and bitumen. Fuel 85, 1–11.
Boczkaj, G., Kamiński, M., Momotko, M., Chruszczyk, D., 2015. Sorbent, Kolumna Sorpcyjna Lub Chromatograficzna: Sposób Wykonania Tych Kolumn Oraz Sposób Ich Wykorzystania. *Patent registration* - P.412584.
Boczkaj, G., Momotko, M., Chruszczyk, D., Przyjazny, A., Kamiński, M., 2016. Novel stationary phases based on asphaltenes for gas chromatography. J. Sep. Sci. 39, 2527–2536.
Derakhshesh, M., Bergmann, A., Gray, M.R., 2013. Occlusion of polyaromatic compunds in asphaltene precipitates suggests porous nanoaggregates. Energy & Fuels 27, 1748–1751.
Ferris, S.W., Black, E.P., Clelland, J.B., 1967. Aromatic structure in asphalt fractions. Ind. Eng. Chem. Prod. Res. Dev. 6, 127–132.
Groenzin, H., Mullins, O.C., 2000. Molecular size and structure of asphaltenes from various sources. Energy Fuels. 14, 677–684.
Hu, Y.-F., Guo, T.-M., 2001. Effect of temperature and molecular weight of n-alkane precipitants on asphaltene precipitation. Fluid Phase Equilib. 192, 13–25.
Hubbard, R.L., Stanfield, K.E., 1948. Determination of asphaltenes, oils, and resins in asphalt. Anal. Chem. 20, 460–465.
Idris, M., Okoro, L.N., 2013. The effects of asphaltenes on petroleum processing. Eur. Chem. Bull. 2, 393–396.
Jiang, C., Larter, S.R., Noke, K.J., Snowdon, L.R., 2008. TLC-FID (Iatroscan) analysis of heavy oil and tar sand samples. Org. Geochem 39, 1210–1214.
Kleinschmidt, L.R., 1955. Chromatographic method for the fractionation of asphalt into distinctive groups of components. J. Res. Natl. Bur. Stand 54, 163–166 (1934).
Kokal, S.L., Sayegh, S.G., 1995. Asphaltenes: the cholesterol of petroleum. In: SPE Middle East oil show. P. Pap. SPE 29787.
Koots, J.A., Speight, J.G., 1975. Relation of petroleum resins to asphaltenes. Fuel 54, 179–184.
León, O., Contreras, E., Rogel, E., Dambakli, G., Acevedo, S., Carbognani, L., Espidel, J., 2002. Adsorption of native resins on asphaltene particles: a correlation between adsorption and activity. Langmuir 18, 5106–5112.
Leyva, C., Ancheyta, J., Berrueco, C., Millán, M., 2013. Chemical characterization of asphaltenes from various crude oils. Fuel Process. Technol. 106, 734–738.
Liao, Z., Zhou, H., Graciaa, A., Chrostowska, A., Creux, P., Geng, A., 2005. Adsorption/occlusion characteristics of asphaltenes: some implication for asphaltene structural features. Energy Fuels. 19, 180–186.
Liao, Z., Geng, A., Graciaa, A., Creux, P., Chrostowska, A., Zhang, Y., 2006. Different adsorption/occlusion properties of asphaltenes associated with their secondary evolution processes in oil reservoirs. Energy Fuels. 20, 1131–1136.
Linton, L.A., 1894. On the technical analysis of asphaltum. J. Am. Chem. Soc. 16, 809–822.
Maqbool, T., Srikiratiwong, P., Fogler, H.S., 2011. Effect of temperature on the precipitation kinetics of asphaltenes. Energy Fuels 25, 694–700.
Marcusson, J., 1911. Chemische Zusammensetzung und Unterscheidung der naturlichen un kunstlichen Asphalte. Chem. Rev. Fett- Harz-Ind 19, 166–171.
Mitchell, D.L., Speight, J.G., 1973. The Solubility of Aspahtlenes in hydrocarbon solvents. Energy Fuels. 52, 149–152.
Moschopedis, S.E., Speight, J.G., 1975. Oxidation of a bitumen. Fuel 54, 210–212.
Mullins, O.C., 2010. The modified yen model. Energy Fuels. 24, 2179–2207.
Mullins, O.C., 2011. The asphaltenes. Annu. Rev. Anal. Chem. 4, 393–418.
Murgich, J., 2002. Intermolecular forces in aggregates of asphaltenes and resins. Pet. Sci. Technol. 20, 983–997.
O'Donnell, G., Snider, L.T., Rietz, E.G., 1951. Separating asphalt into its chemical constituents. Anal. Chem. 23, 894–898.
Parr, S.W., Mears, B., Weatherhead, D.L., 1909. The chemical examination of asphaltic material. J. Ind. Eng. Chem. 1, 751–754.
Pineda, L.A., Trejo, F., Ancheyta, J., 2007. Correlation between properties of asphaltenes and precipitation conditions. Pet. Sci. Technol. 25, 105–119.
Pomerantz, A.E., Wu, Q., Mullins, O.C., Zare, R.N., 2015. Laser-based mass spectrometric assessment of asphaltene molecular weight, molecular architecture, and nanoaggregate number. Energy Fuels. 29, 2833–2842.
Ramirez-Jaramillo, E., Lira-Galeana, C., Manero, O., 2006. Modeling asphaltene deposition in production pipelines. Energy Fuels. 20, 1184–1196.
Rostler, F.S., Sternberg, H.W., 1949. Compounding rubber with petroleum products - correlation of chemical characteristics with compounding properties and analysis of petroleum products used as compounding ingredients in rubber. Ind. Eng. Chem. 41, 598–608.
Schuler, B., Meyer, G., Peña, D., Mullins, O.C., Gross, L., 2015. Unraveling the molecular structures of asphaltenes by atomic force microscopy. J. Am. Chem. Soc. 137, 9870–9876.
Sharma, B.K., Sarowha, S.L.S., Bhagat, S.D., Tiwari, R.K., Gupta, S.K., Venkataramani, P.S., 1998. Hydrocarbon group type analysis of petroleum heavy fractions using the TLC-FID technique. Fresenius. J. Anal. Chem. 360, 539–544.
Speight, J.G., 2004. Petroleum asphaltenes - Part 1: asphaltenes, resins and the structure of petroleum. Oil Gas. Sci. Technol. 59, 467–477.
Speight, J.G., Long, R.B., Trowbridge, T.D., 1984. Factors influencing the separation of asphaltenes from heavy petroleum feedstocks. Fuel 63, 616–620.
Strausz, O.P., Torres, M., Lown, E.M., Safarik, I., Murgich, J., 2006. Equipartitioning of precipitant solubles between the solution phase and precipitated asphaltene in the precipitation of asphaltene. Energy Fuels. 20, 2013–2021.
Strieter, O.G., 1941. Method for determining the components of asphalts and crude oils. Part J. Res. Natl. Bur. Stand 26, 415–418.
Trejo, F., Centeno, G., Ancheyta, J., 2004. Precipitation, fractionation and characterization of asphaltenes from heavy and light crude oils. Fuel 83, 2169–2175.

Gdańsk, 01.03.2022 r.

mgr inż. Maksymilian Plata-Gryl

Department of Process Engineering and Chemical Technology

Gdańsk University of Technology

Gabriela Narutowicza 11/12 Street

80-233 Gdańsk

e-mail: makgryl@student.pg.edu.pl

STATEMENT

on the contribution and participation in the publication

I declare that my contribution to the work:

M. Plata-Gryl, C. Jungnickel, G. Boczkaj, An improved scalable method of isolating asphaltenes, *J. Pet. Sci. Eng.* 167 (2018) 608.

was to develop the research plan (in cooperation with my supervisor), perform all experiments, analyse the data, write the initial draft and further revise the manuscript.

I estimate my contribution to the final publication to be 60 %.

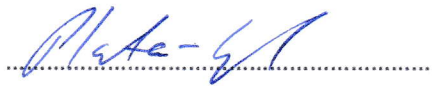

Gdańsk, 01.03.2022 r.

dr hab. Christian Jungnickel, prof. PG
Department of Colloid and Lipid Science
Gdańsk University of Technology
Gabriela Narutowicza 11/12 Street
80-233 Gdańsk
e-mail: christian.jungnickel@pg.edu.pl

STATEMENT

on the contribution and participation in the publication

I declare that my contribution to the work:

M. Plata-Gryl, C. Jungnickel, G. Boczkaj, An improved scalable method of isolating asphaltenes, *J. Pet. Sci. Eng.* 167 (2018) 608.

was to participate in corrections of the initial draft and revised version of the manuscript.

I estimate my contribution to the final publication to be 10 %.

Gdańsk, 28.02.2022 r.

dr hab. inż. Grzegorz Boczkaj, prof. PG

Department of Process Engineering and Chemical Technology

Gdańsk University of Technology

Gabriela Narutowicza 11/12 Street

80-233 Gdańsk

e-mail: grzegorz.boczkaj@pg.edu.pl

STATEMENT

on the contribution and participation in the publication

I declare that my contribution to the work:

M. Plata-Gryl, C. Jungnickel, G. Boczkaj, An improved scalable method of isolating asphaltenes, *J. Pet. Sci. Eng.* 167 (2018) 608.

was to participate in the conceptualization of the research, supervision of experiments, reviewing and editing initial draft and the revised version of the manuscript.

I estimate my contribution to the final publication to be 30 %.

G. B.

.....

Separation and Purification Technology 224 (2019) 315–321

Contents lists available at ScienceDirect

Separation and Purification Technology

journal homepage: www.elsevier.com/locate/seppur

Highly effective asphaltene-derived adsorbents for gas phase removal of volatile organic compounds

Maksymilian Plata-Gryl[a], Malwina Momotko[a], Sławomir Makowiec[b], Grzegorz Boczkaj[a,*]

[a] Gdansk University of Technology, Faculty of Chemistry, Department of Process Engineering and Chemical Technology, Poland
[b] Gdansk University of Technology, Faculty of Chemistry, Department of Organic Chemistry, Poland

ARTICLE INFO

Keywords:
Asphaltenes
Adsorption
VOC
Waste gases
Treatment
Adsorption isotherms

ABSTRACT

A novel nitrated asphaltene-derived adsorbent (Asf-Nitro) was prepared using facile isolation and modification procedures. The successful modification was confirmed by Fourier-transform infrared spectroscopy (FTIR). The nitrated adsorbent was evaluated in terms of dispersive and specific interactions, Lewis acid-base properties and adsorption isotherms by means of inverse gas chromatography (IGC). Nitration was found to be extremely effective in enhancing adsorption properties of asphaltenes towards variety of chemical compounds. Asf-Nitro adsorbent exhibits superior dispersive interactions ($197.50 \pm 1.12\,mJ\,m^{-2}$ at 423 K), as compared to unmodified asphaltenes, which are comparable with activated carbons, zeolites or alumina. Examination of the specific interactions revealed a shift from basic to acidic character of the surface, what will be beneficial for adsorption of alkaline gases. Additionally, adsorption isotherms revealed that developed surface properties of the Asf-Nitro results in more than doubled monolayer adsorption capacity. Obtained results demonstrates the applicability of the asphaltene-derived materials in adsorption processes as highly effective and low cost adsorbents. This studies revealed a highly effective adsorption of environmentally important VOCs, e.g. *n*-butanol (odorous compound), trichloromethane (chlorinated hydrocarbon) and benzene (carcinogenic).

1. Introduction

Volatile organic compounds (VOCs) are a large group of organic chemical compounds having vapor pressure of at least 0.01 kPa at standard conditions [1]. They are present as gaseous airborne chemicals and as chemicals adsorbed on solids (indoor surfaces, airborne particular matter) [2,3]. The effects of some groups of VOCs on human health as well as ecosystems [4] relate to number of acute or chronic hazards e.g.: cancer, allergies, respiratory and immune effects, central nervous systems dysfunctions, formation of tropospheric ozone and photochemical smog [5–7].

Apart from increased health risk and ecosystems deterioration, VOCs can be problematic even if their toxicity is not confirmed. Odorous compounds emitted from industries and landfills can decrease the quality of life and pose a problem for a company's image, since odors are commonly perceived as an indicator of harmful and toxic activity [8,9]. This issue is gaining particular importance due to development of both industrial and residential areas [10,11].

The issue of VOCs emission from anthropogenic sources is acknowledged and demand for VOCs emission control is increasing an enforcement of environmental legislations, e.g. European Union obliged member states to cut the emission of VOCs by 40% till 2030 [12]. Development of separation techniques is a part of remedial measures to reduce emission of VOCs.

Among the available technologies for removal of VOCs, adsorption-based processes proved their usefulness and effectiveness in purification and separation of gaseous streams [13,14]. Since the key parameter in adsorption processes is a type of adsorbent, the main developments in this field are focused on new adsorbents [15]. To replace commonly used activated carbon, zeolites, silica or polymers, new adsorbent must exhibit unique adsorption properties or/and its application must be economically feasible. Three main trends in the research on new adsorbents can be observed:

(1) synthesis of new types of adsorbents e.g. carbon nanotubes, graphene [16], molecular organic frameworks [17],
(2) development of low-cost activated carbon prepared from waste materials [18–20]
(3) direct application of natural materials as bio-adsorbents [21,22]

* Corresponding author at: Gdansk University of Technology, Faculty of Chemistry, Department of Process Engineering and Chemical Technology, G. Narutowicza St. 11/12, 80-233 Gdansk, Poland.
E-mail address: grzegorz.boczkaj@pg.edu.pl (G. Boczkaj).

https://doi.org/10.1016/j.seppur.2019.05.041
Received 29 January 2019; Received in revised form 8 May 2019; Accepted 9 May 2019
Available online 10 May 2019
1383-5866/

An interesting alternative for traditional sorbents can be asphaltenes. They are carbonaceous material with high C:H ratio of about 1–1.2 and the most aromatic fraction of the crude oil and the heaviest products of its processing, quantitatively remaining in residue from vacuum distillation. Asphaltenes are numerous group of polycyclic aromatic hydrocarbons (PACs) defined on the basis of solubility - as a fraction insoluble in *n*-alkanes and soluble in toluene or benzene. They are comprised of 4–10 fused aromatic rings, peripherally attached alkyl chains and polar functional groups, with tendency to stacking and formation of graphite-like structure. Besides carbon and hydrogen, heteroatoms such as oxygen, sulfur, nitrogen and trace amount of metals can be found in their backbone [23–28].

Asphaltenes structure i.e. aromatic ring, alkyl chains, polar functional groups (carboxylic, phenol, pyridine) is a source of a vast variety of interactions e.g. van der Waals, coulombic, hydrogen bonding and π-π stacking [29].

In petroleum industry uncontrolled asphaltene precipitation is a source of severe technological issues during crude oil processing eg. well-bore and pipeline clogging, catalyst deactivation, fouling, coke and emulsion formation [30,31]. The only practical application of asphaltenes is production of bitumen and bitumen mixtures. In petroleum industry there is significant interest in separating asphaltene fraction from process streams. Due to this reasons, asphaltenes can be treated as a undesired by product or waste.

Recently it was shown that asphaltenes can be applied as sorbents in separation techniques, due to their unique selectivity and thermal stability [32] and simplified isolation procedure of asphaltenes using residue from vacuum distillation of crude oil was proposed [33]. Their application as sorbents would lead to valorization of the by-product, reduction of the costs and would enhance company's competitiveness.

Modification of the surface chemistry can be a feasible direction toward novel applications [34]. Surface modifications that can improve or extend adsorption properties of adsorbents are widely investigated [34–39]. Heteroatoms present on a surface of an adsorbent affects the adsorption capacity and selectivity. In the literature studies on the sulfonation [39], amination [38], methylation [37], nitration [36], ammonia [35] or ozone treatment effects on the adsorption properties can be found. The diverse structure of asphaltene molecules make them especially prone to chemical modifications, thus opening many routes toward tuning their properties for particular adsorption applications [34].

The objective of this study was to evaluate the possibility of utilizing asphaltene fraction in adsorption-based processes. To enhance the surface and adsorption properties of the asphaltene fraction, its properties were tuned by a chemical modification. To evaluate the effect of the chemical modification on the performance of the asphaltene-based sorbents in adsorption processes, inverse gas chromatography (IGC) technique was used. It is a variant of gas chromatography in which a material to be investigated is placed inside a column and characterized by monitoring of the retention of probe molecules with known properties under dynamic conditions. IGC measurements can be carried out at infinite dilution and finite concentration. At infinite dilution adsorbate-adsorbent interactions are the leading cause of adsorption effects and the retention data can be converted into e.g. dispersive and specific components of the free energy of adsorption. At finite concentration, for example, adsorption isotherms can be obtained. Among test probes were environmentally important VOCs, e.g. *n*-butanol (odorous compound), trichloromethane (chlorinated hydrocarbon) and benzene (carcinogenic).

2. Experimental

Informations about the origin of bitumen samples and the asphaltene isolation method and purity control procedure can be found in Text S1.

2.1. Chemical modification (nitration) of the asphaltene fraction

Nitrated asphaltenes were modified as follows: HNO_3 (65%, 6.4 cm^3, 91 mmol) was added to a stirred solution of asphaltene (1.59 g) in CH_2Cl_2 (50 ml). The mixture was refluxed and stirred for 16 h. After this time, solvent was removed under reduced pressure (ca. 10 mmHg). Residue was suspended in methanol (50 ml) and filtered off. The precipitate was washed with methanol (20 ml) and dried under vacuum at 80 °C for 8 h. Successful modification was confirmed by the Fourier-transform infrared spectroscopy (FTIR). Details of the FTIR analysis procedure are described in Text S2.

2.2. Adsorbent preparation

Asphaltene-derived adsorbents (raw asphaltenes – Asf and nitrated asphaltenes – Asf-Nitro) were prepared by coating the Chromosorb W AW DMCS 80/100 mesh (Johns-Manville, USA) with asphaltenes (adsorbent). Chromosorb W (further denoted as Ch-W) is a hydrophobic support with large irregular pores and has BET surface area of 0.6–1.3 $m^2 g^{-1}$. Textural properties (i.e. low surface area values, absence of micropores) of the support ensures that only surface's characteristic influences the adsorption experiments. Moreover it eliminates issues with diffusion into pores and on a surface of an adsorbent.

Detailed description of the coating procedure can be found in [32]. The content of the adsorbent on the support was 10% by mass. It is worth to mention that during the immobilization of asphaltenes on the Ch-W a total coverage is obtained, thus support characteristics in terms of molecular interactions with solutes is negligible.

2.3. Inverse gas chromatography measurements

IGC measurements were carried out using Clarus 500 gas chromatograph equipped with flame ionization detector (Perkin Elmer, USA). Preliminary studies revealed that sorption properties of asphaltenes strongly depend on the temperature and that there is nonlinear change in asphaltene's surface properties at about 453 K. To observe that change in detail, measurements were carried out in the 423–473 K temperature range with 5 K increments. Since retention on Ch-W was insufficient at that temperatures, it was lowered to the 313–333 K range with 5 K increments. Temperature of both the injection port and the detector were 573 K. The carrier gas was nitrogen (N5.0, Linde Gas, Poland) and a flow rate of 20 ml min^{-1} was used. The FID detector was supplied by N5.5 hydrogen from the PGXH2 500 generator (Perkin Elmer, USA) and air from the GC 3000 zero air generator (Perkin Elmer, USA).

To perform IGC experiments at infinite dilution (near zero surface coverage), when adsorption is described by Henry's law, repeatedly smaller samples of vapors from the headspace of the probe compounds were injected by a gas-tight syringe into the GC injector operated in splitless mode. Each probe was injected separately. Retention time was calculated from the peak maximum when there was no change in retention time for three consequent injections. To determine dead (void) time, methane was used as a non-interacting, with a stationary phase, compound at conditions used in this study. Test probes used in IGC experiments are listed in Table S1. *n*-Alkanes were used as standard compounds to evaluate dispersive interactions. Selected polar test probes represents various chemical groups of compounds with different chemical and physical properties. It allows to precisely characterize surface's adsorption properties.

Main parameter calculated in IGC experiments is the net retention volume [40] or specific retention volume (per gram of adsorbent) [41–43]. Here it was calculated according to Eq. (1):

$$V_N = \frac{j}{m} F(t_R - t_0) \quad (1)$$

where t_R (min) is the retention time of given probe, t_0 (min) is the void

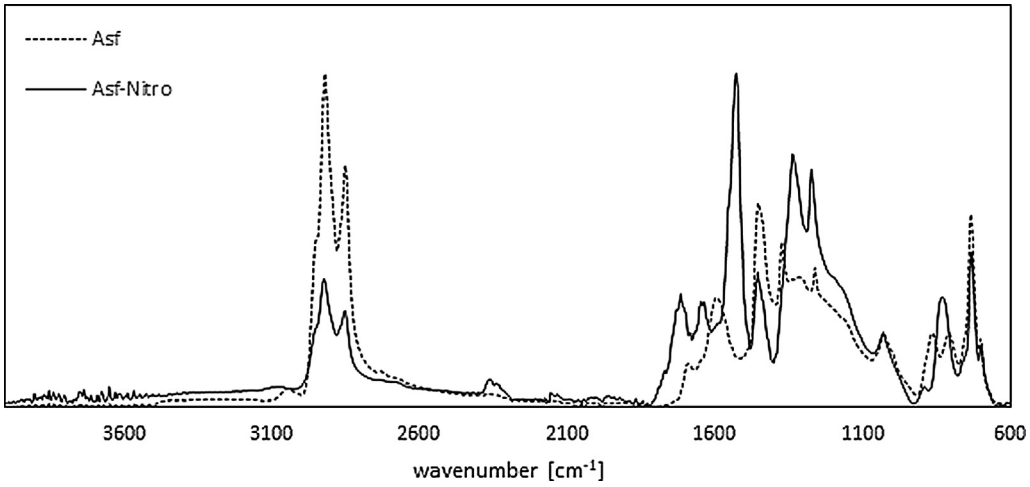

Fig. 1. Normalized FTIR spectra of the asphaltene samples.

time measured with a non–interacting probe (methane), F (mL min^{-1}) is the flow rate measured at the temperature of experiment, j (–) is the James-Martin correction factor taking into account the compressibility of the gas [44] and m (g) is the mas of the adsorbent coated onto support.

Based on V_N value, the molar free energy of adsorption ΔG_A (J mol^{-1}) can be calculated by Eq. (2):

$$\Delta G_A = -RT\ln V_N + C \quad (2)$$

where R (J K^{-1} mol^{-1}) is the gas constant, T (K) is the absolute temperature and C is a constant.

The differential heat of adsorption ΔH_A (J mol^{-1}) and the standard entropy of adsorption ΔS_A (J mol^{-1}) can be derived from the well-known van't Hoff equation.

The free surface energy of a solid is a sum of dispersive (γ_S^D) and specific components (γ_S^{SP}). For non-polar probes, such as alkanes, only dispersive interactions occurs with the surface of the solid. Hence, the value of γ_S^D can be obtained from the ΔG_A values calculated for the series of n-alkanes [45]. To obtain the value of the γ_S^D, the Dorris-Gray method was used [46] in which it is calculated from Eq. (3). Fig. S1 summarize the method of γ_S^D determination.

$$\gamma_S^D = \frac{(-\Delta G_{CH2})^2}{4N^2(a_{CH2})^2\gamma_{CH2}} \quad (3)$$

where N is the Avogadro's number (mol^{-1}), ΔG_{CH_2} (J mol^{-1}) is the free energy of adsorption per methylene group. It can be obtained from the slope of the ΔG_A versus the number of carbon atoms in the n-alkane molecule. a_{CH_2} (m^2) is the surface area of methylene group. In this work the most common value of 6 Å^2 was used, although other values can be found in the literature [45]. γ_{CH_2} (J mol^{-1}) is the surface energy of the polyethylene-type polymer with finite molecular weight and is calculated according to Eq. (4) [45]:

$$\gamma_{CH2} = (35.6 + 0.058(293 - T))\cdot 10^{-3} \quad (4)$$

By injecting polar probes into the column, specific interactions between polar probes and an adsorbent can be observed. Extent of that interactions can be measured with different methods [45] all based on the same assumption that:

$$\Delta G_A = \Delta G_A^d + \Delta G_A^{sp} \quad (5)$$

where ΔG_A^{SP} (J mol^{-1}) refers to specific interactions (the specific free energy of adsorption) of a polar molecule adsorbed on a solid.

Specific free energies of adsorption were calculated using Papirer's method [47,48]. Plotting values of ΔG_A for series of n-alkanes against the logarithm of the vapor pressure (P^0) of the probe at the experimental temperature, will result in a straight line. ΔG_A^{SP} can be calculated as a difference between ΔG_A obtained for the polar probe and ΔG_A of a hypothetical alkane with the same vapor pressure. The principle of the measurement is presented in Fig. S2. The advantage of the Papirer's method are easily accessible P^0 values for test probes in wide temperature ranges.

Knowing the extent of the specific interactions, the acidic (electronacceptor) and basic (electrondonor) properties of a solid can be determined. Calculations of specific interactions revealed nonlinear dependence of $\Delta G_A^{SP}/T$ versus $1/T$ (R^2 = 0.7–0.95), thus ΔH_A^{SP} could not be determined, at least without enormous uncertainty. It prevent usage of donor (DN) and acceptor (AN) numbers that are commonly used to assess acidic and basic properties of a solid, when specific interactions varies linearly with temperature. Instead, Good and van Oss equation [49] was used to obtain the acidic (γ_S^+) and basic (γ_S^-) parameters of the asphaltene adsorbents. Based on the values of aforementioned parameters, the specific component of the surface free energy can be determined (γ_S^{SP}). Details of the calculation procedure are presented in Text S3.

Adsorption isotherms were determined according to the peak maximum method at finite concentration as described elsewhere [50,51]. Adsorption isotherms were measured at three temperatures i.e. 423, 448 and 473 K for selected noxious VOCs i.e. TCM (chlorinated hydrocarbon), benzene (carcinogenic) and n-butanol (odorous). The isotherm calculation method is described in more depth in Text S4 and in Fig. S3.

Experimental data were fitted by non-linear regression to BET isotherm model. Computations were performed in R [52] using minipack.ln package which utilizes Levenberg-Marquardt nonlinear least-squares algorithm [53]. Based on the maximum monolayer adsorption capacity, surface areas occupied by the adsorbate were calculated. Details are provided in Text S5.

2.4. Quality assurance of data

All data points obtained by GC measurements and presented in this paper are an average of three injections. The values reported in the following section are given with 95% confidence interval.

3. Results and discussion

Fig. 1 presents infrared absorption spectra of raw (Asf) and modified (Asf-Nitro) asphaltenes. FTIR-ATR spectroscopy was used to determine functional group types in tested samples. FTIR spectra of both samples revealed intensive bands near 2920, 2850 and 1455 cm^{-1} because of the CH_2 and CH_3 groups. For that groups peak at 1375 cm^{-1} is also characteristic [54]. It is clearly visible in the spectrum for Asf, while on

Asf-Nitro spectrum it is overlaid by stronger absorption band at 1337 cm^{-1}. Bands at 2920, 2850, 1450 and 1375 cm^{-1} corresponds to vibrations of the methyl group in aliphatic chains. Interestingly, no absorption above 3100 cm^{-1} was observed, indicating lack of OH groups. Small band visible in both spectra, at around 700 cm^{-1} can be related to alkyl chains longer than 4 methylene units [55]. The absorbance bands observed between 730 and 870 cm^{-1} can be assigned to the aromatic C—H out-of-plane bending vibrations [56]. Cleary visible band close to 1030 cm^{-1} can be related to sulfoxide functional group [57] or to ester linkages [58]. Absorption bands at 1262 (Asf) and 1274 (Asf-Nitro) cm^{-1} can be attributed to groups containing singly bonded oxygen eg. esters or ethers [59]. Distinct band observed at the 1600 cm^{-1} in the Asf spectrum is related to the aromatic C=C stretching vibration [55]. In the Asf-Nitro spectrum that band is overlaid by the strong absorption at 1337 cm^{-1}. Three new intensive bands, that can be observed in the Asf-Nitro spectrum, at 1529, 1337 and 1272 cm^{-1} are a clear confirmation of successful nitration of the asphaltenes, as they can be related to the asymmetrical and symmetrical aromatic C-NO_2 and N=O stretching, respectively [60]. Additional new peak in the Asf-Nitro spectrum at 1715 cm^{-1} corresponds to the carbonyl functionality [61], what may be a result of the oxidation and together with the increased absorption at 1274 cm^{-1} indicates increased presence of ester functionalities.

Quantitative assessment of the structural features and the effect of the chemical modification on the structure of asphaltenes can be determined based on an approach that can be found e.g. in [62,63]. It is based on the absorption intensity ratios of characteristic bands and the results are presented in Text S6 and Table S2.

Table 1 presents values of the enthalpy and entropy of adsorption of test probes on the investigated materials. Obtained values of enthalpies confirmed that the process is exothermic and negative values of ΔS_A implies that the degree of freedom decreased at the gas-solid interface, what is expected in adsorption process. Compared to ΔH_{liq} (see Table S1), ΔH_A have much lower values (higher absolute values) on Asf and Asf-Nitro, which indicate that measured enthalpies of adsorption are not only due to condensation but also due to physic-chemical interactions between adsorbate and adsorbent. As a result of nitration the value of enthalpy of adsorption increased about one and a half times compared to unmodified asphaltenes. The biggest change was observed for *n*-butanol (1.81 times higher) and the smallest for TCM (1.30 times higher). Similar change in the value of ΔH_A for both the alkanes and polar probes indicates that the most significant difference is in dispersion forces, since alkanes are not capable of specific interaction. The change in the value of entropies followed the same trend as in case of enthalpies.

For Chromosorb W adsorption experiments at temperatures suitable for asphaltene sorbents were infeasible, thus measurements were conducted at 40–60 °C interval with 5 °C increments. It means that for Ch-W lower number of data points (5 instead of 9) were obtained, what resulted in smaller number of the degrees of freedom. As a result, the confidence intervals had extended. Although direct comparison between the results for asphaltene based sorbents and Ch-W is difficult, nevertheless it can be seen that the affinity (indicated by the value of ΔH_A) of probe molecules is stronger for the surface of Asf and Asf-Nitro sorbents, as compared to Ch-W, despite the three times higher temperature during experiments with asphaltene sorbents.

Table 2
Values of the dispersive component of the surface free energy for the Asf and Asf-Nitro adsorbents.

T [K]	γ_S^D (mJ m^{-2})				Asf-Nitro/Asf
	Asf	R^2	Asf-Nitro	R^2	
423	57.72 ± 0.01	1.000	197.50 ± 1.12	0.997	3.42 ± 0.02
428	55.32 ± 0.00	1.000	186.04 ± 0.69	0.998	3.36 ± 0.01
433	52.00 ± 0.03	1.000	175.64 ± 0.06	1.000	3.38 ± 0.00
438	49.79 ± 0.02	1.000	165.35 ± 0.29	0.999	3.32 ± 0.01
443	48.14 ± 0.06	0.999	146.80 ± 0.52	0.998	3.05 ± 0.01
448	44.17 ± 0.06	0.999	159.30 ± 0.42	0.998	3.36 ± 0.01
453	42.68 ± 0.04	0.999	155.87 ± 1.67	0.993	3.65 ± 0.04
458	36.07 ± 0.28	0.995	144.50 ± 1.13	0.995	4.01 ± 0.06
463	37.39 ± 0.09	0.998	130.24 ± 1.03	0.995	3.48 ± 0.04
468	37.58 ± 0.03	0.999	118.85 ± 0.74	0.996	3.16 ± 0.02
473	40.97 ± 0.33	0.999	113.09 ± 0.41	0.997	2.76 ± 0.03

The forces responsible for the adsorption (intermolecular adsorbent-adsorbate interactions) can be generally divided into dispersive (γ_S^D) and specific (γ_S^{SP}) components of the surface free energy, corresponding to the dispersion and specific interactions, respectively. The dispersive component is unspecific for all molecules and is caused by London forces. In the Table 2 values of the γ_S^D for asphaltene sorbents are given along with the value comparing the difference (Asf-Nitro/Asf) that arise after chemical modification. The plot for the data in Table 2 can be found in Fig. S4.

Determination coefficient values for alkane reference lines were above 0.995 at almost all experimental temperatures. Obtained values of the γ_S^D indicate that asphaltene sorbents are very active and exhibit strong dispersive interaction, as compared to Ch-W (64.90 ± 0.16 mJ m^{-2} at 313 K) despite that measurements for asphaltene sorbents were carried out at temperatures 3–4 times higher. It is clearly visible that the nitration promoted the dispersive interactions Asf-Nitro adsorbent have γ_S^D values 2.7–4 times higher than Asf adsorbent. The difference is the most substantial at lower temperatures and is diminishing as the experimental temperature increases. The

Table 1
Values of enthalpies and entropies of adsorption. TCM – chloroform, THF – tetrahudrofuran, EtOAc – ethyl acetate, nBuOH – *n*-butanol. NA – not applicable; at the experimental conditions the retention was insufficient or excessive.

T [K]	Ch-W 313–333		Asf 423–473		Asf-Nitro 423–473	
Probe	ΔH_A (kJ/mol)	ΔS_A (J/mol)	ΔH_A (kJ/mol)	ΔS_A (J/mol)	ΔH_A (kJ/mol)	ΔS_A (J/mol)
C5	NA	NA	NA	NA	−52.06 ± 8.44	−98 ± 19
C6	−34.12 ± 8.34	−112 ± 26	−43.89 ± 8.13	−90 ± 18	−71.82 ± 17.60	−133 ± 39
C7	−59.83 ± 18.62	−182 ± 58	−59.24 ± 4.89	−119 ± 11	−94.28 ± 8.09	−173 ± 18
C8	−70.05 ± 22.83	−203 ± 71	−69.47 ± 2.70	−136 ± 6	−111.91 ± 8.21	−202 ± 18
C9	−77.76 ± 9.30	−217 ± 29	−80.36 ± 3.39	−155 ± 8	−124.81 ± 12.32	−220 ± 27
C10	−93.77 ± 14.59	−259 ± 45	−88.15 ± 4.21	−167 ± 9	NA	NA
TCM	−33.92 ± 7.30	−112 ± 23	−50.40 ± 9.38	−101 ± 21	−66.48 ± 5.32	−117 ± 12
THF	−43.11 ± 2.76	−113 ± 9	−54.12 ± 2.33	−106 ± 5	−81.70 ± 6.40	−144 ± 14
EtOAc	−53.09 ± 10.99	−144 ± 34	−61.54 ± 5.27	−123 ± 12	−97.74 ± 8.81	−174 ± 20
nBuOH	−44.04 ± 9.53	−109 ± 30	−55.32 ± 3.50	−101 ± 8	−100.97 ± 6.78	−175 ± 15
acetone	−38.70 ± 5.59	−102 ± 17	−48.96 ± 5.88	−96 ± 13	−83.18 ± 4.76	−148 ± 11
benzene	−34.01 ± 8.03	−110 ± 25	−51.49 ± 2.43	−100 ± 5	−76.64 ± 5.06	−133 ± 11

increase in the γ_S^D value for the Asf-Nitro can be connected with the shortening of the side chains (see the FTIR analysis results), which can lower the steric hindrance and increase the access of the adsorbate molecules to the cores of the asphaltenes, which consists mostly of polycondensed aromatic rings.

Values of the γ_S^D obtained for Asf-Nitro adsorbent are similar to those obtained for zeolite 13X and higher than those for alumina. Compared to values of γ_S^D found in the literature for activated carbon, Asf-Nitro exhibits slightly weaker dispersive interactions [64].

Analysis of the γ_S^D values obtained for tested sorbents at different temperatures revealed a temporary increase of the γ_S^D value at around 448 K. It could be explained with changes in the adsorption mechanism. As at the elevated temperatures the asphaltenes could swell and partial absorption phenomena could occur. In the previous GC studies an increased efficiency (narrower peaks) were observed for compounds eluting at higher temperatures during analyses with temperature programming, what is characteristic for gas-liquid chromatography. However similar trend should be observed for Asf adsorbent and while there are fluctuations of the γ_S^D value at around 448 K, but they are not statistically significant. Another possible explanation is that the mentioned increase in the dispersive interactions can be attributed to the surface modification and relaxation/deactivation of some surface groups leading to stronger interaction with the aromatic rings present in the core of the asphaltene structure.

For all adsorbents the value of γ_S^D is gradually decreasing with the temperature. The decrease in the γ_S^D value is the most evident for the Asf-Nitro. It is lowering at a rate of about $-3.0\,mJ\,m^{-2}\,K^{-1}$ up to 448 K and $-1.9\,mJ\,m^{-2}\,K^{-1}$ above 448 K, while for Asf and Ch-W adsorbents it is about -0.5 and $-1.0\,mJ\,m^{-2}\,K^{-1}$, respectively. While this is tangential for adsorption step, during desorption it can be advantageous. 2–3 times higher decrease rate of dispersive interactions with increased temperature for Asf-Nitro, compared to Asf, means increased performance during regeneration process and higher economic feasibility.

Table S2 presents values of specific free energy change (ΔG_A^{SP}) for different polar molecules adsorbed on the investigated adsorbents at different temperatures. Both asphaltene adsorbents demonstrate fairly stable specific interactions in the range of experimental temperatures. Relative standard deviation (RSD%) of ΔG_A^{SP} for probe compounds is at the level of 10–15%. Examining changes of the ΔG_A^{SP} value for Asf-Nitro a sudden drop can be observed at around 458 K, which can be caused by lowering of the interactions provided by functional groups.

It is observed that values of specific interactions with basic compounds (THF and EtOAc) are largely higher for the Asf-Nitro, as compared to the Asf. That indicates increased acidity of the Asf-Nitro surface and is an expected result of nitration, as nitro groups should enhance acidic properties of a solid's surface. Contrary, there is no noticeable change in the value of ΔG_A^{SP} for TCM (acidic probe) between asphaltene adsorbents. Values of ΔG_A^{SP} for TCM and EtOAc reveals an amphoteric character of the Asf adsorbent, whereas Asf-Nitro surface displays enhanced acidic properties. In case of neutral compounds i.e. *n*-BuOH, acetone and benzene, only acetone exhibit significant change in the strength of specific interactions (caused by interactions of carbonyl group of acetone with nitro group of modified asphaltene). Thus, the considerable change (decrease) in the enthalpy of adsorption (see Table 1) for nBuOH and benzene is mainly a result of increased dispersive interactions, which is in line with measured γ_S^D values.

While strong specific interactions would be beneficial for removal of variety of compounds with different acceptor and donor-properties, extensive electron-acceptor character of Asf-Nitro surface will promote an adsorption of alkaline gases e.g. ammonia, pyridines or amines.

In Fig. 2, values of γ_S^+ to γ_S^- ratio for examined asphaltene adsorbents are presented. Exact values of the γ_S^+ and γ_S^- can be found in Table S3. Presented values are consistent with former discussion about ΔG_A^{SP} values. Asf exhibit a predominance of basic (electron-donor) properties over acidic, due to the presence of free electron pairs. Acid-base

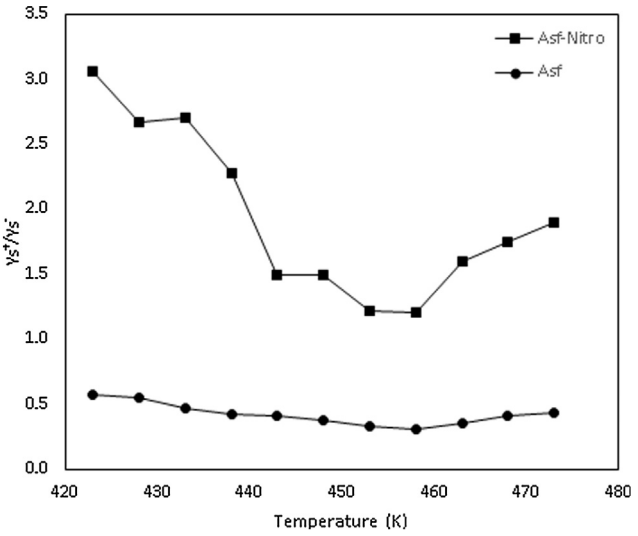

Fig. 2. Values of acidic to basic parameter ratios of examined asphaltene adsorbents.

properties of the Asf surface are virtually stable over the range of experimental temperatures. The lower the γ_S^+ to γ_S^- ratio, the greater basicity of the solid's surface. It is evident that nitration shifted the character of the asphaltene's surface from basic to acidic. Electron-acceptor properties of Asf-Nitro are over 3 times stronger than electron-donor at 423 K and decrease with temperature increase. At 460 K acidity and basicity of Asf-Nitro surface is similar. Above that temperature, an increase of acidity is observed.

Values of the total surface energy (γ_S), divided into dispersive (γ_S^D) and specific (γ_S^{SP}) components, are shown in Fig. 3. It visualizes the aforementioned substantial increase in dispersive component of the free surface energy. According to values of γ_S, Asf-Nitro adsorbent exhibits significantly higher surface activity than unmodified adsorbent, being 3–4 times higher. For both examined asphaltene adsorbents, dispersive interactions dominate over specific interactions. Closer examination of results revealed the increased contribution of specific components to the total surface energy. Taking into account that the surface energy has an immense impact on the adsorbent-adsorbate interactions, nitration appears as a favorable and uncomplicated modification that improve adsorption properties of asphaltenes and will increase the performance of asphaltene based sorbents.

To evaluate the impact of modification on asphaltene adsorbents capacity, measurements at finite concentration were carried out.

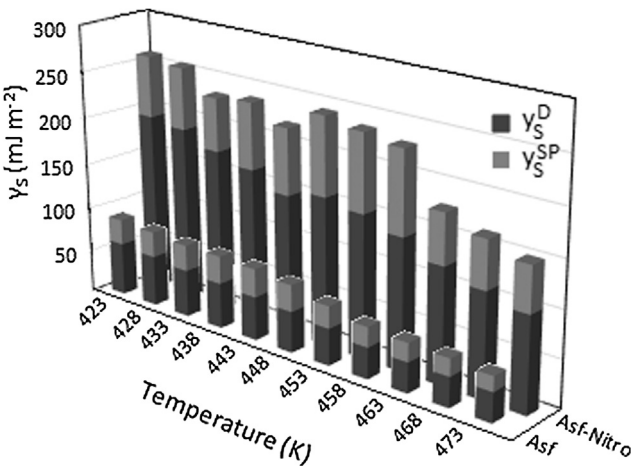

Fig. 3. Total surface energy of asphaltene adsorbents divided into dispersive and specific components.

Table 3
BET constant C, monolayer capacity q_{mono} and surface area of asphaltene adsorbent occupied by the adsorbate at 423–473 K. NA – retention was insufficient at experimental conditions to collect at least 5 data points.

Adsorbate	T (K)	q_{mono} (mg g^{-1})	C	R^2	SA (m^2 g^{-1})
	Asf				
Benzene	423	2.301 ± 0.522	110 ± 39	0.996	0.82 ± 0.19
	448	1.137 ± 0.185	165 ± 41	0.998	0.40 ± 0.07
	473	NA	NA	NA	NA
nBuOH	423	3.404 ± 0.738	51 ± 17	0.997	1.08 ± 0.23
	448	2.555 ± 0.709	66 ± 27	0.998	0.81 ± 0.23
	473	NA	NA	NA	NA
TCM	423	2.333 ± 0.312	215 ± 53	0.996	0.81 ± 0.09
	448	1.531 ± 0.483	355 ± 160	0.998	0.58 ± 0.22
	473	NA	NA	NA	NA
	Asf-Nitro				
Benzene	423	6.275 ± 0.795	804 ± 210	0.994	2.23 ± 0.28
	448	5.717 ± 0.664	569 ± 141	0.997	2.03 ± 0.24
	473	4.637 ± 0.655	479 ± 115	0.999	1.64 ± 0.23
nBuOH	423	7.647 ± 1.002	796 ± 357	0.993	2.43 ± 0.32
	448	6.574 ± 0.850	628 ± 225	0.994	2.09 ± 0.27
	473	4.636 ± 0.409	678 ± 147	0.998	1.47 ± 0.13
TCM	423	9.155 ± 1.198	891 ± 215	0.998	3.11 ± 0.41
	448	8.406 ± 0.683	656 ± 100	0.999	2.85 ± 0.23
	473	4.091 ± 1.778	1223 ± 352	0.985	1.39 ± 0.60

Adsorption isotherms for TCM, n-BuOH and benzene were determined and fitted to the BET isotherm model. The results are presented in the Table 3. The monolayer adsorption capacity of the Asf-Nitro as a consequence of nitration was more than doubled. Increased q_{mono} values for benzene and nBuOH can be easily explained by increased dispersive interactions and in the case of BuOH by enhanced specific interactions as well.

What is intriguing is the Asf-Nitro's outstanding adsorption capacity for TCM (chloroform). TCM acts as an acid and it is expected to establish repulsive forces with the acidic surface of the Asf-Nitro. It may be explained by the predominance of the dispersive interactions and presence of basic adsorption centers. Although in the minority, they can diminish the repulsive effect of acidic moieties. Third factor can be the geometry of the molecules. TCM is not linear as n-BuOH or flat as benzene molecules and can be more "tightly" packed in the monolayer, even if cross-sectional areas of molecules are fairly similar.

To give a more detailed description about the augmented adsorption properties of asphaltene sorbents, the surface area occupied by the adsorbate was calculated. The first thing that stands out is the similarity of the calculated SA for Asf adsorbent, to those provided by the manufacturer for N_2 adsorption (0.5–1.5 m^2 g^{-1}). The change in the SA values between asphaltene adsorbents is just the derivative of the aforementioned increased monolayer capacity and can be an indication of an introduction of a new adsorption sites to the surface.

4. Conclusion

The research revealed that a facile chemical modification can greatly increase the adsorption properties of asphaltene fraction. The nitrated adsorbent exhibits high surface activity that arise from enhanced dispersive and specific interactions. Compared to unmodified asphaltenes, a shift in Lewis acid-base properties after nitration was observed – from basic to acidic character of the surface. Moreover, in terms of dispersive interactions, nitrated sorbent is comparable with activated carbons, zeolites or alumina. Improved strength of the dispersive and specific interactions of nitrated asphaltenes lead to higher adsorption capacity for volatile organic compounds, as compared to unmodified sorbent.

Furthermore, wasted adsorbent can be regenerated at lower temperatures comparing to activated carbon. An alternative solution can be its incorporation into road bitumen – the asphaltene content in the bitumen is desired due to its valuable properties regarding improvement of basic bitumen applicational parameters such as penetration value or softening point.

Considering the above-mentioned assets of nitrated asphaltenes and the nature of the raw material (undesired by-product, facile isolation and modification method), nitrated asphaltenes appears to be an highly effective and low-cost adsorbent for gas phase removal of volatile organic compounds. Utilization of asphaltenes in separation processes would solve, at least partially, petroleum industry's problem with undesired and problematic by-product by its valorization. Moreover, asphaltene fraction's applications could be probably extended to liquid phase adsorption and other separation techniques e.g. membranes. Future studies should target the exploration of inexpensive porous supports for the asphaltene fraction that would facilitate the adsorption through the capillary condensation process as in case of activated carbons.

Acknowledgments

The authors gratefully acknowledge the financial support from the National Center for Research and Development, Warsaw, Poland – Project LIDER, no. LIDER/036/573/L-5/13/NCBR/2014. This work was financially supported by the project "INTERPHD2" no. POWR.03.02.00-IP.08-00-DOC/16.

Appendix A. Supplementary material

Supplementary data to this article can be found online at https://doi.org/10.1016/j.seppur.2019.05.041.

References

[1] J.H. Duffus, M. Nordberg, D.M. Templeton, Glossary of terms used in toxicology, Pure Appl. Chem. 79 (2007), https://doi.org/10.1351/pac200779071153.
[2] F.I. Khan, A.Kr. Ghoshal, A.K. Ghoshal, Removal of volatile organic compounds from polluted air, J. Loss Prev. Process Ind. 13 (2000) 527–545, https://doi.org/10.1016/S0950-4230(00)00007-3.
[3] I. Kourtchev, C. Giorio, A. Manninen, E. Wilson, B. Mahon, J. Aalto, M. Kajos, D. Venables, T. Ruuskanen, J. Levula, M. Loponen, S. Connors, N. Harris, D. Zhao, A. Kiendler-Scharr, T. Mentel, Y. Rudich, M. Hallquist, J.F. Doussin, W. Maenhaut, J. Bäck, T. Petäjä, J. Wenger, M. Kulmala, M. Kalberer, Enhanced volatile organic compounds emissions and organic aerosol mass increase the oligomer content of atmospheric aerosols, Sci. Rep. 6 (2016), https://doi.org/10.1038/srep35038.
[4] A. Mellouki, T.J. Wallington, J. Chen, Atmospheric chemistry of oxygenated volatile organic compounds: impacts on air quality and climate, Chem. Rev. 115 (2015) 3984–4014, https://doi.org/10.1021/cr500549n.
[5] L. Mølhave, B. Bach, O.F. Pedersen, Human reactions to low concentrations of volatile organic compounds, Environ. Int. 12 (1986) 167–175, https://doi.org/10.1016/0160-4120(86)90027-9.
[6] D.A. Sarigiannis, S.P. Karakitsios, A. Gotti, I.L. Liakos, A. Katsoyiannis, Exposure to major volatile organic compounds and carbonyls in European indoor environments and associated health risk, Environ. Int. 37 (2011) 743–765, https://doi.org/10.1016/J.ENVINT.2011.01.005.
[7] S.H. Hong, D.C. Shin, Y.J. Lee, S.H. Kim, Y.W. Lim, Health risk assessment of volatile organic compounds in urban areas, Hum. Ecol. Risk Assess. 23 (2017) 1454–1465, https://doi.org/10.1080/10807039.2017.1325714.
[8] R. Muñoz, E.C. Sivret, G. Parcsi, R. Lebrero, X. Wang, I.H. Suffet, R.M. Stuetz, Monitoring techniques for odour abatement assessment, Water Res. 44 (2010) 5129–5149, https://doi.org/10.1016/j.watres.2010.06.013.
[9] R. Iranpour, H.H.J. Cox, M.A. Deshusses, E.D. Schroeder, Literature review of air pollution control biofilters and biotrickling filters for odor and volatile organic compound removal, Environ. Prog. 24 (2005) 254–267, https://doi.org/10.1002/ep.10077.
[10] M. Nowicki, Planning of industrial sites in a city from the point of view of air pollution control, Energy Build. 11 (1988) 171–179, https://doi.org/10.1016/0378-7788(88)90034-5.
[11] P. Mudu, B. Terracini, M. Martuzzi (Eds.), Human Health in Areas with Industrial Contamination, WHO Regional Office for Europe, Copenhagen, 2014.
[12] European Parliament, European Council, Directive 2008/50/EC on ambient air quality and cleaner air for Europe, Off. J. Eur. Communities 152 (2008) 1–43.
[13] O. Penciu, M. Gavrilescu, Survey on the treatment of gaseous streams containing volatile organic compounds, Environ. Eng. Manag. J. 2 (2003).
[14] K.L. Foster, J. Economy, R.G. Fuerman, S.M. Larson, M.J. Rood, Adsorption

characteristics of trace volatile organic compounds in gas streams onto activated carbon fibers, Chem. Mater. 4 (1992) 1068–1073, https://doi.org/10.1021/cm00023a026.
[15] W.J. Thomas, B. Crittenden, Adsorption Technology and Design, Elsevier, Oxford, 1998.
[16] X. Zhang, B. Gao, A.E. Creamer, C. Cao, Y. Li, Adsorption of VOCs onto engineered carbon materials: a review, J. Hazard. Mater. 338 (2017) 102–123, https://doi.org/10.1016/j.jhazmat.2017.05.013.
[17] J.-R. Li, R.J. Kuppler, H.-C. Zhou, Selective gas adsorption and separation in metal–organic frameworks, Chem. Soc. Rev. 38 (2009) 1477, https://doi.org/10.1039/b802426j.
[18] I.D. Manariotis, K.N. Fotopoulou, H.K. Karapanagioti, Preparation and characterization of biochar sorbents produced from malt spent rootlets, Ind. Eng. Chem. Res. 54 (2015) 9577–9584, https://doi.org/10.1021/acs.iecr.5b02698.
[19] Z. Chen, B. Chen, C.T. Chiou, Fast and slow rates of naphtalene sorption to biochars produced at different temperatures, Environ. Sci. Technol. 46 (2012) 11104–11111, https://doi.org/10.1021/es302345e.
[20] B.H. Hameed, A.A. Rahman, Removal of phenol from aqueous solutions by adsorption onto activated carbon prepared from biomass material, J. Hazard. Mater. 160 (2008) 576–581, https://doi.org/10.1016/J.JHAZMAT.2008.03.028.
[21] F.A.A. Al-Rub, M.H. El-Naas, I. Ashour, M. Al-Marzouqi, Biosorption of copper on Chlorella vulgaris from single, binary and ternary metal aqueous solutions, Process Biochem. 41 (2006) 457–464, https://doi.org/10.1016/j.procbio.2005.07.018.
[22] N. Maaloul, P. Oulego, M. Rendueles, A. Ghorbal, M. Díaz, Novel biosorbents from almond shells: characterization and adsorption properties modeling for Cu(II) ions from aqueous solutions, J. Environ. Chem. Eng. 5 (2017) 2944–2954, https://doi.org/10.1016/j.jece.2017.05.037.
[23] O.C. Mullins, The asphaltenes, Annu. Rev. Anal. Chem. 4 (2011) 393–418, https://doi.org/10.1146/annurev-anchem-061010-113849.
[24] L.A. Pineda, F. Trejo, J. Ancheyta, Correlation between properties of asphaltenes and precipitation conditions, Pet. Sci. Technol. 25 (2007) 105–119, https://doi.org/10.1080/10916460601054248.
[25] A.E. Pomerantz, Q. Wu, O.C. Mullins, R.N. Zare, Laser-based mass spectrometric assessment of asphaltene molecular weight, molecular architecture, and nanoaggregate number, Energy Fuels 29 (2015) 2833–2842, https://doi.org/10.1021/ef5020764.
[26] M.R. Gray, G. Assenheimer, L. Boddez, W.C. McCaffrey, Melting and fluid behavior of asphaltene films at 200–500 C, Energy Fuels 18 (2004) 1419–1423, https://doi.org/10.1021/ef049923w.
[27] C. Leyva, J. Ancheyta, C. Berrueco, M. Millán, Chemical characterization of asphaltenes from various crude oils, Fuel Process. Technol. 106 (2013) 734–738, https://doi.org/10.1016/j.fuproc.2012.10.009.
[28] B. Schuler, G. Meyer, D. Peña, O.C. Mullins, L. Gross, Unraveling the molecular structures of asphaltenes by atomic force microscopy, J. Am. Chem. Soc. 137 (2015) 9870–9876, https://doi.org/10.1021/jacs.5b04056.
[29] J. Murgich, Intermolecular forces in aggregates of asphaltenes and resins, Pet. Sci. Technol. 20 (2002) 983–997, https://doi.org/10.1081/LFT-120003692.
[30] K. Akbarzadeh, A. Hammami, A. Kharrat, D. Zhang, S. Allenson, J. Creek, S. Kabir, A. Jamaluddin, A.G. Marshall, R.P. Rodgers, O.C. Mullins, T. Solbakken, Asphaltenes—problematic but rich in potential, Oilf. Rev. (2007) 22–43.
[31] E. Ramirez-Jaramillo, C. Lira-Galeana, O. Manero, Modeling asphaltene deposition in production pipelines, Energy Fuels 20 (2006) 1184–1196, https://doi.org/10.1021/ef050262s.
[32] G. Boczkaj, M. Momotko, D. Chruszczyk, A. Przyjazny, M. Kamiński, Novel stationary phases based on asphaltenes for gas chromatography, J. Sep. Sci. 39 (2016) 2527–2536, https://doi.org/10.1002/jssc.201600183.
[33] M. Plata-Gryl, C. Jungnickel, G. Boczkaj, An improved scalable method of isolating asphaltenes, J. Pet. Sci. Eng. 167 (2018) 608–614, https://doi.org/10.1016/j.petrol.2018.04.039.
[34] W. Shen, Z. Li, Y. Liu, Surface chemical functional groups modification of porous carbon, Recent Patents Chem. Eng. (2012), https://doi.org/10.2174/2211334710801010027.
[35] M.S. Shafeeyan, W.M.A.W. Daud, A. Houshmand, A. Arami-Niya, Ammonia modification of activated carbon to enhance carbon dioxide adsorption: effect of preoxidation, Appl. Surf. Sci. (2011), https://doi.org/10.1016/j.apsusc.2010.11.127.
[36] M.S. Shafeeyan, A. Houshmand, A. Arami-Niya, H. Razaghizadeh, W.M.A.W. Daud, Modification of activated carbon using nitration followed by reduction for carbon dioxide capture, Bull. Korean Chem. Soc. (2015), https://doi.org/10.1002/bkcs.10100.
[37] W.D. Samuels, N.H. LaFemina, V. Sukwarotwat, W. Yantasee, X.S. Li, G.E. Fryxell, Chloromethylated activated carbon: a useful new synthon for making a novel class of sorbents for heavy metal separations, Sep. Sci. Technol. (2010), https://doi.org/10.1080/01496390903423550.
[38] M. Abe, K. Kawashima, K. Kozawa, H. Sakai, K. Kaneko, Amination of activated carbon and adsorption characteristics of its aminated surface, Langmuir (2000), https://doi.org/10.1021/la990976t.
[39] H. Ikeda, Y. Takeuchi, H. Asaba, Removal of H_2S, CH_3SH and $(CH_3)_3N$ from air by use of chemically treated activated carbon, J. Chem. Eng. Jpn. (1988), https://doi.org/10.1252/jcej.21.91.
[40] J. Schultz, L. Lavielle, C. Martin, The role of the interface in carbon-fiber epoxy composites, J. Adhes. 23 (1987) 45–60.
[41] E. Papirer, J. Schultz, C. Turchi, Surface properties of a calcium carbonate filler treated with stearic acid, Eur. Polym. J. 20 (1984) 1155–1158, https://doi.org/10.1016/0014-3057(84)90181-2.
[42] P.P. Ylä-Mäihäniemi, J.Y.Y. Heng, F. Thielmann, D.R. Williams, Inverse gas chromatographic method for measuring the dispersive surface energy distribution for particulates, Langmuir 24 (2008) 9551–9557, https://doi.org/10.1021/la801676n.
[43] F. Thielmann, Introduction into the characterisation of porous materials by inverse gas chromatography, J. Chromatogr. A 1037 (2004) 115–123, https://doi.org/10.1016/J.CHROMA.2004.03.060.
[44] A.T. James, A.J.P. Martin, Gas-liquid partition chromatography. A technique for the analysis of volatile materials, Analyst 77 (1952) 915–931, https://doi.org/10.1039/AN9527700915.
[45] A. Voelkel, B. Strzemiecka, K. Adamska, K. Milczewska, Inverse gas chromatography as a source of physiochemical data, J. Chromatogr. A. 1216 (2009) 1551–1566, https://doi.org/10.1016/J.CHROMA.2008.10.096.
[46] G.M. Dorris, D.G. Gray, Adsorption of n-alkanes at zero surface coverage on cellulose paper and wood fibers, J. Colloid Interface Sci. 77 (1980) 353–362, https://doi.org/10.1016/0021-9797(80)90304-5.
[47] C. Saint Flour, E. Papirer, Gas-solid chromatography. A method of measuring surface free energy characteristics of short glass fibers. 1. Through adsorption isotherms, Ind. Eng. Chem. Prod. Res. Dev. 21 (1982) 337–341, https://doi.org/10.1021/i300006a029.
[48] C. Saint Flour, E. Papirer, Gas-solid chromatography. A method of measuring surface free energy characteristics of short glass fibers. 2. Through retention volumes measure near zero surface coverage, Ind. Eng. Chem. Prod. Res. Dev. 21 (1982) 666–669, https://doi.org/10.1021/i300006a029.
[49] C.J. van Oss, R.J. Good, M.K. Chaudhury, Additive and nonadditive surface tension components and the interpretation of contact angles, Langmuir 4 (1988) 884–891, https://doi.org/10.1021/la00082a018.
[50] P.J. Kipping, D.G. Winter, Measurement of adsorption isotherms by a gas chromatographic technique, Nature 205 (1965) 1002–1003, https://doi.org/10.1038/2051002a0.
[51] J.F.K. Huber, R.G. Gerritse, Evaluation of dynamic gas chromatographic methods for the determination of adsorption and solution isotherms, J. Chromatogr. A 58 (1971) 137–158, https://doi.org/10.1016/S0021-9673(00)96607-X.
[52] R: A Language and Environment for Statistical Computing, 2008. http://www.r-project.org.
[53] T. V. Elzhov, K.M. Mullen, A.-N. Spiess, B. Bolker, minpack.lm: R Interface to the Levenberg-Marquardt nonlinear least-squares algorithm found in MINPACK, plus support for bounds, 2016.
[54] S. Akmaz, O. Iscan, M.A. Gurkaynak, M. Yasar, The structural characterization of saturate, aromatic, resin, and asphaltene Fractions of Batiraman crude oil, Pet. Sci. Technol. 29 (2011) 160–171, https://doi.org/10.1080/10916460903330361.
[55] O.C. Mullins, E.Y. Sheu, Structures and Dynamics of Asphaltenes, Plenum Press, New York, 1998.
[56] B.K. Wilt, W.T. Welch, J. Graham Rankin, Determination of asphaltenes in petroleum crude oils by Fourier transform infrared spectroscopy, Energy Fuels 12 (1998) 1008–1012, https://doi.org/10.1021/ef980078p.
[57] S.I. Andersen, Separation of asphaltenes by polarity using liquid-liquid extraction, Pet. Sci. Technol. 15 (1997) 185–198, https://doi.org/10.1080/10916469708949650.
[58] V.M. Malhotra, H.A. Buckmaster, 34 GHz EPR FTIR spectra of chromatographically separated Boscan asphaltene fractions, Prepr. from ACS Symp. Trace Elem. Pet. Geochemistry, Dallas, 1989, pp. 185–191.
[59] M.F. Ali, M.N. Siddiqui, A.A. Al-Hajji, Structural studies on residual fuel oil asphaltenes by RICO method, Pet. Sci. Technol. 22 (2004) 631–645, https://doi.org/10.1081/LFT-120034205.
[60] M.N. Siddiqui, I.W. Kazi, Chlorination, nitration, and amination reactions of asphaltene, Pet. Sci. Technol. 32 (2014) 2987–2994, https://doi.org/10.1080/10916466.2014.924528.
[61] J. Douda, Ma.E. Llanos, A.R. Alvarez, J.N. Bolaños, Structure of Maya asphaltene−resin complexes through the analysis of soxhlet extracted fractions, Energy Fuels 18 (2004) 736–742, https://doi.org/10.1021/EF034057T.
[62] L.M. Petrova, N.A. Abbakumova, T.R. Foss, G.V. Romanov, Structural features of asphaltene and petroleum resin fractions, Pet. Chem. 51 (2011) 252–256, https://doi.org/10.1134/S0965544111040062.
[63] H.H. Ibrahim, R.O. Idem, Correlations of characteristics of Saskatchewan crude oils/asphaltenes with their asphaltenes precipitation behavior and inhibition mechanisms: differences between CO_2- and n-heptane-induced asphaltene precipitation, Energy Fuels 18 (2004) 1354–1369, https://doi.org/10.1021/ef034044f.
[64] E. Díaz, S. Ordóñez, A. Vega, J. Coca, Adsorption characterisation of different volatile organic compounds over alumina, zeolites and activated carbon using inverse gas chromatography, J. Chromatogr. A 1049 (2004) 139–146, https://doi.org/10.1016/j.chroma.2004.07.061.

Gdańsk, 01.03.2022 r.

mgr inż. Maksymilian Plata-Gryl
Department of Process Engineering and Chemical Technology
Gdańsk University of Technology
Gabriela Narutowicza 11/12 Street
80-233 Gdańsk
e-mail: makgryl@student.pg.edu.pl

STATEMENT

on the contribution and participation in the publication

I declare that my contribution to the work:

M. Plata-Gryl, M. Momotko, S. Makowiec, G. Boczkaj, Highly effective asphaltene-derived adsorbents for gas phase removal of volatile organic compounds, *Sep. Purif. Technol.* 224 (2019) 315

was to develop the research plan (in cooperation with my supervisor), perform experiments (except preparation of chemically modified asphaltenes), analyse the data, write the initial draft and further revise it.

I estimate my contribution to the final publication to be 65 %.

.....

Gdańsk, 28.02.2022 r.

mgr inż. Malwina Momotko

Department of Process Engineering and Chemical Technology

Gdańsk University of Technology

Gabriela Narutowicza 11/12 Street

80-233 Gdańsk

e-mail: malmomot@student.pg.edu.pl

STATEMENT

on the contribution and participation in the publication

I declare that my contribution to the work:

M. Plata-Gryl, M. Momotko, S. Makowiec, G. Boczkaj, Highly effective asphaltene-derived adsorbents for gas phase removal of volatile organic compounds, *Sep. Purif. Technol.* 224 (2019) 315

was to participate in data analysis and visualization, as well as in initial draft preparation.

I estimate my contribution to the final publication to be 10 %.

Malwina Momotko

Gdańsk, 25.02.2022 r.

dr hab. Sławomir Makowiec, prof. PG
Department of Organic Chemistry
Gdańsk University of Technology
Gabriela Narutowicza 11/12 Street
80-233 Gdańsk
e-mail: mak@pg.edu.pl

STATEMENT

on the contribution and participation in the publication

I declare that my contribution to the work:

M. Plata-Gryl, M. Momotko, S. Makowiec, G. Boczkaj, Highly effective asphaltene-derived adsorbents for gas phase removal of volatile organic compounds, *Sep. Purif. Technol.* 224 (2019) 315

was to participate in the experimental part of the research, by preparing chemically modified asphaltenes.

I estimate my contribution to the final publication to be 10 %.

.....

Gdańsk, 28.02.2022 r.

dr hab. inż. Grzegorz Boczkaj, prof. PG

Department of Process Engineering and Chemical Technology

Gdańsk University of Technology

Gabriela Narutowicza 11/12 Street

80-233 Gdańsk

e-mail: grzegorz.boczkaj@pg.edu.pl

STATEMENT

on the contribution and participation in the publication

I declare that my contribution to the work:

M. Plata-Gryl, M. Momotko, S. Makowiec, G. Boczkaj, Highly effective asphaltene-derived adsorbents for gas phase removal of volatile organic compounds, *Sep. Purif. Technol.* 224 (2019) 315

was to participate in the conceptualization of the research, supervision of the research activity, planning and execution, participation in preparation of the initial draft and the revised, published manuscript.

I estimate my contribution to the final publication to be 15 %.

Chemical Papers (2020) 74:995–1008
https://doi.org/10.1007/s11696-019-00938-z

ORIGINAL PAPER

Application of cyanated asphaltenes in gas-phase adsorption processes for removal of volatile organic compounds

Maksymilian Plata-Gryl[1] · Malwina Momotko[1] · Sławomir Makowiec[2] · Grzegorz Boczkaj[1]

Received: 4 June 2019 / Accepted: 14 September 2019 / Published online: 21 September 2019

Abstract

The paper presents an innovative, chemically modified (methylcyanated) asphaltene-based adsorbent that can be an interesting low-cost alternative for traditional adsorbents. Adsorption properties of adsorbents were examined by inverse gas chromatography technique, adsorption isotherms, and breakthrough curves. A significant increase in retention volume for pyridine, 2-pentanone, nitropropane, toluene, and 1-butanol was observed. Rohrschneider–McReynolds constants revealed an increase in strength of interactions as a result of the modification, especially in strong proton–acceptor interaction (by a factor of 4.6). The surface-free energy of asphaltene adsorbents increased from 136.71 to 169.95 mJ m^{-2} after modification. It is similar to the surface-free energy of silica or alumina. Moreover, modified adsorbent shows very high adsorption potential for pyridine. Adsorption isotherms revealed that monolayer adsorption capacity for pyridine increased 1.5 times after modification. Breakthrough curves of pyridine indicate that chemical modification increased the adsorption capacity, removal efficiency, and throughput. Scale-up calculations revealed that adsorption column packed with modified asphaltene adsorbent would be almost two times smaller compared to a column packed with unmodified one.

Graphic abstract

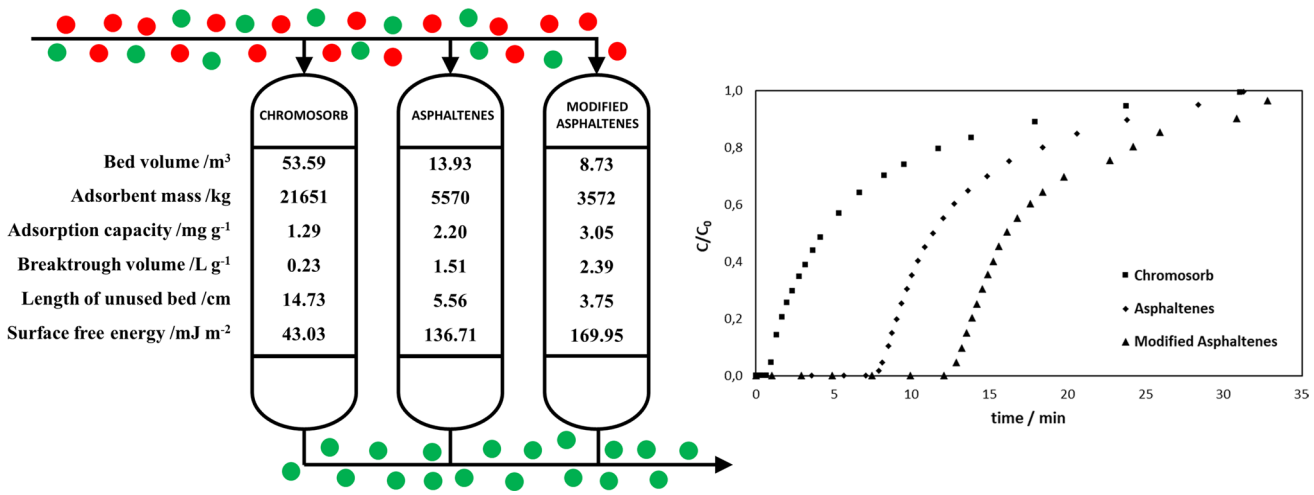

This work was presented at the 44th International Conference of Slovak Society of Chemical Engineering held in Tatranské Matliare on May 21–25, 2018.

Electronic supplementary material The online version of this article (https://doi.org/10.1007/s11696-019-00938-z) contains supplementary material, which is available to authorized users.

Extended author information available on the last page of the article

Keywords Asphaltenes · Adsorption · Adsorbent · Adsorption isotherms · Breakthrough · VOCs removal

Introduction

Volatile organic compounds (VOC), according to European Union regulations, it is any organic compound having an initial boiling point less than or equal to 250 °C measured at a standard pressure of 101.3 kPa (EU 2004). They can cause different diseases and physiological disorders, as well as deteriorate ecosystems (Mellouki et al. 2015; Sarigiannis et al. 2011). VOCs are emitted to the environment from both anthropogenic (e.g., industrial facilities and vehicles) and biogenic sources.

Currently, air quality is gaining more attention as a serious health problem. It leads to tighter legislation standards and increased demand for emission control and waste gas purification techniques. Among those techniques are: thermal oxidation, catalytic oxidation (Huang et al. 2015), absorption (Lin et al. 2006), adsorption (Zhang et al. 2017), biological methods (Gospodarek et al. 2019), and condensation and membrane separation (Belaissaoui et al. 2016).

Adsorption technique is one of the most economical and versatile VOCs' emission control strategies. It is characterized by low energy and maintenance costs, simplicity, and reliability, and can be effectively used to purify waste gases with a low concentration of VOCs. In practice, activated carbons, zeolites, silica, and alumina are used as adsorbents.

Asphaltenes are a class of compounds present in crude oil and products of its processing. It is a fraction insoluble in linear alkanes and soluble in toluene. They quantitatively remain in the residue from vacuum distillation (Mullins 2010, 2011). From a structural standpoint, asphaltenes are polycyclic aromatic hydrocarbons with peripherally attached alkyl chains and graphite-like structure with heteroatoms, e.g., oxygen, nitrogen, sulfur, vanadium, and nickel (Groenzin and Mullins 2000; Schuler et al. 2015). In the petroleum industry, they are a source of severe technological issues (Akbarzadeh et al. 2007). The only practical application of asphaltenes is in the pavement technology as a part of bituminous mixtures.

High thermal stability, feasible procedure of isolation and chemical structure, that can be a source of a vast variety of physicochemical interactions, makes asphaltenes an interesting alternative for traditional adsorbents. In addition, the use of asphaltenes as adsorbents will lead to the valorization of low-value refinery streams (vacuum distillation residues) and will improve waste management. Recently, the applicability of asphaltenes in separation processes was demonstrated (Boczkaj et al. 2016b).

Above-mentioned diverse chemical structure of asphaltene molecules makes them prone to modifications (Plata-Gryl et al. 2019). This work develops the concept of asphaltene adsorbents, by enhancing asphaltene's adsorption properties through feasible chemical modification. Interactions with noxious VOCs were investigated. For evaluation of surface properties, adsorption capacity and performance before and after modification, breakthrough experiments, and inverse gas chromatography (IGC) were performed. IGC is a versatile characterization technique that is used to investigate surface and bulk properties of solids, e.g., surface-free energy, free energy, enthalpy and entropy of adsorption, and adsorption isotherms (Voelkel et al. 2009).

Experimental

Asphaltene fraction isolation and chemical modification

Road bitumen 20/30 SDA (Lotos Group, Gdansk, Poland) and *n*-heptane EMPLURA® (Merck, Darmstadt, Germany) were used to isolate asphaltene fraction. A detailed description of the isolation procedure can be found in (Plata-Gryl et al. 2018).

Chemical modification was performed by dissolving the isolated asphaltene fraction in methylene chloride (p.a., POCH, Gliwice, Poland) in ratio 30 mg:1 mL. Next, 1.7 mg of chloroacetonitrile and 0.7 mg of $ZnCl_2$ per 1 mg of asphaltene were added. The obtained mixture was boiled and continuously stirred in an argon atmosphere for 21 h. Afterward, the solvent was evaporated under reduced pressure. The residue was mixed with methanol (p.a., POCH, Gliwice, Poland), and filtered and rinsed with distilled water and methanol. Subsequently, it was dried under vacuum at 82 °C for 8 h.

The effect of chemical modification on surface structural properties was investigated by Fourier-transform infrared spectroscopy (FTIR) carried out using Bruker TENSOR 27 spectrophotometer (Bruker Optik, Germany) equipped with ATR (Attenuated Total Reflectance) attachment. Asphaltene samples were deposited on the surface of the crystal of the ATR attachment from solution in methylene chloride. Data were recorded in the MIR spectral range from 4000 to 375 cm^{-1} at a spectral resolution of 4 cm^{-1}. 256 scans were averaged for both background and sample spectra.

Adsorbent preparation

For adsorption experiments, asphaltenes were coated onto inert support, namely Chromosorb W-AW-DMCS 80–100 mesh (Johns Manville, Denver, USA). Full description of the support preparation and coating procedures can be

found in (Boczkaj et al. 2016b). The aforementioned procedure ensures complete coating of the support's surface and eliminates its interaction with test probes. Prepared adsorbents were dry-packed into stainless steel columns of internal diameter 2.1 mm. Ends of the column were plugged with silanized glass wool. Before adsorption experiments, columns were conditioned in 250 °C for 5 h in carrier gas (nitrogen) flow. Prepared adsorbents were denoted as Ch-W (uncoated support), Asf (non-modified asphaltenes), and AsfCN (cyanated asphaltenes).

General retention characteristics and selectivity

General retention characteristics and selectivity of asphaltene-based adsorbents were examined by gas chromatography (GC) technique, based on test mixtures containing various chemical compounds, e.g., aromatics, ketones, alcohol, and sulfides having a concentration of ca. 500 ppm of each probe compound in carbon disulfide (p.a. Merck, Darmstadt, Germany). Full list of test compounds is presented in Table S1. To determine Rohrschneider–McReynolds constants, a standard test mixture of *n*-alkanes from *n*-C_5 to *n*-C_{15} (Analytical Controls, Rotterdam, The Netherlands) was used. The void time was determined based on methane retention time as a non-interacting probe (a gas mixture of methane in nitrogen was used for this purpose). GC analyses were performed on the Clarus 500 gas chromatograph (Perkin Elmer, Waltham, USA) equipped with a flame-ionization detector (FID). For this purpose, 3 m columns were used. In all of the analyses, the injection volume of the test mixture was 1 µL. During analyses, the following gases were used: nitrogen (carrier gas), air (for FID) (5 N, Linde Gas, Gdansk, Poland), and hydrogen (5.5 N) from hydrogen generator PGXH$_2$ 500 (Perkin Elmer, Waltham, USA). Chromatographic separations were carried out with temperature programming: 5 min @ 40 °C, 10 °C/min, 5 min @ 250 °C. Based on retention time values, the following parameters were calculated: capacity factor (k), selectivity coefficient (α), and linear retention index (LRI).

Linear retention index of a given compound on the investigated stationary is calculated according to the following equation:

$$\mathrm{LRI} = 100\left(\frac{t_{\mathrm{r,i}} - t_{\mathrm{r},z}}{t_{\mathrm{r},z+1} - t_{\mathrm{r},z}}\right) + 100z, \tag{1}$$

where $t_{\mathrm{r,i}}$ is the retention time of a compound of interest, $t_{\mathrm{r},z}$ and $t_{\mathrm{r},z+1}$ are the retention time of *n*-alkanes eluting before and after the compound of interest, respectively, and z is the carbon atom number in the *n*-alkane molecule eluting before compound of interest.

Rohrschneider–McReynolds constants are a widely used concept in gas chromatography to characterize intermolecular forces between separated solutes and the stationary phase. Specific constants are calculated as the difference between retention indices of some specific compounds on the stationary phase studied and squalane (non-polar reference stationary phase). The sum of constants is termed as "polarity" of the stationary phase. Test probes used to determine the Rohrschneider–McReynolds constants and type of interactions which they represent are described in details in Table S2.

Adsorption properties of the adsorbent's surface studies by inverse gas chromatography (IGC)

To evaluate the surface-free energy of adsorbents, the IGC is performed at infinite dilution (near zero surface coverage). At these conditions, adsorption is described by Henry's law and only adsorbate–adsorbent interactions are observed. To achieve this, small volumes of vapors from the headspace of the probe compounds were injected. Each probe was injected separately.

For IGC experiments, the same apparatus as mentioned above was used. Temperature of GC oven during experiments was maintained at 303 K and carrier gas flow rate was set to 20 mL min^{-1}. The basic parameter used in IGC is net retention volume V_{N}. It was calculated according to Eq. (2):

$$V_{\mathrm{N}} = \frac{j}{m}F(t_{\mathrm{R}} - t_0), \tag{2}$$

where t_{R} (min) is the retention time of a test compound, t_0 (min) is the void time measured with methane, F (mL min^{-1}) is the flow rate measured at the temperature of experiment, j (–) is the James–Martin correction factor for compressibility of the gas (James and Martin 1952), and m (g) is the mass of the adsorbent.

Based on V_{N}, the molar free energy of adsorption ΔG_{A} (J mol^{-1}) was calculated by Eq. (3):

$$\Delta G_{\mathrm{A}} = -RT\ln V_{\mathrm{N}} + C, \tag{3}$$

where R (J K^{-1} mol^{-1}) is the gas constant, T (K) is the absolute temperature, and C is a constant.

To calculate the free surface energy of a solid, the value of dispersive and specific components must be known. Dispersive component of the surface-free energy $\gamma_{\mathrm{S}}^{\mathrm{D}}$ was calculated from the retention data of *n*-alkanes, since for non-polar probes, only dispersive interactions occur (Voelkel et al. 2009). To calculate the value of $\gamma_{\mathrm{S}}^{\mathrm{D}}$, the Dorris–Gray method was used (Dorris and Gray 1980). Dispersive component was calculated by Eq. (4):

$$\gamma_{\mathrm{S}}^{\mathrm{D}} = \frac{\left(-\Delta G_{\mathrm{CH_2}}\right)^2}{4N^2\left(a_{\mathrm{CH_2}}\right)^2\gamma_{\mathrm{CH_2}}}, \tag{4}$$

where N is the Avogadro's number (mol^{-1}) and ΔG_{CH_2} (J mol^{-1}) is the free energy of adsorption per methylene group. ΔG_{CH_2} is obtained from the slope of the ΔG_A versus the number of carbon atoms in the n-alkane molecule. a_{CH_2} (m^2) is the surface area of methylene group. For calculation, the most common value of 6 $Å^2$, found in the literature, was used. γ_{CH_2} (J mol^{-1}) is the surface-free energy of the polyethylene-type polymer with finite molecular weight. It was calculated according to Eq. (5) (Voelkel et al. 2009):

$$\gamma_{CH_2} = (35.6 + 0.058(293 - T)) \times 10^{-3}. \tag{5}$$

To estimate specific interactions, polar test compounds were used. The extent of those interactions can be measured based on the assumption that:

$$\Delta G_A = \Delta G_A^D + \Delta G_A^{SP}, \tag{6}$$

where ΔG_A^D is the dispersive component of the free energy of adsorption (equal to ΔG_A of n-alkanes) and ΔG_A^{SP} (J mol^{-1}) is the specific component of the free energy of adsorption. ΔG_A^{SP} was calculated by Papirer's method (Saint Flour and Papirer 1982). In this method, a plot of ΔG_A for series of n-alkanes against the logarithm of the saturated vapor pressure (P^0) at the experimental temperature is required. It should give straight line and ΔG_A^{SP} can be calculated as a difference between ΔG_A for a polar probe and a hypothetical n-alkane with the same vapor pressure.

Based on the values of ΔG_A^{SP}, the acidic (electron acceptor) and basic (electron donor) properties of a solid can be estimated. In this work, the Good and van Oss approach (van Oss et al. 1988) was used to obtain acidic (γ_S^+) and basic (γ_S^-) parameters of the asphaltene adsorbents according to Eq. (7):

$$\Delta G_A^{SP} = 2 \times N \times a_P \left(\left(\gamma_l^+ \gamma_S^-\right)^{\frac{1}{2}} + \left(\gamma_l^- \gamma_S^+\right)^{\frac{1}{2}} \right), \tag{7}$$

where a_P (m^2) is the cross-sectional area of an adsorbate, and γ_l^+ and γ_l^- (J m^{-2}) are the electron acceptor and electron donor parameters of a probe molecules, respectively. Similarly, γ_S^+ and γ_S^- (J m^{-2}) are the electron acceptor (acidic) and electron donor (basic) parameters of a solid's surface, respectively. When using monopolar acid (γ_l^- is 0.0 J m^{-2}), Eq. 7 reduces to:

$$\gamma_S^- = \frac{(\Delta G_A^{SP})^2}{4 \times N^2 \times a^2 \times \gamma_l^+} \tag{8}$$

conversely; when monopolar base is used (γ_l^+ is 0.0 J m^{-2}), Eq. (7) simplifies to:

$$\gamma_S^+ = \frac{(\Delta G_A^{SP})^2}{4 \times N^2 \times a^2 \times \gamma_l^-}. \tag{9}$$

In this work, chloroform (TCM) was used as a monopolar acid (γ_l^+ is 0.0015 J m^{-2}) and ethyl acetate (EtOAc) was used as a monopolar base (γ_l^- is 0.0062 J m^{-2}) (van Oss 1993). Using the acidic and basic parameters, the specific component of the surface-free energy γ_S^{SP} can be calculated according to the following equation:

$$\gamma_S^{SP} = 2\sqrt{\gamma_S^+ \gamma_S^-}. \tag{10}$$

To determine adsorption isotherms, IGC at finite concentration and peak maximum method were used. Details about the method and calculations can be found in (Huber and Gerritse 1971; Kipping and Winter 1965). Experimental conditions (temperature and carrier gas flow rate) were the same as in IGC at infinite dilution experiments. Experimental data were fitted to Langmuir and Freundlich isotherm models.

Langmuir model is a two-parameter model that describes the adsorption on flat homogenous surface with finite number of equivalent adsorption centers which can hold one molecule. According to this model, only monolayer coverage is possible. In non-linear form, Langmuir model is as follows (Langmuir 1918):

$$q_e = \frac{Q_{mon} K_L P}{1 + K_L P}, \tag{11}$$

where q_e is the amount of adsorbed probe compound (adsorbate) per gram of adsorbent (mg g^{-1}), P is the partial pressure of an adsorbate in gas phase (Pa), K_L is the Langmuir constant (Pa^{-1}), and Q_{mon} is the maximum monolayer capacity (mg g^{-1}).

Freundlich model is an empirical model which describes non-linear reversible adsorption on energetically heterogeneous surfaces, and in its non-linear form, it is described by Eq. (12) (Jaroniec 1975):

$$q_e = K_F P^{1/n}, \tag{12}$$

where K_F is the Freundlich constant (mg g^{-1} $Pa^{-1/n}$) which can be treated as a rough adsorption capacity indicator and n is the dimensionless constant related to an intensity of adsorption. The lower the value of n, the more favorable is adsorption.

Experimental data were fitted by non-linear regression. Computations were performed by R programming language (R: a language and environment for statistical computing 2008) using the minipack.ln package which utilizes Levenberg–Marquardt non-linear least-squares algorithm (Elzhov et al. 2016)

Breakthrough experiments

Breakthrough curves were measured on modified Autosystem XL gas chromatograph (Perkin Elmer, Waltham, USA) with FID using a 20 cm (2.1 mm ID) long SS columns. As a model contaminant, pyridine in nitrogen (gas mixture, C=0.88 mg

L^{-1}) was used. All measurements were done in triplicate at 30 °C and at 50 mL/min flow rate. A breakthrough point was set to $C_t/C_0 = 0.05$, where C_t is an effluent concentration and C_0 is an influent concentration.

Maximum adsorption capacity q_{max} (mg) of the adsorbent was calculated as follows:

$$q_{max} = F \int_{t=0}^{t_e} C_r dt, \tag{13}$$

where $C_r = (C_0 - C_t)$ is the pyridine removal (mg L^{-1}) concentration, C_0 is the initial pyridine concentration (mg L^{-1}), C_t is the pyridine concentration in effluent at given time (mg L^{-1}), and t_e is exhaustion time (min). The adsorption capacity until breakthrough was calculated from the same formula by changing the integral bound t_e to t_b (breakthrough time at $C_t/C_0 = 0.05$). In text, adsorption capacities are reported per gram of adsorbent as Q_{max} and Q_{break} (mg g^{-1}).

Breakthrough volume V_{break} (L) was calculated according to Eq. (14):

$$V_{break} = \frac{F \times t_b}{1000 \times m}. \tag{14}$$

In this work, effective adsorption capacity Q_{eff} is defined as a part of adsorption capacity of an adsorbents utilized up to the breakthrough point and was calculated as:

$$Q_{eff} = \frac{Q_{break}}{Q_{max}} \times 100. \tag{15}$$

Percentage removal of pyridine RE (%) was calculated by Eq. (16):

$$RE = \frac{q_{max}}{P_{total}} \times 100, \tag{16}$$

where P_{total} (mg) is the total amount of pyridine that entered the column calculated according to Eq. (17):

$$P_{total} = \frac{C_0 F t_e}{1000}. \tag{17}$$

The mass-transfer zone (MTZ) (cm) is the part of packed bed where adsorption takes place. The shorter the MTZ, the better the performance of adsorption column. MTZ was calculated by the following equation:

$$MTZ = L\left(\frac{t_e - t_b}{t_e}\right), \tag{18}$$

where L is the length of the adsorbent in the column (cm).

Length of unused bed LUB (cm) is the distance of the adsorbent bad, which is not saturated at the breakthrough time. It was calculated as follows:

$$LUB = L\left(\frac{t_s - t_b}{t_s}\right), \tag{19}$$

where t_s is the time at which $C_t/C_0 = 0.5$.

Adsorbent exhaustion rate ARE (g L^{-1}) is the mass of adsorbent deactivated per volume of the gas that flew through the column up to breakthrough point. Lower values of AER indicate better column performance. ARE was calculated by Eq. (20):

$$AER = \frac{m}{V_{break}}. \tag{20}$$

For a given adsorbent bed, the performance of a column depends on the number of bed volumes of gas NBV (1) treated before the breakthrough occurs. NBV is expressed as follows:

$$NBV = \frac{V_{break}}{V_{bed}}, \tag{21}$$

where V_{bed} (L) is the volume of the adsorbent's bed in the adsorption column.

To analyze the dynamic behavior of pyridine adsorption onto the packed-columns with studied adsorbents, a few frequently used models were used, i.e., Thomas, Yoon–Nelson, Dose Response (DRM), and Bed Depth Service Time (BDST) models were applied to the experimental data. Models were fitted to the data in the same way as in case of adsorption isotherms.

Thomas model can be used to calculate the maximum adsorption capacity. It assumes that the adsorption process follows the second-order reversible kinetics, Langmuir isotherm of adsorption and there is no axial dispersion (Thomas 1944). The mathematical form of Thomas model is as follows:

$$\frac{C_t}{C_0} = \frac{1}{1 + \exp\left(\frac{k_{Th} q_{Th} m}{F} - k_{Th} C_0 t\right)}, \tag{22}$$

where t is the experimental time (h), k_{Th} is the Thomas rate constant (L h^{-1} mg^{-1}), q_{Th} is the maximum adsorption capacity of the adsorbent (mg g^{-1}), and F is the flow rate in L h^{-1}.

The Yoon–Nelson is a simple model originally developed for the adsorption of gases on activated carbons (Yoon and Nelson 1984). The model is expressed as follows:

$$\frac{C_t}{C_0} = \frac{1}{1 + \exp\left(k_{Yn}\left(t_{50} - t\right)\right)}, \tag{23}$$

where k_{Yn} is the rate constant (min^{-1}) and t_{50} is the time required to reach the point in which $C_t/C_0 = 0.5$.

The DRM model (Yan et al. 2001) is represented by Eq. (24):

$$\frac{C_t}{C_0} = 1 - \frac{1}{1 + \left(\frac{C_0 F t}{q_{DRM} m}\right)^a}, \tag{24}$$

where a is the constant and q_{DRM} (mg g^{-1}) is the maximum adsorption capacity predicted by the model.

The last model used in this work was the BDST model. The model assumes that adsorption is limited by the adsorbent–adsorbate interactions. It focuses on predicting the time (service time) required to remove a specific amount of adsorbate before exhaustion. The equation describing BDST model is as follows (Hutchins 1973):

$$\frac{C_t}{C_0} = \frac{1}{1 + \exp\left[k_{BDST} C_0 \left(\frac{N_0}{C_0 u} L - t\right)\right]}, \tag{25}$$

where k_{BDST} (L mg^{-1} min^{-1}) is the adsorption rate constant that describes the mass transfer from the gas phase to the solid phase and N_0 (mg L^{-1}) is the maximum volumetric adsorption capacity of adsorbent's bed.

For scale-up calculations, the breakthrough curves and following kinetic equation were used:

$$\frac{C_t}{C_0} = \frac{1}{1 + \exp\left(\frac{k_1}{F}\left(q_0 m - C_0 V\right)\right)}, \tag{26}$$

where k_1 (L kg^{-1} s^{-1}) is the rate constant, q_0 (kg kg^{-1}) is the maximum adsorption capacity, and V (L) is the throughput volume. The advantage of this approach is the possibility to select a breakthrough volume in the design of a column.

Quality assurance of data

Except for the general retention characteristics, all measurements were performed in triplicates and results are given with 95% confidence interval CI. It was calculated as:

$$\mathrm{CI} = t_{\alpha/2,df} \times \mathrm{SE}, \tag{27}$$

where $t_{\alpha/2,df}$ is a t Student statistic for 95% confidence level and for given degrees of freedom df. SE is a standard error of a mean value.

To confirm the fit of the data to the models, the determination coefficient R^2 and Chi-square coefficient χ^2 were used. The expressions of R^2 and χ^2 are given below:

$$R^2 = \frac{\sum \left(y_c - \bar{y}_e\right)^2}{\sum \left(y_e - \bar{y}_e\right)^2}, \tag{28}$$

$$\chi^2 = \sum \frac{\left(y_e - y_c\right)^2}{y_c}, \tag{29}$$

where y_c, y_e, and $\bar{y}_e$ are values calculated by a model, experimental, and experimental mean, respectively.

Results and discussion

Figure S1 presents the FTIR-ATR spectra of raw and modified asphaltenes. Obtained spectra are convoluted and only general features of the surface structure can be identified. Absorption bands near 2920, 2850, 1455, and 1375 cm^{-1} are characteristics for CH_2 and CH_3 groups in aliphatic chains. No absorption above 3100 cm^{-1} indicates lack of OH groups on the surface of asphaltenes. Absorption bands between 730 and 870 cm^{-1} can be assigned to aromatic C–H out-of-plane bending vibrations (Malhotra and Buckmaster 1989). Band near 1030 cm^{-1} can be related to ester linkages or sulfoxides (Wilt et al. 1998). Band near 1260 cm^{-1} can be attributed to groups containing singly bonded oxygen, e.g., esters or ethers (Carbognani and Espidel 2003). The distinct band observed at 1600 cm^{-1} is related to the aromatic C=C-stretching vibrations. In the spectrum of Asf, a band from ketonic carbonyl oxygen (band at 1700–1680 cm^{-1}) (Ali et al. 2004) is observed, while in AsfCN spectrum, it is missing indicating a change in the surface functional group structure.

Studies by IR spectroscopy revealed slight changes in the surface structure of asphaltenes. It is probably due to complex matrix as asphaltene fraction, which is consisting of hundreds/thousands of different chemical compounds. Strong signal from oxygen containing moieties can shield the signal produced by the functional groups introduced by chemical modification. Moreover, FTIR technique may not be sensitive enough to detect small number of –CN functional groups. Nevertheless, following results of adsorption studies clearly demonstrate that chemical modification significantly enhanced adsorption performance of asphaltene adsorbents.

General retention characteristics

Table S1 presents a comparison of the capacity factors (k), selectivity factors with respect to n-heptane (α_{C7}), and linear retention indices (LRIs) for the raw and cyanated adsorbents. Based on the values of capacity factors, it can be noticed that chemical modification has changed the selectivity of asphaltenes. On unmodified adsorbent thiophenes, thiols, sulfides, and disulfides presented the order of elution according to the boiling point (lack of unique selectivity) and on cyanated asphaltenes only sulfides, disulfides, and additionally ketones exhibited retention proportional to boiling points. On modified adsorbent, sulfides and disulfides eluted according to boiling points even when considered as one group of compounds. This demonstrates the lack of specific interactions with compounds carrying the sulfur-containing functional groups.

Interesting retention pattern was revealed for pyridine and its methylated derivatives on the cyanated adsorbent. The elution order was inversely proportional to temperature. The bigger the number of methyl groups attached to the pyridine ring, the lowest retention was observed. It indicates strong interactions with pyridine ring and additional methyl groups introduce steric hindrance that constricts adsorbate–adsorbent interactions.

In general, increased strength of interactions between cyanated adsorbent and test compounds can be observed, comparing to non-modified asphaltenes. Analysis of the values of LRIs indicates uniform change upon modification. An increase in the value of LRIs is about 1.4–1.5 times comparing to non-modified asphaltenes. It was the highest for aromatic hydrocarbons (1.48) and the lowest for alcohols (1.41). Similarly, the most significant change in the selectivity was found for the aromatic hydrocarbons. The biggest increase of α_{C7} was for nitrobenzene (×1.80) and pyridine (×1.65) and the lowest for 2-pentanone (×1.20). Moreover, increase in capacity factor for nitrobenzene and pyridine was observed. It implies that those compounds (and similar ones) can be effectively adsorbed and removed from gaseous streams by the cyanated adsorbent. Consequently, pyridine was selected for experiments in dynamic conditions (breakthrough studies). The second aspect of pyridine selection relates to its odorous character with low odor threshold as well as toxicity.

To preliminary compare types of interactions between adsorbent and adsorbate, the Rohrschneider–McReynolds constants are calculated and presented in Table 1. For comparison purposes, values for adsorbents commonly used in gas chromatography are given as well.

Chemical modification of asphaltenes leads to increased values of all constants indicating an increase in the intermolecular forces between test probes and the adsorbent. The smallest change was observed for X', which means that there is relatively small change in the dispersion forces and polarizability character of the adsorbent. Cyanation had the most profound effect on the value of the constant S', which represent the acidic character of the adsorbent. Its value increased over four times. That implies stronger interactions with proton–acceptor and polar molecules, such as pyridine. In general, overall "polarity" of the AsfCN was raised by 2.5 times and indicates much stronger interactions (prolonged retention) with adsorbates as compared to unmodified asphaltenes. It must be emphasized that "polarity" of the stationary phase, defined as the sum of the Rohrschneider–McReynolds constants, cannot be equated with selectivity. Simply, the higher the sum ("polarity"), the higher the retention time. Based on the Σ, AsfCN can be classified as the medium "polarity" adsorbent.

For more in-depth information about surface adsorption properties, the IGC technique was used. Figure 1 compares the retention volumes (expressed as bed volumes, BV) for volatile organic compounds on the investigated adsorbents. The highest retention volume was observed for pyridine. At the same time, the most significant change (over two times) upon modification was observed for pyridine, nitropropane, *n*-butanol, DEE, and TCM. However, in case of DEE and TCM, the overall retention is low as compared to, e.g., pyridine. It is in great part related to differences in boiling points.

Surface characterization by inverse gas chromatography

In Table 2, values of the dispersive component of the surface-free energy (γ_S^D) and the change of the free enthalpy of adsorption per methylene group (ΔG_{CH_2}) for investigated adsorbents are presented. In addition, values reported in the literature for other adsorbents are given. Measurements revealed slight change in the value of γ_S^D as a result of chemical modification of asphaltenes. It is in line with small change in the value of Rohrschneider–McReynolds's X' constant. Both the constant X' and parameter γ_S^D represent the ability of an adsorbent to interact by non-specific dispersion forces. It is evident that cyanation did not change that property significantly. Consequently, the differences in retention volumes presented in Fig. 1 have arisen from the change in specific interactions. To some extent, it was disclosed by the aforementioned Rohrschneider–McReynolds constants. Nevertheless, both asphaltene-based adsorbents display

Table 1 Values of the Rohrschneider–McReynolds constants. Under the constant sign, type of represented interaction is given

Adsorbent	X' π–π interaction	Y' Hydrogen bonding	Z' Proton–acceptor	U' Dipole–dipole	S' Strong proton–acceptor interaction	Σ
Asf	88	97	172	182	171	710
AsfCN	102	293	276	325	785	1781
Apiezon J (non-polar, hydrocarbon type)	38	36	27	49	57	207
Carbowax 6000 (very polar, polyglycol)	322	540	369	577	512	2320
OV-275® (highly polar, silicone)	629	872	763	1106	849	4219

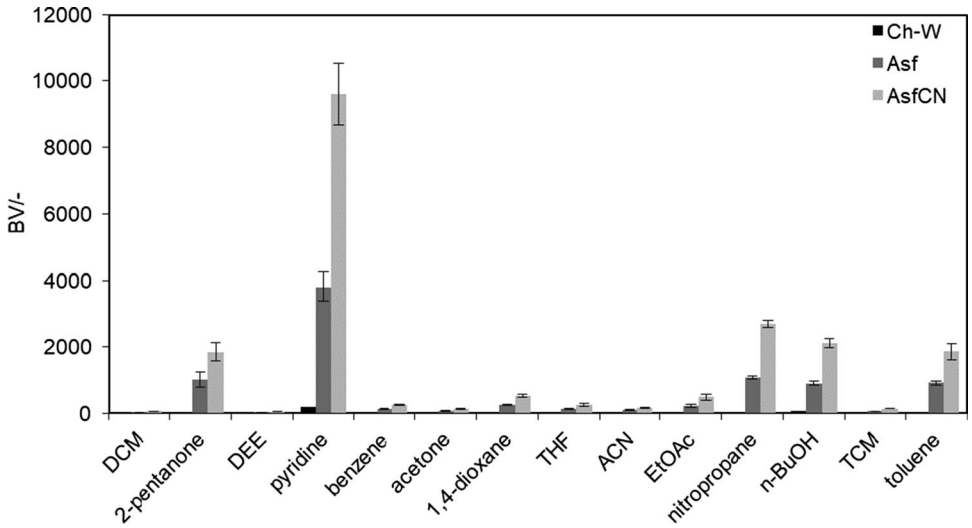

Fig. 1 Retention volumes (reported as bed volumes) for volatile organic compounds measured at infinite dilution conditions

Table 2 Values of the dispersive component of the surface-free energy and the change of the free enthalpy of adsorption per methylene group for investigated adsorbents and selected adsorbents reported in the literature

Adsorbent	*T*/*K*	γ_S^D (mJ m^{-2})	ΔG_{CH_2} (kJ mol^{-1})	References
Ch-W	303	26.02 ± 0.01	2.18 ± 0.08	This work
Asf	303	106.66 ± 0.64	4.42 ± 0.53	This work
AsfCN	303	118.03 ± 0.05	4.65 ± 0.15	This work
Alumina	473	59.3	NA	Díaz et al. (2004)
Zeolite 13X	473	154.9	NA	Díaz et al. (2004)
Carbon nanofiber	473	18.4	NA	Díaz et al. (2007)
Fumed silica	293	98.2 ± 2	NA	Vidal et al. (1987)
Silica	353	61.3	6.97	Tijburg et al. (1991)

much stronger dispersion forces than diatomaceous earth (Ch-W). The value of γ_S^D is over five times higher for Asf and AsfCN as compared to Ch-W. When contrasted with literature data for other adsorbents, asphaltene-based adsorbents have similar γ_S^D values as silica derived adsorbents but much lower than for example Zeolite 13X—considering the fact that γ_S^D value for zeolite was measured at 473 K (strength of dispersion forces is inversely proportional to temperature).

In Table 3, the specific component of the free enthalpy of adsorption for selected VOCs is presented. The highest relative change of the strength of specific interactions was observed for 1,4-dioxane (over three times), but overall, the adsorption was weak regardless the type of adsorbent. In absolute values, the biggest difference was noticed for DEE, TCM, and pyridine. It was 1.34, 1.09, and 1.03 kJ mol^{-1}, respectively. Increased interactions with TCM (electron acceptor compound) and pyridine (electron donor compound) suggest that new adsorption centers were introduced on the surface of asphaltene, having electron donor (basic) as well as electron acceptor character (acidic).

To investigate the acid–base character and specific interactions as a whole, van Oss approach was used. Figure 2 provides the information about the contribution of specific interactions (γ_S^{SP}) to the total free surface energy (γ_S^T) along with acid (γ_S^+) and base (γ_S^-) components of the specific interactions.

Table 3 Specific component of the free enthalpy of adsorption for selected VOCs, measured at 303 K on asphaltene-based adsorbents

$-\Delta G_A^{SP}$ (kJ mol^{-1})		
Test probe	Asf	AsfCN
DCM	4.19 ± 0.01	5.04 ± 0.05
2-Pentanone	3.40 ± 0.028	3.72 ± 0.38
DEE	4.26 ± 0.17	5.60 ± 0.23
Pyridine	4.79 ± 0.15	5.81 ± 0.24
Benzene	1.89 ± 0.11	2.65 ± 0.09
Acetone	3.57 ± 0.16	4.32 ± 0.14
1,4-Dioxane	0.16 ± 0.13	0.76 ± 0.24
THF	4.13 ± 0.14	4.59 ± 0.43
ACN	1.38 ± 0.11	1.31 ± 0.11
EtOAc	3.36 ± 0.20	4.21 ± 0.52
Nitropropane	NA	NA
n-BuOH	NA	NA
TCM	2.87 ± 0.04	3.96 ± 0.06
Toluene	2.33 ± 0.08	2.86 ± 0.33

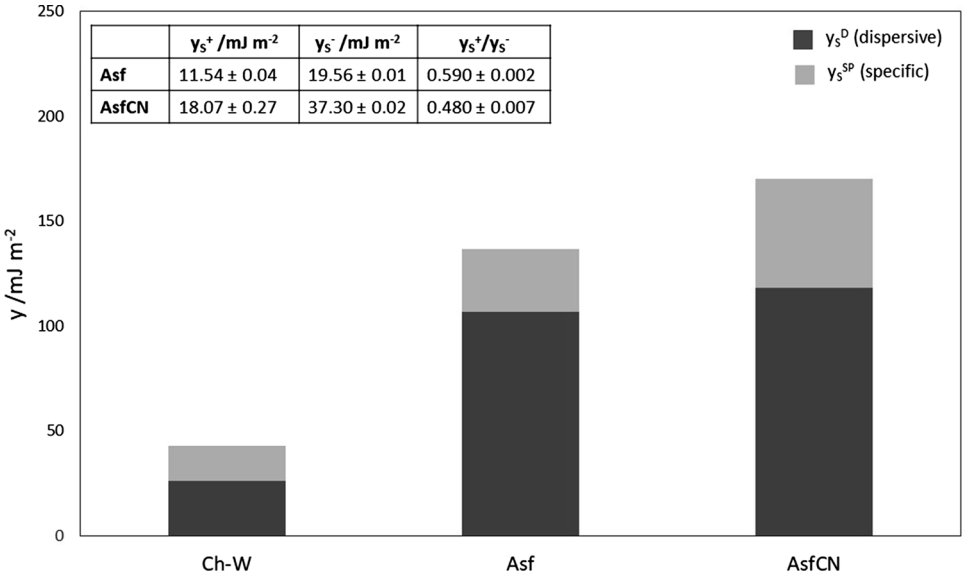

Fig. 2 Contribution of specific and dispersive components to the total surface-free energy. Inserted table presents the strength of acid (electron acceptor) and base (electron donor) interactions of asphaltene adsorbents

It is clear that the biggest part of adsorbent–adsorbate interactions is due to dispersive forces. That type of interactions has non-specific character and will contribute to the adsorption of chemical compounds regardless their chemical nature. It will be beneficial in case of purification of waste gases containing wide variety of contaminants. Moreover, measurements revealed that most profound difference between the raw and modified asphaltene adsorbent is in the specific component of the surface-free energy. As a result of modification, both acid (electron acceptor) and base (electron donor) adsorption centers were introduced, which is observed by the increased values of the γ_S^+ and γ_S^-. That change was not equal and the surface character, measured by γ_S^+/γ_S^- ratio, shifted slightly towards more electron donor (basic). Although the difference is not that substantial and asphaltene adsorbents can be effective in removal of both alkaline and acidic gases.

Adsorption isotherms

To learn more about adsorption potential of asphaltene adsorbents, an adsorption isotherm for pyridine at 303 K was measured by IGC at finite concentration. Figure 3 presents the experimental adsorption isotherms together with model isotherms (Langmuir and Freundlich), and in Table 4, the values of the parameters of the isotherm models are presented.

Values of the R^2 indicate that Freundlich isotherm model fits better to the experimental data. It implies that the surface

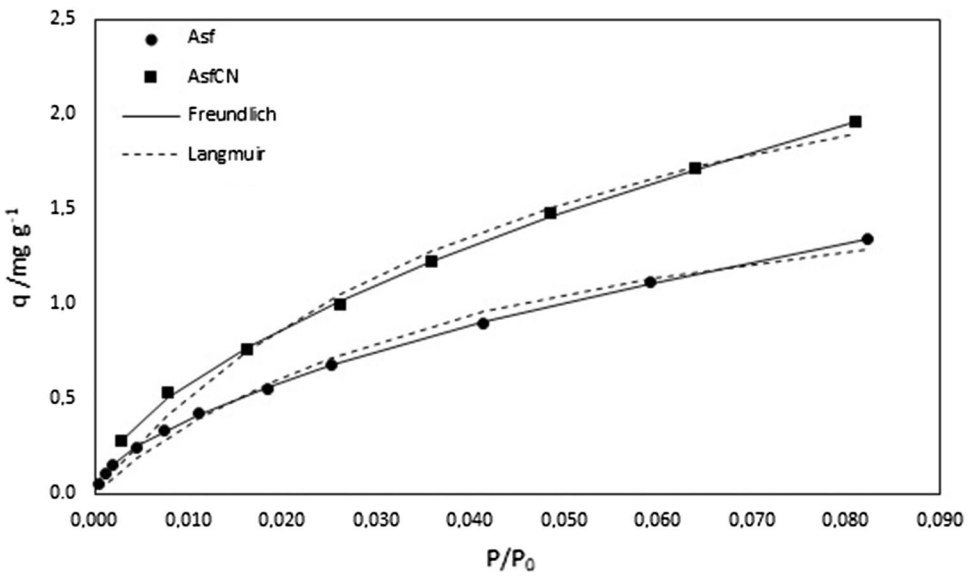

Fig. 3 Experimental and model adsorption isotherms for pyridine at 303 K on asphaltene adsorbents

Table 4 Results of the isotherm models fitting to the experimental data

	Asf	AsfCN
Langmuir		
Q_{mon} (mg g^{-1})	1.970 ± 0,335	3.076 ± 0.612
K_L (Pa^{-1})	0.0063 ± 0.0021	0.0055 ± 0.0021
R^2	0.991	0.990
Freundlich		
n (–)	1.717 ± 0.029	1.725 ± 0.047
K_F (mg g^{-1} $Pa^{-1/n}$)	0.049 ± 0.002	0.073 ± 0.006
R^2	1.000	0.999

Table 5 Operational parameters of investigated columns for adsorption of pyridine at 303 K and 50 mL min^{-1} flowrate

Parameter	Ch-W	Asf	AsfCN
RE (%)	23.03 ± 1.38	45.24 ± 1.96	54.26 ± 4.73
MTZ (cm)	19.29 ± 0.12	14.50 ± 0.48	12.53 ± 0.51
LUB (cm)	14.73 ± 0.65	5.56 ± 0.20	3.75 ± 0.39
NBV (–)	81 ± 1	589 ± 8	890 ± 33
AER (g L^{-1})	0.16 ± 0.01	0.18 ± 0.01	0.16 ± 0.01
Q_{eff} (%)	15.46 ± 2.70	60.63 ± 2.75	68.78 ± 2.24
Q_{max} (mg $g^{-1)}$	1.29 ± 0.06	2.20 ± 0.08	3.05 ± 0.23
Q_{break} (mg g^{-1})	0.20 ± 0.03	1.33 ± 0.02	2.10 ± 0.16
V_{break} (L g^{-1})	0.23 ± 0.03	1.51 ± 0.02	2.39 ± 0.18

of the adsorbents is heterogeneous. At the same time, similar value of the n parameter of the Freundlich model indicates that chemical modification did not influenced significantly the heterogeneity of the asphaltene adsorbent's surface. K_F parameter can be correlated with the adsorption capacity. Its higher value for AsfCN demonstrates the increased adsorption capacity which is in line with the calculated, from the Langmuir model, monolayer capacity (Q_{mon}). The monolayer capacity has increased by 56% as a result of chemical modification.

Breakthrough experiments

Since most of the adsorption processes are performed in fixed bed columns with constant flow of a contaminated gas, it was important to evaluate the adsorption performance of the investigated adsorbents in dynamic conditions. Figure 4 presents experimental breakthrough curves, and in Table 5, parameters calculated based on breakthrough data are given.

From breakthrough curves shapes, it is clear that chemical modification enhanced the adsorption properties of asphaltene adsorbent. Calculated maximum adsorption capacity (Q_{max}) is in very good agreement with the monolayer capacity (Q_{mon}) obtained from the Langmuir isotherm model. The experiment confirmed previous observations that both asphaltene adsorbents are superior as compared to Ch-W adsorbent. The highest pyridine removal efficiency was obtained for AsfCN and goes along with the highest maximum adsorption capacity (Q_{max}), adsorption capacity till breakthrough (Q_{break}), and breakthrough volume (V_{break}). Moreover, for AsfCN, the highest effectiveness of adsorption capacity exploitation was observed. Up to the breakthrough point, the AsfCN was exhausted in almost 70%. In the case of Ch-W and Asf, it was 15 and 60%, respectively. Since the exhaustion time was virtually the same for all adsorbents, the change in breakthrough point must have been a result of mass-transfer zone-length change. For AsfCN, the length of MTZ was reduced by 35% as compared to Ch-W and by 13.6% as compared to the Asf adsorbent. Furthermore, considerable change was observed in the value of NBV. For modified adsorbent, the volume of fluid treated till breakthrough (expressed as bed volumes) was equal to 890. For

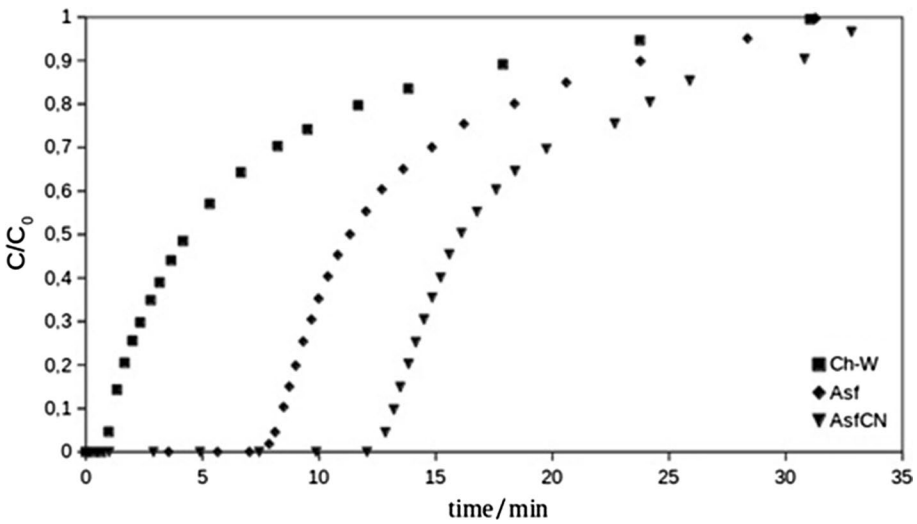

Fig. 4 Breakthrough curves for pyridine (0.88 mg L^{-1}) at 303 K and at flow rate of 50 mL min^{-1}

performance, effectiveness and also from an economic point of view, very important is the change in the value of LUB. It describes the part of an adsorbent bed in the column which remains unused when the breakthrough point occurs. In the case of chemically modified asphaltene adsorbent, it was reduced by 400 and 50% compared to Ch-W and Asf, respectively.

Tested adsorption columns undergo three adsorption–desorption cycles. Obtained results showed that the adsorbent can be recycled/reused. Based on the standard deviation value, for three repetitions, it can be seen that prepared adsorbent retained its adsorption properties after several regenerations (Table 5).

To further analyze the obtained breakthrough curves, the experimental data were modeled by the Thomas and BDST models. The results of modeling are presented in Table 6 and Figure S2.

All models used described the experimental data in a reasonably good manner. The determination coefficient was above 0.930 in all cases. However, models failed to predict the experimental breakthrough curve near the inflection points. On both sides of the curve (near the breakthrough and saturation points), models underestimated the performance of adsorbent. Interestingly, three models (Thomas, Yoon–Nelson, and BDST) predicted the breakthrough curve shape in virtually the same way.

The maximum adsorption capacity predicted by Thomas (q_{Th}) and DRM (q_{DRM}) models is similar but lower than the experimental value. Also Yoon–Nelson model miscalculated the performance of adsorbents. Value of the t_{50} parameter (time at which $C_t/C_0 = 0.05$) for all adsorbents was lower than experimental.

The rate constant k_{BDST} calculated by BDST model describes the rate of adsorbate transfer from the gas phase to the solid phase. It increased for both asphaltene adsorbents as compared to Ch-W, but for AsfCN, it is lower than for Asf. The N_0 parameter characterizes the adsorption capacity of the bed per unit bed volume. Since it is correlated with adsorption capacity, it is not a surprise that AsfCN adsorbent has the highest N_0 value.

Above-mentioned results and former literature reports on utilization of asphaltenes for waste gas purification indicate that the presented application can be used in petrochemical industry for adsorption of volatile compounds containing sulfur, nitrogen, oxygen, as well as aromatic hydrocarbons. These compounds are typically present in waste gases emitted from process streams (Boczkaj et al. 2016a; Boczkaj et al. 2017; Makos et al. 2018a, b).

Table 6 Thomas, Yoon–Nelson, DRM, and BDST model parameters

	Ch-W	Asf	AsfCN
Thomas			
k_{Th} (L h^{-1} mg^{-1})	1498 ± 384	1702 ± 362	1552 ± 354
q_{Th}/mg g^{-1}	0.898 ± 0.120	1.813 ± 0.077	2.655 ± 0.088
R^2	0.937	0.957	0.950
χ^2	0.670	0.587	0.542
Yoon–Nelson			
t_{50} (min)	5.32 ± 0.74	12.12 ± 0.52	16.99 ± 0.56
t_{50} Experimental (min)	4.41 ± 0.51	11.34 ± 0.44	16.06 ± 0.37
k_{YN} (min^{-1})	0.366 ± 0.094	0.416 ± 0.088	0.379 ± 0.086
R^2	0.937	0.957	0.951
χ^2	0.670	0.587	0.542
DRM			
a (–)	1.501 ± 0.096	4.617 ± 0.672	6.013 ± 1.035
q_{DRM} (mg g^{-1})	0.805 ± 0.034	1.950 ± 0.061	2.881 ± 0.078
R^2	0.996	0.975	0.965
χ^2	0.110	0.381	0.393
BDST			
k_{BDST} (L mg^{-1} min^{-1})	0.416 ± 0.108	0.472 ± 0.050	0.4312 ± 0.099
N_0 (mg L^{-1})	338.3 ± 47.1	770.3 ± 32.8	1080.2 ± 36.3
R^2	0.937	0.957	0.950
χ^2	0.670	0.581	0.540

Scale-up of packed bed adsorption column

For scaling-up of the adsorption column, the kinetic equation and experimental breakthrough data from laboratory column were used. The assumption was made that breakthrough occurs at C/C_0 equal to 0.05, influent concentration is equal to laboratory experiment (i.e. 0.88 mg L^{-1}), volumetric flow rate of designed column is 2000 m^3 h^{-1}, required breakthrough volume is equal to 10,000 m^3, and unit gas flowrate is the same as in laboratory scale column, i.e., 241 L s^{-1} m^{-2}. Table 7 gives calculated parameters of scaled-up columns.

Aforementioned results of adsorption column scaling-up clearly indicate that favorable adsorption characteristics of asphaltene-based adsorbents (especially AsfCN) lead to substantial reduction of the size of a potential adsorption unit in case of process-scale operations. Results revealed that

Table 7 Calculated parameters of the scaled-up columns

Parameter	Adsorbent		
	Ch-W	Asf	AsfCN
ρ_{bed} (kg m^{-3})	404	400	409
M (kg)	21,651	5570	3572
V_{bed} (m^3)	53.59	13.93	8.73
D (m)	1.71	1.71	1.71
H (m)	23.25	6.04	3.79

application of the 10 wt% cyanated asphaltene-based adsorbent reduced the required adsorbent's mass over six times. It is of utmost importance when considering economic feasibility. The advantageous characteristic of asphaltene-based adsorbents can be further improved using a different support with higher surface area.

Conclusions

These studies revealed that small quantities of asphaltenes can be effectively used as an adsorption active component for removal of toxic volatile organic compounds from the gas phase. Moreover, it was proved that feasible chemical modification significantly enhanced performance of asphaltene adsorbents. Classification by *Rohrschneider–McReynolds* constants showed that overall strength of interactions increased more than two times. The biggest change was observed for pyridine. Cyanation increased the value of the dispersive and specific components of the surface-free energy from 106 to 118 mJ m^{-2} and from 30 to 52 mJ m^{-2}, respectively. Dispersive component's value is comparable to silica or alumina. Moreover, modification resulted in increased concentration of both acidic and basic adsorption centers on the adsorbent's surface. It indicates that asphaltene adsorbents can be effective in removal of both alkaline and acidic gases.

Analysis of adsorption isotherms reveals that monolayer capacity was increased by 56% after modification. The adsorption process was better described by the Freundlich model and results suggest that energetically heterogeneous characteristic of the adsorbent's surface did not change significantly upon chemical modification.

Breakthrough curves have explicitly demonstrated the applicability of asphaltenes to adsorption processes and waste gas purification. Calculated operational parameters indicate significant increase in performance of modified asphaltene adsorbent. Results of scale-up calculations revealed that mass of adsorbents required to achieve desired pyridine removal decreased from 21651 for uncoated support to 5570 and 3572 kg for raw asphaltene adsorbent and cyanated asphaltene adsorbent, respectively. Hence, the chemical modification leads not only to enhanced adsorption properties of asphaltenes but also to higher economic feasibility, in case of potential process-scale applications.

Above-mentioned advantages of asphaltene adsorbents: undesired by-product, facile isolation and chemical modification methods, strong adsorbent–adsorbate interactions of asphaltenes, and its chemically modified derivative seem to be an effective and low-cost adsorbent for waste gas purification. Further developments in asphaltene-based adsorbents are required—inexpensive porous support (with high surface area) will further facilitate their performance.

Acknowledgements The authors gratefully acknowledge the financial support from the National Center for Research and Development, Warsaw, Poland—Project LIDER, no. LIDER/036/573/L-5/13/NCBR/2014. This work was financially supported by the project "INTERPHD2" no. POWR.03.02.00-IP.08-00-DOC/16.

References

Akbarzadeh K, Hammani A, Zhang D, Alleson S, Creek J, Kabir S, Jamaluddin AJ, Marshall AG, Rodgers RP, Mullins OC, Solbakken T (2007) Asphaltenes—problematic but rich in potential. Oilf Rev 19:22–43

Ali MF, Siddiqui MN, Al-Hajji AA (2004) Structural studies on residual fuel oil asphaltenes by RICO method. Pet Sci Technol 22:631–645. https://doi.org/10.1081/LFT-120034205

Belaissaoui B, Le Moullec Y, Favre E (2016) Energy efficiency of a hybrid membrane/condensation process for VOC (volatile organic compounds) recovery from air: a generic approach. Energy 95:291–302. https://doi.org/10.1016/j.energy.2015.12.006

Boczkaj G, Makoś P, Fernandes A, Przyjazny A (2016a) New procedure for the control of the treatment of industrial effluents to remove volatile organosulfur compounds. J Sep Sci 39:3946–3956. https://doi.org/10.1002/jssc.201600608

Boczkaj G, Momotko M, Chruszczyk D, Przyjazny A, Kamiński M (2016b) Novel stationary phases based on asphaltenes for gas chromatography. J Sep Sci 39:2527–2536. https://doi.org/10.1002/jssc.201600183

Boczkaj G, Makoś P, Fernandes A, Przyjazny A (2017) New procedure for the examination of the degradation of volatile organonitrogen compounds during the treatment of industrial effluents. J Sep Sci 40:1301–1309. https://doi.org/10.1002/jssc.201601237

Carbognani L, Espidel J (2003) Preparative subfractionation of petroleum resins and asphaltenes. II. Characterization of size exclusion chromatography isolated fractions. Pet Sci Technol 21:1705–1720. https://doi.org/10.1081/LFT-120024558

Díaz E, Ordóñez S, Vega A, Coca J (2004) Adsorption characterisation of different volatile organic compounds over alumina, zeolites and activated carbon using inverse gas chromatography. J Chromatogr A 1049:139–146. https://doi.org/10.1016/j.chroma.2004.07.061

Díaz E, Ordóñez S, Vega A (2007) Adsorption of volatile organic compounds onto carbon nanotubes, carbon nanofibers, and high-surface-area graphites. J Colloid Interface Sci 305:7–16. https://doi.org/10.1016/j.jcis.2006.09.036

Dorris GM, Gray DG (1980) Adsorption of *n*-alkanes at zero surface coverage on cellulose paper and wood fibers. J Colloid Interface Sci 77:353–362. https://doi.org/10.1016/0021-9797(80)90304-5

Elzhov TV, Mullen KM, Spiess AN, Bolker B (2016) minipack.lm: R interface to the Levenberg-Marquardt nonlinear least-squares algorithm found in MINPACK, plus support for bounds

EU (2004) Directive 2004/42/CE on the limitation of emissions of volatile organic compounds due to the use of organic solvents in certain paints and varnishes and vehicle refinishing products

Gospodarek M, Rybarczyk P, Szulczyński B, Gębicki J (2019) Comparative evaluation of selected biological methods for the removal of hydrophilic and hydrophobic odorous VOCs from air. Processes 7:1–22. https://doi.org/10.3390/pr7040187

Groenzin H, Mullins OC (2000) Molecular size and structure of asphaltenes from various sources. Energy Fuels 14:677–684. https://doi.org/10.1021/ef990225z

Huang H, Xu Y, Feng Q, Leung DYC (2015) Low temperature catalytic oxidation of volatile organic compounds: a review. Catal Sci Technol 5:2649–2669. https://doi.org/10.1039/c4cy01733a

Huber JFK, Gerritse RG (1971) Evaluation of dynamic gas chromatographic methods for the determination of adsorption and solution isotherms. J Chromatogr A 58:137–158. https://doi.org/10.1016/S0021-9673(00)96607-X

Hutchins R (1973) New method simplifies desing of activated carbon systems. Chem Eng 80:133–138

James AT, Martin AJP (1952) Gas–liquid partition chromatography. A technique for the analysis of volatile materials. Analyst 77:915–932. https://doi.org/10.1039/AN9527700915

Jaroniec M (1975) Adsorption on heterogeneous surfaces: the exponential equation for the overall adsorption isotherm. Surf Sci 50:553–564

Kipping PJ, Winter DG (1965) Measurement of adsorption isotherms by a gas chromatographic technique. Nature 205:1002–1003

Langmuir I (1918) The adsorption of gases on plane surfaces of glass, mica and platinum. J Am Chem Soc 40:1361–1403

Lin CC, Wei TY, Hsu SK, Liu WT (2006) Performance of a pilot-scale cross-flow rotating packed bed in removing VOCs from waste gas streams. Sep Purif Technol 52:274–279. https://doi.org/10.1016/j.seppur.2006.05.003

Makoś P, Fernandes A, Boczkaj G (2018a) Method for the simultaneous determination of monoaromatic and polycyclic aromatic hydrocarbons in industrial effluents using dispersive liquid–liquid microextraction with gas chromatography–mass spectrometry. J Sep Sci 41:2360–2367. https://doi.org/10.1002/jssc.201701464

Makoś P, Fernandes A, Przyjazny A, Boczkaj G (2018b) Sample preparation procedure using extraction and derivatization of carboxylic acids from aqueous samples by means of deep eutectic solvents for gas chromatographic-mass spectrometric analysis. J Chromatogr A 22:10–19. https://doi.org/10.1016/j.chroma.2018.04.054

Malhotra VM, Buckmaster HA (1989) 34 GHz EPR FTIR spectra of chromatographically separated Boscan asphaltene fractions. In: Preprints from ACS symposium on trace elements in petroleum geochemistry

Mellouki A, Wallington TJ, Chen J (2015) Atmospheric chemistry of oxygenated volatile organic compounds: impacts on air quality and climate. Chem Rev 2015:3984–4014. https://doi.org/10.1021/cr500549n

Mullins OC (2010) The modified Yen model. Energy Fuels 24:2179–2207. https://doi.org/10.1021/ef900975e

Mullins OC (2011) The asphaltenes. Annu Rev Anal Chem 4:393–418. https://doi.org/10.1146/annurev-anchem-061010-113849

Plata-Gryl M, Jungnickel C, Boczkaj G (2018) An improved scalable method of isolating asphaltenes. J Pet Sci Eng 167:608–614. https://doi.org/10.1016/j.petrol.2018.04.039

Plata-Gryl M, Momotko M, Makowiec S, Boczkaj G (2019) Highly effective asphaltene-derived adsorbents for gas phase removal of volatile organic compounds. Sep Purif Technol 224:315–321. https://doi.org/10.1016/j.seppur.2019.05.041

R: a language and environment for statistical computing (2008. https://cran.r-project.org/web/packages/minpack.lm/minpack.lm.pdf

Saint Flour C, Papirer E (1982) Gas-solid chromatography: a method of measuring surface free energy characteristics of short glass fibers. 2. Through retention volumes measured near zero surface coverage. Ind Eng Chem Prod Res Dev 21:666–669. https://doi.org/10.1021/i300008a031

Sarigiannis DA, Karakitsios SP, Gotti A, Liakos IL, Katsoyiannis A (2011) Exposure to major volatile organic compounds and carbonyls in European indoor environments and associated health risk. Environ Int 37:743–756. https://doi.org/10.1016/j.envint.2011.01.005

Schuler B, Meyer G, Peña D, Mullins OC, Gross L (2015) Unraveling the molecular structures of asphaltenes by atomic force microscopy. J Am Chem Soc 137:9870–9876. https://doi.org/10.1021/jacs.5b04056

Thomas HC (1944) Heterogeneous ion exchange in a flowing system. J Am Chem Soc 66:1664–1666

Tijburg I, Jagiello J, Vidal A, Papirer E (1991) Inverse gas chromatographic studies on silica: infinite dilution and finite concentration measurements. Langmuir 7:2243–2247. https://doi.org/10.1021/la00058a044

van Oss CJ (1993) Acid-base interfacial interactions in aqueous media. Colloids Surfaces A Physicochem Eng Asp 78:1–49. https://doi.org/10.1016/0927-7757(93)80308-2

van Oss CJ, Good RJ, Chaudhury MK (1988) Additive and nonadditive surface tension components and the interpretation of contact angles. Langmuir 4:884–891. https://doi.org/10.1021/la00082a018

Vidal A, Papirer E, Wang MJ, Donnet JB (1987) Modification of silica surfaces by grafting of alkyl chains. I—Characterization of silica surfaces by inverse gas-solid chromatography at zero surface coverage. Chromatographia 23:121–128. https://doi.org/10.1007/BF02312887

Voelkel A, Strzemiecka B, Adamska K, Milczewska K (2009) Inverse gas chromatography as a source of physiochemical data. J Chromatogr A 1216:1551–1566. https://doi.org/10.1016/j.chroma.2008.10.096

Wilt BK, Welch WT, Graham Rankin J (1998) Determination of asphaltenes in petroleum crude oils by fourier transform infrared spectroscopy. Energy Fuels 12:1008–1012. https://doi.org/10.1021/ef980078p

Yan G, Viaraghavana T, Chen M (2001) A new model for heavy metal removal in a biosorption column. Adsorpt Sci Technol 19:25–43. https://doi.org/10.1260/0263617011493953

Yoon YH, Nelson JH (1984) Application of gas adsorption kinetics. I. A theoretical model for respirator cartridge service life. Am Ind Hyg Assoc 45:509–516. https://doi.org/10.1080/15298668491400197

Zhang X, Gao B, Zheng Y, Hu X, Creamer AE, Annable MD, Li Y (2017) Biochar for volatile organic compound (VOC) removal: sorption performance and governing mechanisms. Bioresour Technol 245:606–614. https://doi.org/10.1016/j.biortech.2017.09.025

Affiliations

Maksymilian Plata-Gryl[1] · Malwina Momotko[1] · Sławomir Makowiec[2] · Grzegorz Boczkaj[1]

✉ Grzegorz Boczkaj
grzegorz.boczkaj@pg.edu.pl

[1] Department of Process Engineering and Chemical Technology, Faculty of Chemistry, Gdansk University of Technology, G. Narutowicza St. 11/12, 80-233 Gdańsk, Poland

[2] Department of Organic Chemistry, Faculty of Chemistry, Gdansk University of Technology, 80-233 Gdańsk, G. Narutowicza St. 11/12, Poland

Gdańsk, 01.03.2022 r.

mgr inż. Maksymilian Plata-Gryl

Department of Process Engineering and Chemical Technology

Gdańsk University of Technology

Gabriela Narutowicza 11/12 Street

80-233 Gdańsk

e-mail: makgryl@student.pg.edu.pl

STATEMENT

on the contribution and participation in the publication

I declare that my contribution to the work:

M. Plata-Gryl, M. Motoko, S. Makowiec, G. Boczkaj, Application of cyanated asphaltenes in gas-phase adsorption process for removal of volatile organic compounds, *Chem. Pap.* 74 (2020) 995

was to develop the research plan (in cooperation with my supervisor), perform experiments (except preparation of chemically modified asphaltenes), analyse the data, write the initial draft and further revise it.

I estimate my contribution to the final publication to be 70 %.

Gdańsk, 28.02.2022 r.

mgr inż. Malwina Momotko

Department of Process Engineering and Chemical Technology

Gdańsk University of Technology

Gabriela Narutowicza 11/12 Street

80-233 Gdańsk

e-mail: malmomot@student.pg.edu.pl

STATEMENT

on the contribution and participation in the publication

I declare that my contribution to the work:

M. Plata-Gryl, M. Motoko, S. Makowiec, G. Boczkaj, Application of cyanated asphaltenes in gas-phase adsorption process for removal of volatile organic compounds, *Chem. Pap.* 74 (2020) 995

was to participate in data analysis and visualization, as well as in initial draft preparation.

I estimate my contribution to the final publication to be 10 %.

Malwina Momotko

Gdańsk, 25.02.2022 r.

dr hab. Sławomir Makowiec, prof. PG
Department of Organic Chemistry
Gdańsk University of Technology
Gabriela Narutowicza 11/12 Street
80-233 Gdańsk
e-mail: mak@pg.edu.pl

STATEMENT

on the contribution and participation in the publication

I declare that my contribution to the work:

M. Plata-Gryl, M. Motoko, S. Makowiec, G. Boczkaj, Application of cyanated asphaltenes in gas-phase adsorption process for removal of volatile organic compounds, *Chem. Pap.* 74 (2020) 995

was to participate in the experimental part of the research, by preparing chemically modified asphaltenes.

I estimate my contribution to the final publication to be 10 %.

.....

Gdańsk, 28.02.2022 r.

dr hab. inż. Grzegorz Boczkaj, prof. PG
Department of Process Engineering and Chemical Technology
Gdańsk University of Technology
Gabriela Narutowicza 11/12 Street
80-233 Gdańsk
e-mail: grzegorz.boczkaj@pg.edu.pl

STATEMENT

on the contribution and participation in the publication

I declare that my contribution to the work:

M. Plata-Gryl, M. Motoko, S. Makowiec, G. Boczkaj, Application of cyanated asphaltenes in gas-phase adsorption process for removal of volatile organic compounds, *Chem. Pap.* 74 (2020) 995

was to participate in the conceptualization of the research, supervision of the research activity planning and execution, preparation of the initial draft and the revised, published work.

I estimate my contribution to the final publication to be 10 %.

Chemical Engineering Journal 427 (2022) 130653

Contents lists available at ScienceDirect

Chemical Engineering Journal

journal homepage: www.elsevier.com/locate/cej

Characterization of diatomaceous earth coated with nitrated asphaltenes as superior adsorbent for removal of VOCs from gas phase in fixed bed column

Maksymilian Plata-Gryl [a], Malwina Momotko [a], Sławomir Makowiec [b], Grzegorz Boczkaj [a,c,*]

[a] Gdansk University of Technology, Faculty of Chemistry, Department of Process Engineering and Chemical Technology, G.Narutowicza St. 11/12, 80-233 Gdansk, Poland
[b] Gdansk University of Technology, Faculty of Chemistry, Department of Organic Chemistry, G.Narutowicza St. 11/12, 80-233 Gdansk, Poland
[c] EkoTech Center, Gdansk University of Technology, G.Narutowicza St. 11/12, 80-233 Gdansk, Poland

ARTICLE INFO

Keywords:
Asphaltenes
Carbon materials
Volatile organic compounds (VOCs)
Adsorption
Waste gases treatment
Air purification

ABSTRACT

Asphaltenes isolated from bitumen possess unusual adsorption characteristics that can be further enhanced by chemical modifications to promote interactions with VOCs'. Herein, nitrated asphaltenes are used as an active layer coated on a surface of a diatomaceous earth, in order to prepare an efficient adsorbent (AsfNitro). Breakthrough experiments with benzene, pyridine, and 1-nitropropane revealed significant increase in adsorption capacity, after deposition of nitrated asphaltenes, by 26, 12, and 8 times respectively. The adsorption capacity of AsfNitro for benzene per square meter of surface area is far more superior than for other adsorbents in use. Moreover, the AsfNitro exhibited excellent efficiency. For adsorption of 1-nitropropane and pyridine, almost 100% of the adsorbent's bed was effectively used. Inverse gas chromatography measurements proved that nitrated asphaltenes were exclusively responsible for the adsorption properties, and the role of the diatomaceous earth was only to provide the surface area. Presented findings can be extended to other support materials and their inherent limitations for adsorption of VOCs can be overcome. Comparison of adsorption enthalpies demonstrated that common adsorbents e.g. activated carbons, cannot compete with AsfNitro in terms of sorbate-sorbent interactions. Additionally, contribution of chemisorption mechanism was recognized for AsfNitro, which indicate catalytic properties, and opens a new research field about asphaltenes' novel practical applications. Application of asphaltenes in adsorption processes can be an effective procedure for risk mitigation of hazardous VOCs, accompanied by effective waste management and materials' valorisation. Wasted adsorbent can be easily regenerated (without deterioration of surface properties), or blended in bitumen-aggregates mixes for road paving applications.

1. Introduction

Importance of volatile organic compounds (VOCs) removal from waste gases is obvious due to their often toxic [1], and odorous character [2], as well as participation in atmospheric photochemical reactions [3,4]. Exposure to VOCs emitted from both anthropogenic [5–9], and natural sources [10,11] pose a threat to the respiratory and nervous systems [7,8,11,12]. Regardless of adverse health effects, VOCs pollution has attracted a great public attention because of their capability to cause odour problems [13–15]. This type of pollution is becoming an important environmental issue as it is affecting directly the quality and comfort of human life [16,17], event at low concentrations, which are not necessarily dangerous for physical health.

VOCs emission can be controlled and limited by different techniques [18] e.g.: membrane separation, absorption [19], adsorption [20], condensation [21], catalytic oxidation [22], biodegradation [23], thermal oxidation [24] or plasma catalysis [25]. Among these methods, adsorption is regarded as efficient, feasible, robust and economical approach with straightforward design and mild operating conditions [20,26]. Additionally, it allows to recover and reuse an adsorbent and an adsorptive (VOC) through thermal and/or vacuum desorption [27].

Adsorption is based on interaction between the surface of the adsorbent and the adsorptive, present in the fluid phase, via physical interactions (physisorption) or chemical bonding (chemisorption). The

* Corresponding author at: Gdansk University of Technology, Faculty of Chemistry, Department of Process Engineering and Chemical Technology, 80-233 Gdansk, G. Narutowicza St. 11/12, Poland.
E-mail address: grzegorz.boczkaj@pg.edu.pl (G. Boczkaj).

https://doi.org/10.1016/j.cej.2021.130653
Received 10 March 2021; Received in revised form 5 May 2021; Accepted 30 May 2021
Available online 4 June 2021

performance of the adsorption processes is determined by textural properties (surface area, porosity, pore size distribution) and surface functional groups of the adsorbent. While textural properties will provide the adsorption capacity, functional groups will be responsible for the selectivity of adsorption. Adsorbents that are commonly used for removal of VOCs are: activated carbons (ACs), zeolites, hypercrosslinked polymeric resins, and metal organic frameworks (MOFs) [26,28–30].

Since the key parameter in adsorption is the adsorbent, major contributions to the development of this technique were made by the studies on new types of adsorbents e.g. carbon nanotubes [31], graphene [32], MOFs [33]. Significant part of this research is devoted to utilization of waste materials as adsorbents [34,35], since to some extent adsorption takes place on virtually any material. Without a doubt, waste materials in their raw form cannot match AC in terms of adsorption performance, but considering their accessibility and low value they are an interesting alternative for traditional adsorbents, at least in waste gases and wastewater treatment processes.

Asphaltenes are a group of chemical compounds with interesting adsorption properties [36–38], that can fall under the category of waste material. At the present moment their applicability is limited to the paving materials [39,40] – asphaltenes are part of asphalt and bitumen products from oil refineries, and as such asphaltenes can be considered as an unwanted by-product. Generally, they are a source of severe damages to both upstream and downstream oil processing systems, and the oil company's concern is to ensure their separation from process streams, or at least stabilization to prevent uncontrolled precipitation [41,42]. Asphaltenes are the most polar fraction of crude oil with the highest molecular weight. From structural point of view, those are polyromantic hydrocarbons (PAHs) with 4–7 condensed aromatic rings, peripheral alkyl chains, multiple functional groups and heteroatoms - examples of asphaltenes' molecular structure can be found in the Figure S1.

Due to quite complicated structure, asphaltenes are defined on the basis solubility: as a fraction of crude oil insoluble in n–alkanes and soluble in toluene/benzene. The highest content of asphaltenes fraction is observed in asphalts, since non-volatile asphaltenes remains quantitatively in residues from distillation processes. Moreover, during asphalt air blowing processes the structure of asphaltenes is changed by introduction of new oxygen containing functional groups [43–45].

Recently, new emerging applications of asphaltenes have been reported eg.: for adsorption [36–38], catalysis [46], and advanced oxidation processes (AOPs) [47]. In case of adsorption processes, asphaltenes are interesting as contrary to graphene or carbon nanotubes, they are readily soluble in organic solvents. Thus, it is possible to immobilize small amounts of asphaltenes on the surface of materials that possess developed surface area but low adsorption capacity. Proper combination should provide synergistic effect, i.e. strong adsorbent having high surface area.

Moreover the structure of asphaltenes is prone to chemical modifications that can increase their adsorption performance [36,37] and they can be easily isolated from bitumen with high purity [48]. Utilization of asphaltenes in the adsorption processes can be a next step toward effective waste management, waste valorisation and risk mitigation of hazardous VOCs for environment and humans.

In this study an effort was made to test the applicability of diatomaceous earth coated with nitrated asphaltenes for gas purification under dynamic conditions. The adsorption properties were scrutinized by breakthrough curves for VOCs, that are significant environmental pollutants e.g. pyridine (odorous compound), tetrachloroethane (chlorinated hydrocarbon) and benzene (carcinogenic compound) at environmentally relevant concentrations and temperatures. Additionally, the impact of humidity, thermal stability and reusability were tested. The adsorption behaviour between VOCs and nitrated asphaltenes was qualitatively and quantitatively followed by Fourier-transform infrared spectroscopy (FTIR), inverse gas chromatography (IGC) and low temperature nitrogen adsorption.

2. Experimental

2.1. Asphaltenes isolation and purification

Asphaltenes were isolated from bitumen 20/30 SDA (Lotos Group, Poland) by modified precipitation method followed by additional purification in Soxhlet apparatus, for 24 h at the temperature of boiling point of n-heptane (under reflux). Detailed description of the procedures can be found in [48]. For isolation n–heptane EMPLURA (Merck, Germany) was used. The content of asphaltenes in the isolated fraction was 98% as determined by TLC-FID (thin-layer chromatography with flame-ionization detection). The remaining 2% were highly condensed resins.

2.2. Synthesis of nitrated asphaltenes

Nitrated asphaltenes were synthesized by mixing HNO_3 (65%, 6.4 cm^3, 91 mmol, POCH, Poland) with the stirred solution of asphaltenes (1.59 g) in methylene chloride (50 mL, pure p.a., POCH, Poland). Obtained mixture was refluxed and stirred for 16 h. Afterwards, solvent was removed under reduced pressure (ca. 10 mmHg), residue was suspended in methanol (50 mL, pure p.a., POCH, Poland) and filtered off. The precipitate was washed with methanol (20 mL) and dried under vacuum at 80 °C for 8 h. Effects of modification were studied by the FTIR spectroscopy.

Elemental analysis of the nitrated asphaltenes was performed with the Flash 2000 elemental analyser (Thermo Scientific, USA).

2.3. Adsorbent preparation

The KG adsorbent (Kieselgur – diatomaceous earth, 60–80 mesh, Merck, Germany) was used as received from supplier. The AsfNitro adsorbent was prepared using the methods of coating of stationary phases onto solid support. Before coating, the support (KG) was washed with methanol (pure p.a., POCH, Poland) and deionized water, followed by activation in the vacuum drier at 200 °C for 5 h. Next, the support was cooled and transferred to the previously prepared solution of asphaltenes in dichloromethane (pure p.a., POCH, Poland). The amount of nitrated asphaltenes and KG was adjusted to give the final asphaltenes content of 10% m/m. The mixture was mixed in a flask and the solvent was evaporated in a rotary evaporator. After removal of the solvent, the prepared adsorbent, named AsfNitro, was dried in the vacuum drier at 105 °C for 1 h.

Dichloromethane was used for the deposition/immobilization of nitrated asphaltenes on the KG according to our previous practice in this field. It was fully recovered from the rotary evaporator. However, as this compound is considered a hazardous to the environment, in industrial practice it can be substituted by other solvents providing solubility of nitrated asphaltenes e.g. toluene.

2.4. Fourier-transform infrared spectroscopy analysis

Chemical structure of the prepared AsfNitro adsorbent before and after adsorption of target VOCs was determined using Fourier transform infrared spectroscopy (FTIR), performed on a Nicolet Spectrometer IR200 (Thermo Scientific, USA). The device was equipped with attenuated total reflectance (ATR) attachment with diamond crystal. Measurements were made with 1 cm^{-1} resolution in the range from 4000 to 400 cm^{-1}.

2.5. Surface area measurement

Nitrogen adsorption–desorption isotherms (BET method for the calculation of the specific surface area) were recorded using the Micromeritics Gemini V (Norcross, USA) instrument at 77 K (liquid

nitrogen temperature).

2.6. Inverse gas chromatography measurements

IGC measurement were conducted using a Clarus 580 gas chromatograph (Perkin Elmer, USA) with a flame ionization detector (FID). The instrument was interfaced to a PC computer for control and acquisition of chromatograms in TotalChrom 6.3.2 application (Perkin Elmer, USA). Adsorbents were packed into GC stainless steel columns (inner diameter 2.1 mm, length 20 cm) using dry packing method, and were preconditioned twice in a gas chromatograph by passing carrier gas (N5.0 nitrogen, Linde Gas, Poland) in the temperature program (5 min @ 50 °C, 2 °C/min, 120 min @ 250 °C). The flowrate of the nitrogen was set to 20 mL min^{-1}. All test compounds were used as received from supplier, and are listed in the Table S1 together with their basic properties. Methane was used as non-interacting marker to determine void time of columns. The retention time of test probes was determined at peak maximum.

IGC at infinite dilution (IGC-ID) was used to measure: free energy of adsorption (ΔG_A), dispersive (γ_S^D), and specific (γ_S^{SP}) components of the surface free energy, electronacceptor (γ_S^+), and electrondonor (γ_S^-) parameters of a solid's surface. Based on the values of ΔG_A the enthalpy of adsorption (ΔH_A) for test probes was calculated. IGC at finite concentration (IGC-FC) was used to measure sorption isotherms for selected probes. Details of the IGC's experimental methods and calculations are given in the SI – section S1 and S2.

2.7. Breakthrough measurements

Breakthrough curves were measured on a modified Autosystem XL gas chromatograph (Perkin Elmer, USA) with an online FID detection, using 20 cm (2.1 mm inner diameter) long stainless steel columns. As a model contaminants, mixtures of benzene, pyridine and 1-nitropropane in nitrogen were used. All three are representatives of VOC group and their concentration in the air is limited. Benzene is known for its carcinogenic properties, pyridine is an odorous compound with very low odour threshold, and 1-nitropropane is a flammable, odorous, and very volatile compound. Moreover, 1-nitropropane possess a threat of explosion when mixed with air and/or when it is in contact with acids, bases, oxidizing agents or heavy metal oxides [49].

Initial concentrations for benzene, pyridine, and 1-nitropropane were 9.6, 46.5, 275 ppm, respectively. Mixtures were prepared in separate gas cylinders and their concentration was determined by GC-FID technique. The initial concentration of test species were set to be 10 times higher than permissible exposure limit (PEL) in the workplace during an 8 h workday as set by the U.S. Occupational Safety and Health Administration [49]. The aim was to collect reliable data about adsorption performance without artificial exaggeration of adsorption performance of the AsfNitro adsorbent, as very often the unrealistic high concentration of test compound can amplify the adsorption capacity.

Measurements were conducted on two relative humidity (RH) levels, i.e. 5 and 80%, to evaluate the influence of low and high levels of water in the gas stream on adsorption performance. RH level was measure by HM2301 humidity sensor (Hanwei, China). Experiments at RH = 80% were performed by sweeping vapours from above the water placed in a heated container.

All measurements were performed at 30 °C and at 30 mL min^{-1} flow rate. Breakthrough point was set to $\frac{C_t}{C_0} = 0.1$, where C_t (mg L^{-1}) is the outlet gas concentration at given time and C_0 (mg L^{-1}) is the influent concentration. Maximum adsorption capacity Q_{max} (mg g^{-1}) of an adsorbent was calculated as follows:

$$q_{max} = F \int_{t=0}^{t_e} \frac{(C_0 - C_t)dt}{m} \quad (1)$$

Where m (g) is the mass of the adsorbent, and t_e (min) is the exhaustion time at $\frac{C_t}{C_0} = 0.95$. Breakthrough adsorption capacity Q_{break} (mg g^{-1}) was calculated from the same equation by changing the integral bound from t_e to t_b (breakthrough time at $\frac{C_t}{C_0} = 0.1$).

Breakthrough volume $BTV_{10\%}$(L) was calculated according to Eq. (2):

$$BTV_{10\%} = \frac{Ft_b}{1000m} \quad (2)$$

The effective adsorption capacity Q_{eff} (mg g^{-1}) is defined as a part of adsorption capacity utilized up to the breakthrough point and was calculated as:

$$Q_{eff} = \frac{Q_{break}}{Q_{max}} \bullet 100 \quad (3)$$

The mass transfer zone MTZ (cm), i.e. a part of packed bed where adsorption takes place, and length of unused bed LUB (cm), i.e. a distance of the adsorbent bed, that is not saturated at the breakthrough time were calculated as follows:

$$MTZ = L\left(\frac{t_e - t_b}{t_e}\right) \quad (4)$$

$$LUB = L\left(\frac{t_s - t_b}{t_s}\right) \quad (5)$$

where t_s (min) is the time at which $\frac{C_t}{C_0} = 0.5$.

2.8. Regeneration ability

The regeneration ability of the AsfNitro was tested with benzene. After saturation, the adsorbent was regenerated by thermal desorption. A N_2 stream was passed through the column with a 30 mL min^{-1} flowrate, at 200 °C until the detector's signal after the desorption stage was stable. Next, the adsorbent was reused to measure the adsorption capacity. Mentioned procedure was repeated 10 times.

2.9. Quality assurance of data

All data points obtained by GC measurements and presented in this paper are an average of three injections. To minimize error caused by linearization of the isotherm and breakthrough curve models, experimental data were fitted by non-linear regression. Computations were performed by R programming language [50] using the Levenberg-Marquardt non-linear least-square algorithm provided by the MINPACK library [51].

Although, data was fitted to the nonlinear forms of the isotherm and breakthrough curve models, the goodness of fit was evaluated by both: the Chi-square coefficient X^2, and the R^2, as the R^2 is more instinctively comprehended:

$$X^2 = \frac{\sum (y_e - y_c)^2}{y_c} \quad (6)$$

$$R^2 = \frac{\sum \left(y_c - \overline{y}_e\right)^2}{\sum \left(y_e - \overline{y}_e\right)^2} \quad (7)$$

where y_c, y_c, and $\overline{y}_e$ are values calculated by a model, experimental, and experimental mean, respectively.

3. Results and discussion

For preparation of the adsorbent with nitrated asphaltenes, the Kieselgur was used as a support. Kieselgur, also known as diatomite or diatomaceous earth, is a fossil material made from siliceous (mainly amorphous hydrated silica) skeletons of diatoms. It was chosen for

several reasons: 1) it is a low-cost material, as the diatomaceous silica is the most abundant form of silica known, 2) it has highly developed bimodal (macro and meso) porosity which makes it a popular adsorbent (mesopores enhance the specific surface area and macropores facilitates the mass transport and diffusion), 3) it has high mechanical and chemical resistance, and 4) the rigid structure of diatomite particles allows to maintain a high filtering velocity and avoid blocking of the filter with tiny solid particles, if present in the processed stream. It is also noteworthy to mention that some attention was already paid to modifying the surface of diatomite to improve its adsorption properties [52,53]. The proof of successful modification leading to introduction of $–NO_2$ groups to the structure of asphaltenes can be found in our previous study and in the Figure S1 [36]. Also, the elemental composition of raw and nitrated asphaltenes proved the fact of successful modification. The nitrogen content increased from 1.28 to 6.25% wt., and oxygen from 1.79 to 18.81% wt. Analysis of the results reveals that $–NO_2$ groups account for 16.40% wt. of nitrated asphaltenes (0.0036 mol of $–NO_2$ per gram). The molar ratio of introduced oxygen and nitrogen (O/N) equal to 3 indicate that apart from $–NO_2$ groups, also other oxygen-containing groups were added to the structure of asphaltenes, because of oxidation. It is in line with the results of FTIR published previously [36]. At the same tame molar ratio of C/H, for both raw and nitrated asphaltenes is close to 1. It is a typical value for asphaltenes, and demonstrates their high aromaticity.

The low temperature nitrogen adsorption revealed that textural properties of both adsorbents were similar. Neither the BET surface area, nor the total pore volume was changed by the deposition of nitrated asphaltenes on the surface of diatomaceous earth (KG). The BET surface area of the KG and the AsfNitro was 1.480 ± 0.020 and 1.491 ± 0.037 $m^2\ g^{-1}$, respectively. The total pore volume was the same for both adsorbents i.e. 0.0015 $cm^3\ g^{-1}$. It proves that KG, and other similar mesoporous materials, can be a suitable support and surface area provider for asphaltenes.

To evaluate adsorption properties of the adsorbent, the equilibrium (isotherms) and dynamic (breakthrough curves) experiments has been conducted with pyridine, benzene, and 1-nitropropane.

3.1. Breakthrough curves

In real life applications adsorption processes are usually operated under dynamic conditions (i.e. continuous flow of contaminated gas), and with formation of multilayer adsorption. Breakthrough analysis is the method to assess the applicability of the prepared adsorbent through characterization of adsorption capacity, kinetics and selectivity. Breakthrough experiments were performed with controlled temperature of 30 °C in a practical flow-through configuration that mimics conditions used in industrial separations. Fig. 1 presents breakthrough curves for low humidity gas stream (RH = 5% ± 2). Breakthrough curves revealed significant change in the adsorption capacity for all test compounds in favour of AsfNitro adsorbent. The highest change was observed for pyridine and benzene. Interesting observation was made about the shape of the curve for benzene and AsfNitro adsorbent. It is clearly less steep compared to curve for KG. The steepness of the curve is correlated to the efficiency of the adsorption and effective usage of the adsorbent. The more steep is the curve, the smaller width of the mass transfer zone (zone with the highest mass transfer speed) is. More slanted curve may indicate that there is a change in heterogeneity of the surface between KG and AsfNitro. The adsorption centres for benzene may have a wider adsorption potential distribution compared do pyridine and 1-nitropropane. More information about adsorption process were obtained from parameters derived from breakthrough curves that describe performance of columns at RH = 5%, and are presented in the Table 1.

$BTV_{10\%}$, Q_{max}, and Q_{break} parameters characterize the adsorption capacity of the adsorbent, which is considerably superior for AsfNitro adsorption capacity compared to KG, regardless of the test compound. In case of waste gas purification, especially important is the substantial

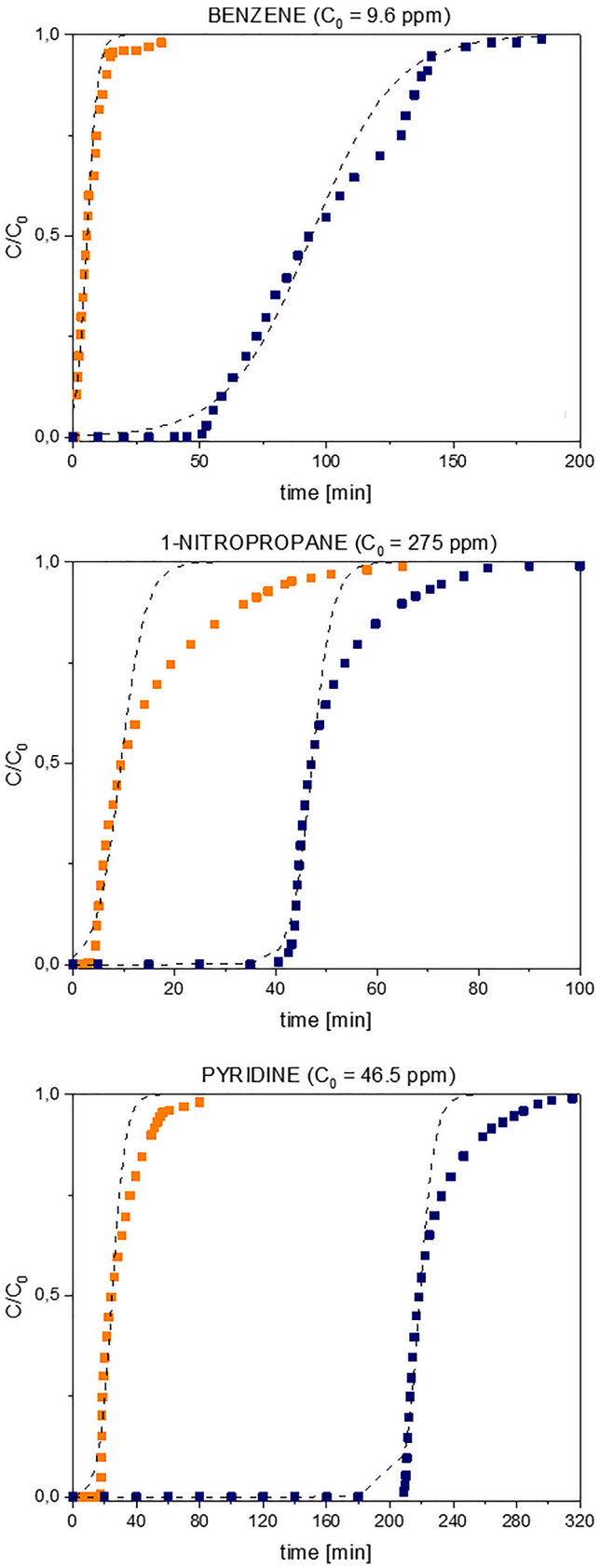

Fig. 1. Breakthrough curves of benzene, pyridine and 1-nitropropane on the KG (■) and AsfNitro (■) adsorbent. Dashed line (– – –) represents logistic growth model. Relative humidity of gas stream was 5%.

Table 1
Operational parameters of investigated columns (with KG and AsfNitro adsorbents) used for adsorption of benzene, pyridine and 1-nitropropane, measured at RH = 5%.

Parameter	$BTV_{10\%}$	Q_{max}	Q_{break}	Q_{eff}	MTZ	LUB
Unit	[L g^{-1}]	[mg g^{-1}]	[mg g^{-1}]	[%]	[cm]	[cm]
benzene						
KG	0.46 ± 0.03	0.048 ± 0.003	0.014 ± 0.001	29.4 ± 3.8	17.3 ± 0.4	12.1 ± 1.1
AsfNitro	12.07 ± 0.77	0.570 ± 0.060	0.360 ± 0.040	68.7 ± 6.6	11.0 ± 0.5	4.3 ± 0.4
pyridine						
KG	3.61 ± 0.21	0.924 ± 0.013	0.544 ± 0.031	58.8 ± 2.5	14.2 ± 0.6	5.4 ± 0.2
AsfNitro	43.86 ± 1.17	7.084 ± 0.210	6.608 ± 0.177	92.3 ± 0.3	4.5 ± 0.3	0.7 ± 0.1
1-nitropropane						
KG	1.10 ± 0.07	3.277 ± 0.127	1.096 ± 0.066	33.4 ± 0.7	17.6 ± 0.1	9.9 ± 0.1
AsfNitro	9.28 ± 0.09	11.045 ± 0.125	9.272 ± 0.091	84.0 ± 1.8	8.7 ± 0.6	1.4 ± 0.1

increase of the breakthrough adsorption capacity (Q_{break}) and breakthrough volume ($BTV_{10\%}$). Higher value of $BTV_{10\%}$ is advantageous as it increases the adsorbent bed service life, and simultaneously decreases required adsorbent mass.

Beside enhancement of adsorption capacity, analysis of breakthrough curves revealed the improvement of the adsorption efficiency. The mass transfer zone (MTZ) reduced after modification of KG with nitrated asphaltenes. The shorter the MTZ, the better the performance of adsorption column. The adsorbent bed was used more effectively leading to a shorter length of unused bed (LUB) – a portion of adsorbent bed that was not exhausted when breakthrough was observed. To give better idea about the efficiency change, the effective adsorption capacity (Q_{eff}) was calculated, i.e. the part of adsorption capacity that was used before the breakthrough occurred. It was two times higher for AsfNitro compared to KG. That value was outstanding for pyridine and 1-nitropropane. AsfNitro adsorbent was exhausted in 92 (pyridine) and 84% (1-nitropropane) when the breakthrough was observed. It is around two times higher than for KG adsorbent. The fact of improved adsorption efficiency is certainly not without significance for the economics of the adsorption process.

The breakthrough data was modelled by three popular mathematical expressions i.e. Bohart-Adams, Thomas and Yoon-Nelson. However, to estimates the values of those parameters a logistic equation was used:

$$\frac{C}{C_0} = \frac{1}{1 + \exp(a - bt)} \tag{8}$$

the definition of a and b parameters, in regard to the Bohart-Adams, Thomas and Yoon-Nelson models, is presented in the Table 2. The abovementioned approach is applicable, because at the ground level all three mentioned models are one and the same, just with different definitions for a and b parameters, and can be expressed as the logistic growth function with two parameters [54].

Table 3 summarizes the results of logistic growth model fitting, including calculated values of abovementioned models. Although, experimental curves for both adsorbents where fairly well described by the logistic growth equation, regression analysis derived from Eq. (8) of the experimental breakthrough data obtained for test probes gave better agreements with the AsfNitro's breakthrough curves. It is reflected by the difference between measured and calculated values of τ, q_0, and N_0. For AsfNitro it was below 10%, which is an acceptable agreement of results for such purpose.

The values of models' constants revealed that modification of KG with asphaltenes didn't change significantly the kinetics, except for benzene. For that compound a substantial decrease of k_{YN}, k_T, and k_{BA} was observed. It was expected based on the analysis of the breakthrough

Table 2
Meaning of the a and b parameters in regard to the breakthrough curve's models.

Model	Logistic growth function	
	a	b
Yoon-Nelson	$k_{YN}\tau$	k_{YN}
Thomas	$\frac{k_T q_0 m}{F}$	$k_T C_0$
Bohart-Adams	$\frac{k_{BA} N_0 L}{u}$	$k_{BA} C_0$
Parameter	**Definition**	**Unit**
k_{YN}	Yoon-Nelson rate coefficient	min^{-1}
τ	time required for 50% breakthrough	min
k_T	Thomas rate coefficient	$cm^3\ mg^{-1}\ min^{-1}$
q_0	maximum adsorption capacity	mg g^{-1}
F	volumetric flowrate	$cm^3\ min^{-1}$
m	mass of the adsorbent	g
k_{BA}	Bohart-Adams rate coefficient	$cm^3\ mg^{-1}\ min^{-1}$
N_0	adsorption capacity of the adsorbent per unit volume of the bed	mg cm^{-3}
L	bed depth	cm
u	superficial velocity	cm min^{-1}

curve's shape. Nitrated asphaltenes on the surface of KG have introduced large number of new active centres with wide distribution of adsorption potential compared to pure KG. As the most active centres are progressively occupied towards the less active, the enthalpy of adsorption decrease. This is illustrated as a decrease in the gradient of the breakthrough curve of benzene on the AsfNitro adsorbent (Fig. 3). Overall, the drop in the rate of benzene adsorption is fully compensated by large increase of adsorption capacity.

The adsorption performance of AsfNitro adsorbent toward benzene was compared with other adsorbents reported in the literature in terms of 10% breakthrough capacity (Q_{break}). Data for 1 Pa inlet partial pressure was extracted from [30]. In this work nitrated asphaltenes are intended to be used as an active layer used to coat a surface area of an inexpensive support. As such, the adsorption capacity will depend on the choice of the support. To highlight it, Fig. 2 was prepared where Q_{break}, measured at RH = 5%, was normalized against the specific surface area of the adsorbents. The adsorption capacity per meter square of surface area is superior to all other adsorbents listed. Results in the Fig. 2 points out the direction for further development of nitrated asphaltenes-based adsorbents – search for materials with suitable surface area e.g. natural minerals, clays, or rocks that are easily available in the target destination. Small particles of inorganic support covered with asphalthenes can be easily utilized. As asphalthenes are a component of bitumen used for road paving applications as well as sealants – the wasted adsorbent bed can be blended with bitumen during preparation of bitumen-aggregates mix. In case of hot mix operations under controlled conditions it would be possible to desorb the VOCs and treat them by proper technology, while wasted adsorbent incorporation as asphalt component. This approach is already used for utilization of post-process ashes which are blended with asphalt.

To test the effect of water vapour on adsorption, measurements at 80 ± 2% relative humidity were performed for benzene and 1-nitropropane. Collected data revealed that the relative humidity had a negative influence on the breakthrough curves. Table S2 lists breakthrough parameters of columns operated under humid conditions.

The breakthrough adsorption capacity decreased under humid conditions. This drop can be attributed to the competitive adsorption of water molecules on the surface of adsorbents. The AsfNitro adsorbent bed become depleted by benzene and 1-nitropropane about 6 and 2 times faster, respectively, compared to dry conditions. The drop of adsorption capacity toward benzene was similar as for e.g. activated carbon prepared from peat [55]. Nevertheless, the AsfNitro retains

Table 3
Results of logistic growth model fitting.

	k_{YN}(min^{-1})	τ(min)	k_T(cm^3 mg^{-1} min^{-1})	q_0(mg g^{-1})	k_{BA}(cm^3 mg^{-1} min^{-1})	N_0(mg cm^{-3})	X^2(R^2)
KG							
benzene	0.473 ± 0.026	5.6 ± 0.1	15458 ± 852	0.037 ± 0.001	15458 ± 852	0.007 ± 0.001	0.366 (0.979)
pyridine	0.239 ± 0.017	24.8 ± 0.2	1583 ± 112	0.804 ± 0.001	1583 ± 112	0.162 ± 0.001	0.850 (0.960)
1-nitropropane	0.413 ± 0.027	9.5 ± 0.1	413 ± 27	2.046 ± 0.004	413 ± 27	0.412 ± 0.001	0.684 (0.961)
AsfNitro							
benzene	0.061 ± 0.002	94.1 ± 0.1	1993 ± 76	0.619 ± 0.001	1993 ± 76	0.125 ± 0.001	0.338 (0.985)
pyridine	0.213 ± 0.015	219.0 ± 0.2	1411 ± 96	7.113 ± 0.005	1411 ± 96	1.433 ± 0.005	0.492 (0.975)
1-nitropropane	0.492 ± 0.033	47.2 ± 0.1	492 ± 33	10.157 ± 0.004	492 ± 33	2.047 ± 0.002	0.399 (0.973)

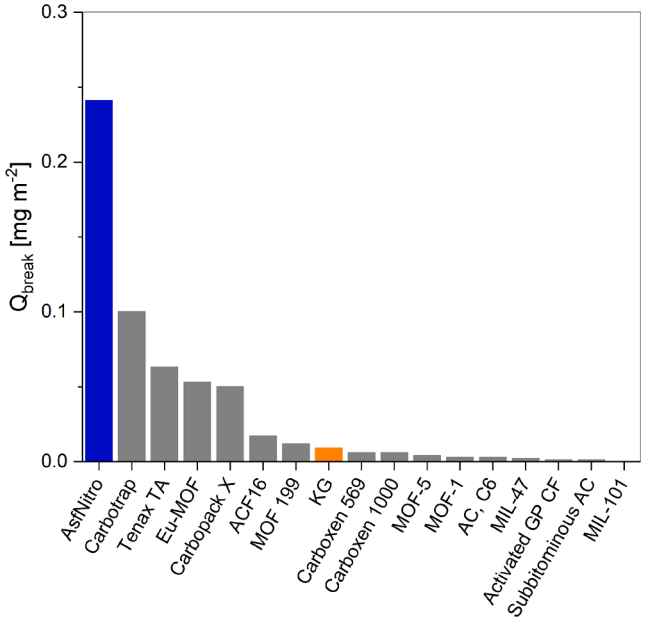

Fig. 2. Adsorption capacities (Q_{break}, breakthrough adsorption capacity), measured at RH = 5%, of AsfNitro, KG and other adsorbents for benzene per surface area of an adsorbent.

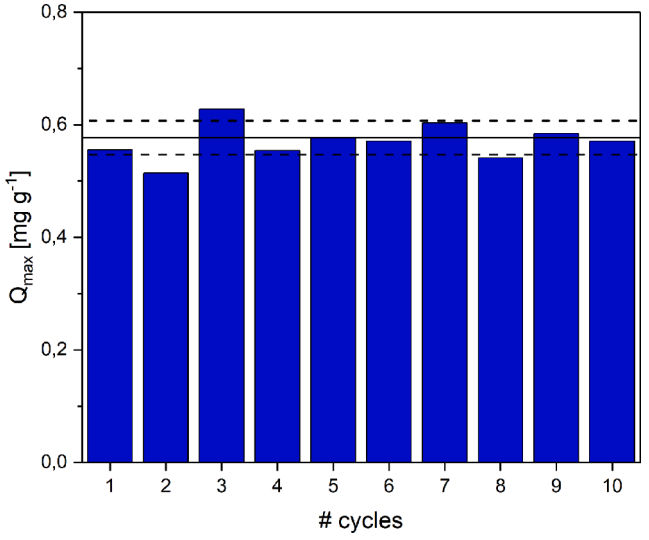

Fig. 3. Reusability of AsfNitro adsorbent for benzene adsorption. Solid line represents mean value, dotted line standard deviation.

partially its favourable adsorption properties.

The reuse potential of the AsfNitro adsorbent was evaluated by monitoring the changes of Q_{max} value for benzene between consequent adsorption–desorption cycles. The regeneration of adsorbent bed was achieved by thermal desorption at 250 °C in pure nitrogen stream. The relative humidity of gas stream, for both adsorption and desorption step, was 5 ± 2%. The results are presented in the Fig. 3.

The AsfNitro represents satisfactory reusability. The maximum adsorption capacity was stable in the course of the 10 consequent adsorption–desorption cycles. The RSD for measured values was around 5%. Moreover, the mentioned result indicate a favourable thermal stability of the AsfNitro, since it was regenerated by the thermal desorption (250 °C). In process scale the desorption can be aided by vacuum, and performed in lower temperatures. It will extend the life cycle of the AsfNitro adsorbent.

Moreover, the adsorption–desorption stability of the adsorbent's performance demonstrates the durability of the chemical modification with –NO_2. It is further supported by IGC results, presented in the next sections. After each analysis, adsorbent was thermally regenerated to ensure full desorption of a test probe, and the accuracy of the IGC results indicate that it did not affect the surface properties of AsfNitro.

3.2. Inverse gas chromatography

Both tested adsorbents have similar surface area and porosity. Thus, it can be concluded that the differences in the adsorption performance, observed in breakthrough experiments are not caused by the differences in textural properties and diffusion, but are the result of the different strengths of adsorbate-adsorbent interactions. Those interactions arise from chemical structure of the surface and presence of the specific sorption sites. It leads to preferential adsorption of certain compounds over others. To investigate in detail the thermodynamic equilibrium separation mechanism, the IGC technique was used. In the Table S2 the ΔG_A, ΔH_A and ΔS_A value for all test probes are reported.

3.2.1. Adsorption isotherms

The adsorption isotherms were used to reveal the relationship between the equilibrium concentration in the gas phase and the amount of VOC adsorbed on the surface of KG and AsfNitro adsorbents at low surface coverage ($\theta < 1$). The adsorption equilibrium data were fitted to two well-known isotherm models, to evaluate their utility and to simulate the experimental data. Measurements were done for the same test probes as in breakthrough experiments. The equilibrium adsorption properties were compared in the temperature range between 100 and 140 °C.

Langmuir model is the most extensively used isotherm model. It assumes that adsorption is limited to a one molecular layer, all adsorption sites on the surface are energetically identical, and there is no interaction between adsorbate's molecules [56]. Langmuir model is described by Eq. (9):

$$q_e = q_0 \frac{K_L P}{1 + KP} \tag{9}$$

where q_0 (mg g^{-1}) is the maximum adsorption capacity of the adsorbent, K_L (Pa^{-1}) is the Langmuir equilibrium constant related to the heat of adsorption, and P (Pa) is the partial pressure of the adsorbate in gas phase.

The Freundlich isotherm is an empirical model applicable to adsorption process on heterogeneous surface [57]. The equation for Freundlich model is as follows:

$$q_e = K_F P^{\frac{1}{n}} \tag{10}$$

where K_F (mg g^{-1} Pa$^{-1/n}$) is the parameter related to the adsorption capacity, parameter n (-) characterizes the heterogeneity of the adsorbent's surface and the adsorption intensity. The lower the value of n, the more favourable is adsorption.

Using values of K_L for different temperatures, the heat of adsorption can be estimated from the following van't Hoff equation, which relates the Langmuir equilibrium constant to the temperature [58]:

$$K_L = K_0 exp\left[\frac{-E_A}{RT}\right] \tag{11}$$

where E_A (J mol^{-1}) is the activation energy of adsorption and K_0 is the adsorption equilibrium constant. The relation between the $\ln K_L$ and $\frac{1}{T}$ are given in the SI (Figure S4).

Due to very low retention of benzene on KG, the isotherm was measured only for 100 °C and the E_A value couldn't be calculated for that adsorbate-adsorbent pair. For pyridine and 1-nitropropane it was 12.21 ± 1.54 and 3.89 ± 0.14 kJ mol^{-1}, respectively. For AsfNitro the E_A values for benzene, pyridine and 1-nitropropane were 59.94 ± 2.99, 47.85 ± 4.55 and 29.55 ± 3.63, respectively. It is evident that adsorption performance of AsfNitro originates exclusively from presence of nitrated asphaltenes. The E_A increased almost 4 times for pyridine, and over 7 times for 1-nitropropane. For benzene it would be even greater. The magnitude of E_A indicates the character of adsorption i.e. physisorption or chemisorption. Typically, range 5–40 kJ mol^{-1} corresponds to a physisorption and 40–800 kJ mol^{-1} to a chemisorption [59], however that distinction is not rigid.

Values of adsorption energy for AsfNitro falls between two mentioned ranges. It suggest that test probes are bounded to the surface of AsfNitro by synergistic combination of very strong physical interactions and chemical interactions with functional groups on the surface. Before deposition of asphaltenes on the KG's surface the fundamental interacting force were of van der Waals type, and the adsorption process was based solely on physisorption.

To model the experimental data, the Langmuir and Freundlich adsorption isotherm models were used. Full set of results, together with examples of adsorption isotherms at 100 °C, can be found in the SI (Table S3 and Figure S5). The Freundlich model was more adequate for experimental data, however both models explained it correctly, as indicated by high R^2 values. Those results mean that the surface of both adsorbents is not homogenous in terms of adsorption centres' energy. It is further supported by the results presented in the section 3.2.2. Moreover the n values, for all test probes, are lower for AsfNitro adsorbent, meaning more favourable adsorption.

In the Fig. 4 monolayer adsorption capacities, derived from Langmuir model, are compared. The deposition of nitrated asphaltenes on the surface of KG enormously enhanced its adsorption capacity. Generally, the extent of Q_{mono} of test compounds is following the boiling point i.e. the compound with the highest boiling point has the highest monolayer adsorption capacity. For 1-nitropropane, and benzene at 100 °C, the difference between Q_{mono} of adsorbents was around 70 times in favour of AsfNitro, and was quite stable in the whole range of temperature. For pyridine, the difference increases with temperature. From 79 at 100 °C, to 92 times more at 140 °C. It suggests that interactions between pyridine and KG weaken faster with temperature increase, comparing to pyridine and AsfNitro. Less rapid reduce of strength of interactions is favourable for the stability and predictability of the adsorption process.

3.2.2. Surface's heterogeneity

Surface's energy heterogeneity was described by the adsorption potential distribution, which was calculated from the sorption isotherm

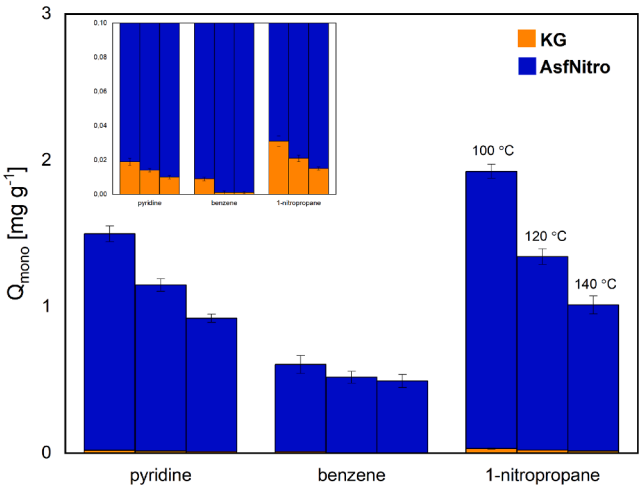

Fig. 4. Values of monolayer adsorption capacities, derived from Langmuir model.

determined by the ECP method [60]. Adsorption potential A (J mol^{-1}) is calculated by conversion of a partial pressure according to Eq. (12):

$$A = RT\ln\left(\frac{P_0}{P}\right) \tag{12}$$

where P_0 is (Pa) the saturation pressure. The distribution parameter ∅ (mol mol g^{-1} J^{-1}), which is correlated with the number of adsorption sites, is calculated according to Eq. (13):

$$\varnothing = -\frac{dn}{dA} \tag{13}$$

where n (mol) is an adsorbed amount of the probe.

Fig. 5 compares the adsorption potential distribution for test probes used to determine adsorption isotherms at 100 °C, for the surface coverage in the range between 0 and 0.5. It is obvious that adsorption potential distribution of KG and AsfNitro are dissimilar, and it illustrates markedly different chemistry of the surface. The area under the curves is directly related to the uptake of the different energy sites, and it indicates that AsfNitro adsorbent has a larger number of adsorption centres on its surface, compared to KG, which are responsible for its superior adsorption capacity. For all test compounds, and both adsorbents, lower energy sites have a bigger population then the high energy.

Benzene's adsorption potentials distribution revealed that both adsorbents possess adsorption centres with similar energy, but their number on AsfNitro is greater. A sharp increase of distribution potential (∅) on the left side (at half surface coverage) of AsfNitro's adsorption potential distribution illustrates that most of the adsorption capacity towards benzene is due to lower energy sites, that originates from aromatic rings in the structure of asphaltenes. Moreover, both distributions are rather flat, without distinct peaks in the adsorption potential range considered. It was predictable as benzene molecule is non-polar and interacts mostly by dispersive interactions.

More significant differences are observed for 1-nitropropane and pyridine adsorption potential distributions. The distributions not only indicate increased number of adsorption sites, but also a shift toward lower energy sites, for the considered range of surface's coverage (0–0.5), and multiple peaks one the AsfNitro's curves. Those peaks indicate that there are certain types of adsorption centres specific for 1-nitropropane and pyridine molecules. Insets of the Fig. 5b and c shows that surface of KG don't exhibit any specific adsorption sites for any of test compounds, at the 0–0.5 surface coverage.

Adsorbate-adsorbents interactions responsible for the observed differences in the adsorption capacity of KG and AsfNitro adsorbents, can be divided into two categories: dispersive and specific. Both were analysed by the IGC technique.

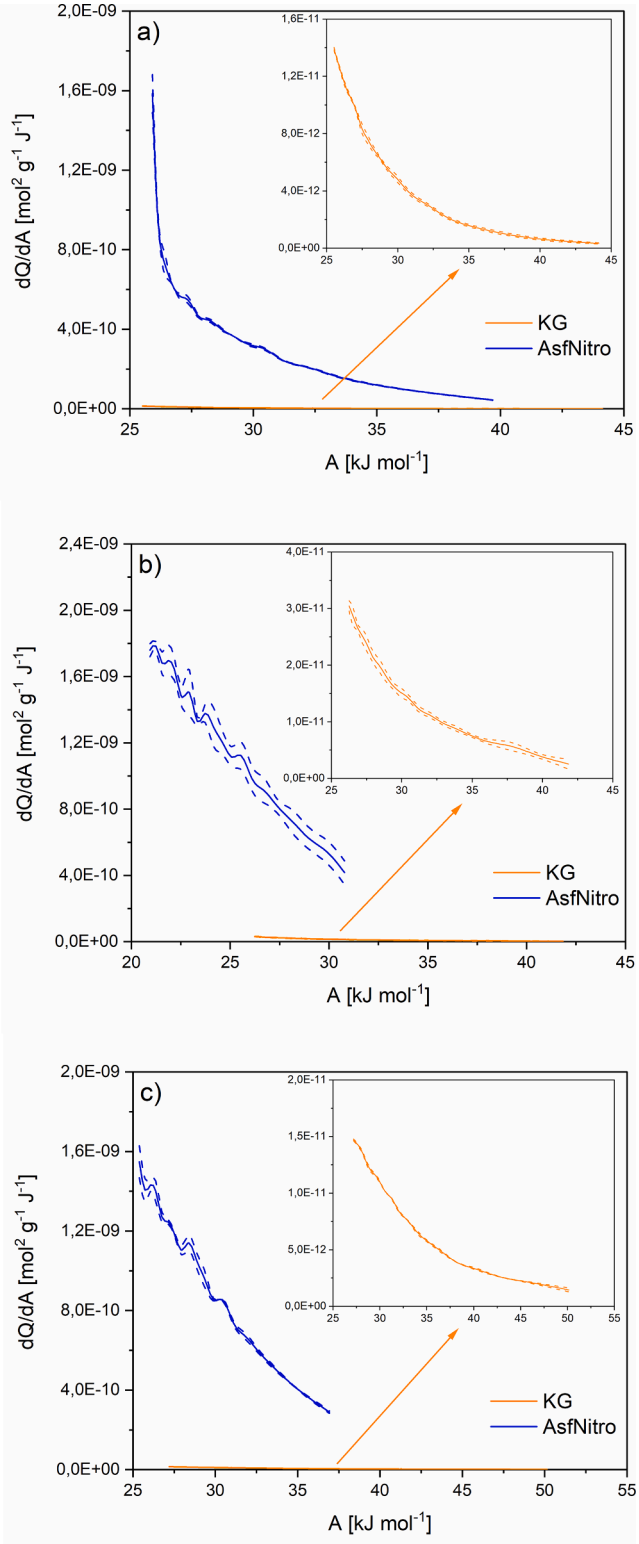

Fig. 5. Adsorption potential distribution for a) benzene, b) 1-nitropropane, c) pyridine at 100 °C.

3.2.3. *Dispersive interactions*

Dispersive interactions were revealed by retention of non-polar probes (e.g. n-alkanes) which interact with the surface only through dispersive interactions. Based on it, the dispersive component of the surface free energy (γ_S^D) was calculated. It is important for evaluation of activity of the surface, and is correlated with the unspecific London interactions and heterogeneity of the surface. Generally, micro and mesoporous materials with active surface have values of γ_S^D above 200 mJ m^{-2} [60–62]. In practice, the higher the surface energy, the more interactive is the surface.

Fig. 6 compares values of γ_S^D for KG and AsfNitro and how they changes with temperature. Obtained values of γ_S^D indicate that the surface of both adsorbents (KG and AsfNitro) is relatively active, at 60 °C the value of γ_S^D is above 200 mJ m^{-2}. The result for AsfNitro is similar to previously reported, where nitrated asphaltenes were deposited on the surface of silanized support (Chromosorb W AW DCMS) [36]. In comparison to KG, dispersive interactions were only slightly enhanced by the deposition of asphaltenes on the surface of diatomaceous earth. It is in line with the small changes in ΔH_A (see Table S3) observed for n-alkanes. The value of γ_S^D for both adsorbents is linearly increasing with the temperature decrease, which is a typical behaviour for adsorbents. As the temperature decrease, the magnitude of weak London dispersion interactions is increasing because molecules of adsorbate, having less kinetic energy, reside longer on the surface of the adsorbent. Interestingly, the strength of dispersive interactions is decreasing faster, with increase of temperature, for the AsfNitro. This fact can be advantageous during thermal desorption and adsorbent regeneration as the adsorbed molecules will be more easily desorbed. This will lead to faster regeneration in lower temperature, and lower thermal stress will be imposed on adsorbent particles. Hence, particles of the AsfNitro should be more resilient to fracturing and deformations as compared to the KG. Moreover, relatively small slope of the γ_S^D versus temperature plot imply good adsorption performance stability if there will be changes of surrounding temperature.

For better understanding of results presented in the Fig. 6, comparison of γ_S^D values for different adsorbents was compiled in the Table 4. Retention of test probes (e.g. n-alkanes) strongly depends on the experimental temperature, hence there is no standard temperature used for the measurement of the γ_S^D. The experimental conditions and range of n-alkanes is selected individually for a given adsorbent in order to achieve acceptable values of retention time. Thus, the information in the Table 4 should be analysed carefully. Nevertheless, knowing that the γ_S^D is increasing with decrease of the temperature, it is apparent that the AsfNitro has a very active surface, exceeding some of the emerging adsorbents (e.g. MOFs) and comparable with carbonaceous materials (CNTs, AC). Results indicate that deposition of asphaltenes on the surface of materials is an effective method to obtain very good activity and adsorption performance.

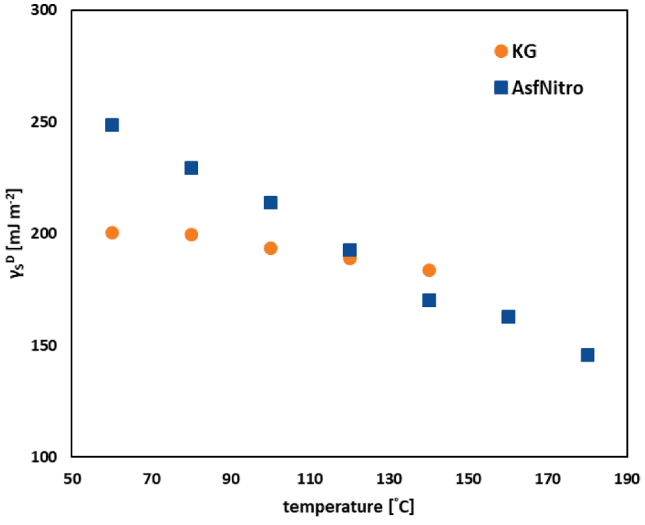

Fig. 6. Value of the dispersive component of the surface free energy γ_S^D in different temperatures for KG and AsfNitro adsorbents.

Table 4
Comparison of dispersive surface energy for various adsorbents.

Adsorbent	T [°C]	γ_S^D [mJ m^{-2}]	Reference
IRMOF	180	91	[63]
CNT	200	125	[64]
HKUST-1 (MOF)	90	144.5	[65]
AsfNitro	**80**	**229.54 ± 0.18**	**This work**
RD granular silica gel	90	93.14	[61]
SBA-16 (porous silica)	93	71,93	[66]
Maxsorb III (AC)	140	213.98	[67]
Chemviron F400	350	208.20	[60]
High surface area graphite	200	115	[68]

While the γ_S^D measured by IGC at infinite dilution is a useful parameter in materials characterization, it can be criticised for the fact that only high energy adsorption sites are probed. In some cases, as for example waste gas purification, the distribution of active sites may be more important than high energy sites. To get more insight into dispersive interactions, the adsorption potential distribution was determined for n-heptane at 100 °C. It is presented in the Fig. 7.

The adsorption potential distributions presented in the Fig. 7 were collected for the surface coverage between 0 and 0.2. This part of the studies revealed that nitrated asphaltenes are solely responsible for the adsorption potential of AsfNitro. There is a colossal increase in the number of active sites participating in the adsorption of n-heptane after coating asphaltenes on the diatomaceous earth. It shows the tremendous difference in dispersive interactions between AsfNitro and KG is not in the adsorption centres with the highest energy but in the abundance of adsorption sites with lower energy that were introduced by nitrated asphaltenes. That difference was also reflected in the n–heptane's monolayer adsorption capacity. It was over 130 times higher after deposition of asphaltenes (2.406 and 0.018 mg g^{-1}, respectively).

3.2.4. Specific interactions

As revealed by results presented in the Table S4, deposition of nitrated asphaltenes on the surface of diatomaceous earth has also a prominent effect on the specific interactions. For all test probes a decrease of ΔG_A values was observed for AsfNitro, as compared to KG adsorbent. Generally, lower value of the ΔG_A means that adsorbate is adsorbed to a greater extent. Negative values of the ΔG_A indicate that the adsorption process is thermodynamically feasible and spontaneous. For all test probes the free energy of adsorption is increasing as the temperature of measurement increase. It indicates that adsorbate molecules residence time on the surface is becoming shorter and adsorption in higher temperatures is less favourable. It is a typical phenomenon and a foundation of desorption process (regeneration of adsorbent). Based on ΔG_A values determined at different temperatures, the ΔH_A and ΔS_A were calculated. The obtained values are natural for adsorption process, i.e. negative values of enthalpy and entropy implies respectively that the adsorption is exothermic and that the degree of freedom decreases at the gas–solid interface. Comparison of ΔH_A for both adsorbents disclose the difference in the strength of adsorption in favour of AsfNitro adsorbent (see Table S4). Coating of KG with nitrated asphaltenes resulted in ca. 1.5–2 times increase of the ΔH_A value. The smallest change was observed for nonpolar compounds (e.g. alkanes, benzene). It is a premise that introduction of nitrated asphaltenes altered the adsorption to a greater extent through specific, than by dispersive interactions. Moreover examination of coefficient of determination (R^2) revealed that the mechanism of specific interactions of AsfNitro adsorbent may be susceptible to temperature in non-obvious manner. For KG adsorbent, value of R^2 for plot of $\frac{\Delta G_A}{T}$ versus $\frac{1}{T}$ is high for all adsorbates, whereas in case of AsfNitro very high linearity is obtained only for n-alkanes.

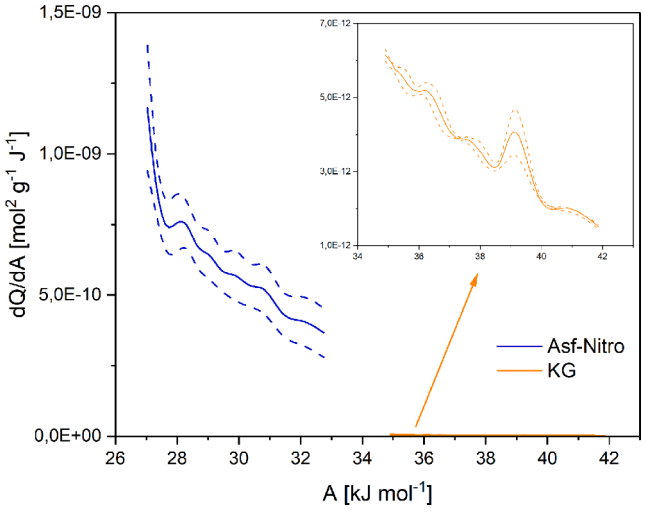

Fig. 7. Adsorption potential distribution for n-heptane at 100 °C.

Table 5 compares enthalpies of adsorption, measured at infinite dilution, for selected adsorbents. Red colour indicates values lower, and green higher or equal to values calculated for material coated with nitrated asphaltenes. It is clear that AsfNitro adsorbent is superior in this respect. The adsorbents that can compete with nitrated asphaltenes are high-tech, novel materials like metal–organic frameworks (MOFs) or graphene. Moreover, the ΔH_A values of AsfNitro are above the range typically assigned to physical adsorption and fall into chemisorption range. Obtained results indicates that nitrated asphaltenes may have catalytic properties. Similar results were recently reported for oxidized asphaltenes [46]. These findings can open new paths for research about asphaltenes' properties and their novel practical applications.

Specific interactions can also be described in terms of Lewis acid-base theory. Electron donor (γ_S^-) and electron acceptor (γ_S^+) properties of the surface were revealed by measuring the retention of monopolar acid (chloroform) and monopolar base (ethyl acetate). Fig. 8 presents the ratio of γ_S^-/γ_S^+ that is describing the basicity of the surface. The higher the value, the more electrondonor the surface is. The experiment revealed the fundamentally different character of the surface of AsfNitro adsorbent, as compared to KG. The AsfNitro surface is predominantly electrondonor (basic) in the nature (the KG has mainly electron acceptor nature) that originates in the free electron rich nitro groups in the structure of nitrated asphaltenes. The specific interactions change with temperature. As it increase, the γ_S^-/γ_S^+ value decrease and the surface is becoming less electrondonor. Above 170 °C the character of the surface becomes acidic ($\gamma_S^-/\gamma_S^+ < 1$). The KG surface's character is electron acceptor in the whole range of experimental temperatures. Thus the electron rich surface of the AsfNitro adsorbent will favourably adsorb molecules with electron-acceptor capabilities.

3.3. Mechanism of adsorption.

Since BET analysis revealed that both adsorbents have similar surface areas, high adsorption capacity of AsfNitro (compared to KG) can't be ascribed to differences in specific surface area. The difference have to arise from the chemistry of the surface of AsfNitro adsorbent. In previous work [38] it was demonstrated that asphaltene-based stationary phases presents satisfactory batch-to-batch stability of adsorption properties.

Fig. 9 presents FTIR-ATR spectra of AsfNitro before and after adsorption of test probes. In the AsfNitro spectrum the presence of nitro group is manifested by three intensive bands at 1530, 1335, and 1275 cm^{-1}. They can be assigned to the asymmetrical and symmetrical aromatic C-NO_2 and N = O stretching, respectively [75]. Original asphaltenes have oxygen functionalities, which content may be further enhanced by acid used for nitration, as indicated by the elemental analysis results. The bands at 1720, and 1642 cm^{-2} are due to the presence of ester and amide carbonyl functionalities [76]. Bands at 2953, 2923, 2851, and 1451 cm^{-1} are attributed to the CH_2 and CH_3

Table 5
Enthalpies of adsorption ΔH_A (kJ mol^{-1}) measured by IGC-ID for different adsorbents.

	AsfNitro	AC1	ACF	PP-resin	CNTs	Graphene	HSAG300	CNT	GO	rGO	HKUST-1	Cu-BTC	IRMOF-1
acetone	78.9	33.3	61.7	58.7	49.9	–	–	–	–	–	–	70.6	74.4
DEE	101.7	–	–	–	–	–	–	–	56.1	68.4	75.4	–	84.7
THF	81.7	–	–	–	–	–	–	–	51.8	50.4	77.5	78.5	–
EtOAc	76.8	53.0	63.5	65.0	–	48.1	–	–	133.2	62.5	–	75.1	81.2
TCM	75.1	59.0	55.7	57.1	–	–	33.2	30.8	41.0	76.0	–	–	39.2
benzene	79.9	51.0	55.5	55.9	22.9	34.3	52.5	34.7	–	–	51.2	68.9	46.7
T (°C)	80–120	70–100	70–100	70–100	30–90	30–60	200–250	200–250	130–150	140–150	220–250	200–230	200
SA (m^2 g^{-1})	1.5	1068	1222	861	108	510	312	186	2	321	1168	1400	781
Ref.	This study	[69]			[70]	[71]	[64]		[72]		[73]	[74]	[63]

AC-activated carbon, ACF – activated carbon fiber, PP – porous polymeric, CNT – carbon nanotubes, HSAG – high surface area graphite, GO – graphene oxide, rGO – reduced graphene oxide, HKUST–1/Cu-BTC/IRMOF-1 – different types of metal–organic frameworks.

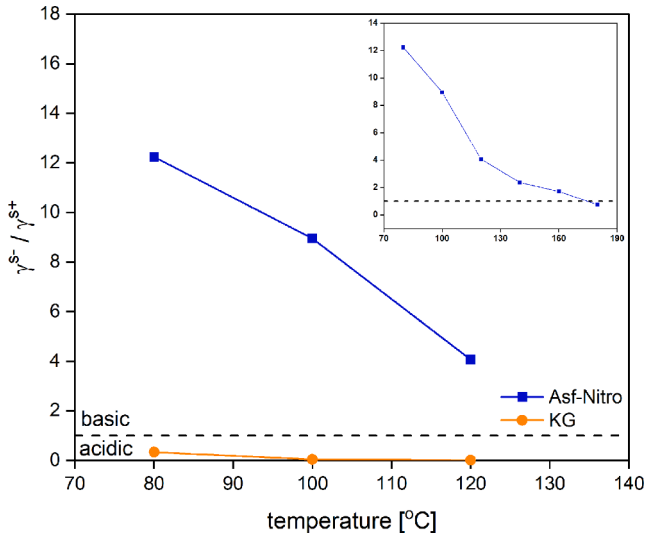

Fig. 8. Electron donor γ_S^- (basic) and electron acceptor γ_S^+ (acidic) character of KG and AsfNitro surface. The inset presents the evolution of γ_S^-/γ_S^+ in a broader range of temperature for AsfNitro.

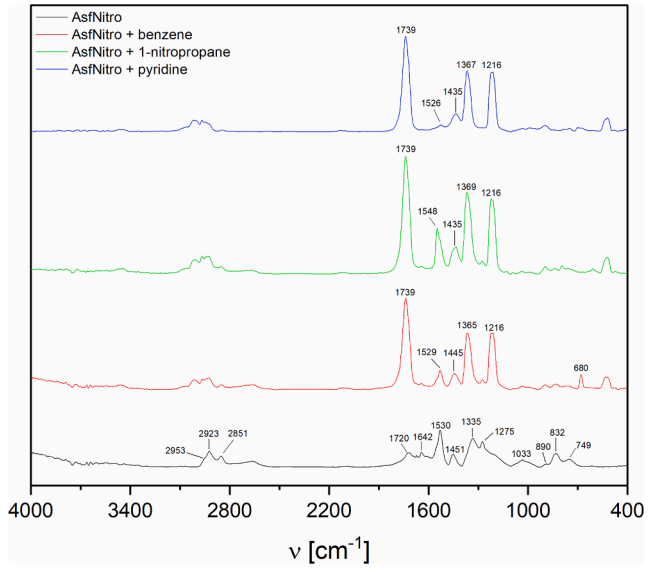

Fig. 9. FTIR-ATR spectra of AsfNitro before and after adsorption of test probes.

groups, in aliphatic chains. The signals from substituted aromatic rings, forming the backbone of asphaltenes, are visible for lower wavenumber values (bands at 890, 832, 749 cm^{-1}). The band located at 1033 may be assigned to the sulfoxide groups, but also the C–H in-plane bending bands of aromatics occur in this region [77].

To a great extent, adsorption properties of the AsfNitro are determined by the presence of NO_2 groups. As a strong electron withdrawing group, it should greatly reduce the overall electron density in aromatic rings of asphaltene molecule. As a result, the aromatic core of nitrated asphaltene may act as acceptor, and electron rich nitro group as donor in donor–acceptor (charge transfer) complexes, which are partially covalent in nature, and may explain high adsorption enthalpies of test compounds [78].

The contribution of nitro group, to adsorption of VOCs is clearly manifested by changes in intensity and position of IR absorption bands [80] characteristic for NO_2 group, after adsorption. The band located at 1530 cm^{-1} shifted after adsorption of benzene, pyridine and 1-nitropropane to 1529, 1526, and 1548 cm^{-1}, respectively. At the same time a substantial decrease of intensity was observed for benzene and pyridine indicating interaction with –NO_2 group. On the other hand, for the 1-nitropropane and increased intensity was observed, that comes from –NO_2 groups present in the structure of 1-nitropropane molecules, adsorbed on the surface of AsfNitro.

The position of other band, originating from –NO_2 in AsfNitro have also changed. The band located at 1335 cm^{-1} shifted after adsorption to 1367 cm^{-1}, for all test compounds. For 1275 cm^{-1} band, a substantial decrease of intensity was observed, along with slight red-shift (1275 – 1273 cm^{-1}). Bands' position shifts are a clear indication of interaction between nitro group and adsorbates.

Molecular interaction responsible for abovementioned position shifts of absorption bands can have different nature depending on the adsorbate. For aromatic molecules they can be a n-electron and π system of the aromatic molecule interactions, or dipole interactions for 1-nitropropane molecule [80]. In case of pyridine, interaction can occur through charge transfer between –NO_2 group and the aromatic nitrogen [79].

Moreover, considering the structure of AsfNitro, adsorptivity of aromatic compounds (benzene, and pyridine) can be promoted by the π-π stacking interactions with the polyaromatic structure of asphaltenes. The contribution of asphaltenes' aromatic rings is proved by lower intensity of bands attributed to the substituted aromatic rings (900–750 cm^{-1} region). The stacking mechanism can be enhanced by defects in the aromatic structure of AsfNitro, introduced by the chemical modification, as carbon materials with distributed π systems possess higher adsorption capacity, than carbon materials with conjugated π systems [80,81].

Apart from specific interactions, substantial contribution to adsorption properties of AsfNitro is from dispersive interactions, which promotes adsorption of organic molecules. It is supported by the comparison of polarizability of test molecules and the adsorption capacity of AsfNitro. The capacity increase with the polarizability of the adsorbate (Figure S6, R^2 = 0.935) - as the polarizability increase, dispersion forces become stronger.

Dispersive interactions are also proved by contribution of alkyl chains. For benzene, and pyridine, intensity of bands attributed to CH_2

and CH_3 groups (2953, 2923, 2851) decreased. For 1-nitropropane increase of intensity was observed. As in the case of $–NO_2$ group, increase is explained by the presence of alkyl chains in adsorbed molecules.

One more distinctive change was observed on the spectra after adsorption. A strong bands at 1740, and 1216 cm^{-1} appeared, which were assigned to the ester group (C = O, and C-O, respectively). As any of the adsorbates doesn't have carbonyl moiety in its structure, it may by an evidence of a formation of a new functional group on the surface. It is also, another signal (next to adsorption enthalpies at infinite dilution) of chemisorption on the surface of AsfNitro, and a premise for catalytic properties of nitrated asphaltenes.

4. Conclusions

This study presents an efficient adsorbent prepared by coating the porous support material (diatomaceous earth) with 10 %wt. of nitrated asphaltenes. Breakthrough curves and IGC measurements revealed that nitrated asphaltenes were exclusively responsible for the adsorption properties, and the role of the support was only to provide the surface area. Those findings can be extended to other support materials and their inherent limitations for adsorption of volatile organic compounds can be overcame.

The breakthrough experiments with selected VOCs, i.e. benzene, pyridine, and 1-nitropropane revealed significant increase in adsorption capacity after deposition of nitrated asphaltenes. Adsorption capacity of benzene calculated per gram of nitrated asphaltenes was comparable with e.g. Carboxen 1000, Tenax TA or MIL-47. Since nitrated asphaltenes are intended as the additive for coating support materials with developed surface area, the adsorption capacity of benzene was normalized by surface area of the AsfNitro. From this point of view, the AsfNitro's adsorption capacity is far more superior than for activated carbons or metal–organic frameworks. Moreover, deposition of nitrated asphaltenes was favourable for efficiency of the adsorbent. For 1-nitropropane and pyridine, the AsfNitro's bed was exhausted in 94, and 84% when breakthrough occurred - two times higher than for uncoated support material. It is certainly not without significance for the economics of the adsorption process – almost 100% of the bed was effectively used in waste gas purification. Breakthrough tests under humid conditions demonstrated that AsfNitro adsorbent is susceptible to the presence of water to the same extent as activated carbons.

IGC measurements supported the conclusion that nitrated asphaltenes are solely the source of remarkably strong interactions with adsorbates. Adsorption isotherms showed a significant increase of adsorption capacity, after coating the support with asphaltenes, that can be explained by increase of both dispersive and specific interactions – mainly of electrondonor nature. Comparison of adsorption enthalpies at infinite dilution demonstrated that activated carbons cannot compete in that matter with AsfNitro. The only comparable adsorbents (still falling behind AsfNitro) were metal–organic frameworks and graphene. Additionally, the values of adsorption enthalpies for AsfNitro indicated contribution of chemisorption to overall adsorption. This is a premise, supported by FTIR measurement, that nitrated asphaltenes may have catalytic properties. If such, than it opens a new path for research about asphaltenes' novel practical applications.

Presented results explicitly demonstrate the applicability of nitrated asphaltenes in adsorption processes and waste gas purification, and durability of the chemical modification with $–NO_2$ groups. Unique structure of AsfNitro is a source of various interactions that promote VOCs' adsorption, and facile coating of nitrated asphaltenes on a support, easily available in the target destination (e.g. natural clays, rocks), can be an effective procedure for risk mitigation of hazardous VOCs, accompanied by effective waste management and valorisation of a material that is considered a waste in petroleum industry.

Declaration of Competing Interest

The authors declare that they have no known competing financial interests or personal relationships that could have appeared to influence the work reported in this paper.

Acknowledgements

The authors gratefully acknowledge the financial support from the National Center for Research and Development, Warsaw, Poland – Project LIDER, no. LIDER/036/573/L-5/13/NCBR/2014.

This work was financially supported by the project "INTERPHD2" no. POWR.03.02.00-IP.08-00-DOC/16.

Appendix A. Supplementary data

Supplementary data to this article can be found online at https://doi.org/10.1016/j.cej.2021.130653.

References

[1] G. Boczkaj, P. Makoś, A. Fernandes, A. Przyjazny, New procedure for the examination of the degradation of volatile organonitrogen compounds during the treatment of industrial effluents, J. Sep. Sci. 40 (6) (2017) 1301–1309, https://doi.org/10.1002/jssc.201601237.

[2] G. Boczkaj, A. Przyjazny, M. Kamiński, Characteristics of volatile organic compounds emission profiles from hot road bitumens, Chemosphere 107 (2014) 23–30, https://doi.org/10.1016/j.chemosphere.2014.02.070.

[3] N.P.R.I. (Canada), Guide for reporting to the National Pollutant Release Inventory, 2016.

[4] European Parliament; European Council, Directive 2004/42/CE, 2004.

[5] Na Li, Qi Jiang, Fusong Wang, Peide Cui, Jun Xie, Jiashuo Li, Shaopeng Wu, Diego Maria Barbieri, Comparative assessment of asphalt volatile organic compounds emission from field to laboratory, J. Clean. Prod. 278 (2021) 123479, https://doi.org/10.1016/j.jclepro.2020.123479.

[6] C. Geng, W. Yang, X. Sun, X. Wang, Z. Bai, X. Zhang, Emission factors, ozone and secondary organic aerosol formation potential of volatile organic compounds emitted from industrial biomass boilers, J. Environ. Sci. (China) 83 (2019) 64–72, https://doi.org/10.1016/j.jes.2019.03.012.

[7] Yuxiu Zhang, Chaohai Wei, Bo Yan, Emission characteristics and associated health risk assessment of volatile organic compounds from a typical coking wastewater treatment plant, Sci. Total Environ. 693 (2019) 133417, https://doi.org/10.1016/j.scitotenv.2019.07.223.

[8] R. Tong, L. Zhang, X. Yang, J. Liu, P. Zhou, J. Li, Emission characteristics and probabilistic health risk of volatile organic compounds from solvents in wooden furniture manufacturing, J. Clean. Prod. 208 (2019) 1096–1108, https://doi.org/10.1016/j.jclepro.2018.10.195.

[9] Maria Rosa Ras, Rosa Maria Marcé, Francesc Borrull, Characterization of ozone precursor volatile organic compounds in urban atmospheres and around the petrochemical industry in the Tarragona region, Sci. Total Environ. 407 (14) (2009) 4312–4319, https://doi.org/10.1016/j.scitotenv.2009.04.001.

[10] Alex Guenther, C. Nicholas Hewitt, David Erickson, Ray Fall, Chris Geron, Tom Graedel, Peter Harley, Lee Klinger, Manuel Lerdau, W.A. Mckay, Tom Pierce, Bob Scholes, Rainer Steinbrecher, Raja Tallamraju, John Taylor, Pat Zimmerman, A global model of natural volatile organic compound emissions, J. Geophys. Res. 100 (D5) (1995) 8873, https://doi.org/10.1029/94JD02950.

[11] Y. Ren, Z. Qu, Y. Du, R. Xu, D. Ma, G. Yang, Y. Shi, X. Fan, A. Tani, P. Guo, Y. Ge, J. Chang, Air quality and health effects of biogenic volatile organic compounds emissions from urban green spaces and the mitigation strategies, Environ. Pollut. 230 (2017) 849–861, https://doi.org/10.1016/j.envpol.2017.06.049.

[12] E. Nie, G. Zheng, Z. Shao, J. Yang, T. Chen, Emission characteristics and health risk assessment of volatile organic compounds produced during municipal solid waste composting, Waste Manag. 79 (2018) 188–195, https://doi.org/10.1016/j.wasman.2018.07.024.

[13] Ruoyu Hu, Guijian Liu, Hong Zhang, Huaqin Xue, Xin Wang, Paul Kwan Sing Lam, Odor pollution due to industrial emission of volatile organic compounds: A case study in Hefei, China, J. Clean. Prod. 246 (2020) 119075, https://doi.org/10.1016/j.jclepro.2019.119075.

[14] Nicole E. Rabaud, Susan E. Ebeler, Lowell L. Ashbaugh, Robert G. Flocchini, Characterization and quantification of odorous and non-odorous volatile organic compounds near a commercial dairy in California, Atmos. Environ. 37 (7) (2003) 933–940, https://doi.org/10.1016/S1352-2310(02)00970-6.

[15] R.M. Fisher, N. Le-Minh, E.C. Sivret, J.P. Alvarez-Gaitan, S.J. Moore, R.M. Stuetz, Distribution and sensorial relevance of volatile organic compounds emitted throughout wastewater biosolids processing, Sci. Total Environ. 599–600 (2017) 663–670, https://doi.org/10.1016/j.scitotenv.2017.04.129.

[16] J. Badach, P. Kolasińska, M. Paciorek, W. Wojnowski, T. Dymerski, J. Gębicki, M. Dymnicka, J. Namieśnik, A case study of odour nuisance evaluation in the context of integrated urban planning, J. Environ. Manage. 213 (2018) 417–424, https://doi.org/10.1016/j.jenvman.2018.02.086.

[17] M. Keck, K. Mager, K. Weber, M. Keller, M. Frei, B. Steiner, S. Schrade, Odour impact from farms with animal husbandry and biogas facilities, Sci. Total Environ. 645 (2018) 1432–1443, https://doi.org/10.1016/j.scitotenv.2018.07.182.
[18] F.I. Khan, A. Kr, A.K. Ghoshal Ghoshal, Removal of volatile organic compounds from polluted air, J. Loss Prev. Process Ind. 13 (2000) 527–545, https://doi.org/10.1016/S0950-4230(00)00007-3.
[19] Maurizio Sansotera, Sina Geran Malek Kheyli, Alberto Baggioli, Claudia L. Bianchi, Maria Pia Pedeferri, Maria Vittoria Diamanti, Walter Navarrini, Absorption and photocatalytic degradation of VOCs by perfluorinated ionomeric coating with TiO2 nanopowders for air purification, Chem. Eng. J. 361 (2019) 885–896, https://doi.org/10.1016/j.cej.2018.12.136.
[20] C. Yang, G. Miao, Y. Pi, Q. Xia, J. Wu, Z. Li, J. Xiao, Abatement of various types of VOCs by adsorption/catalytic oxidation: A review, Chem. Eng. J. 370 (2019) 1128–1153, https://doi.org/10.1016/j.cej.2019.03.232.
[21] Xin Li, Jie Ma, Xiang Ling, Design and dynamic behaviour investigation of a novel VOC recovery system based on a deep condensation process, Cryogenics (Guildf). 107 (2020) 103060, https://doi.org/10.1016/j.cryogenics.2020.103060.
[22] M.S. Kamal, S.A. Razzak, M.M. Hossain, Catalytic oxidation of volatile organic compounds (VOCs) - A review, Atmos. Environ. 140 (2016) 117–134, https://doi.org/10.1016/j.atmosenv.2016.05.031.
[23] M. Gospodarek, P. Rybarczyk, B. Szulczyński, J. Gębicki, Comparative evaluation of selected biological methods for the removal of hydrophilic and hydrophobic odorous VOCs from air, Processes. 7 (2019) 12–15, https://doi.org/10.3390/pr7040187.
[24] M. Tomatis, M.T. Moreira, H. Xu, W. Deng, J. He, A.M. Parvez, Removal of VOCs from waste gases using various thermal oxidizers: A comparative study based on life cycle assessment and cost analysis in China, J. Clean. Prod. 233 (2019) 808–818, https://doi.org/10.1016/j.jclepro.2019.06.131.
[25] M.F. Mustafa, X. Fu, Y. Liu, Y. Abbas, H. Wang, W. Lu, Volatile organic compounds (VOCs) removal in non-thermal plasma double dielectric barrier discharge reactor, J. Hazard. Mater. 347 (2018) 317–324, https://doi.org/10.1016/j.jhazmat.2018.01.021.
[26] Xiuquan Li, Li Zhang, Zhongqing Yang, Peng Wang, Yunfei Yan, Jingyu Ran, Adsorption materials for volatile organic compounds (VOCs) and the key factors for VOCs adsorption process: A review, Sep. Purif. Technol. 235 (2020) 116213, https://doi.org/10.1016/j.seppur.2019.116213.
[27] H. Sui, P. An, X. Li, S. Cong, L. He, Removal and recovery of o-xylene by silica gel using vacuum swing adsorption, Chem. Eng. J. 316 (2017) 232–242, https://doi.org/10.1016/j.cej.2017.01.061.
[28] X. Zhang, B. Gao, A.E. Creamer, C. Cao, Y. Li, Adsorption of VOCs onto engineered carbon materials: A review, J. Hazard. Mater. 338 (2017) 102–123, https://doi.org/10.1016/j.jhazmat.2017.05.013.
[29] G. Zhang, Y. Liu, S. Zheng, Z. Hashisho, Adsorption of volatile organic compounds onto natural porous minerals, J. Hazard. Mater. 364 (2019) 317–324, https://doi.org/10.1016/j.jhazmat.2018.10.031.
[30] J.E. Szulejko, K.H. Kim, J. Parise, Seeking the most powerful and practical real-world sorbents for gaseous benzene as a representative volatile organic compound based on performance metrics, Sep. Purif. Technol. 212 (2019) 980–985, https://doi.org/10.1016/j.seppur.2018.11.001.
[31] Mei-syue Li, Siang Chen Wu, Yang-hsin Shih, Characterization of volatile organic compound adsorption on multiwall carbon nanotubes under different levels of relative humidity using linear solvation energy relationship, J. Hazard. Mater. 315 (2016) 35–41, https://doi.org/10.1016/j.jhazmat.2016.04.004.
[32] L. Yu, L. Wang, W. Xu, L. Chen, M. Fu, J. Wu, D. Ye, Adsorption of VOCs on reduced graphene oxide, J. Environ. Sci. (China) 67 (2017) 171–178, https://doi.org/10.1016/j.jes.2017.08.022.
[33] K. Vellingiri, J.E. Szulejko, P. Kumar, E.E. Kwon, K.H. Kim, A. Deep, D. W. Boukhvalov, R.J.C. Brown, Metal organic frameworks as sorption media for volatile and semi-volatile organic compounds at ambient conditions, Sci. Rep. 6 (2016) 27813, https://doi.org/10.1038/srep27813.
[34] R.R. Gil, B. Ruiz, M.S. Lozano, M.J. Martín, E. Fuente, VOCs removal by adsorption onto activated carbons from biocollagenic wastes of vegetable tanning, Chem. Eng. J. 245 (2014) 80–88, https://doi.org/10.1016/j.cej.2014.02.012.
[35] Alba Anfruns, María J. Martin, Miguel A. Montes-Morán, Removal of odourous VOCs using sludge-based adsorbents, Chem. Eng. J. 166 (3) (2011) 1022–1031, https://doi.org/10.1016/j.cej.2010.11.095.
[36] M. Plata-Gryl, M. Momotko, S. Makowiec, G. Boczkaj, Highly effective asphaltene-derived adsorbents for gas phase removal of volatile organic compounds, Sep. Purif. Technol. 224 (2019) 315–321, https://doi.org/10.1016/j.seppur.2019.05.041.
[37] Maksymilian Plata-Gryl, Malwina Momotko, Sławomir Makowiec, Grzegorz Boczkaj, Application of cyanated asphaltenes in gas-phase adsorption processes for removal of volatile organic compounds, Chem. Pap. 74 (3) (2020) 995–1008, https://doi.org/10.1007/s11696-019-00938-z.
[38] Grzegorz Boczkaj, Malwina Momotko, Dorota Chruszczyk, Andrzej Przyjazny, Marian Kamiński, Novel stationary phases based on asphaltenes for gas chromatography, J. Sep. Sci. 39 (13) (2016) 2527–2536, https://doi.org/10.1002/jssc.201600183.
[39] N.K. Rajan, V. Selvavathi, B. Sairam, J.M. Krishnan, Influence of asphaltenes on the rheological properties of blended paving asphalts, Pet. Sci. Technol. 28 (4) (2010) 331–350, https://doi.org/10.1080/10916460802640282.
[40] A. Seitllari, Y.S. Kumbargeri, K.P. Biligiri, I. Boz, A soft computing approach to predict and evaluate asphalt mixture aging characteristics using asphaltene as a performance indicator, Mater. Struct. Constr. 52 (2019) 1–11, https://doi.org/10.1617/s11527-019-1402-5.
[41] Chen Wang, Tiantai Li, Hui Gao, Jinsheng Zhao, Yuan Gao, Quantitative study on the blockage degree of pores due to asphaltene precipitation in low-permeability reservoirs with NMR technique, Elsevier B.V. 163 (2018) 703–711, https://doi.org/10.1016/j.petrol.2017.11.021.
[42] K. Akbarzadeh, A. Hammami, A. Kharrat, D. Zhang, S. Allenson, J. Creek, S. Kabir, A. Jamaluddin, A.G. Marshall, R.P. Rodgers, O.C. Mullins, T. Solbakken, Asphaltenes—problematic but rich in potential, Oilf, Rev. (2007) 22–43.
[43] Oliver C. Mullins, The asphaltenes, Annu. Rev. Anal. Chem. 4 (1) (2011) 393–418, https://doi.org/10.1146/annurev-anchem-061010-113849.
[44] Henning Groenzin, Oliver C. Mullins, Molecular size and structure of asphaltenes from various sources, Energy Fuels. 14 (3) (2000) 677–684, https://doi.org/10.1021/ef990225z.
[45] Bruno Schuler, Gerhard Meyer, Diego Peña, Oliver C. Mullins, Leo Gross, Unraveling the Molecular Structures of Asphaltenes by Atomic Force Microscopy, J. Am. Chem. Soc. 137 (31) (2015) 9870–9876, https://doi.org/10.1021/jacs.5b04056.
[46] H. Jung, C.W. Bielawski, Asphaltene oxide promotes a broad range of synthetic transformations, Commun. Chem. 2 (2019) 1–9, https://doi.org/10.1038/s42004-019-0214-4.
[47] Kirill Fedorov, Maksymilian Plata-Gryl, Javed Ali Khan, Grzegorz Boczkaj, Ultrasound-assisted heterogeneous activation of persulfate and peroxymonosulfate by asphaltenes for the degradation of BTEX in water, J. Hazard. Mater. 397 (2020) 122804, https://doi.org/10.1016/j.jhazmat.2020.122804.
[48] M. Plata-Gryl, C. Jungnickel, G. Boczkaj, An improved scalable method of isolating asphaltenes, J. Pet. Sci. Eng. 167 (2018) 608–614, https://doi.org/10.1016/j.petrol.2018.04.039.
[49] National Institute for Occupational Safety and Health, Pocket Guide to Chemical Hazards, 2007.
[50] R: A language and environment for statistical computing, (2008). http://www.r-project.org.
[51] T.V. Elzhov, K.M. Mullen, A.-N. Spiess, B. Bolker, minpack.lm: R Interface to the Levenberg-Marquardt nonlinear least-squares algorithm found in MINPACK, plus support for bounds, (2016).
[52] M. Al-Ghouti, M.A.M. Khraisheh, M.N.M. Ahmad, S. Allen, Thermodynamic behaviour and the effect of temperature on the removal of dyes from aqueous solution using modified diatomite: A kinetic study, J. Colloid Interface Sci. 287 (1) (2005) 6–13, https://doi.org/10.1016/j.jcis.2005.02.002.
[53] Wen-Tien Tsai, Chi-Wei Lai, Kuo-Jong Hsien, Characterization and adsorption properties of diatomaceous earth modified by hydrofluoric acid etching, J. Colloid Interface Sci. 297 (2) (2006) 749–754, https://doi.org/10.1016/j.jcis.2005.10.058.
[54] Khim Hoong Chu, Breakthrough curve analysis by simplistic models of fixed bed adsorption: In defense of the century-old Bohart-Adams model, Chem. Eng. J. 380 (2020) 122513, https://doi.org/10.1016/j.cej.2019.122513.
[55] Andrei Veksha, Eiji Sasaoka, Md. Azhar Uddin, The influence of porosity and surface oxygen groups of peat-based activated carbons on benzene adsorption from dry and humid air, Carbon N. Y. 47 (10) (2009) 2371–2378, https://doi.org/10.1016/j.carbon.2009.04.028.
[56] I. Langmuir, Adsorption of gases on plain surfaces of glass mica platinum, J. Am. Chem. Soc. 40 (1918) 1361–1403.
[57] M. Jaroniec, Adsorption on heterogeneous surfaces: The exponential equation for the overall adsorption isotherm, Surf. Sci. 50 (2) (1975) 553–564, https://doi.org/10.1016/0039-6028(75)90044-8.
[58] Thio Christine Chandra, M.M. Mirna, Y. Sudaryanto, S. Ismadji, Adsorption of basic dye onto activated carbon prepared from durian shell: Studies of adsorption equilibrium and kinetics, Chem. Eng. J. 127 (1-3) (2007) 121–129, https://doi.org/10.1016/j.cej.2006.09.011.
[59] S.J. Gregg, K. Sing, Adsorption, surface area and porosity, Academic Press, Michigan, 1982.
[60] Frank Thielmann, Introduction into the characterisation of porous materials by inverse gas chromatography, J. Chromatogr. A. 1037 (1-2) (2004) 115–123, https://doi.org/10.1016/j.chroma.2004.03.060.
[61] M.L. Palash, Animesh Pal, Tahmid Hasan Rupam, Byung-Duck Park, Bidyut Baran Saha, Surface energy characterization of different particulate silica gels at infinite dilution, Colloids Surfaces A Physicochem. Eng. Asp. 603 (2020) 125209, https://doi.org/10.1016/j.colsurfa.2020.125209.
[62] Pirre P. Ylä-Mäihäniemi, Jerry Y.Y. Heng, Frank Thielmann, Daryl R. Williams, Inverse gas chromatographic method for measuring the dispersive surface energy distribution for particulates, Langmuir 24 (17) (2008) 9551–9557, https://doi.org/10.1021/la801676n.
[63] Matthew T. Luebbers, Tianjiao Wu, Lingjuan Shen, Richard I. Masel, Trends in the adsorption of volatile organic compounds in a large-pore metal-organic framework, IRMOF-1, Langmuir 26 (13) (2010) 11319–11329, https://doi.org/10.1021/la100635r.
[64] Eva Díaz, Salvador Ordóñez, Aurelio Vega, Adsorption of volatile organic compounds onto carbon nanotubes, carbon nanofibers, and high-surface-area graphites, J. Colloid Interface Sci. 305 (1) (2007) 7–16, https://doi.org/10.1016/j.jcis.2006.09.036.
[65] A.S. Münch, F.O.R.L. Mertens, Investigation of n-alkane adsorption on HKUST-1 and determination of intrinsic interfacial energy contributions, Microporous Mesoporous Mater. 270 (2018) 180–188, https://doi.org/10.1016/j.micromeso.2018.05.012.
[66] M. Rückriem, A. Inayat, D. Enke, R. Gläser, W.-D. Einicke, R. Rockmann, Inverse gas chromatography for determining the dispersive surface energy of porous silica, Colloids Surfaces A Physicochem. Eng. Asp. 357 (1-3) (2010) 21–26, https://doi.org/10.1016/j.colsurfa.2009.12.001.

[67] A. Pal, A. Kondor, S. Mitra, K. Thu, S. Harish, B.B. Saha, On surface energy and acid–base properties of highly porous parent and surface treated activated carbons using inverse gas chromatography, J. Ind. Eng. Chem. 69 (2019) 432–443, https://doi.org/10.1016/j.jiec.2018.09.046.
[68] Montserrat R. Cuervo, Esther Asedegbega-Nieto, Eva Díaz, Salvador Ordóñez, Aurelio Vega, Ana Belén Dongil, Inmaculada Rodríguez-Ramos, Modification of the adsorption properties of high surface area graphites by oxygen functional groups, Carbon N. Y. 46 (15) (2008) 2096–2106, https://doi.org/10.1016/j.carbon.2008.08.025.
[69] Huijuan Liu, Bowen Xu, Keyan Wei, Yansong Yu, Chao Long, Adsorption of low-concentration VOCs on various adsorbents: Correlating partition coefficient with surface energy of adsorbent, Sci. Total Environ. 733 (2020) 139376, https://doi.org/10.1016/j.scitotenv.2020.139376.
[70] Yang-hsin Shih, Mei-syue Li, Adsorption of selected volatile organic vapors on multiwall carbon nanotubes, J. Hazard. Mater. 154 (1-3) (2008) 21–28, https://doi.org/10.1016/j.jhazmat.2007.09.095.
[71] Petr Lazar, František Karlický, Petr Jurečka, Mikuláš Kocman, Eva Otyepková, Klára Šafářová, Michal Otyepka, Adsorption of small organic molecules on graphene, J. Am. Chem. Soc. 135 (16) (2013) 6372–6377, https://doi.org/10.1021/ja403162r.
[72] H. Grajek, J. Jonik, L. Rutkowski, M. Purchała, T. Wawer, The optimisation of chromatographic conditions for determination of acceptor-donor properties of graphene oxide and reduced graphene oxide, Acta Innov. 26 (2018) 5–20.
[73] Alexander S. Münch, Florian O.R.L. Mertens, The Lewis acidic and basic character of the internal HKUST-1 surface determined by inverse gas chromatography, CrystEngComm 17 (2) (2015) 438–447, https://doi.org/10.1039/C4CE01327A.
[74] Giselle Autié-Castro, Edilso Reguera, Celio L. Cavalcante, Antonio S. Araujo, Enrique Rodríguez-Castellón, Surface acid-base properties of Cu-BTC and Fe-BTC MOFs. An inverse gas chromatography and n-butylamine thermo desorption study, Inorganica Chim. Acta. 507 (2020) 119590, https://doi.org/10.1016/j.ica.2020.119590.
[75] M.N. Siddiqui, I.W. Kazi, Chlorination, nitration, and amination reactions of asphaltene, Pet. Sci. Technol. 32 (24) (2014) 2987–2994, https://doi.org/10.1080/10916466.2014.924528.
[76] J. Douda, M.E. Llanos, R. Alvarez, J. Navarrete Bolaños, Structure of Maya asphaltene−resin complexes through the analysis of soxhlet extracted fractions, Energy Fuels 18 (3) (2004) 736–742, https://doi.org/10.1021/ef034057t.
[77] Morteza Asemani, Ahmad Reza Rabbani, Detailed FTIR spectroscopy characterization of crude oil extracted asphaltenes: Curve resolve of overlapping bands, J. Pet. Sci. Eng. 185 (2020) 106618, https://doi.org/10.1016/j.petrol.2019.106618.
[78] L. Emmett, G.M. Prentice, G.D. Pantoş, Donor-acceptor interactions in chemistry, Annu. Reports Prog. Chem. - Sect. B. 109 (2013) 217–234, https://doi.org/10.1039/c3oc90004e.
[79] Sandeep Kumar, D.R. Sharma, N. Thakur, N.S. Negi, V.S. Rangra, Molecular associations in binary mixture of pyridine and nitrobenzene in benzene solution using microwave absorption data, Z. Phys. Chem. 219 (12_2005) (2005) 1649–1654, https://doi.org/10.1524/zpch.2005.219.12.1649.
[80] Xiaoxiao Chen, Baoliang Chen, Macroscopic and spectroscopic investigations of the adsorption of nitroaromatic compounds on graphene oxide, reduced graphene oxide, and graphene nanosheets, Environ. Sci. Technol. 49 (10) (2015) 6181–6189, https://doi.org/10.1021/es5054946.
[81] Jun Wang, Baoliang Chen, Baoshan Xing, Wrinkles and folds of activated graphene nanosheets as fast and efficient adsorptive sites for hydrophobic organic contaminants, Environ. Sci. Technol. 50 (7) (2016) 3798–3808, https://doi.org/10.1021/acs.est.5b04865.

Gdańsk, 01.03.2022 r.

mgr inż. Maksymilian Plata-Gryl

Department of Process Engineering and Chemical Technology

Gdańsk University of Technology

Gabriela Narutowicza 11/12 Street

80-233 Gdańsk

e-mail: makgryl@student.pg.edu.pl

STATEMENT

on the contribution and participation in the publication

I declare that my contribution to the work:

M. Plata-Gryl, M. Momotko, S. Makowiec, G. Boczkaj, Characterization of diatomaceous earth coated with nitrated asphaltenes as superior adsorbent for removal of VOCs from gas phase in fixed bed column, *Chem. Eng. J.* 427 (2022) 130653

was to develop the research plan (in cooperation with my supervisor), perform experiments (except preparation of chemically modified asphaltenes and their elemental analysis), analyse the data, write the initial draft and further revise it.

I estimate my contribution to the final publication to be 65 %.

Plata-Gryl

Gdańsk, 28.02.2022 r.

mgr inż. Malwina Momotko

Department of Process Engineering and Chemical Technology

Gdańsk University of Technology

Gabriela Narutowicza 11/12 Street

80-233 Gdańsk

e-mail: malmomot@student.pg.edu.pl

STATEMENT

on the contribution and participation in the publication

I declare that my contribution to the work:

M. Plata-Gryl, M. Momotko, S. Makowiec, G. Boczkaj, Characterization of diatomaceous earth coated with nitrated asphaltenes as superior adsorbent for removal of VOCs from gas phase in fixed bed column, *Chem. Eng. J.* 427 (2022) 130653

was to participate in data analysis and visualization, as well as in initial draft preparation.

I estimate my contribution to the final publication to be 10 %.

Malwina Momotko

Gdańsk, 25.02.2022 r.

dr hab. Sławomir Makowiec, prof. PG
Department of Organic Chemistry
Gdańsk University of Technology
Gabriela Narutowicza 11/12 Street
80-233 Gdańsk
e-mail: mak@pg.edu.pl

STATEMENT

on the contribution and participation in the publication

I declare that my contribution to the work:

M. Plata-Gryl, M. Momotko, S. Makowiec, G. Boczkaj, Characterization of diatomaceous earth coated with nitrated asphaltenes as superior adsorbent for removal of VOCs from gas phase in fixed bed column, *Chem. Eng. J.* 427 (2022) 130653

was to participate in the experimental part of the research, by preparing chemically modified asphaltenes.

I estimate my contribution to the final publication to be 10 %.

.....

Gdańsk, 28.02.2022 r.

dr hab. inż. Grzegorz Boczkaj, prof. PG
Department of Process Engineering and Chemical Technology
Gdańsk University of Technology
Gabriela Narutowicza 11/12 Street
80-233 Gdańsk
e-mail: grzegorz.boczkaj@pg.edu.pl

STATEMENT

on the contribution and participation in the publication

I declare that my contribution to the work:

M. Plata-Gryl, M. Momotko, S. Makowiec, G. Boczkaj, Characterization of diatomaceous earth coated with nitrated asphaltenes as superior adsorbent for removal of VOCs from gas phase in fixed bed column, *Chem. Eng. J.* 427 (2022) 130653

was to participate in the conceptualization of the research, supervision of the research activity planning and execution, preparation of the initial draft and the revised, published work.

I estimate my contribution to the final publication to be 15 %.